UNIVERSITÀ
DEGLI STUDI
FIRENZE

DOTTORATO DI RICERCA IN SCIENZE CHIMICHE

CICLO XXVIII

COORDINATORE Prof. ANDREA GOTI

Organic Synthesis Applied to Photovoltaics: New Efficient Sensitizers for Transparent and Near Infrared (NIR) Absorbing Dye-Sensitized Solar Cells

Settore Scientifico Disciplinare CHIM/06

Dottorando
Dott. Alessio Dessì

_____

Tutore
Dr.ssa Gianna Reginato

_____

Co-tutore
Dr. Lorenzo Zani

_____

Coordinatore
Prof. Andrea Goti

_____

Anni 2012/2015

Table of Contents

Abstract

Presently, Dye-Sensitized Solar Cells (DSSCs) are considered one of the most promising technologies to convert solar energy in electric current due to their low cost of production, their innovative aesthetic properties and their easy integration in buildings and objects. The dye, which can be a completely organic molecule, is the photoactive material and is considered the heart of the DSSC. Exceeding the current record efficiency is not the unique goal which can be pursued in order to make DSSC the most relevant photovoltaic technology: stability, transparency and color are pivotal properties for a future worldwide commercialization of DSSCs. During this Ph.D., these targets have been pursued by working on the structure of new organic photosensitizers. A careful design of the structures through computational analysis has been accomplished, then the synthesis of the selected dyes has been planned and executed, and the optimization of reaction conditions using sustainable procedure has been carried out when possible. Finally, the photovoltaic performances of the solar cells built with our dyes have been assessed and compared with those of reference dyes.

Chapter 1

Introduction

1.1. The energy issue

In the last two centuries our world has faced many important changes. Old agricultural-based economies were abandoned to embrace industrial and technological societies, and one of the most expensive price to pay for this change has been a huge increase of the energy demand and the exploitation of every possible natural resource. Every year, the world energy consumption increases and, in 2014, amounted to almost 18 TW* of required power: quite significantly, as depicted in Figure 1.1, the increase of nearly 37% from 2000 is mostly due to developing countries, such as China and India, whose industries are becoming more and more important in the world manufacturing and economic scenario.[1]

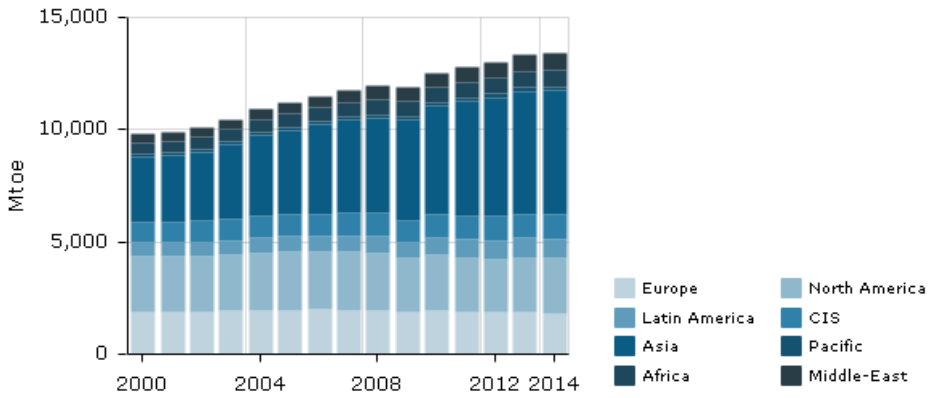

Figure 1.1. World Energy Consumption 2000-2014.[1]

Although, for the first time, the growth of China total energy consumption in the last year was nearly zero, outlooks for the next twenty years forecast a further increase in world energy demand, estimating a value of required power of 23-24 TW in 2035.[2] Nowadays fossil fuels are still the main energy source (78.4% - Figure 1.2), but their massive use is causing pollution, because of the large carbon dioxide emissions deriving from their combustion, and will also result in their depletion in a medium-long term period. For these reasons, the development of alternative energetic sources cannot be postponed anymore.

* 1000 MToe ≈ 1.33 TW.

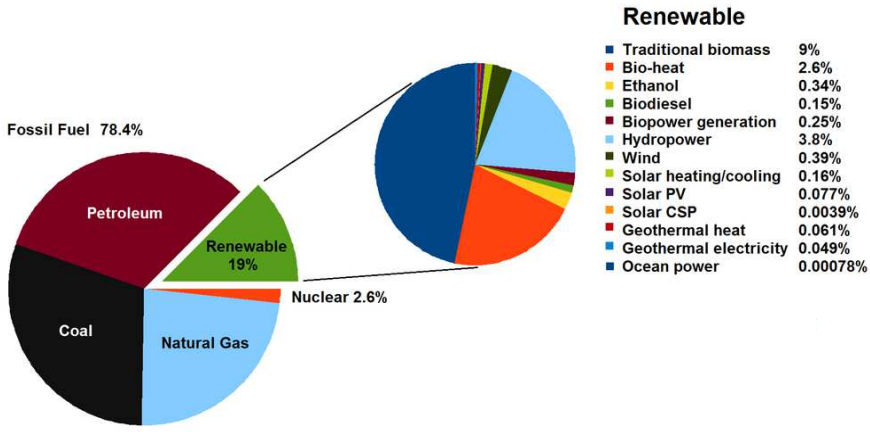

Figure 1.2. Total world energy consumption by source (2013).[3]

Renewable energy sources would be the perfect solution to the problem of increasing energetic demand, because they are practically inexhaustible (at least on the timescale associated with human technology) and their environmental impact is low. Nowadays, the principal renewable sources exploited are biomass, hydropower and bio-heat (Figure 1.2), but wind and solar are growing rapidly as well: data for 2013 show that renewable electricity generation overtook natural gas becoming the second largest source of electricity worldwide by producing 22% of total electricity (Figure 1.3a)[4], while the shares of solar and wind in this production grew dramatically in the last fifteen years (Figure 1.3b).[1] These data are encouraging, but not satisfying enough yet to discard fossil fuels definitively.

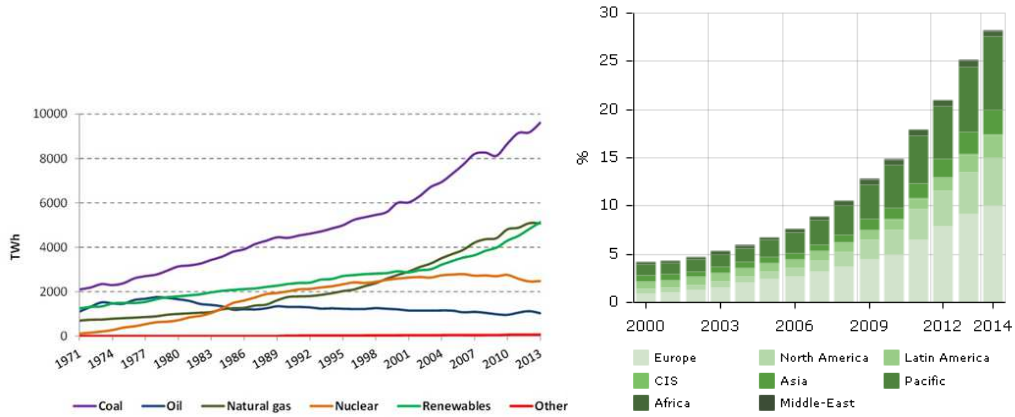

Figure 1.3. a) World electricity production by source from 1973 to 2013. b) Share of wind and solar in electricity production.

Among all the possible renewable sources, solar energy is widely considered to have the highest potential to become the world principal energy supply. Annual solar irradiation to the Earth is ten thousand times higher than the world annual needs and orders of magnitude larger than any of the other energy sources combined together (Figure 1.4).[5] Even considering that only 600 of 1.7×10^5 TW provided by the Sun are realistically exploitable, solar cells with an efficiency of just 10% could produce three times the energy necessary to feed the Earth energetic needs.[6]

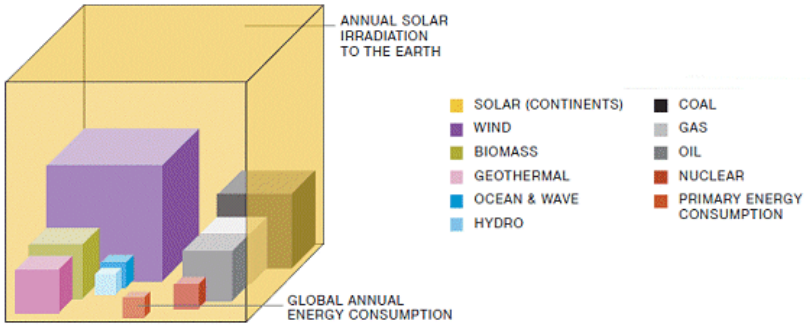

Figure 1.4. Comparison of finite and renewable planetary energy reserves.[7]

This free, inexhaustible and widely distributed kind of energy can be converted in electric current by photovoltaics (PV). Photovoltaic devices contain semiconducting materials which exhibit the photoelectric effect, that is electron emission promoted by light. Using solar light, photovoltaics generate clean energy, without producing any pollution, even if the environmental profile of PV devices during its whole cycle of life, from raw materials extraction to end-of-life and disposal phase, is not negligible anyway.[8] The principal drawbacks of PV technology, which are still limiting its large-scale employment, are the not constant production of energy, because of day/night alternation and the variation of solar light intensity and incidence during the day, and the relatively high cost of produced energy (0.20 – 0.30 $/KWh), which is still superior to that of the electricity generated from coal (0.09 – 0.14 $/KWh) and natural gas (0.06 – 0.12 $/KWh), and results from the high production costs of photovoltaic devices.[9] In view of these drawbacks, advances in technology, increases in manufacturing scale and research on new materials and new methods for energy storage are required to reduce costs of production and increase device efficiencies, in order to make photovoltaics a real alternative to fossil fuels.

1.2. The photovoltaic technology

Physical principles at the base of photovoltaic technologies were already known in 19th century, but the first practical photovoltaic device, also known as solar cell, was publicly demonstrated in the mid-50's at Bell Laboratories.[10] Solar cells were readily used for space applications and improvements were gradual over the next two decades, with a rapid drop of production costs from the 70's. Nowadays there are three principal classes of solar cells which differ for the materials used in their fabrications as well as their appearance and physical properties (in particular thickness and flexibility):

i. Silicon-based solar cells
ii. Thin-film solar cells
iii. Emerging photovoltaics (organic and hybrid solar cells)

1.2.1. Silicon-based solar cells

Historically, the first class of solar cells ever developed contained mono- or polycrystalline silicon as bulk semiconducting material, and today it is still the most commercially predominant PV technology. Monocrystalline silicon solar modules (i.e. arrays of cells connected in series and/or in parallel) are more efficient than polycrystalline ones (22-23% vs. 18-19%, for a definition of photovoltaic efficiency see below), but much more expensive too (due to their more complicated production procedures), so polysilicon cells are the most common type used in photovoltaics.[11] Typical crystalline silicon wafers for solar cells have a thickness between 160 and 240 µm.

These cells are entirely based around the concept of a *p*-*n* junction, created by doping of the growing crystals of silicon with atoms of Group III (B or Al for positive junction) and Group V (P o As for negative junction): diffusion of electrons from *n*-side to *p*-side occurs with formation of an electric field. Sunlight photons promote electrons from the valence band of the semiconductor to the conduction band generating holes and the inbuilt electric field pushes electrons and holes to the *n* and *p*-side respectively. The cycle is over when electrons on the *n*-side pass through the external circuit to fill the holes at the *p*-side.[12]

Besides the high efficiency, silicon solar cells have a long durability (almost 20-25 years) and the installation cost is low, but the manufacturing process is complex and quite expensive because the construction of the cell requires a relatively high amount of extra-pure silicon. Furthermore, Si-cells are appropriate for wide installations in desert places, but their integration in buildings and cities is less straightforward, being hindered by their thickness, low flexibility and unsightly look.

1.2.2. Thin-film solar cells

Thin-film solar cells are made by coating one or more thin layers of photovoltaic material on a substrate, such as glass, plastic or metal. Film thickness can vary from a few nanometres to tens of micrometres, making such devices much thinner than the first-generation crystalline silicon solar cells. As a consequence, thin-film cells are flexible, lighter, and have less drag or friction. For these reasons they can be used in building-integrated photovoltaics (BIPV) to replace conventional building materials such as the roof, skylights, or façades.[13] Thin-film technology reduces the amount of active material in comparison with silicon-based cells, so the manufacturing process is easier and cheaper. Their working principle is also based on a *p*-*n* junction, with cadmium sulfide (CdS) as *n*-side and different photovoltaic materials as light-harvesting *p*-side. The principal classes of thin-film cells are the following:

i. Amorphous silicon:[14] it is the most well-developed thin-film technology to-date. The amount of silicon required for these cells is lower than traditional silicon-based cells and manufacturing is more economic and easier, but efficiencies are still low (12-14%).
ii. Cadmium telluride (CdTe):[15] CdTe is the only thin film material which could rival crystalline silicon in terms of cost/watt ratio. CdTe has lower production costs and higher efficiencies (20-21% for lab cells, 16-17% for modules) than amorphous silicon, but tellurium supplies are limited and cadmium is highly toxic, so disposal of such a cell at the end of its life cycle could be very hard.
iii. Copper indium gallium selenide (CIGS):[16] this material has an extremely high absorption coefficient, so CIGS films can be much thinner than other semiconductors. High efficiencies of 20-21% are obtained for lab cells and beyond 15% for modules, while costs are analogous to monocrystalline silicon, but the use of toxic and rare elements such as indium and gallium produces not negligible environmental problems.

iv. Copper zinc tin sulfide and selenide (CZTSSe):[17] this material, also known as kesterite, could be an attracting alternative to CIGS because it is made from non-toxic, earth-abundant and low-cost materials, but its efficiencies (up to 11-12%) are still much lower than those obtained by CIGS.
v. Gallium arsenide (GaAs):[18] although GaAs cells are very expensive, they hold the world's record in efficiency for a single-junction solar cell at 28.8%. Because of the high cost, GaAs is mostly used for solar panels on spacecrafts.

Despite some evident qualities, market-share of thin-film cells never reached more than 20 percent in the last two decades and has been declining in recent years to about 9 percent of worldwide photovoltaic installation in 2013.[19]

1.2.3. Emerging photovoltaics

Silicon-based and thin-film solar cells described in previous paragraphs are devices containing a single *p*-*n* junction: for this reason, their maximum theoretical efficiency cannot overcome the so-called Shockley-Queisser limit,[20] which depends on the band gap energy of the photovoltaic material inside the cell (31-41%).

Emerging photovoltaics are new generation solar cells which are potentially able to overcome the Shockley-Queisser limit to achieve higher efficiencies, possibly with lower costs. This goal can be pursued in two different ways, building multi-junction solar cells containing multiple thin films of photovoltaic materials with different band gap energy to absorb a broader range of wavelengths of solar spectrum (i) or designing devices which exploit different mechanisms to convert solar energy in electric current (ii).

Multi-junction solar cells (i) have obtained impressive results in terms of efficiency and the world record of 46% has been achieved in 2014 with a four-junction cell under a concentrator photovoltaic system,[21] but their very high cost of production has limited, for the moment, their application to spacecrafts.

Other emerging photovoltaic devices with different working mechanisms (ii) are now under study and, even if their efficiencies are still lower than silicon-based and thin-film solar cells (Figure 1.5, orange lines), their extremely interesting electronic, optical and technological features, as well as their low cost of production, identify this new generation of solar cells as the most promising alternative for the future world energy production. This class of emerging photovoltaics devices is

characterized by the use of organic and hybrid materials and includes dye-sensitized solar cells (DSSCs), perovskite solar cells, organic/polymer solar cells and quantum dots.

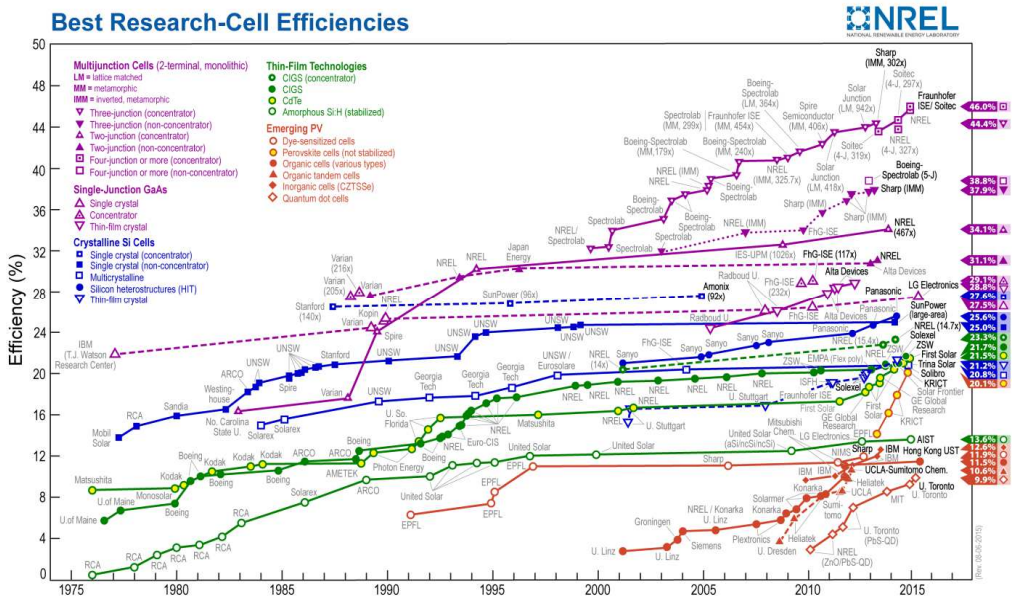

Figure 1.5. Efficiency chart for every solar cell technology.[22]

Big attention was recently focused on perovskite solar cells,[23] because their efficiencies rose from below 10%, as described in their first report in 2009, to over 20% in 2015, becoming a hot topic in the solar cells field. Perovskites for solar cell applications are organometallic compounds containing halides of lead and alkylammonium or formamidinium ions with the same crystalline structure of natural perovskite ($CaTiO_3$). These materials were initially used as sensitizers for traditional DSSC cells, but their different working mechanism has allowed the development of devices without a semiconducting metal oxide which is instead necessary for DSSCs (see paragraph 1.3.1.2), achieving efficiencies beyond 20%.[24] Despite these important results, a possible large scale application of perovskites is hampered, for the moment, by the use of toxic lead salts and their low long-term stability, due to fast degradation in the presence of water.

Photovoltaic devices with low environmental impact, good stability and charming electronic and optical properties are dye-sensitized solar cells, which are the subject of this Ph.D. thesis and will be carefully described in next paragraphs.

1.3. Dye-Sensitized Solar Cells (DSSCs)

Dye-sensitized solar cells have been described for the first time in 1991 by Grätzel and O'Regan.[25] Unlike conventional PV cells, the working mechanism of a DSSC is similar to natural photosynthesis: likewise the chlorophyll, which absorbs photons but does not participate to the electron transfer, photoreceptor and charge carrier are implemented by different components in DSSCs. This is contrary to conventional PV cells where a semiconductor assumes both functions. This separation of functions leads to lower purity demands on raw materials and consequently makes DSSCs a lower-cost alternative to traditional PV cells. Moreover, even if the power conversion efficiencies of DSSCs are still lower (max. efficiency 14.7% in laboratory tests)[26] than that of silicon-based and thin-film solar cells, DSSCs have many potential advantages such as easy manufacturing, good performance under diffuse light and high temperature, higher environmental compatibility compared with traditional photovoltaic devices and huge flexibility in terms of shape, color and transparency. All these features make DSSC as the most interesting photovoltaic technology for integration of solar cells inside buildings and small electronic objects (decorative solar lamps and chargers, flexible mobile phone chargers, solar bags, etc.).

1.3.1. DSSC components and working principle

There are five principal components inside the structure of a DSSC (Figure 1.6): a conductive substrate (i), a semiconducting thin-film (ii), a photosensitizer (iii), an electrolyte solution containing a redox couple (iv) and a counterelectrode (v).[6,27,28]

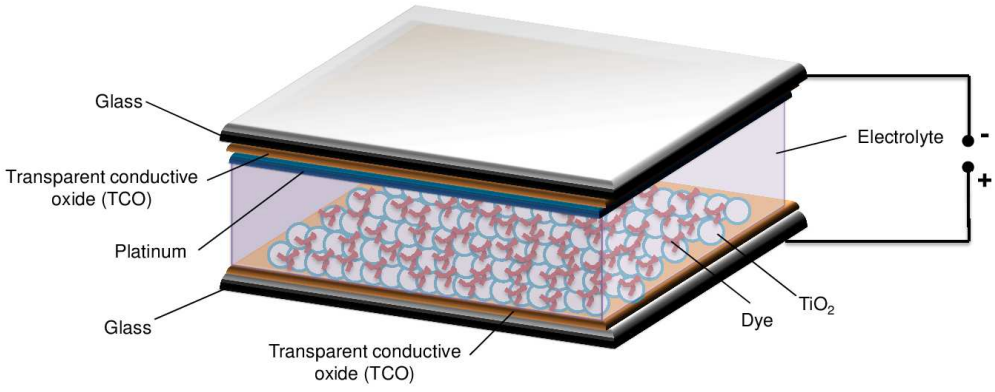

Figure 1.6. Schematic representation of a dye-sensitized solar cell.

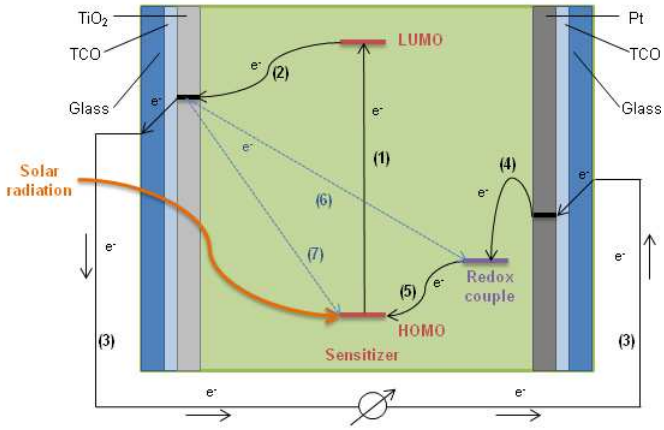

Figure 1.7. Photoelectrochemical processes inside a dye-sensitized solar cell.

Figure 1.7 summarizes the principal electrochemical reactions which enable the generation of electron current.[6,27] Initially, the photosensitizer absorbs solar light, gathering the required energy to excite one electron from HOMO to LUMO **(1)**. The electron in the excited state has a short lifetime and can return to its fundamental state by means of radiative processes or be transferred to the conduction band of semiconductor (injection) **(2)**, which is usually kinetically favored. Injected electrons move through the conducting layer by diffusion, then pass through the external circuit **(3)** to the counterelectrode and, here, the reduction of the redox shuttle occurs **(4)**. Finally, the oxidized dye is regenerated by reduction from the redox couple **(5)**; thus, the cycle is over with production of electric current and without any permanent chemical modification. There are also some undesired reactions which negatively affect the whole process reducing the electron flux through the external circuit and the voltage between the two electrodes. The most relevant one is the recombination of injected electrons in the conduction band of the semiconductor both with redox shuttle ions **(6)** or with the oxidized dye **(7)**.

1.3.1.1. Conducting substrate

The backbone of a DSSC is constituted by two glass electrodes coated with a transparent conductive oxide (TCO), which is usually tin oxide doped with fluorine (FTO) or indium-tin oxide (ITO). Recently some TCO-free alternatives, such as highly conductive polymers[29] or colloidal graphite,[30] have been developed to get rid of the expensive conductive oxides and replace the conventional glass with flexible plastic substrates.

1.3.1.2. Semiconducting thin-film

The most used semiconducting material is titanium dioxide (TiO_2, also known as titania), which is air-stable, nontoxic and commercially available at a low price. Several crystal forms of TiO_2 occur naturally: rutile, anatase, and brookite. Although rutile is the thermodynamically most stable form, anatase is the preferred structure in DSSCs, because it has a larger bandgap (3.2 *vs.* 3.0 eV for rutile) and a higher conduction band edge energy, E_c. Titania is layered on the conducting substrate as a mesoporous nanocrystalline thin-film: the most common technique to prepare TiO_2 nanoparticles is the acid- or base-catalyzed hydrolysis of a titanium precursor such as titanium (IV) alkoxide with an excess of water, followed by hydrothermal growth and crystallization. Acid or basic hydrolysis gives materials of different shapes and properties, while rate of hydrolysis, temperature and water content can be tuned to produce particles of different sizes. The produced particles are formulated in a paste with polymer additives and deposited onto conducting glass substrates using doctor blading or screen printing techniques. Finally, the film is sintered at about 450 °C in air to remove the organic components and to make electrical connection between the nanoparticles. The porosity of the resulting mesoporous film can be controlled by changing the amount of polymer in the paste. The average thickness of TiO_2 layer is about 10 µm, while TiO_2 nanoparticles diameter is in the range 10-30 nm. In several cases, the mesoporous light absorption layer of TiO_2 is deposited between a 50 nm-thick TiO_2 blocking layer,[31] which must prevent contact between the redox mediator and the TCO, and a very thin light-scattering layer,[32] with or without an overcoating of TiO_2 on the whole structure, deposited by means of chemical bath deposition using aqueous $TiCl_4$.[33]

A possible alternative to TiO_2 is zinc oxide (ZnO).[34] The bandgap and conduction band edge of ZnO is similar to that of titania, and ZnO even has a higher electron mobility which should favor electron transport, but its chemical stability is poor compared with that of TiO_2. Solar cells with SnO_2,[35] $SrTiO_3$ and Nb_2O_5[36] as semiconductors have been reported as well.

1.3.1.3. Photosensitizer

The photosensitizer or dye is an organic or organometallic molecule able to bind the semiconductor, harvest solar light and transfer electrons to TiO_2, initiating the process of electric current generation. Anchoring of the dye to the semiconductor occurs by dipping the glass electrode containing the semiconducting thin-film in a solution of the photosensitizer in organic solvent for some hours: the system

composed by substrate/semiconductor/dye is called photoanode. The principal characteristics of the dyes will be fully described in paragraph 1.3.3.

1.3.1.4. Electrolyte solution

The space between the two electrodes is filled with an electrolyte, which can consist of a solution or gel containing a redox couple, or a solid hole-conducting material. The electrolyte is responsible for the inner charge carrier transport between electrodes and continuously regenerates the dye and itself during DSSC operation. The electrolyte must have long-term stability, including chemical, thermal, optical, electrochemical and interfacial stability; moreover, it should not cause desorption and degradation of the sensitizing dye and should not exhibit a significant absorption in the range of visible light.

Regarding liquid electrolytes, they show several advantages such as easy preparation, high conductivity, low viscosity and good interfacial wetting between electrolytes and electrodes. Today, liquid electrolytes are still the most widely used transport medium for DSSCs. The most used solvents are organic polar liquids like high-boiling point nitriles (propionitrile, methoxyacetonitrile, 3-methoxyproprionitrile) and ionic liquids, but simple water has been tested, too.[37] Iodide/triiodide is the simplest and most used redox couple because it has a suitable redox potential to provide a rapid dye regeneration; moreover such couple has good solubility, high conductivity and low cost, so it has been the preferred redox shuttle since the beginning of DSSC development. A common I^-/I_3^--based electrolyte solution is prepared dissolving I_2 in a proper solvent with an excess amount of an iodine-containing salt, such as LiI, NaI or NH_4I. Many additives are often used to optimize the photovoltaic performance of DSSCs: for instance, 4-*tert*-butylpyridine (TBP)[38] was used for the first time as an additive in the electrolyte, resulting in a significant improvement of the open circuit potential of DSSC (see paragraph 1.3.2.3). Later, many nitrogen-containing heterocycles have been studied as additives, exhibiting similar effects to TBP. Another class of frequently used additives contains specific cations, such as lithium ions (Li^+) or guanidinium ions [$C(NH_2)_3^+$],[39] which should cause a shift of the conduction band edge of TiO_2 toward lower energies, resulting in an increase of the electron injection yield and electron lifetime.[40]

Though the I^-/I_3^- redox couple shows remarkable performance in DSSCs, there are several negative features limiting its further application: (i) iodine is extremely corrosive to many sealing materials, especially metals, causing difficult assembling

and sealing for large-area DSSC and poor long-term stability;[41] (ii) iodine has a relatively high vapor pressure, which makes it efficient device encapsulation challenging; (iii) the I_3^- ion absorbs part of the visible light, lowering the conversion efficiency of the devices.[42] Some halogen- or pseudohalogen-based alternatives, such as Br^-/Br_3^-,[43] $SCN^-/(SCN)_3^-$ and $SeCN^-/(SeCN)_3^-$,[44] have been tested, exhibiting very good values of efficiency, but their poor stability limited the development of DSSCs based on them. Otherwise, metallorganic $[Co]^{2+/3+}$ complexes have aroused great interest as iodine-free redox mediators because they are nonvolatile, noncorrosive, light-colored and have tunable potential through modification of the ligands.[45] Right now, Co-complex mediators are the most efficient redox couples for DSSCs, as demonstrated by the highest efficiency of more than 14% obtained for traditional devices.[26] Other metal complexes and clusters, such as Ni(III)/Ni(IV), Cu(I)/Cu(II), Mn(III)/Mn(IV) and ferrocene/ferricenium (Fc/Fc^+), have also been investigated.[46]

In the assembling of large area DSSCs liquid electrolytes have shown some drawbacks mainly due to the leakage and volatilization of solvent and the significant dissociation of the adsorbed dye, electrode and sealing materials, which causes loss of the cell efficiency in a long term period. For these reasons some alternatives have been investigated, such as (i) quasi-solid-state electrolytes, [47] which are macromolecular or supramolecular nano-aggregate systems, characterized by a remarkable ionic conductivity and both the cohesive property of solid and the diffusive property of liquid, and (ii) solid-state transport materials,[48] including ionic conductors, inorganic hole-transport salts and oxides and organic hole-transport polymers.

1.3.1.5. Counterelectrode

The most common counterelectrodes for DSSCs with iodide/triiodide electrolytes can be prepared by deposition of a thin catalytic layer of platinum onto a conductive substrate. Pt is able to catalyze the reduction of the redox couple and reduce the charge transfer resistances to less than 1 $\Omega\,cm^2$. Pt films can be deposited using a range of methods such as electrodeposition, spray pyrolysis, sputtering, and vapor deposition. Because of the high cost of platinum, the investigation of Pt-free counterelectrodes is very active and many materials, such as mixtures of graphite and carbon black,[49] carbon nanotubes,[50] conducting polymers[51] and cobalt sulfide[52] have been tested.

1.3.2. Photovoltaic parameters and DSSC characterization

The photovoltaic performances of DSSCs are mainly evaluated by some conventional parameters which allow the comparison between different cells. These parameters will be fully described in next paragraphs.[6,27]

1.3.2.1. Incident Photon-to-Current Conversion Efficiency (IPCE)

The IPCE parameter is defined as the ratio between the number of electrons flowing through the external circuit and the number of incident photons and is represented by equation (1).

$$IPCE\ (\%) = \frac{1240\ (eV\ nm)\ J_{ph}\ (mA\ cm^{-2})}{\lambda\ (nm)/I\ (mW\ cm^{-2})} \quad (1)$$

λ and I are the wavelength and the intensity of the monochromatic light which generates the short-circuit photocurrent density, J_{ph}. A plot of IPCE vs. excitation wavelength is named IPCE spectrum and is very useful for the evaluation of a new sensitizer for DSSCs.

IPCE can also be expressed as the product of four factors, as represented in equation (2):

$$IPCE\ (\lambda) = LHE\ (\lambda) \times \Phi_{inj}\ (\lambda) \times \Phi_{reg} \times \eta_{CC}\ (\lambda) \quad (2)$$

LHE (λ) is the light-harvesting efficiency for photons of wavelength λ, Φ_{inj} and Φ_{reg} are the quantum yields for electron injection and dye regeneration, respectively, and η_{CC} is the charge collection efficiency. IPCE is therefore correlated to the absorption properties of the dye, the amount of adsorbed dye on TiO_2 electrode and all electron transfer processes from the dye to the external circuit. The maximum IPCEs for DSSCs lie in the 80–85% range; they do not reach 100% experimentally because of reflection and absorption losses (10–15%) due to the conductive glass.

1.3.2.2. Photocurrent/voltage (J/V) curves

The photovoltaic performance of a DSSC can be easily evaluated by means of the measurement of the J/V curves (Figure 1.8) under standard AM 1.5 simulated sunlight (100 mW cm^{-2}). The key-parametres which are typically extracted by J/V curves are open-circuit voltage (V_{oc}), short-circuit photocurrent density (J_{sc}), fill factor (*ff*) and solar energy-to-electricity conversion yield (η).

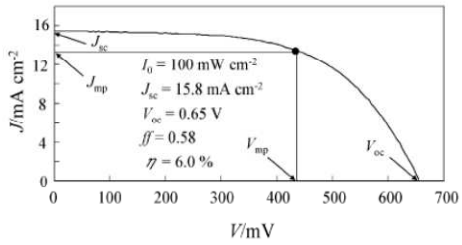

Figure 1.8. Typical J/V curve of a DSSC.[27]

1.3.2.3. Open-circuit voltage (V_{oc})

The V_{oc} parameter is the difference in electric potential between the two electrodes of a cell under illumination when the circuit is open. V_{oc} can be mathematically expressed by equation (3):

$$V_{oc} = E_F - E_{redox} \qquad \text{where } E_F = \frac{E_{cb}}{e} + \frac{k_B T}{e}\ln\left(\frac{n}{N_{cb}}\right) \qquad (3)$$

e is the elementary charge, k_B is the Boltzmann constant, *T* is the absolute temperature, E_{cb} is the energy level of the conduction band of TiO_2, *n* is the density of conduction band electrons in TiO_2, N_{cb} is the effective density of conduction band states and E_{redox} is the redox potential of the redox couple. E_F is the Fermi level at the equilibrium and its value is set by the conduction band energy (E_{cb}) of the TiO_2, but depends also on the electron density (*n*) in the conduction band of the semiconductor; *n* is intimately connected with the electron injection and recombination kinetics and, accordingly, with the dye properties. Therefore, the maximum V_{oc} value is the difference between the Fermi level (–0.5 to –0.4 V *vs*. NHE) at the equilibrium and the redox potential of the electrolyte: if the redox couple is I^-/I_3^- (E_{redox} = 0.4 V *vs*. NHE), V_{oc} is theoretically in the 0.8–0.9 V range, but electron recombination [reaction **(6)** and **(7)**, Figure 1.7] usually reduces this value.

V_{oc} can be slightly modified adding some additives to the electrolyte because E_{cb} is dependent on the molecular dipole at the TiO_2/dye interface: a dipole moment pointing away from the TiO_2 surface shifts the conduction band of TiO_2 to more negative values, leading to an increase in V_{oc}. This is the effect generated by adding 4-*tert*-butylpyridine (TBP) to the electrolyte mixture (see paragraph 1.3.1.4) since TBP adsorbed on the TiO_2 surface is supposed to induce a negative shift of the E_{cb} of TiO_2. Moreover, adsorbed TBP prevents a direct contact between I_3^- ions and the TiO_2 surface, reducing the possibility of electron recombination. The total resulting effect is an improved V_{oc} value.[38]

V_{oc} can be increased by replacing I^-/I_3^- with redox couples with a more positive E_{redox} such as Br^-/Br_3^- (1.1 V *vs*. NHE) or cobalt complexes [e.g. $Co^{II/III}$tris(bipyridyl): 0.56 V *vs*. NHE].

1.3.2.4. Short-circuit photocurrent density (J_{sc})

The J_{sc} value is the photocurrent per unit area (mA cm^{-2}) when a DSSC under irradiation is short-circuited, that is when electrical impedance and difference in electric potential are next to zero. J_{sc} is the maximum value of photocurrent density produced by an ideal cell under irradiation. This value is intimately connected with the interaction between dye and TiO_2 and depends on light-absorption capability of the dye, electron-injection efficiency from dye to the conduction band of TiO_2 and dye-regeneration efficiency. An increase in J_{sc} can be achieved through fine design of the structure of the dyes and consequent proper modification of their photo-electrochemical properties.

1.3.2.5. Fill factor (*ff*)

Fill factor is defined as the ratio between the maximum power output ($J_{mp}V_{mp}$) and the product of J_{sc} and V_{oc} (eq. 4).

$$ff = \frac{J_{mp}\,V_{mp}}{J_{sc}\,V_{oc}} \qquad (4)$$

ff is determined from the J/V curve and is an indication of how much of the area of the rectangle for $J_{sc}V_{oc}$ is filled by that described by $J_{mp}V_{mp}$ (Figure 1.8). Thus, maximum *ff* is equal to unity. In a real cell, power is dissipated through the resistance of the contacts and during charge transport (equivalent to a resistance in series, R_s), and through leakage currents, such as recombination and dark current (equivalent to a resistance in parallel, R_{sh}). When R_s is higher than zero and R_{sh} is not infinite, fill factor is in the 0–1 range and the photovoltaic performance of the cell is reduced. Careful fabrication of the device is important to minimize the charge transport resistance and minimize leakage currents.

1.3.2.6. Solar energy-to-electricity conversion efficiency (η)

The η value is defined as the ratio between the maximum output electrical power of a DSSC and the energy of incident sunlight (I_0, generally 100 mW cm^{-2}). Equation (5) collects all the photovoltaic parameters (V_{oc}, J_{sc}, *ff*) previously described.

$$\eta\ (\%) = \frac{J_{sc}\,(mA\ cm^{-2})\,V_{oc}\,(V)\,ff}{I_0\ (mW\ cm^{-2})} \qquad (5)$$

High η values are obtained by optimization of the J_{sc}, V_{oc}, and *ff* values of the cell. Every component inside the structure of a DSSC is important, but the molecular design of sensitizers is crucial to increase the η value dramatically. Therefore it is important to modify the structures of known dyes to optimize the photophysical and electrochemical properties of the dyes themselves and control their molecular orientation and arrangement on semiconductor surface.

In the next paragraphs, structures and properties of the most important classes of sensitizers will be described.

1.3.3. Sensitizers

Starting from 1991, when Grätzel and O'Regan published their first paper on DSSCs,[25] thousands of different sensitizers have been tested, but the synthesis of new dyes for DSSCs is nevertheless still a very important research field because of the crucial role they play within the working mechanism of DSSCs. A good sensitizer must own some essential properties, which can be described as follows:[6,27,53,54]

I. The absorption spectrum of the dye must cover the visible and near-infrared region of the solar spectrum as much as possible, and the dyes must have high molar absorption coefficients to achieve a high light-harvesting efficiency.
II. The dye must have at least one anchoring group to form a strong linkage to the TiO_2 electrode, decrease the interface resistance and secure stable bonding for a long time.
III. Energy levels of the frontier molecular orbitals of the dye must match with those of the semiconductor and the electrolyte (Figure 1.7). The energy level of the lowest unoccupied molecular orbital (LUMO) must be higher (more negative) than the conduction band edge of the TiO_2 electrode to achieve good electron injection from the excited dye. On the other hand, the energy level of the highest occupied molecular orbital (HOMO) must be lower (more positive) than the redox potential of redox couple to achieve efficient regeneration of the oxidized dye.
IV. Aggregation of the dye on the TiO_2 surface should be avoided because it reduces the electron-injection efficiency owing to intermolecular energy transfer. A precise optimization of the structure of the dye and addition of additives can minimize these aggregation phenomena.

V. High thermal, photo- and electrochemical stability of the dye is requested to achieve durable DSSCs.

Three different classes of dyes for DSSC have been studied so far and their main properties will be described in next paragraphs.

1.3.3.1. Transition metal complexes

The first transition metal complexes which have been studied as sensitizers for DSSCs are ruthenium-based complexes. They have a wide absorption spectrum of visible light, owing to the metal-to-ligand charge transfer (MLCT) process, energy levels which match well with those of TiO_2 and the I^-/I_3^- redox couple, a relatively long excited-state lifetime and a good chemical and electrochemical stability. Ligands, typically bipyridines or terpyridines containing carboxylic acids as anchoring groups, can be tuned by different substituents to change the photophysical and electrochemical properties of the complexes and thus improve the photovoltaic performances of the cells. Indeed, after their first report in 1991,[25] Grätzel and co-workers published a series of Ru-complexes which exhibited outstanding properties (Figure 1.9). **N3** dye,[55] bearing two carboxylated bipyridines and two thiocyanate groups as ligands, has been the first one which showed a broad visible light absorption spectrum, good anchoring to the TiO_2 electrode, an IPCE spectrum extending to 800 nm and an efficiency (η) of 10%.

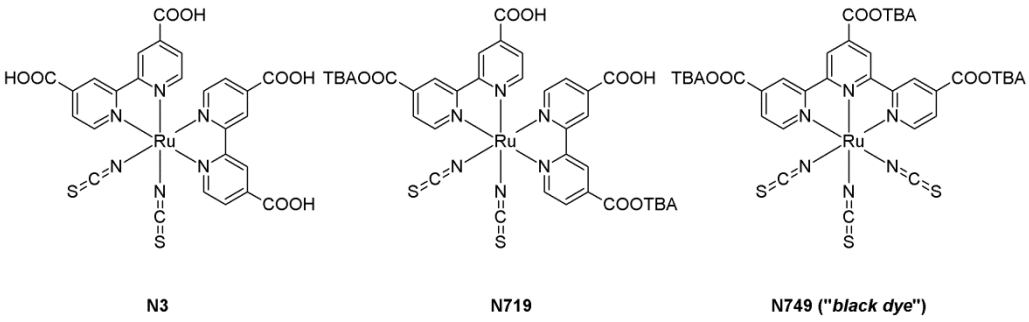

Figure 1.9. Structures of first Ru-based sensitizers.

Starting from the structure of **N3**, analogous results were obtained by deprotonation of the most acidic carboxylic residues (**N719**)[56] or replacement of the ligands (***black dye***)[57]: **N719** showed an higher power conversion efficiency (11%) than **N3** thanks to the shift of reduction and oxidation potentials to more negative values, while ***black dye*** extended the IPCE spectrum into the near-IR region up to 920 nm, achieving

10.4% efficiency. **N3**, **N719** and ***black dye*** are still considered as reference dyes for DSSCs.

In order to increase the molar extinction coefficient, suppress dye aggregation on the semiconductor and optimize the redox potential of the sensitizer, many modifications on the structures of ligands have been carried out (Figure 1.10), such as introduction of alkyl chains,[58] vinyl groups,[59] donor groups,[60] thiophenes,[61] EDOTs,[62] carbazoles[63] and other heterocycles or combinations of these elements,[64] achieving power efficiencies similar or higher than **N3**.

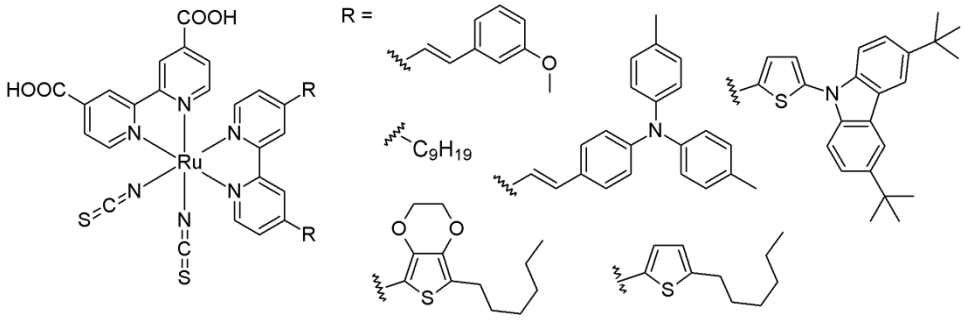

Figure 1.10. Some modifications of N3 skeleton.

Substitution of isothiocyanate ligands has been investigated too, because they seem to be the weakest part of Ru-complex from a chemical stability point of view: for example, cyclometalated ruthenium complexes have been tested achieving a remarkable efficiency of 10.1%.[65]

Despite the above-mentioned high power conversion efficiencies, Ru-based complexes have some drawbacks, such as low abundance, high cost and toxicity of the metal center. Some alternatives to ruthenium have been investigated: osmium (II) polypyridines have a broader MLCT absorption band than Ru-containing analogues and extended IPCE spectra up to 1100 nm, but lower photocurrent efficiency. [66] Square-planar platinum (II) complexes containing thiols and polypyridines or phenanthrolines as ligands have absorption spectra which cover the entire visible spectrum of solar light, but cell efficiencies were never superior to 3%.[67] Cyclometalated iridium (III) complexes allow faster electron transfer between oxidized dye and redox couple compared to Ru-complexes, but a low V_{oc} limit the overall power conversion efficiency to 2.9%.[68] Similar results have been obtained with copper (I)[69] complexes, while rhenium (I),[70] iron (II)[71] and nickel (II)[72] sensitizers recorded even lower efficiencies.

1.3.3.2. Porphyrins and phthalocyanines

Ruthenium complexes exhibit high power conversion efficiencies, but have small molar extinction coefficients and limited absorption in the near-infrared region of the solar spectrum. Porphyrins, which play an important role in chlorophyll photosynthesis, show very high absorption bands in the visible region of the solar spectrum and efficient electron injection in the conduction band of TiO_2,[73] and so could also be potential sensitizers for DSSCs.[6,74] The first application of a porphyrin-based dye for DSSC was reported in 1993 by Grätzel *et al.*,[75] who used copper as metal center (**1**, Figure 1.11) obtaining IPCE values of 70-80% in the visible region and a power conversion efficiency of 2.6%.

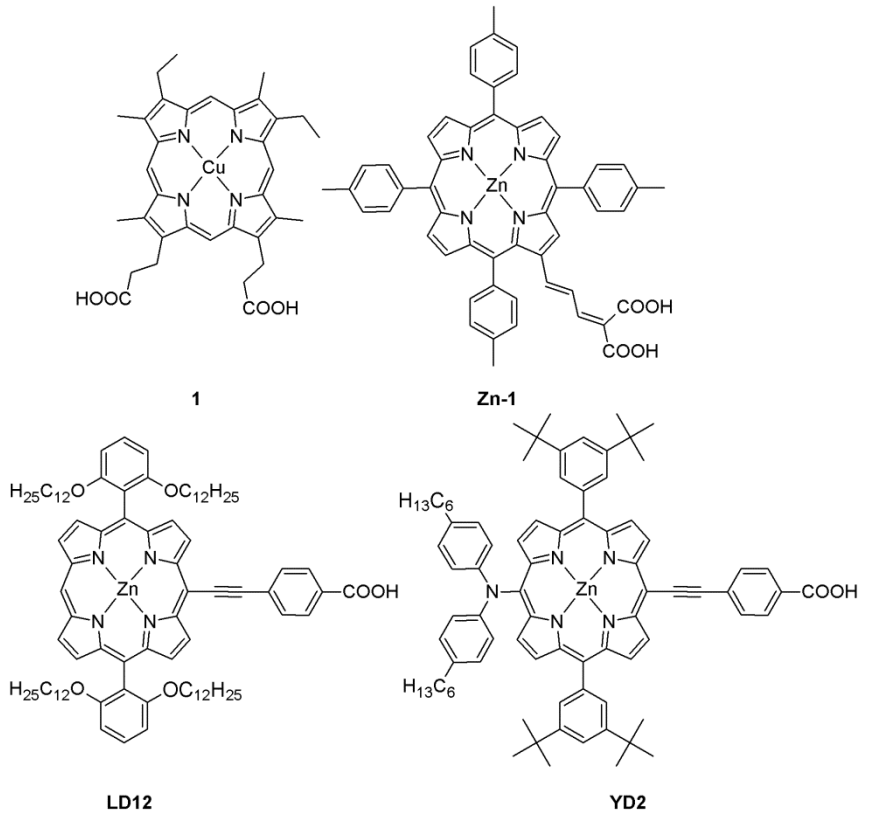

Figure 1.11. Some examples of porphyrins sensitizers.

Substitution of copper with zinc (**Zn-1**, Figure 1.11, η = 7.0%)[76] allowed a great improvement of the efficiency, while introduction of *ortho*-alkoxyphenyl groups (**LD12**, Figure 1.11, η = 7.43%)[77] on the porphyrin core minimized the aggregation of the dye on TiO_2 and retarded the charge recombination by a blocking effect.

Push-pull type porphyrins have been widely investigated owing to their broad and intense absorption spectral features as well as efficient electron injection due to intramolecular charge transfer (ICT) character.[74] Many porphyrins containing different donor and acceptor groups have been synthesized: for example, **YD2** (Figure 1.11, η ≈ 11%), bearing a strong electron-donating diarylamino group at *meso* position, has been the first porphyrin sensitizer with an η-value of more than 10%,[78] while 8-hydroxyquinoline,[79] salicylic acid[80] and tropolone[81] have been tested as anchoring groups instead of benzoic acid in order to improve cell stability and electron injection to the TiO_2.

Grätzel *et al.*[82] have recently recorded the record power conversion efficiency of 13% with a porphyrin dye employing **SM315** (Figure 1.12) and a cobalt-based redox shuttle: a fine optimization of the structure of the dye, with the introduction of bulky chains in *ortho*-position and a benzodithiazole unit as a more strongly electron-withdrawing group, ensured a very broad absorption of visible and near-infrared solar light and minimized the aggregation of the dye on the TiO_2 electrode.

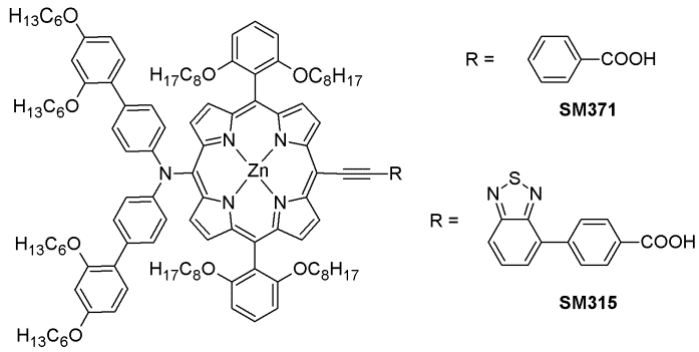

Figure 1.12. Structure of SM315 and SM371 porphyrins dyes.

Phthalocyanines are synthetic analogues of porphyrins and, like them, possess an extensively conjugated skeleton resulting in intense absorption of visible and near-infrared light. For these reasons phthalocyanines have also been studied as sensitizers for DSSCs.[6,83] The first examples of DSSCs containing phthalocyanines gave poor results, with overall efficiencies below 1%,[84] probably because of a substantial aggregation of the sensitizer on the TiO_2 electrode.

To overcome this drawback, chemical modifications of the phthalocyanine core have been carried out, such as introduction of bulky aliphatic groups: **TT1**-based cells[85] (Figure 1.13) recorded a promising efficiency of 3.5%, but only in the presence of

chenodeoxycholic acid as a coadsorbent to prevent aggregation.[86] Bulkier groups are necessary to suppress completely the π-stacking and minimize recombination by blocking the interactions between the electrolyte and the aromatic surface of the phthalocyanines. This purpose has been accomplished by introducing 2,6-disubstituted phenoxy groups on the phthalocyanines skeleton: **PcS18**[87] and **TT40**[88,89] (Figure 1.13) did not need any coadsorbent to prevent aggregation and recorded extremely high efficiencies (5.9% and 6.49%, respectively) for phthalocyanines.

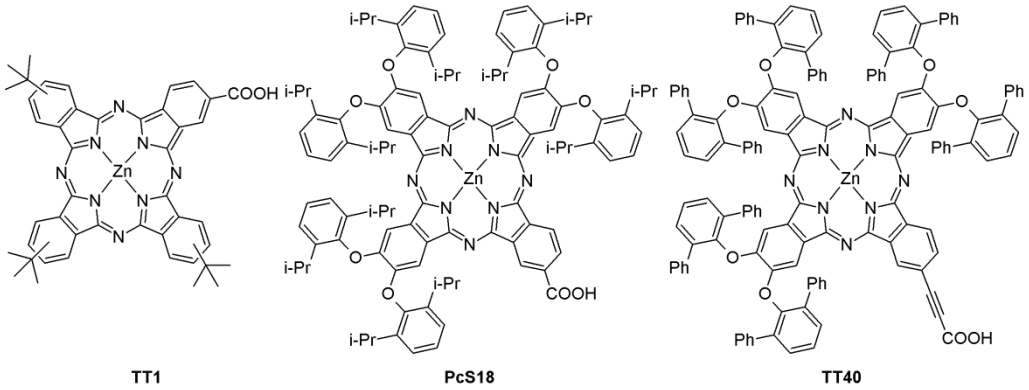

Figure 1.13. Some examples of phthalocyanines sensitizers.

Ru(II), Ti(IV) and Si(IV) have been tested as alternative metal center for phthalocyanines in order to take advantage of their ability to coordinate axial substituents which could inhibit molecular aggregation and recombination. Phthalocyanines containing Ru(II)[90] and Ti(IV)[91] yielded scarce results, while the employment of Si(IV)[92] as metal center was more productive, giving cells with very high short-circuit current density (≈ 19 mA cm^{-2}) and an overall efficiency of 4.5%.

1.3.3.3. *Metal-free* organic dyes

The last class of sensitizers includes organic dyes which do not contain any metal cation. These compounds have attracted much interest as potential alternatives to ruthenium-based sensitizers because they have much lower production costs and environmental impact than Ru-complexes, their molar extinction coefficients are usually higher and their photophysical and electrochemical properties can be easily tuned by fine optimization of their structure. The most common design for an organic dye presents a D-π-A structure (Figure 1.14), where donor (D) and acceptor (A) groups are connected by a π-conjugated spacer.[6,53] The acceptor group has to anchor the dye to the semiconductor too.

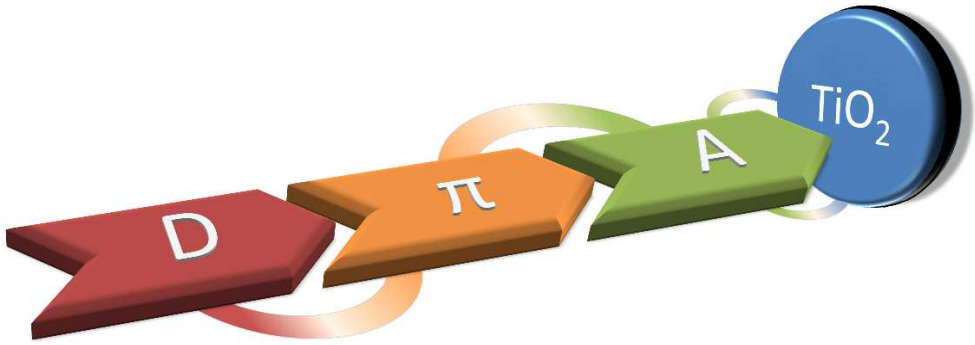

Figure 1.14. Drawing of a D-π-A structure.

Thanks to the *push-pull* structure, the HOMO is mostly delocalized on the donor group, while the LUMO is located on the acceptor moiety: when the dye absorbs light, intramolecular charge transfer (ICT) occurs, through the π-spacer, from the donor to the acceptor group, which is directly bound to the semiconductor layer. This ICT process promotes a fast electron injection from the excited dye to the conduction band of the TiO_2 and restricts recombination between the injected electron and the oxidized dye. HOMO/LUMO energy levels, which must be matched to the conduction band edge of the TiO_2 electrode and to the redox potential of the electrolyte (see Paragraph 1.3.3.III), can be tuned by the expansion of π-spacer and the introduction of stronger, or weaker, electron-donating and -accepting substituents. In the D-π-A concept, introduction of a stronger electron-donating group will shift the HOMO level to higher energy, while a stronger electron-withdrawing group will shift the LUMO to lower energy: in this way, the HOMO-LUMO band gap can be easily decreased, resulting in a red-shift of the absorption peaks.

The principal drawbacks of organic dyes are related to (i) the aggregation of the dyes on the TiO_2 surface and (ii) the poor near-infrared light harvesting properties of most dyes. In the first case, π-stacking between dye molecules reduces the electron-injection yield from the dye to the conduction band of TiO_2 owing to intermolecular energy transfer, although the introduction of sterically hindered substituents into the planar structure of the dye and/or the use of chenodeoxycholic acid (CDCA) as a co-adsorbent can minimize this effect.[93] In the latter case, the low light-harvesting properties of a dye could be improved by extending π-conjugation or introducing additional acceptor units inside the π-bridge (D-A-π-A structure).[94]

The main features of every portion of the dye are the following:[6,53,54,95,96]

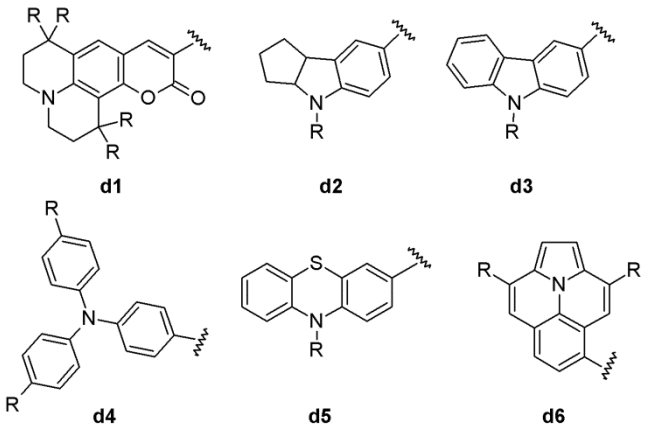

Figure 1.15. Some examples of structures of donor groups.

I. **Donor groups** (Figure 1.15): the choice of an appropriate donor group affects the HOMO energy level of the dye, the absorption properties of the molecule, the dye aggregation and the charge recombination rate. Triphenylamine (**d4**) has been the most widely used donor group because of its strong electron-donating ability and hole-transport properties: its first application as donor group for a DSSC dye goes back to 2004.[97] In the last years a large number of triarylamine-based dyes has been synthesized which differ for the introduction of different substituents in the 4,4'-positions, such as alkyl chains,[98] alkyloxy,[99] alkylthioxy[100] and phenyldialkyloxy[101] groups or other aromatic and heteroaromatic rings (so-called *starburst donors*),[102] or for the substitution of one or more benzene rings with other polycycles, such as naphthalene,[103] fluorene[104] and truxene.[105] Best triarylamine-based dyes as donor groups exhibited efficiencies up to 10.3%.[101] Replacing a triarylamine unit with an indoline (**d2**) shifts the absorption spectrum of the dye to higher wavelengths owing to its more powerful electron-donating capability.[106] Moreover, indoline dyes are characterized by high molar extinction coefficients and good stability. Recently, an impressive power conversion efficiency of 10.65% has been obtained with a dye containing a bulky-indoline moiety and a cobalt-based redox shuttle.[107] Carbazoles (**d3**), which are structurally similar to indolines, have also been employed as donor groups in many DSSC-dyes.[108] Recently a DSSC containing a carbazole-based sensitizer yielded the highest efficiency of 12.5%[109] (14.3%[26,110] by co-sensitizing with a second dye) among the cells with *metal-free* dyes by using a cobalt-based redox shuttle. Other donor groups which have been studied in last years are coumarin (**d1**),[111] phenothiazine (**d5**)[112] and ullazine (**d6**).[113]

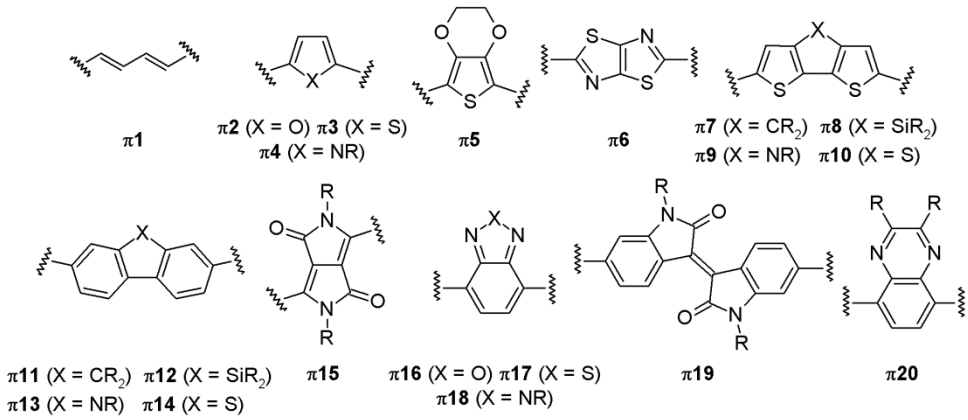

Figure 1.16. Some examples of structures of π-spacers.

II. **π-spacers** (Figure 1.16): the first role of the conjugated bridge is the transfer of electron density from the donor to the acceptor group, facilitating charge separation upon excitation. However, fine tuning of the π-bridge allows also to adjust the HOMO/LUMO energy levels, to extend light absorption to higher wavelengths, to raise up molar extinction coefficients and to minimize dye aggregation and recombination rate. Both electronrich and electronpoor units have been employed in the π-bridge for all these purposes. Initially, dyes just employed simple double or triple bonds and small aromatic or heteroaromatic rings or combination of both of them (**π1-4**)[114] as conjugated bridges, but the light-harvesting properties of these dyes were not sufficient to achieve high power conversion efficiencies, and so more complex structures have been designed. The substitution of a simple thiophene (**π3**) with an ethylenedioxythiophene (EDOT; **π5**) resulted in an higher efficiency of the cell (5.2% vs. 7.3%) and a broader absorption spectrum.[115] Polycyclic heteroaromatic structures such as **π7-9** and **π11-13** have found many applications as π-spacers thanks to their conjugated planar structures, which enhance the light absorption properties of the dye, and the presence of long alkyl chains which inhibit the recombination and the aggregation on the TiO_2.[116] Another powerful tool to increase dye performance is the incorporation of additional electron-withdrawing groups in the bridging framework, getting a D-A-π-A type structure.[94] The additional unit is expected to act as electron trap to separate charge and to facilitate migration to the final acceptor. Moreover, this incorporation has often provided a better long term stability of the dye and a downshift of the LUMO energy level, which means a more intense light

absorption in the near-IR region of the spectrum. Some examples of additional acceptor groups are benzannulated heterocycles, such as benzooxadiazole (**π16**), [117] benzothiadiazole (**π17**), [118] benzotriazole (**π18**) [119] and quinoxaline (**π20**),[120] diketopyrrolepyrrole (**π15**)[121] and isoindigo (**π19**).[122]

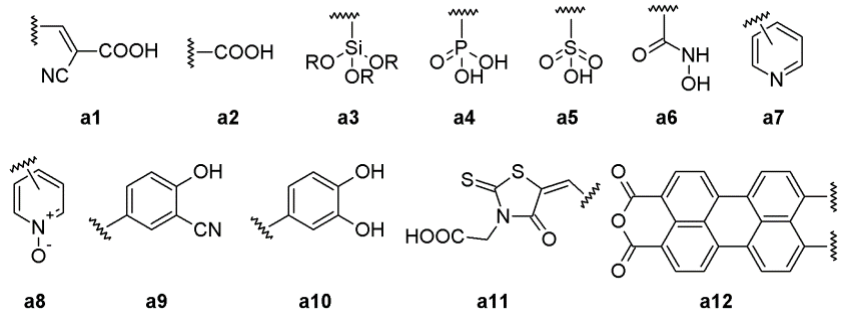

Figure 1.17. Some examples of structures of acceptor/anchoring groups.

III. **Acceptor/anchoring groups** (Figure 1.17): these moieties must ensure (i) the long term stability of the cell by a strong binding of the dye on the semiconductor surface and (ii) a good electron injection from the chromophore to the TiO_2 layer. The traditional anchors for DSSC dyes are cyanoacrylic (**a1**) and carboxylic acids (**a2**), but **a1**, which conjugates the electron-withdrawing properties of the cyano group with the binding properties of the carboxylic moiety, is by far the most used one.[6,123] Cyanoacrylic acids ensure good electron injection and strong anchoring to the semiconductor by forming an ester linkage with TiO_2, so this moiety is always used as reference when a new anchoring group for DSSC dye is tested. Nevertheless, the long term stability of the cells can be compromised by cleavage of the cyanoacrylic moiety from the semiconductor in the presence of water and bases. For this reason, many potential alternative anchoring groups have been investigated in the last years to ensure better long term stability as well as efficient electron injection. Alkoxysilyl-anchors (**a3**),[109,110] phosphoric acids (**a4**),[124] sulfonic acids (**a5**)[125] and hydroxamic acids (**a6**)[126] have been considered because of their structural similarity to carboxylic acids. Even if the binding between these anchors and TiO_2 is more stable and resistant to water than the corresponding carboxylates, only dyes containing **a3** and **a6**[126b] moieties recorded similar or even better photovoltaic performances than **a1**. Remarkably, test cells containing the alkoxysilyl dye **ADEKA-1** (Figure 1.18) have recently recorded the highest efficiency of 12.5% among *metal-free* sensitizers by employing a large number of

additives in the electrolyte solution with a cobalt-based redox shuttle and treating the TiO_2 electrodes with $TiCl_4$, $Al(O^iPr)_3$ and $Mg(OEt)_2$ to prevent recombination reactions.[109] Higher efficiencies up to 14.3% were obtained cosensitizing ADEKA-1 with a carboxy-anchor dye.[26]

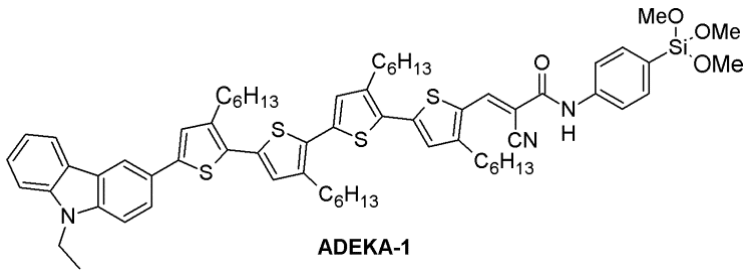

ADEKA-1

Figure 1.18. Structure of dye ADEKA-1.

A different type of anchor to TiO_2 is provided by pyridine (**a7**) and its derivatives or analogues: unlike carboxylic acids, which have interactions with Brønsted basic sites of TiO_2, pyridine can coordinate the Lewis acidic sites of the semiconductor, leading to an efficient electron injection and a bathochromic shift of light absorption when the dye is adsorbed onto TiO_2.[127] To obtain a stronger linkage with TiO_2, pyridines substituted with cyano[128] groups and carboxylic acids,[129] N-oxides (**a8**),[130] pyrazines[131] and pyridinium ions[132] have been investigated: even if the long term stability of dyes with these anchors is very good, photovoltaic performances are often lower than the corresponding carboxylates. A completely different way to inject electrons into TiO_2 can be accomplished by using catechols (**a10**). The 1,2-dihydroxyl moiety of catechol ensures a very strong bidentate linkage of the dye to the semiconductor which provides a direct electron injection from the ground state of the dye to the CB of TiO_2 upon photoexcitation.[27,123] Dyes containing catechol as anchoring group belong to *type-II* sensitizers and have been investigated for their extremely strong linkage with the semiconductor, which provides an excellent long term stability of the cell, and for the bathochromic shift of the light absorption spectrum upon dye sensitization of TiO_2. Unfortunately, photovoltaic performances of catechol-based dyes have always been poor owing to the strong recombination of injected electrons with the oxidized dye and the electrolyte.[133]

Application of organic synthesis has theoretically enabled the introduction of any possible functional chemical group inside the structure of a sensitizer. Although a huge research work has been already done in the last years, the search for new structures is still very active, not only to surpass the current record efficiency,[26] but also to improve many other DSSC properties, like stability, transparency and color, which are required for future commercial applications.

1.4. References

[1] *Global Energy Statistics Yearbook 2015*, yearbook.enerdata.net

[2] *BP Energy Outlook 2035*, bp.com/energyoutlook

[3]http://commons.wikimedia.org/wiki/File:Total_World_Energy_Consumption_by_Source_2013.png

[4] http://www.iea.org/newsroomandevents/news/2015/august/renewable-electricity-generation-climbs-to-second-place-after-coal.html

[5] Schiermeier Q., Tollefson J., Scully T., Witze A. *Nature*, **2008**, *454*, 816

[6] Hagfeldt A., Boschloo G., Sun L., Kloo L. Pettersson H. *Chem. Rev.*, **2010**, *110*, 6595

[7] http://www.greenpeace.org/international/Global/international/publications/climate/2011/Final%20SolarGeneration%20VI%20full%20report%20lr.pdf

[8] Parisi M. L., Maranghi S., Basosi R. *Renewable Sustainable Energy Rev.*, **2014**, *39*, 124

[9] Energy Information Administration, Annual Energy Outlook 2011. DOE/EIA-0383(2010)

[10] "April 25, 1954: Bell Labs Demonstrates the First Practical Silicon Solar Cell"**,** *APS News*, **2009**, *18*, 4

[11] Green M. A., Emery K., Hishikawa Y., Warta W., Dunlop E. D. *Prog. Photovolt. Res. Appl.*, **2012**, *20*, 12

[12] Wenham S. R., Green M. A. *Prog. Photovolt. Res. Appl.*, **1996**, *4*, 3

[13] Strong S. "Building Integrated Photovoltaics (BIPV)", *wbdg.org*. Whole Building Design Guide, **2010**

[14] Wronski C. R. *Conference Record of the 28 th IEEE Photovoltaic Specialists Conference, Anchorage, AK*, IEEE: New York, **2000**, p 1-6

[15] a) Britt J., Ferekides C. *Applied Physics Letters*, **1993**, *62*, 2851. b) Ullal H. S. *Proc. 28 th IEEE PVSC*, **2000**, 418

[16] Green M. A. *Third Generation Photovoltaics: Advanced Solar Energy Conversion*; Springer-Verlag: Berlin, Heidelberg, **2003**

[17] a) Siebentritt S., Schorr S. *Prog. Photovolt.: Res. Appl.*, **2012**, *20*, 512. b) Haass S. G., Diethelm M., Werner M., Bissig B., Romanyuk Y. E., Tiwari A. N. *Adv. Energy Mater.*, **2015**, *5* , 1500712.

[18] Yablonovitch E., Miller O. D., Kurtz S. R. *2012 38th IEEE Photovoltaic Specialists Conference*, 001556. ISBN 978-1-4673-0066-7

[19] Green M. A. *Solar Energy*, **2003**, *74*, 181

[20] Shockley W., Queisser H. J. *J. Appl. Phys.*, **1961**, *32*, 510

[21] https://www.ise.fraunhofer.de/en/press-and-media/press-releases/press-releases-2014/new-world-record-for-solar-cell-efficiency-at-46-percent

[22] http://www.nrel.gov/ncpv/images/efficiency_chart.jpg

[23] a) Kim D. W., Shin S. S., Lee S., Cho I. S., Kim D. H., Lee C. W., Jung H. S., Hong K. S. *ChemSusChem*, **2013**, *6*, 449. b) Park N.-G. *Mater. Today*, **2015**, *18*, 65

[24] Yang W. S., Noh J. H., Jeon N. J., Kim Y. C., Ryu S., Seo J., Seok S. I. *Science*, **2015**, *348*, 1234

[25] O'Regan B., Grätzel M. *Nature*, **1991**, *353*,737

[26] Kakiage K., Aoyama Y., Yano T., Oya K., Fujisawa J.-I., Hanaya M. *Chem Commun.*, **2015**, DOI:10.1039/c5cc06759f

[27] Ooyama Y., Harima Y. *ChemPhysChem*, **2012**, *13*, 4032

[28] Wu J., Lian Z., Lin J., Huang M., Huang Y., Fan L., Luo G. *Chem. Rev.*, **2015**, *115*, 2136

[29] a) Lee K. S., Lee H. K., Wang D. H., Park N.-G., Lee J. Y., Park O O., Park J. H. *Chem. Commun.*, **2010**, *46*, 4505. b) Yoo K., Kim J.-Y., Lee J. A., Kim J. S., Lee D.-K., Kim K., Kim J. Y., Kim B. S., Kim H., Kim W. M., Kim J. H., Ko M. J. *ACS Nano*, **2015**, *9*, 3760

[30] Veerappan G., Bojan K., Rhee S.-W. *ACS Appl. Mater. Interfaces*, **2011**, *3*, 857

[31] Ito S., Liska P., Comte P., Charvet R. L., Pechy P., Bach U., Schmidt-Mende L., Zakeeruddin S. M., Kay A., Nazeeruddin M. K., Grätzel M. *Chem. Commun.*, **2005**, 4351

[32] Zhang Z. P., Ito S., O'Regan B., Kuang D. B., Zakeeruddin S. M., Liska P., Charvet R., Comte P., Nazeeruddin M. K., Pechy P., Humphry-Baker R., Koyanagi T., Mizuno T., Grätzel M. *Z. Phys. Chem.*, **2007**, *221*, 319

[33] Sommeling P. M., O'Regan B. C., Haswell R. R., Smit H. J. P., Bakker N. J., Smits J. J. T., Kroon J. M., van Roosmalen J. A. M. *J. Phys. Chem. B*, **2006**, *110*, 19191

[34] Saito M., Fujihara, S. *Energy Environ. Sci.*, **2008**, *1*, 280

[35] Onwona-Agyeman B., Kaneko S., Kumara A., Okuya M., Murakami K., Konno A., Tennakone K. *Jpn. J. Appl. Phys. Part 2*, **2005**, *44*, L731

[36] Guo P., Aegerter M. A. *Thin Solid Films*, **1999**, *351*, 290

[37] Law C., Pathirana S., Li X., Anderson A., Barnes P., Listorti A., Ghaddar T., O'Regan B. *Adv. Mater.*, **2010**, *22*, 4505

[38] Nazeeruddin K., Kay A., Rodicio I., Humphry-Baker R., Mueller E., Liska P., Vlachopoulos N., Grätzel M. *J. Am. Chem. Soc.*, **1993**, *115*, 6382

[39] Liu Y., Hagfeldt A., Xiao X., Lindquist S. *Sol. Energy Mater. Sol. Cells*, **1998**, *55*, 267

[40] Zhang C., Huang Y., Huo Z., Chen S., Dai S. *J. Phys. Chem. C*, **2009**, *113*, 21779

[41] Toivola M., Ahlskog F., Lund P. *Sol. Energy Mater. Sol. Cells*, **2006**, *90*, 2881

[42] Wang M., Grätzel C., Zakeeruddin S. M., Grätzel M. *Energy Environ. Sci.*, **2012**, *5*, 9394

[43] Boschloo G., Hagfeldt A. *Acc. Chem. Res.*, **2009**, *42*, 1819

[44] a) Wang P., Zakeeruddin S., Moser J., Baker R., Grätzel M. *J. Am. Chem. Soc.*, **2004**, *126*, 7164. b) Oskam G., Bergeron B., Meyer G., Searson P. *J. Phys. Chem. B*, **2001**, *105*, 6867. c) Bergeron B, Marton A., Oskam G., Meyer G. *J. Phys. Chem. B*, **2004**, *109*, 937

[45] a) Nusbaumer H., Moser J., Zakeeruddin S., Nazeeruddin M., Grätzel M. *J. Phys. Chem. B*, **2001**, *105*, 10461. b) Nelson J., Amick T., Elliott C. *J. Phys. Chem. C*, **2008**, *112*, 18255. c) Hamann T., Brunschwig B., Lewis N. *J. Phys. Chem. B*, **2006**, *110*, 25514. d) Yella A., Lee H., Tsao H., Yi C., Chandiran A., Nazeeruddin M., Diau E., Yeh C., Zakeeruddin S., Grätzel M. *Science*, **2011**, *334*, 629

[46] a) Bai Y., Yu Q., Cai N., Wang Y., Zhang M., Wang P. *Chem. Commun.*, **2011**, *47*, 4376. b) Gregg B., Pichot F., Ferrere S., Fields C. *J. Phys. Chem. B*, **2001**, *105*, 1422. c) Hamann T., Farha O., Hupp J. *J. Phys. Chem. C*, **2008**, *112*, 19756. d) Feldt S., Cappel U., Johansson E., Boschloo G., Hagfeldt A. *J. Phys. Chem. C*, **2010**, *114*, 10551. e) Daeneke T., Kwon T., Holmes A., Duffy N., Bach U., Spiccia L. *Nat. Chem.*, **2011**, *3*, 211. f) Rangeeka Perera I., Gupta A., Xiang W., Daeneke T., Bach U., Evans R. A., Ohlin C. A., Spiccia L. *Phys. Chem. Chem. Phys.*, **2014**, *16*, 12021

[47] a) Wu J., Hao S., Lan Z., Lin J., Huang M., Huang Y., Fang L., Yin S., Sato T. *Adv. Funct. Mater.*, **2007**, *17*, 2645. b) Wu J., Lan Z., Lin J., Huang M., Hao S., Sato T., Yin S. *Adv. Mater.*, **2007**, *19*, 4006. c) Di Noto V., Lavina S., Giffin G. A., Negro E., Scrosati B. *Electrochim. Acta*, **2011**, *57*, 4. d) Gorlov M., Kloo L. *Dalton Trans.*, **2008**, 2655

[48] a) Li D., Qin D., Deng M., Luo Y., Meng Q. *Energy Environ. Sci.*, **2009**, *2*, 283. b) Li B., Wang L., Kang B., Wang P., Qiu Y. *Sol. Energy Mater. Sol. Cells*, **2006**, *90*, 549. c) Zhang W., Cheng Y., Yin X., Liu B. *Macromol. Chem. Phys.*, **2011**, *212*, 15

[49] Kay A., Grätzel M. *Sol. Energy Mater. Sol. Cells*, **1996**, *44*, 99

[50] Suzuki K., Yamaguchi M., Kumagai M., Yanagida S. *Chem. Lett.*, **2003**, *32*, 28

[51] Yeh M.-H., Lin L.-Y., Lee C.-P., Wei H.-Y., Chen C.-Y., Wu C.-G., Vittal R., Ho K.-C. *J. Mater. Chem.*, **2011**, *21*, 19021

[52] Wang M., Anghel A. M., Marsan B., Cevey Ha N.-L., Pootrakulchote N., Zakeeruddin S. M., Grätzel M. *J. Am. Chem. Soc.*, **2009**, *131*, 15976

[53] Ooyama Y., Harima Y. *Eur. J. Org. Chem.*, **2009**, 2903

[54] Basheer B., Mathew D., George B. K., Reghunadhan Nair C. P. *Solar Energy*, **2014**, *108*, 479

[55] Nazeeruddin M. K., Kay A., Rodicio I., Humphry-Baker R., Mueller E., Liska P., Vlachopoulos N., Grätzel M., *J. Am. Chem. Soc.*, **1993**, *115*, 6382

[56] Nazeeruddin M. K., Zakeeruddin S. M., Humphry-Baker R., Jirousek M., Liska P., Vlachopoulos N., Shklover V., Fischer C. H., Grätzel M. *Inorg. Chem.*, **1999**, *38*, 6298

[57] Nazeeruddin M. K., Pechy P., Grätzel M. *Chem. Commun.*, **1997**, 1705

[58] Wang P., Zakeeruddin S. M., Exnar I., Grätzel M. *Chem. Commun.*, **2002**, 2972

[59] a) Wang P., Zakeeruddin S. M., Moser J. E., Humphry-Baker R., Comte P., Aranyos V., Hagfeldt A., Nazeeruddin M. K., Grätzel M. *Adv. Mater.*, **2004**, *16*, 1806. b) Kuang D., Klein C., Ito S., Moser J.-E., Humphry-Baker R., Evans N., Duriaux F., Grätzel C., Zakeeruddin S. M., Grätzel M. *Adv. Mater.*, **2007**, *19*, 1133

[60] Yum J. H., Jung I., Baik C., Ko J., Nazeeruddin M. K., Grätzel M. *Energy Environ. Sci.*, **2009**, *2*, 100

[61] Chia-Yuan Chen S.-J. W., Chun-Guey W., Jian-Ging C., Kuo-Chuan H. *Angew. Chem. Int. Ed.*, **2006**, *45*, 5822

[62] Chen C.-Y., Wu S.-J., Li J.-Y., Wu C.-G., Chen J.-G., Ho K.-C. *Adv. Mater.* **2007**, *19*, 3888

[63] Chen C.-Y., Chen J.-G., Wu S.-J., Li J.-Y., Wu C.-G., Ho K.-C. *Angew. Chem. Int. Ed.*, **2008**, *47*, 7342

[64] a) Gao F., Wang Y., Shi D., Zhang J., Wang M., Jing X., Humphry-Baker R., Wang P., Zakeeruddin S. M., Grätzel M. *J. Am. Chem. Soc.*, **2008**, *130*, 10720. b) Cao Y. M., Bai Y., Yu Q. J., Cheng Y. M., Liu S., Shi D., Gao F. F., Wang P. *J. Phys. Chem. C*, **2009**, *113*, 6290. c) Chen C. Y., Wang M., Li J. Y., Pootrakulchote N., Alibabaei L., Ngoc-Le C. H., Decoppet J. D., Tsai J. H., Grätzel C., Wu C. G., Zakeeruddin S. M., Grätzel M. *ACS Nano*, **2009**, *3*, 3103. d) Shi-Jhang W., Chia-Yuan C., Jian-Ging C., Jheng-Ying L., Yung-Liang T., Kuo-Chuan H., Chun-Guey W. *Dyes Pigments*, **2010**, *84*, 95. e) Wang S. W., Chou C. C., Hu F. C., Wu K. L., Chi Y., Clifford J. N., Palomares E., Liu S. H., Chou P. T., Wei T. C., Hsiao T. Y., *J. Mater. Chem. A*, **2014**, *2*, 17618

[65] Bessho T., Yoneda E., Yum J.-H., Guglielmi M., Tavernelli I., Imai H., Rothlisberger U., Nazeeruddin M. K., Grätzel M. *J. Am. Chem. Soc.*, **2009**, *131*, 5930

[66] a) Sauve G., Cass M. E., Coia G., Doig S. J., Lauermann I., Pomykal K. E., Lewis N. S. *J. Phys. Chem. B*, **2000**, *104*, 6821. b) Sauve G., Cass M. E., Doig S. J., Lauermann I., Pomykal K., Lewis N. S. *J. Phys. Chem. B*, **2000**, *104*, 3488. c) Altobello S., Argazzi R., Caramori S., Contado C., Da Fre S., Rubino P., Chone C., Larramona G., Bignozzi C. A. *J. Am. Chem. Soc.*, **2005**, *127*, 15342

[67] a) Islam A., Sugihara H., Hara K., Singh L. P., Katoh R., Yanagida M., Takahashi Y., Murata S., Arakawa H., Fujihashi G. *Inorg. Chem.*, **2001**, *40*, 5371. b) Geary E. A. M., Yellowlees L. J., Jack L. A., Oswald I. D. H., Parsons S., Hirata N., Durrant J. R., Robertson N. *Inorg. Chem.*, **2005**, *44*, 242

[68] Ning Z., Zhang Q., Wu W., Tian H. *J. Organomet. Chem.*, **2009**, *694*, 2705

[69] a) Alonso-Vante N., Nierengarten J.-F., Sauvage J.-P. *J. Chem. Soc., Dalton Trans.*, **1994**, 1649. b) Sakaki S., Kuroki T., Hamada T. *J. Chem. Soc., Dalton Trans.*, **2002**, 840. c) Bessho T., Constable E. C.; Grätzel M., Hernandez Redondo A., Housecroft C. E., Kylberg W., Nazeeruddin M. K., Neuburger M., Schaffner S. *Chem. Commun.*, **2008**, 3717

[70] Hasselmann G. M., Meyer G. J. *J. Phys. Chem. B*, **1999**, *103*, 7671

[71] a) Ferrere S., Gregg B. A. *J. Am. Chem. Soc.*, **1998**, *120*, 843. b) Ferrere S. *Chem. Mater.*, **2000**, *12*, 1083. c) Ferrere S. *Inorg. Chim. Acta*, **2002**, *329*, 79

[72] Linfoot C. L., Richardson P., McCall K. L., Durrant J. R., Morandeira A., Robertson N. *Solar Energy*, **2011**, *85*, 1195

[73] a) Cherian S., Wamser C. C. *J. Phys. Chem. B*, **2000**, 104, 3264. b) Fungo F., Otero L., Durantini E. L., Silber J. J., Sereno L. E., *J. Phys. Chem. B*, **2000**, 104, 7644. c) Fungo F., Otero L., Sereno L. E., Silber J. J., Durantini E. L. *J. Mater. Chem.*, **2000**, 10, 645. d) Tachibana Y., Haque S. A., Mercer I. P., Durrant J. R., Klug D. R. *J. Phys. Chem. B*, **2000**, 104, 1198

[74] Higashino T., Imahori H. *Dalton Trans.*, **2015**, *44*, 448

[75] Kay A., Grätzel M. *J. Phys Chem.*, **1993**, 97, 6272 *and references therein*

[76] Campbell W. M., Jolley K. W., Wagner P., Wagner K., Walsh P. J., Gordon K. C., Schmidt-Mende L., Nazeeruddin M. K., Wang Q., Grätzel M., Officer D. L. *J. Phys. Chem. C*, **2007**, *111*, 11760

[77] Chang Y.-C., Wang C.-L., Pan T.-Y., Hong S.-H., Lan C.-M., Kuo H.-H., Lo C.-F., Hsu H.-Y., Lin C.-Y., Diau E. W.-G. *Chem. Commun*., **2011**, *47*, 8910

[78] a) Lu H.-P., Tsai C.-Y., Yen W.-N., Hsieh C.-P., Lee C.-W., Yeh C.-Y., Diau E. W.-G. *J. Phys. Chem. C*, **2009**, *113*, 20990. b) Bessho T., Zakeeruddin S. M., Yeh C.-Y., Diau E. W.-G., Grätzel M. *Angew. Chem., Int. Ed.*, **2010**, *49*, 6646

[79]a) He H., Gurung A., Si L. *Chem. Commun.*, **2012**, *48*, 5910. b) Si L., He H., Zhu K. *New J. Chem.*, **2014**, *38*, 1565

[80] a) Gou F., Jiang X., Li B., Jing H., Zhu Z. *ACS Appl. Mater. Interfaces*, **2013**, *5*, 12631. b) Gou F., Jiang X., Fang R., Jing H., Zhu Z. *ACS Appl. Mater. Interfaces*, **2014**, *6*, 6697

[81] Higashino T., Fujimori Y., Sugiura K., Tsuji Y., Ito S., Imahori, H. *Angew. Chem. Int. Ed.*, **2015**, *54*, 9052

[82] Mathew S., Yella A., Gao P., Humphry-Baker R., Curchod B. F. E., Ashari-Astani N., Tavernelli I., Rothlisberger U., Nazeeruddin M. K., Grätzel M. *Nat. Chem*, **2014**, *6*, 242

[83] Ragoussi M.-E., Ince M., Torres T. *Eur. J. Org. Chem.*, **2013**, 6475

[84] a) Nazeeruddin M. K., Humpry-Baker R., Grätzel M., Murrer B. A. *Chem. Commun.*, **1998**, 719. b) Nazeeruddin M. K., Humphry-Baker R., Grätzel M., Wöhrle D., Schnurpfeil G., Schneider G., Hirth A., Trombach N. *J. Porphyrins Phthalocyanines*, **1999**, *3*, 230. c) He J., Benkö G., Korodi F., Polivka T., Lomoth R., Åkermark B., Sun L., Hagfeldt A., Sundstrom V. *J. Am. Chem. Soc.*, **2002**, *124*, 4922

[85] Cid J.-J., Yum J.-H., Jang S.-R., Nazeeruddin M. K., Martínez-Ferrero E., Palomares E., Ko J., Grätzel M., Torres T. *Angew. Chem. Int. Ed.*, **2007**, *46*, 8358

[86] Yum J.-H., Jang S.-R., Humphry-Baker R., Grätzel M., Cid J.-J., Torres T., Nazeeruddin M. K., *Langmuir*, **2008**, *24*, 5636

[87] Kimura M., Nomoto H., Suzuki H., Ikeuchi T., Matsuzaki H., Murakami T. N., Furube A., Masaki N., Griffith M. J., Mori S. *Chem. Eur. J.*, **2013**, *19*, 7496

[88] Ragoussi M.-E., Cid J.-J., Yum J.-H., de la Torre G., Di Censo D., Grätzel M., Nazeeruddin M. K., Torres T. *Angew. Chem.*, **2012**, *124*, 4451; *Angew. Chem. Int. Ed.*, **2012**, *51*, 4375

[89] Ragoussi M.-E., Yum J.-H., Chandiran A. K., Ince M., de la Torre G., Grätzel M., Nazeeruddin M. K., Torres T. *ChemPhysChem*, **2014**, *15*, 1033

[90] a) Listorti A., López-Duarte I., Martínez-Díaz M. V., Torres T., Dos Santos T., Barnes P. R. F., Durrant J. R. *Energy Environ. Sci.*, **2010**, *3*, 1573. b) Morandeira A., López-Duarte I., O'Regan B., Martínez-Díaz M. V., Forneli A., Palomares E., Torres T., Durrant J. R. *J. Mater. Chem.*, **2009**, *19*, 5016

[91] a) Palomares E., Martínez-Díaz M. V., Haque S. A., Torres T., Durrant J. R. *Chem. Commun.*, **2004**, 2112. b) Rodríguez-Morgade M. S., Pellejà L., Torres T., Palomares E. *J. Porphyrins Phthalocyanines*, **2013**, *17*, 814

[92] Lim B., Margulis G. Y., Yum J.-H., Unger E. L., Hardin B. E., Grätzel M., McGehee M. D., Sellinger A. *Org. Lett.*, **2013**, *15*, 784

[93] Liu D., Fessenden R.W., Hug G. L., Kamat P.V. *J. Phys. Chem. A*, **1997**, *101*, 2583

[94] a) Wu Y., Zhu W.-H. *Chem. Soc. Rev.*, **2013**, *42*, 2039. b) Wu Y., Zhu W.-H., Zakeeruddin S. M., Grätzel M. *ACS Appl. Mater. Interfaces*, **2015**, *7*, 9307

[95] Ahmad S., Guillén E., Kavan L., Grätzel M., Nazeeruddin M. K. *Energy Environ. Sci.*, **2013**, *6*, 3439

[96] Lee C.-P., Lin R. Y.-Y., Lin L.-Y., Li C.-T., Chu T.-C., Sun S.-S., Lin J. T., Ho K.-C. *RSC Adv.*, **2015**, *5*, 23810

[97] Kitamura T., Ikeda M., Shigaki K., Inoue T., Anderson N. A., Ai X., Lian T. Q., Yanagida S. *Chem. Mater.*, **2004**, *16*, 1806

[98] Zeng W., Cao Y., Bai Y., Wang Y., Shi Y., Zhang M., Wang F., Pan C., Wang P. *Chem. Mater.*, **2010**, *22*, 1915

[99] Yella A., Lee H. W., Tsao H. N., Yi C., Chandiran A. K., Nazeeruddin M. K., Diau E. W. G., Yeh C. Y., Zakeeruddin S. M., Grätzel M. *Science*, **2011**, 334, 629

[100] a) Robson K. C. D., Hu K., Meyer G. J., Berlinguette C. P. *J. Am. Chem. Soc.*, **2013**, *135*, 1961. b) Robson K. C. D., Koivisto B. D., Berlinguette C. P. *Inorg. Chem.*, **2012**, *51*, 1501

[101] Tsao H. N., Burschka J., Yi C., Kessler F., Nazeeruddin M. K., Grätzel M. *Energy Environ. Sci.*, **2011**, *4*, 4921

[102] a) Ning Z., Zhang Q., Wu W., Pei H., Liu B., Tian H. *J. Org. Chem.*, **2008**, *73*, 3791. b) Tang J., Hua J., Wu W., Li J., Jin Z., Long Y., Tian H. *Energy Environ. Sci.*, **2010**, *3*, 1736. c) Shi J., Huang J., Tang R., Chai Z., Hua J., Qin J., Li Q., Li Z. *Eur. J. Org. Chem.*, **2012**, 5248

[103] Chang Y. J., Chow T. J. *Tetrahedron*, **2009**, *65*, 4726

[104] Choi H., Raabe I., Kim D., Teocoli F., Kim C., Song K., Yum J.-H., Ko J., Nazeeruddin M. K., Grätzel M. *Chem. Eur. J.*, **2010**, *16*, 1193

[105] Zong X., Liang M., Fan C., Tang K., Li G., Sun Z., Xue S. *J. Phys. Chem. C*, **2012**, *116*, 11241

[106] a) Horiuchi T., Miura H., Uchida S. *Chem. Commun.*, **2003**, 3036. b) Ito S., Miura H., Uchida S., Takata M., Sumioka K., Liska P., Comte P., Pechy P., Grätzel M. *Chem. Commun.*, **2008**, 5194. c) Wu Y., Marszalek M., Zakeeruddin S. M., Zhang Q., Tian H., Grätzel M., Zhu W. *Energy Environ. Sci.*, **2012**, *5*, 8261. d) Pei K., Wu Y., Wu W., Zhang Q., Chen B., Tian H., Zhu W. *Chem. Eur. J.*, **2012**, *18*, 8190

[107] Yang J., Ganesan P., Teuscher J., Moehl T., Kim Y. J., Yi C., Comte P., Pei K., Holcombe T. W., Nazeeruddin M. K., Hua J., Zakeeruddin S. M., Tian H., Grätzel M. *J. Am. Chem. Soc.*, **2014**, *136*, 5722

[108] a) Koumura N., Wang Z.-S., Mori S., Miyashita M., Suzuki E., Hara K. *J. Am. Chem. Soc.*, **2006**, *128*, 14256. b) Wang Z.-S., Koumura N., Cui Y., Takahashi M., Sekiguchi H., Mori A., Kubo T., Furube A., Hara K. *Chem. Mater.*, **2008**, *20*, 3993. c) Koumura N., Wang Z.-S., Miyashita M., Uemura Y., Sekiguchi H., Cui Y., Mori A., Mori S., Hara K. *J. Mater. Chem.*, **2009**, *19*, 4829. d) Lai H., Hong J., Liu P., Yuan C., Li Y., Fang Q. *RSC Adv.*, **2012**, *2*, 2427

[109] Kakiage K., Aoyama Y., Yano T., Otsuka T., Kyomen T., Unno M., Hanaya M. *Chem. Commun.*, **2014**, *50*, 6379

[110] Kakiage K., Aoyama Y., Yano T., Oya K., Kyomen T., Hanaya M. *Chem. Commun.*, **2015**, *51*, 6315

[111] a) Hara K., Kurashige M., Dan-oh Y., Kasada C., Shinpo A., Suga S., Sayama K., Arakawa H. *New J. Chem.*, **2003**, *27*, 783. b) Wang Z. S., Cui Y., Dan-Oh, Y., Kasada C., Shinpo A., Hara K. *J. Phys. Chem. C*, **2008**, *112*, 17011

[112] a) Tian H., Yang X., Chen R., Pan Y., Li L., Hagfeldt A., Sun L. *Chem. Commun.*, **2007**, 3741. b) Manfredi N., Cecconi B., Abbotto A. *Eur. J. Org. Chem.*, **2014**, 7069

[113] Delcamp J. H., Yella A., Holcombe T. W., Nazeeruddin M. K., Grätzel M. *Angew. Chem. Int. Ed.*, **2013**, *52*, 376

[114] a) Kitamura T., Ikeda M., Shigaki K., Inoue T., Anderson N. A., Ai X., Lian T., Yanagida S. *Chem. Mater.*, **2004**, *16*, 1806. b) Hara K., Kurashige M., Ito S., Shinpo A., Suga S., Sayama K., Arakawa H. *Chem. Commun.*, **2003**, 252. c) Hagberg D. P., Edvinsson T., Marinado T., Boschloo G., Hagfeldt A., Sun, L. *Chem. Commun.*, **2006**, 2245. d) Li R., Lv X., Shi D., Zhou D., Cheng Y., Zhang G., Wang P., *J. Phys. Chem. C*, **2009**, *113*, 7469

[115] a) Liu W.-H., Wu I.-C., Lai C.-H., Lai C.-H., Chou P.-T., Li Y.-T., Chen C.-L., Hsu Y.-Y., Chi Y. *Chem. Commun.*, **2008**, 5152. b) Chen B.-S., Chen D.-Y., Chen C.-L., Hsu C.-W., Hsu H.-C., Wu K.-L., Liu S.-H., Chou P.-T., Chi Y. *J. Mater. Chem.*, **2011**, *21*, 1937

[116] a) Li R., Liu J., Cai N., Zhang M., Wang P. *J. Phys. Chem. B*, **2010**, *114*, 4461. b) Ko S., Choi H., Kang M.-S., Hwang H., Ji H., Kim J., Ko J., Kang Y. *J. Mater. Chem.*, **2010**, *20*, 2391. c) Zhu X., Tsuji H., Yella A., Chauvin A.-S., Grätzel M., Nakamura E. *Chem. Commun.*, **2013**, *49*, 582.

[117] Zhu H., Wu Y., Liu J., Zhang W., Wu W., Zhu W.-H. *J. Mater. Chem. A*, **2015**, *3*, 10603

[118] a) Qu S., Qin C., Islam A., Wu Y., Zhu W., Hua J., Tian H., Han L. *Chem. Commun.*, **2012**, *48*, 6972. b) Li R., Zhang M., Yan C., Yao Z., Zhang J., Wang P. *ChemSusChem*, **2015**, *8*, 97

[119] a) Cui Y., Wu Y., Lu X., Zhang X., Zhou G., Miapeh F. B., Zhu W., Wang Z.-S. *Chem. Mater.*, **2011**, *23*, 4394. b) Huang Z.-S., Cai C., Zang X.-F., Iqbal Z., Zeng H., Kuang D.-B., Wang L., Meier H., Cao D. *J. Mater. Chem. A*, **2015**, *3*, 1333

[120] a) Chang D. W., Lee H. J., Kim J. H., Park S. Y., Park S.-M., Dai L., Baek J.-B. *Org. Lett.*, **2011**, *13*, 3880. b) Li S. R., Lee C. P., Liao C. W., Su W. L., Li C. T., Ho K. C., Sun S. S. *Tetrahedron*, **2014**, *70*, 6276

[121] a) Yum J.-H., Holcombe T. W., Kim Y., Yoon J., Rakstys K., Nazeeruddin M. K., Grätzel M. *Chem. Commun.*, **2012**, *48*, 10727. b) Qu S. Y., Qin C., Islam A., Wu Y. Z., Zhu W. H., Hua J. L., Tian H., Han L. Y. *Chem. Commun.*, **2012**, *48*, 6972. c) Yum J.-H., Holcombe T. W., Kim Y., Rakstys K., Moehl T., Teuscher J., Delcamp J. H., Nazeeruddin M. K., Grätzel M. *Sci. Rep.*, **2013**, *3*, 2446

[122] a) Ying W. J., Guo F. L., Li J., Zhang Q., Wu W. J., Tian H., Hua J. L. *ACS Appl. Mater. Interfaces*, **2012**, *4*, 4215. b) Li S.-G., Jiang K.-J., Huang J.-H., Yang L.-M., Song Y.-L. *Chem. Commun.*, **2014**, *50*, 4309

[123] Zhang L., Cole J. M. *ACS Appl. Mater. Interfaces*, **2015**, *7*, 3427

[124] a) Pechy P., Rotzinger F. P., Nazeeruddin M. K., Kohle O., Zakeeruddin S. M., Humphry-Baker R., Grätzel M. *J. Chem. Soc., Chem. Commun.*, **1995**, 65. b) Mulhern K. R., Orchard A., Watson D. F., Detty M. R. *Langmuir*, **2012**, *28*, 7071. c) Abate A., Perez-Tejada R., Wojciechowski K., Foster J. M., Sadhanala A., Steiner U., Snaith H. J., Franco S., Orduna J. *Phys. Chem. Chem. Phys.*, **2015**, *17*, 18780

[125] Yao Q.-H., Shan L., Li F.-Y., Yin D.-D., Huang C.-H. *New J. Chem.*, **2003**, *27*, 1277

[126] a) McNamara W. R., Snoeberger III R. C., Li G., Richter C., Allen L. J., Milot R. L., Schmuttenmaer C. A., Crabtree R. H., Brudvig G. W., Batista V. S. *Energy Environ. Sci.*, **2009**, *2*, 1173. b) Koenigsmann C., Ripolles T. S., Brennan B. J., Negre C. F. A., Koepf M., Durrell A. C., Milot R. L., Torre J. A., Crabtree R. H., Batista V. S., Brudvig G., Bisquert J., Schmuttenmaer C. *Phys. Chem. Chem. Phys.*, **2014**, *16*, 16629

[127] Ooyama Y., Inoue S., Nagano T., Kushimoto K., Ohshita J., Imae I., Komaguchi K., Harima Y. *Angew. Chem. Int. Ed.*, **2011**, *50*, 7429

[128] Mao J., Wang D., Liu S.-H., Hang Y., Xu Y., Zhang Q., Wu W., Chou P.-T., Hua J. *Asian J. Org. Chem.*, **2014**, *3*, 153

[129] Franchi D., Calamante M., Reginato G., Zani L., Peruzzini M., Taddei M., Fabrizi De Biani F., Basosi R., Sinicropi A., Colonna D., Di Carlo A., Mordini A. *Tetrahedron*, **2014**, *70*, 6285

[130] a) Wang L., Yang X., Li S., Cheng M., Sun L. *RSC Adv.*, **2013**, *3*, 13677. b) Cecconi B., Mordini A., Reginato G., Zani L., Taddei M., Fabrizi de Biani F., De Angelis F., Marotta G., Salvatori P., Calamante M. *Asian J. Org. Chem.*, **2014**, *3*, 140. c) Wang L., Yang X., Zhao J., Zhang F., Wang X., Sun L. *ChemSusChem*, **2014**, *7*, 2640

[131] Ooyama Y., Uenaka K., Harima Y., Ohshita J. *RSC Adv.*, **2014**, *4*, 30225

[132] a) Ooyama Y., Yamaguchi N., Ohshita J., Harima Y. *Electrochemistry*, **2013**, *81*, 325. b) Tian J., Yang X., Zhao J., Wang L., Wang W., Li J., Sun L. *RSC Adv.*, **2014**, *4*, 34644. c) Franchi D., Calamante M., Reginato G., Zani L., Peruzzini M., Taddei M., Fabrizi de Biani F., Basosi R., Sinicropi A., Colonna D., Di Carlo A., Mordini A. *Synlett*, **2015**, *26*, 2389

[133] a) Tae E. L., Lee S. H., Lee J. K., Yoo S. S., Kang E. J., Yoon K. B. *J. Phys. Chem. B*, **2005**, *109*, 22513. b) An B.-K., Hu W., Burn P. L., Meredith P. *J. Phys. Chem. C*, **2010**, *114*, 17964. c) Ooyama Y., Yamada T., Fujita T., Harima Y., Ohshita J. *J. Mater. Chem. A*, **2014**, *2*, 8500

Chapter 2

Aim of the work

As explained in the introduction, DSSCs are heterogeneous systems which contain several components: each of them contributes to the overall efficiency of the solar device. However, the sensitizer can be considered the heart of a DSSC since it is directly responsible for the conversion of the solar energy in electric current. This Ph.D. research work, fitting in this contest, has been focused on the design and synthesis of new organic photosensitizers, which could be suitable to be employed in DSSC devices and characterized by good photovoltaic performances. Indeed, it is important to keep in mind that, in order to fulfill special requests from the market, to overcome the current record efficiency must not be the only aim to pursue in designing new dyes. Improvement of many other properties, like stability, transparency and color, which are needful for future commercial applications, is indeed also very important. For these reasons we decided to focus our work in the screening of new structures which could be used as the central core of the dye, the π-spacer. This unit in fact might play a significant role to affect such properties since it is responsible not only for the intramolecular charge transfer process upon photoexcitation, but also for the light absorption properties of the dye and its long-term stability.

In the first part of this work we have investigated the synthesis of new organic dyes having a superior light-harvesting ability. This property is related to the possibility of building transparent thin-layer DSSCs,[1] a kind of cells which can be used in the context of building-integrated photovoltaics (BIPV).[2] Furthermore, dyes with such features could find application for solid-state DSSCs.[3] It is also important to keep in mind that, in order to facilitate the large-scale commercialization of DSSC technology, it is necessary to employ fabrication techniques as simple as possible. Indeed, the application of surface treatments on both the conductive glass and the inorganic semiconductor, the consecutive deposition of multiple TiO_2 layers of different average particle size and shape,[4] or the introduction of several additives and co-adsorbents both in the sensitizing baths and cell electrolytes[5] are usually required to obtain high efficiencies. For these reasons we have selected our structures with the aim to obtain new sensitizers able to give good photovoltaic efficiencies under simplified conditions. This fact would allow to reduce the economic and environmental costs of DSSCs,[6] thus helping to make this technology more sustainable.

In the second part of this work we have focused on the synthesis of new dyes having an appropriate chromophore able to extend the light absorption spectrum of the

dyes in the red/near-infrared (NIR) region. First of all, the absorption of a greater fraction of the incident light should correspond to an increase of the photocurrent density (J_{sc}) and, consequently, of the overall efficiency of the solar device.[7] Moreover, dyes with such light-harvesting properties should show an unusual blue-green color, a feature which is currently owned by few commercial sensitizers[8] and, thus, highly requested.

Finally, in planning the synthesis of our target molecules we have always tried to optimize the synthetic procedures employed in view of a possible scale–up. Optimization of reaction conditions using sustainable procedure such as non conventional MW activation and catalytic processes has been carried out when possible.

References

[1] De Sousa S., Olivier C., Ducasse L., Le Bourdon G., Hirsch L., Toupance T. *ChemSusChem*, **2013**, *6*, 993

[2] Yoon S., Tak S., Kim J., Jun Y., Kang K., Park J. *Build. Environ.*, **2011**, *46*, 1899

[3] Miyasaka T. *J. Phys. Chem. Lett.*, **2011**, *2*, 262

[4] Ito S., Murakami T. N., Comte P., Liska P., Grätzel C., Nazeeruddin M. K., Grätzel M. *Thin Solid Films*, **2008**, *516*, 4613

[5] Kakiage K., Aoyama Y., Yano T., Otsuka T., Kyomen T., Unno M., Hanaya M. *Chem. Commun.*, **2014**, *50*, 6379

[6] Parisi M. L., Maranghi S., Basosi R. *Renew. Sust. Energ. Rev.*, **2014**, *39*, 124

[7] Hamann T. W., Jensen R. A., Martinson A. B. F., Van Ryswykac H., Hupp J. T. *Energy Environ. Sci.*, **2008**, *1*, 66

[8] http://www.dyenamo.se/dyenamo_dyes.php#dnf10

Chapter 3

Microwave-activated synthesis of thiazolo[5,4-*d*]thiazoles

Dessì A., Calamante M., Mordini A., Zani L., Taddei M., Reginato G.

RSC Adv., **2014**, *4*, 1322

3.1. Introduction and background

The first spacer we decided to take into account was thiazolo[5,4-*d*]thiazole (TzTz – Figure 3.1), a bicyclic system formally derived from the [3.3.0] fusion of two thiazole rings. The first TzTz derivative (R = phenyl) was synthesized by Ephraim in 1891 through the condensation of benzaldehyde with dithiooxamide,[1] but a wrong structure containing two four-membered rings was assigned to the product (Figure 3.1).

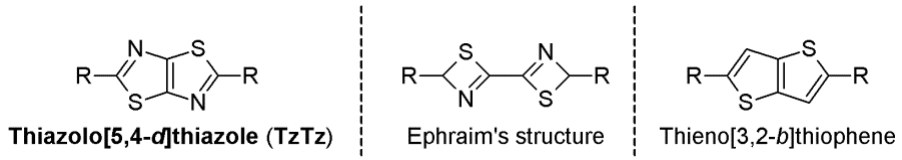

Figure 3.1. General structure of the TzTz ring system (left), the structure assigned by Ephraim (center) and its corresponding thiophene derivative (right).

Several years later, in 1960, Johnson and Ketcham established the right structure of Ephraim's condensation product through a series of spectroscopic and derivatization studies and improved the original synthetic protocol preparing a wide range of diaryl-analogues using different aromatic aldehydes.[2] After that, the number of studies concerning the chemistry of thiazolothiazoles did not increase sensibly until 2000s, when the TzTz ring system started to attract great interest in the field of organic electronics due to its rigid and planar backbone, which could be easily included in an extended π-conjugated electronic structure.[3]

Compared to the corresponding thiophene derivative, thieno[3,2-*b*]thiophene (Figure 3.1), the TzTz ring is more electron-deficient, due to the presence of the additional nitrogen atoms, and therefore shows a superior oxidative stability, reflected in its resistance to attack by nitric or sulfuric acid at room temperature, direct bromination and Friedel-Crafts acylations.[4] Furthermore, TzTz-derivatives show strong π-π stacking and overlapping of the orbitals in the solid state,[5] often resulting in high charge-carrier mobility, which is a crucial property for optoelectronic applications.[6] As a consequence, interest in this class of compounds has grown dramatically in the last decade, especially due to some early studies concerning their employment in optoelectronic devices such as light-emitting diodes (OLEDs)[7] and organic field-effect transistors (OFETs).[8,9] Following these initial reports, an ever increasing number of small molecules and polymeric materials incorporating the thiazolo[5,4-*d*]thiazole

unit has been described in the literature[3,10] and application in various fields, including photovoltaics, has been investigated.

Despite this large amount of work and the encouraging results obtained in the above-mentioned fields, employment of thiazolo[5,4-*d*]thiazoles as photosensitizers for DSSCs was not described. Therefore, we decided to prepare new organic dyes containing this heterocyclic core, expecting a beneficial effect on the photophysical, spectroscopic and stability properties of the final dyes. The first problem we had to face was to find a general and efficient method to synthesize the thiazolo[5,4-*d*]thiazole core.

Considering the large number of publications appeared in recent years, it was quite surprising to ascertain the lack of a general and efficient synthetic procedure for the preparation and functionalization of such molecules. Indeed, many of the papers concerning the synthesis of thiazolothiazoles still applied the old procedure by Ketcham,[2] which required to heat to reflux a mixture of dithiooxamide (**2**) and a moderate-to-large excess of an aromatic aldehyde (4.0-13.0 eq.), either in solvent-free conditions or in the presence of phenol as a high boiling point solvent (Scheme 3.1).

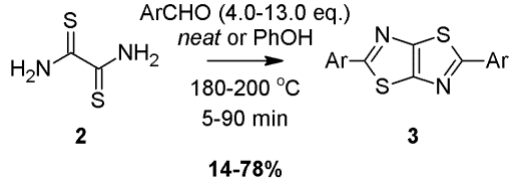

Scheme 3.1. Condensation of dithiooxamide (2) with aromatic aldehydes to give diaryl-thiazolo[5,4-d]thiazoles (3).

Compounds **3** are usually insoluble solids, which can be recovered from the reaction mixture by filtration and recrystallized from different solvents. Clearly, the reaction conditions shown in Scheme 3.1 were quite harsh, requiring temperatures above 180 °C to start the condensation reaction; moreover a large amount of aldehyde was often required and only few examples recorded yields over 60%. Finally, under these conditions the conversion of aliphatic substrates was unsuccessful.

Indeed, following the first reports by Ketcham and co-workers,[2,4] some later studies slightly modified the original reaction conditions by changing solvent, temperature and reaction time. For example, the condensation reaction between aromatic or

heteroaromatic aldehydes and dithiooxamide (**2**) worked with moderate yields by using *N*,*N*-dimethylformamide[11] or *o*-dichlorobenzene[12] as solvents, although even in this case heating at 150-160°C for several hours was necessary. Better results were obtained by Pope *et al.*[13] by using nitrobenzene as solvent and heating at 130°C for 24 hours: under these conditions, a small series of thiazolo[5,4-*d*]thiazoles was prepared in moderate to good yields, just using a stoichiometric amount of aromatic and heteroaromatic aldehydes. Over time, some alternative procedures have been described, but they usually consisted of two or more synthetic steps requiring the use of non-commercially available starting materials, which limited their practical application.[14] Therefore, the traditional procedure by Johnson and Ketcham[2] and its subsequent modifications were still the only methodology generally applied for the preparation of aromatic thiazolo[5,4-*d*]thiazole-containing derivatives, although a systematic study to find optimal and more general conditions was still necessary.

In search for new and more efficient reaction conditions, in a preliminary experiment we observed that the yield of thiazolo[5,4-*d*]thiazole **3a** could be significantly enhanced if the reaction was carried out in solvent-free conditions, using four equivalents of aldehyde **4a**, under MW-irradiation (Scheme 3.2).

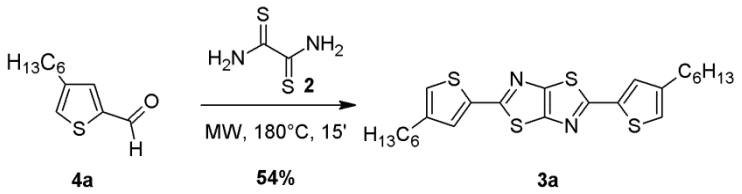

Scheme 3.2. MW-assisted synthesis of thiazolo[5,4-d]thiazole 3a.

The efficiency of the reaction was improved compared to the usual thermal process;[15] moreover, the reaction time was notably shortened to just 15 minutes, while the amount of byproducts at the end of reaction was reduced. Prompted by this result and in consideration of the demonstrated utility of thiazolo[5,4-*d*]thiazoles,[3,10] before approaching the synthesis of new thiazolothiazole-containing dyes, we decided to study in more detail the effect of microwave activation in the condensation of dithioxoamide (**2**) with aromatic and heteroaromatic aldehydes, aiming to find a general and mild synthetic procedure.

3.2. Results and discussion

3.2.1. Optimization of the reaction

The advent of microwave-assisted organic synthesis has contributed significantly to the development of mild and sustainable procedures for the preparation of organic compounds as it often leads to a remarkable decrease in reaction times and chemical waste, an increase in yields and an easier product workup.[16] This technique has found useful application in the synthesis of heterocycles,[17] and this fact led us to think it could also be exploited for thiazolothiazole synthesis. To optimize the reaction conditions, 2-methoxybenzaldehyde (**4b**) was chosen as a model substrate (Table 3.1), because it is an inexpensive and commercially available reagent.

Table 3.1. Optimization of reaction conditions for the preparation of thiazolothiazole 3b from 2-methoxybenzaldehyde (4b).

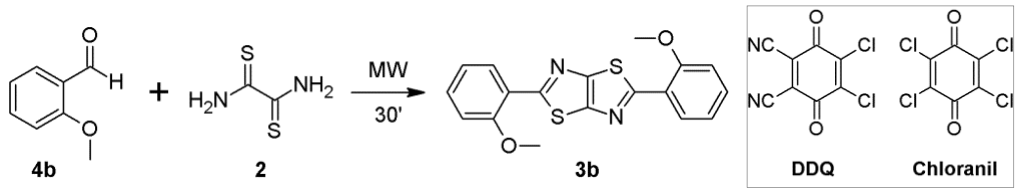

Entry	**4b**[a]	T (°C)	DDQ[a]	Yield[b]
1	4.0	150	-	48%
2	4.0	150	0.25	61%
3	4.0	150	0.50	70%
4	4.0	150	0.50[c]	68%
5[d]	4.0	150	0.50	48%
6	3.0	150	0.75	61%
7	4.0	100	0.50	-
8	4.0	180	0.75	52%
9[e]	4.0	150	0.50	59%
10[e]	3.0	150	0.50	63%
11[e]	2.0	150	0.50	55%

[a] Equivalents used in the reaction relative to dithiooxamide. [b] Yield of isolated compound. [c] Chloranil was used instead of DDQ as the oxidant. [d] Reaction performed without MW activation. [e] Nitrobenzene ($C_6H_5NO_2$) was used as the solvent.

Furthermore the corresponding condensation product, 2,5-bis(2-methoxyphenyl)-thiazolo[5,4-*d*]-thiazole (**3b**), could be easily obtained in high purity by a simple precipitation followed by recrystallization from chloroform or *o*-xylene. When a

mixture of aldehyde **4b** and dithiooxamide (**2**) (ratio **4b**:**2** = 4:1) was irradiated in a MW reactor under solventless conditions at 150°C for 30 min, product **3b** was obtained in 48% yield after recrystallization (entry 1).

The aldehyde/dithiooxamide 4:1 ratio, instead of the stechiometric 2:1, was necessary to achieve complete dissolution of dithiooxamide under *solvent free* conditions. Such result was already comparable to that obtained with the classical thermal procedure by employing a much larger amount of aldehyde **4b** (47% yield, 8.0 eq.) at an higher temperature (T > 238°C, b.p. **4b**).[2] However, analysis of the ^{1}H-NMR spectrum of the crude reaction mixture revealed the presence of a byproduct, which was identified as the symmetrical compound **5** (Figure 3.2), based on the assignment of the relevant spectral peaks.

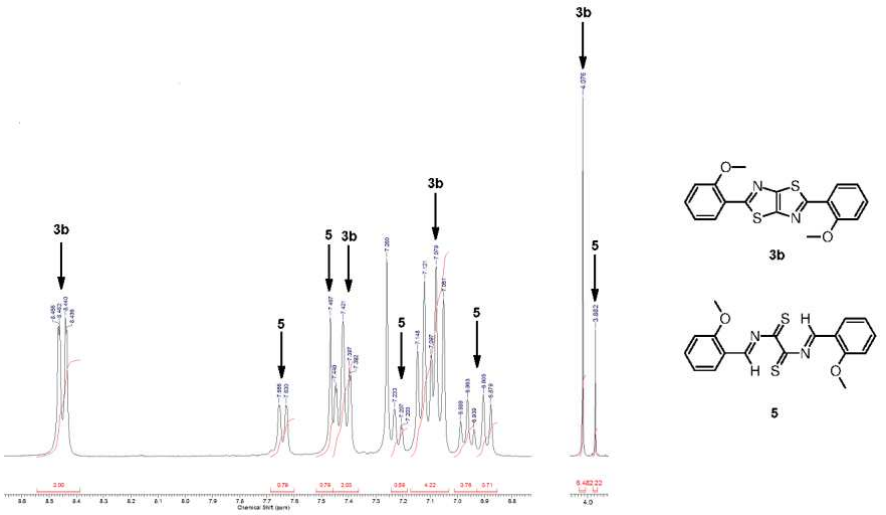

Figure 3.2. ^{1}H-NMR spectrum of crude reaction mixture containing product 3b and byproduct 5.

Formation of this byproduct can be explained by considering the reaction mechanism as reported in Scheme 3.3: the reaction starts with the condensation between the aldehyde and the first $-NH_2$ group of dithiooxamide (**2**), then proceeds with a nucleophilic attack of a sulfur atom on the imine carbon to get the first five-membered ring. After proton rearrangement, the same mechanism is repeated again with the formation of the bicyclic structure, leading to a partially hydrogenated intermediate. Finally, the latter has to undergo spontaneous dehydrogenation to give final product **3**; to carry out the last oxidation the reaction usually has to be conducted under air.

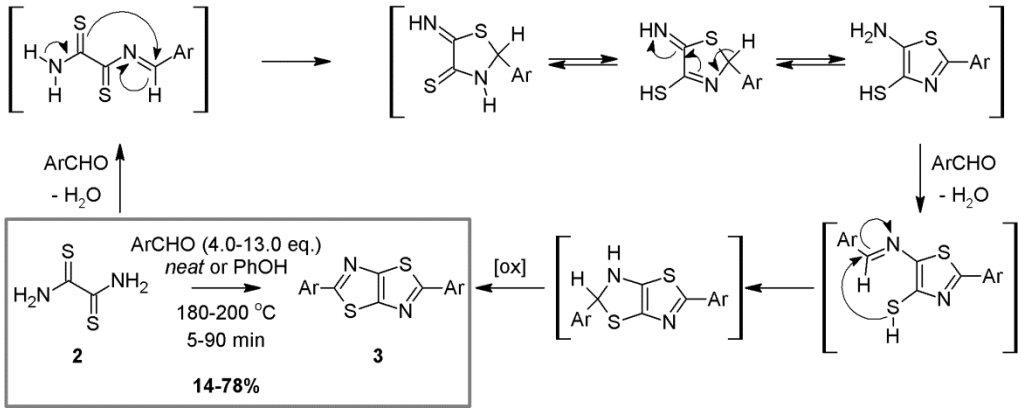

Scheme 3.3. Reaction mechanism for the condensation of dithiooxamide (2) with aromatic aldehydes.

Compound **5**, which could be obtained by double condensation of **2** with two equivalents of **3b**, is a likely intermediate in the cyclization pathway we have depicted in Scheme 3.3;[3] similar products were already observed in the thermal reaction of salicylaldehyde with dithiooxoamide by Ketcham[2] and in that case authors demonstrated that they could be converted to the desired product by heating at 250–270°C, with or without addition of a mild oxidant like sulfur.

Since the last dehydrogenation step is irreversible and affects all the equilibria towards the formation of product **3**, we supposed that the presence of intermediate **5** could be due to an inefficient dehydrogenation step, despite the high temperature and the presence of air. Therefore, we assumed that the yield of our reaction could be further improved by addition of an oxidant, in order to facilitate the last dehydrogenation step and achieve full conversion of the intermediates to product **3b**. Indeed, when the crude mixture was directly dissolved in THF and reacted with 0.25 eq. of a dehydrogenating reagent such as DDQ (Table 1, entry 2) at reflux for 10 min, the yield was improved to 61%. An increase of the amount of DDQ (0.5 eq., entry 3) led to a further enhancement to 70% (entry 3), while the employment of a cheaper, structurally related oxidant such as chloranil gave practically the same result (68%, entry 4). Importantly, a control test using conventional thermal heating under the same conditions was carried out and a lower yield of the desired compound was obtained (48%, entry 5), showing that MW activation is beneficial for the reaction outcome. Finally, a reasonable yield could still be obtained when lowering the amount of aldehyde to 3.0 eq. (entry 6), while further experiments showed that variation of the temperature (entries 7 and 8) or employment of a longer reaction time were not beneficial in this case.

Although these optimized conditions were better than any other alternative procedure reported in the literature in terms of yield, time and temperature required, our MW-activated reaction under *solvent-free* conditions could not be used in the case of solid reaction partners or when a large excess of one reagent should be avoided because of its high cost or complex preparation. For this reason, we decided to investigate also the reaction outcome using nitrobenzene as the reaction medium, a solvent previously employed in thermal procedures.[13] The results obtained are reported in Table 3.1. Unfortunately the reaction was less efficient if compared to the *solvent-free* conditions (entry 9), but we could observe that, in the presence of a solvent, it was possible to lower the amount of aldehyde maintaining a reasonable yield of the product (2.0 eq., 55%, entry 11) even using a stoichiometric ratio, proving these as the best conditions to be used with valuable or solid substrates.

3.2.2. Scope of the reaction

With two different sets of efficient reaction conditions in our hand, the scope of these MW-assisted procedures was assessed by reacting a range of different aldehydes both under *solvent-free* conditions (method **A**) and in solution (method **B**).

The results obtained are reported in Table 3.2, where they are compared with the best results previously described in the literature for known compounds. The expected products were obtained in good yields (up to 81%) and high purity in most of the cases by employing two different methods. *Solvent-free* conditions (method **A**) generally provided better results, except in the cases of products **3d**,**e** (entries 3, 4). The procedure was suitable both for substituted aromatic (entries 1–7) and heteroaromatic (entries 8–13) aldehydes: in many examples higher yields than those reported in the literature were obtained (up to 76%, entries 1, 3, 8, 9, 11), while in a few cases our methodology afforded similar results to the literature (entries 5, 10), even when using a smaller excess of aldehyde (entries 2, 4). The best result was obtained with EDOT-aldehyde **4n**, which gave the corresponding product in 81% yield (entry 13). Unfortunately, a complete spectroscopic characterization of compounds **3g** and **3h** was hindered by their almost completely insolubility in a wide range of the most common organic solvents (entries 6–7). Despite that, in the case of compound **3h**, direct infusion mass spectrometry made its identification possible by detecting the corresponding molecular peaks and showing the typical distribution pattern of a tetrachloro-substituted compound.

Table 3.2. Scope of MW activated condensation/oxidation sequence to thiazolo[5,4-d]thiazoles.

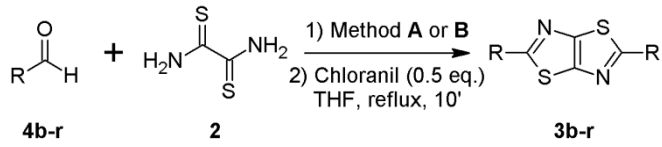

4b-r **2** **3b-r**

Entry	R	Product	Method[a,b]	Isolated Yield	Lit. Yield (eq. of **4**)
1	2-CH_3O-Ph (**4b**)	**3b**	**A**	68%	47% (ref. 2) (8)
			B	55%	
2	Ph (**4c**)	**3c**	**A**	73%	78% (ref. 2) (10)
			B	66%	
3	2-Br-Ph (**4d**)	**3d**	**A**	35%	35% (ref. 18) (10)
			B	58%	
4	4-*t*Bu-Ph (**4e**)	**3e**	**A**	46%	52% (ref. 19) (3.5)
			B	47%	
5	2-OH-Ph (**4f**)	**3f**	**A**	46%	45% (ref. 18) (2)
			B	30%	
6	3,5-Br_2-Ph (**4g**)	**3g**	**B**	69%[c]	-
7	2,4-Cl_2-Ph (**4h**)	**3h**	**B**	72%[c]	-
8	2-Thienyl (**4i**)	**3i**	**A**	72%	36% (ref. 11b) (2)
			B	49%	
9	2-Furyl (**4j**)	**3j**	**B**	66%	40% (ref. 2) (13)
10	4-Pyridyl (**4k**)	**3k**	**B**	66%	60% (ref. 13) (2)
11	2-Pyridyl (**4l**)	**3l**	**B**	76%	60% (ref. 13) (2)
12	5-Thiazolyl (**4m**)	**3m**	**B**	75%	-
13	2-(3,4-Ethylenedioxy) thienyl (**4n**)	**3n**	**B**	81%	-
14	*n*-Hexyl (**4o**)	**3o**	**A**	54%[d]	-
			B	40%[d]	
15	Cyclohexyl (**4p**)	**3p**	**A**	40%	-
			B	21%	
16	*tert*-Butyl (**4q**)	**3q**	**B**	33%[d]	-
17	Styryl (**4r**)	**3r**	**A**	6%	7% (ref. 2) (9)
			B	9%	

[a] Method **A**: aldehyde **4** (4.0 eq.), dithiooxamide **2** (1.0 eq.) MW, 150°C, 30', *neat*. [b] Method **B**: aldehyde **4** (2.0 eq.), dithiooxamide **2** (1.0 eq.), nitrobenzene, MW, 150°C, 30'. [c] Due to the almost complete insolubility in a wide range of organic solvents, full characterization was not possible. [d] Purified by flash column chromatography.

On the other hand, in order to confirm indirectly the formation of compound **3g** and verify the possibility to do chemical transformations on such insoluble materials, we decided to modify it by introducing some long alkyl chains. Therefore, the solid obtained after crystallization was reacted with oct-1-yne under heterogeneous Pd-catalyzed Sonogashira conditions,[20] and the soluble tetraalkyl-substituted bisaryl-thiazolothiazole **6** was isolated after flash column chromatography (Scheme 3.4).

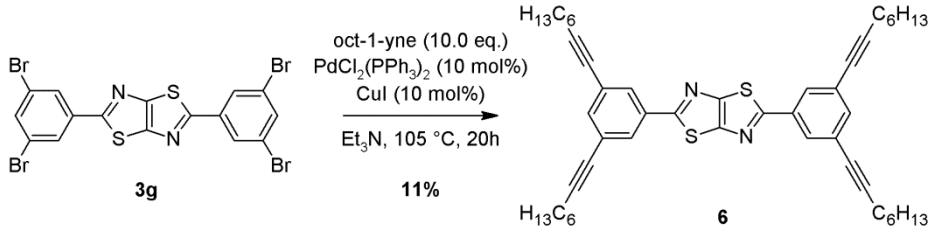

Scheme 3.4. Elaboration of compound 3g by means of a Pd-catalyzed Sonogashira reaction.

It is noteworthy that, even working under substantially heterogeneous conditions, this reaction allowed the formation of four new carbon–carbon bonds, albeit with a low yield. Preparation of compound **6**, besides proving the actual formation of **3g**, demonstrated the synthetic utility of the present procedure when starting from halo-substituted aryl aldehydes.

Finally, we tested our optimized procedures with more challenging substrates such as primary, secondary and tertiary aliphatic aldehydes **4o**–**q**, whose conversion was usually unsuccessful under classic conditions.[2] The last dehydrogenation step is actually less favored for aliphatic aldehydes than aromatic ones, because the final π-system is shorter and less stabilized, and consequently, the thermodynamic driving force for the reaction is smaller. Indeed, to date, the preparation of only one aliphatic product has been described.[19,21] Moreover enolizable aldehydes can afford aldol-type byproducts which can lower the reaction yield. Despite that, our MW-activated procedure allowed to overcome such disadvantages and aliphatic TzTz derivatives could be prepared, albeit with moderate yields (33–54%, entries 14–16). Unlike all the other TzTz-derivatives, compounds **3o** and **3q** were much more soluble in common organic solvents and thus a flash column chromatography purification was necessary to isolate pure compounds. Therefore, for the first time, it has been possible to describe a synthetic procedure for the preparation of thiazolo[5,4-*d*]thiazoles which is effective both on aromatic and aliphatic substrates. Finally, the method found a limitation in the use of α,β-unsaturated aldehydes: when

cinnamaldehyde **4r** was subjected to the reaction conditions, the corresponding product could be isolated only in very low yield (entry 17).

Interestingly, another research group recently tested a modification of this procedure on three different aromatic aldehydes, replacing chloranil with SeO_2:[22] even though the yield of **3c** was comparable to those obtained with our procedure, the use of selenium dioxide, which is a more toxic reagent than chloranil, is neither profitable nor advisable.

3.3. Experimental Section

3.3.1. General Procedure A

In a microwave vial equipped with a magnetic stirrer were introduced aldehyde **4** (8.0 mmol, 4.0 eq.) and dithiooxamide **2** (2.0 mmol, 1.0 eq.). The resulting mixture was heated under microwave irradiation at 150 °C for 30 min, then allowed to cool down to room temperature. The reaction mixture was diluted with THF (ca. 5 mL) and transferred in a flask, then chloranil (1.0 mmol, 0.5 eq.) was added to the reaction mixture, which was heated to reflux and stirred for 10 min. After this time heating was interrupted and methanol (ca. 10 mL) was added. After cooling down to 0 °C a precipitated was formed. The solid was filtered and washed with methanol, then recrystallized from THF to give pure thiazolo[5,4-*d*]thiazoles **3**.

3.3.2. General Procedure B

In a microwave vial equipped with a magnetic stirrer were placed aldehyde **4** (2.0 mmol, 2.0 eq.), dithiooxamide **2** (1.0 mmol, 1.0 eq.) and nitrobenzene (1 mL). The resulting mixture was heated under microwave irradiation at 150 °C for 30 min, after which it was allowed to cool down to room temperature. THF (ca. 5 mL) and chloranil (0.5 mmol, 0.5 eq.) were added to the reaction mixture, which was transferred to a flask, heated to reflux and stirred for 10 min. After this time heating was interrupted and methanol (ca. 10 mL) was added to the reaction mixture, which was cooled down to 0 °C. The resulting solid was filtered, washed with methanol and recrystallized from THF to give pure thiazolo[5,4-*d*]thiazoles **3**.

2,5-Bis(2-methoxyphenyl)-thiazolo[5,4-*d*]thiazole (3b).[2]

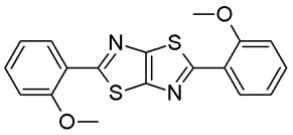

3b

Aldehyde **4b** (1.09 g, 8.00 mmol) was reacted with dithiooxamide **2** (240 mg, 2.00 mmol) following general procedure **A**. After purification, compound **3b** (482 mg, 68% yield) was obtained as a pale brown solid.

(**3b**): mp = 260–261 °C (lit.2 253–254 °C). ^{1}H-NMR (300 MHz, $CDCl_3$): δ = 8.45 (dd, *J* = 7.9 and 1.7 Hz, 2H), 7.42 (td, *J* = 7.4 and 1.7 Hz, 2H), 7.12 (t, *J* = 8.2 Hz, 2H), 7.06 (d, *J* = 8.3 Hz, 2H), 4.08 (s, 6H) ppm. ^{13}C-NMR (100 MHz, $CDCl_3$): δ = 163.5, 156.6, 152.1, 131.1, 128.6, 123.1, 121.4, 111.8, 55.9 ppm. IR (KBr): $\tilde{\nu}$ = 3078, 2832, 1582 cm^{-1}. ESI-MS: *m/z* = 355 $[M+H]^+$.

2,5-Diphenylthiazolo[5,4-*d*]thiazole (3c).[2]

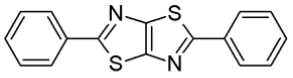

3c

Aldehyde **4c** (849 mg, 8.00 mmol) was reacted with dithiooxamide **2** (240 mg, 2.00 mmol) following general procedure **A**. After purification, compound **3c** (430 mg, 73% yield) was obtained as a yellow solid.

(**3c**): mp = 196–198 °C (lit.2 209–210 °C). ^{1}H-NMR (300 MHz, $CDCl_3$): δ = 7.99–8.02 (m, 4H), 7.47–7.50 (m, 6H) ppm. ^{13}C-NMR (75 MHz, $CDCl_3$): δ = 169.3, 151.0, 134.1, 130.8, 129.3, 126.5 ppm. IR (KBr): $\tilde{\nu}$ = 3059, 1570 cm^{-1}. ESI-MS: *m/z* = 295 $[M+H]^+$.

2,5-Bis(2-bromophenyl)-thiazolo[5,4-*d*]thiazole (3d).[18]

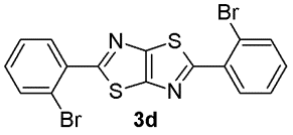

3d

Aldehyde **4d** (370 mg, 2.00 mmol) was reacted with dithiooxamide **2** (120 mg, 1.00 mmol) in 1.0 mL of nitrobenzene, following general procedure **B**. After purification, compound **3d** (262 mg, 58% yield) was obtained as a pale green solid.

(**3d**): mp = 228–229 °C. ^{1}H-NMR (300 MHz, $CDCl_3$): δ = 8.06 (dd, *J* = 8.0 and 1.6 Hz, 2H), 7.75 (dd, *J* = 8.0 and 1.2 Hz, 2H), 7.46 (td, *J* = 7.6 and 1.2 Hz, 2H), 7.33 (td, *J* = 8.0 and 1.6 Hz, 2H) ppm. ^{13}C-NMR (100 MHz, $CDCl_3$): δ = 166.8, 151.9, 134.5, 134.4, 132.1, 131.3, 127.9, 121.7 ppm. IR (KBr): $\tilde{\nu}$ = 3055, 1570, 1026 cm^{-1}. ESI-MS: *m/z* = 453 $[M+H]^+$.

2,5-Bis(4-tert-butylphenyl)-thiazolo[5,4-*d*]thiazole (3e).[19]

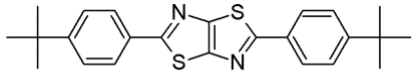

3e

Aldehyde **4e** (324 mg, 2.00 mmol) was reacted with dithiooxamide **2** (120 mg, 1.00 mmol) in 1.0 mL of nitrobenzene, following general procedure **B**. After purification, compound **3e** (187 mg, 47%yield) was obtained as a pale yellow solid.

(**3e**): mp = 285–287 °C. ^{1}H-NMR (300MHz, $CDCl_3$): δ = 7.92 (d, *J* = 8.1Hz, 4H), 7.49 (d, *J* = 8.4 Hz, 4H), 1.37 (s, 18H) ppm. ^{13}C-NMR (75 MHz, $CDCl_3$): δ = 169.1, 154.3, 150.7, 131.5, 126.3, 126.2, 35.1, 31.3 ppm. IR (KBr): $\tilde{\nu}$ = 3058, 2962, 1517 cm^{-1}. ESI-MS: *m/z* = 407 $[M+H]^+$.

2,5-Bis(2-hydroxyphenyl)-thiazolo[5,4-*d*]thiazole (3f).[2,13]

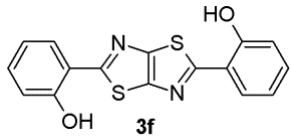

3f

Aldehyde **4f** (977 mg, 8.00 mmol) was reacted with dithiooxamide **2** (240 mg, 2.00 mmol) following general procedure **A**. After purification, compound **3f** (300 mg, 46% yield) was obtained as a light brown solid.

(**3f**): mp = 303–305 °C (lit.2 300–302 °C). ^{1}H-NMR (300 MHz, $CDCl_3$): δ = 11.39 (s, 2H), 7.65 (d, *J* = 7.9 Hz, 2H), 7.38 (t, *J* = 8.3 Hz, 2H), 7.10 (d, *J* = 8.3 Hz, 2H), 6.98 (t, *J* = 8.1 Hz, 2H) ppm. ^{13}C-NMR (75 MHz, pyridine-d_5): δ = 166.7, 157.2, 151.3, 132.2, 128.6,

121.2, 120.4, 117.9 ppm. IR (KBr): $\tilde{\nu}$ = 3212, 3038, 1576 cm^{-1}. ESI-MS: *m/z* = 327 $[M+H]^+$.

2,5-Bis(3,5-dibromophenyl)-thiazolo[5,4-*d*]thiazole (3g).

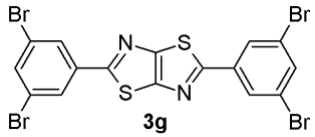

3g

Aldehyde **4g** (528 mg, 2.01 mmol) was reacted with dithiooxamide **2** (120 mg, 1.00 mmol) in 1.0 mL of nitrobenzene, following general procedure **B**. After purification, compound **3g** (419 mg, 69% yield) was obtained as a pale brown solid, which was insoluble in all the organic solvents tested.

(**3g**): IR (KBr): $\tilde{\nu}$ = 3074, 1580, 1038 cm^{-1}.

2,5-Bis(2,4-dichlorophenyl)-thiazolo[5,4-*d*]thiazole (3h).

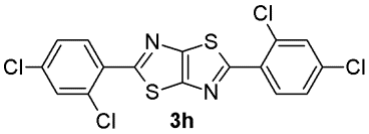

3h

Aldehyde **4h** (350 mg, 2.01 mmol) was reacted with dithiooxamide **2** (120 mg, 1.00 mmol) in 1.0 mL of nitrobenzene, following general procedure **B**. After purification, compound **3h** (311 mg, 72% yield) was obtained as a brown solid, which was insoluble in all the organic solvents tested.

(**3h**): IR (KBr): $\tilde{\nu}$ = 3071, 1582, 1065 cm^{-1}. ESI-MS: *m/z* = 431 (75%), 433 $[M+H]^+$ (100%), 435 (50%), 437 (11%), 439 (1%).

2,5-Bis(thiophen-2-yl)-thiazolo[5,4-*d*]thiazole (3i).[11a,b]

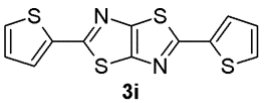

3i

Aldehyde **4i** (897 mg, 8.01 mmol) was reacted with dithiooxamide **2** (240 mg, 2.00 mmol) following general procedure **A**. After purification, compound **3i** (441 mg, 72% yield) was obtained as a yellow solid.

(**3i**): mp = 244–245 °C (lit.11a 246 °C). ^{1}H-NMR (400 MHz, $CDCl_3$): δ = 7.58 (dd, *J* = 3.7 and 1.1 Hz, 2H), 7.47 (dd, *J* = 5.0 and 1.1 Hz, 2H), 7.12 (dd, *J* = 5.0 and 3.7 Hz, 2H) ppm. ^{13}C-NMR (75 MHz, $CDCl_3$): δ = 162.7, 149.9, 137.7, 128.8, 128.3, 126.9 ppm. IR (KBr): $\tilde{\nu}$ = 3116, 1571 cm^{-1}. ESI-MS: *m/z* = 307 $[M+H]^+$.

2,5-Bis(fur-2-yl)-thiazolo[5,4-*d*]thiazole (3j).[2,11a]

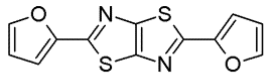

3j

Aldehyde **4j** (192 mg, 2.00 mmol) was reacted with dithiooxamide **2** (120 mg, 1.00 mmol) in 1.0 mL of nitrobenzene, following general procedure **B**. After purification, compound **3j** (181 mg, 66% yield) was obtained as a dark green solid.

(**3j**): mp = >250 °C (dec.) (lit.2 238–240 °C). ^{1}H-NMR (300 MHz, $CDCl_3$): δ = 7.56 (d, *J* = 1.5 Hz, 2H), 7.08 (d, *J* = 3.3 Hz, 2H), 6.59 (dd, *J* = 3.6 and 2.1 Hz, 2H) ppm. ^{13}C-NMR (75 MHz, $CDCl_3$): δ = 158.8, 150.7, 148.8, 144.4, 112.8, 110.3 ppm. IR (KBr): $\tilde{\nu}$ = 3111, 1497 cm^{-1}. ESI-MS: *m/z* = 275 $[M+H]^+$.

2,5-Bis(pyridine-4-yl)-thiazolo[5,4-*d*]thiazole (3k).[11c,13]

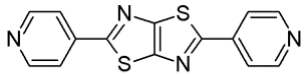

3k

Aldehyde **4k** (214 mg, 2.00 mmol) was reacted with dithiooxamide **2** (120 mg, 1.00 mmol) in 1.0 mL of nitrobenzene, following general procedure **B**. After purification, compound **3k** (196 mg, 66% yield) was obtained as a light brown solid.

(**3k**): mp = 301–304 °C (lit.13 300–302 °C). ^{1}H-NMR (300 MHz, $CDCl_3$): δ = 8.78 (d, *J* = 6.6 Hz, 4H), 7.87 (d, *J* = 6.9 Hz, 4H) ppm. ^{13}C-NMR (100 MHz, $CDCl_3$): δ = 167.6, 152.5, 151.0, 140.6, 120.2 ppm. IR (KBr): $\tilde{\nu}$ = 3038, 1596 cm^{-1}. ESI-MS: *m/z* = 297 $[M+H]^+$.

2,5-Bis(pyridine-2-yl)-thiazolo[5,4-*d*]thiazole (3l).[13,23]

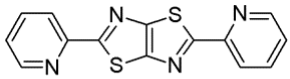

3l

Aldehyde **4l** (214 mg, 2.00 mmol) was reacted with dithiooxamide **2** (120 mg, 1.00 mmol) in 1.0 mL of nitrobenzene, following general procedure **B**. After purification, compound **3l** (225 mg, 76% yield) was obtained as a brown solid.

(**3l**): mp = 334–335 °C (lit.13 325–326 °C). ^{1}H-NMR (300 MHz, $CDCl_3$): δ = 8.66 (d, *J* = 4.5 Hz, 2H), 8.24 (d, *J* = 7.5 Hz, 2H), 7.85 (td, *J* = 7.7 and 1.7 Hz, 2H), 7.37 (dd, *J* = 7.5 and 4.8 Hz, 2H) ppm. ^{13}C-NMR (75 MHz, $CDCl_3$): δ = 171.0, 153.4, 151.6, 149.8, 137.3, 125.2, 120.1 ppm. IR (KBr): $\tilde{\nu}$ = 3056, 1570 cm^{-1}. ESI-MS: *m/z* = 297 $[M+H]^+$.

2,5-Bis(1,3-thiazol-5-yl)-thiazolo[5,4-*d*]thiazole (3m).

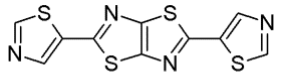

3m

Aldehyde **4m** (226 mg, 2.00 mmol) was reacted with dithiooxamide (120 mg, 1.00 mmol) in 1.0 mL of nitrobenzene, following general procedure **B**. After purification, compound **3m** (231 mg, 75% yield) was obtained as a brown solid.

(**3m**): mp = 295–297 °C. ^{1}H-NMR (300 MHz, $CDCl_3$): δ = 8.91 (s, 2H), 8.37 (s, 2H) ppm. ^{13}C-NMR (100 MHz, $CDCl_3$): δ = 160.0, 155.2, 150.6, 142.5, 133.4 ppm. IR (KBr): $\tilde{\nu}$ = 3048, 1533 cm^{-1}. ESI-MS: *m/z* = 309 $[M+H]^+$. ESI-HRMS (ion trap): *m/z* calcd. for $C_{10}H_5N_4S_4$ $[M+1]^+$ 308.9392. Found 308.9395.

2,5-Bis(2,3-dihydrothieno[3,4-*b*][1,4]-dioxin-5-yl)-thiazolo[5,4-*d*]thiazole(3n).

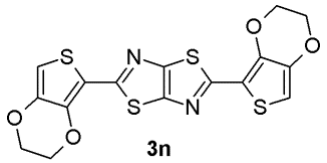

3n

Aldehyde **4n** (340 mg, 2.00 mmol) was reacted with dithiooxamide **2** (120 mg, 1.00 mmol) in 1.0 mL of nitrobenzene, following general procedure **B**. After purification, compound **3n** (341 mg, 81% yield) was obtained as a brown solid.

(**3n**): mp = >350 °C (dec.). ^{1}H-NMR (400 MHz, DMSO-d_6): δ = 6.94 (s, 2H), 4.50–4.53 (m, 4H), 4.33–4.36 (m, 4H) ppm. IR (KBr): $\tilde{\nu}$ = 3107, 2926, 1507, 1065 cm^{-1}. ESI-MS: *m/z* = 423 $[M+H]^+$. ESI-HRMS (ion trap) *m/z* calcd for $C_{16}H_{11}O_4N_2S_4$ $[M+1]^+$ 422.9596. Found 422.9596.

*Note: due to the low solubility of compound **3n** in most organic solvents it was not possible to record a suitable ^{13}C-NMR spectrum.*

2,5-Dihexyl-thiazolo[5,4-*d*]thiazole (3o).

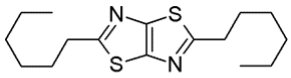

3o

Aldehyde **4o** (228 mg, 2.00 mmol) was reacted with dithiooxamide **2** (120 mg, 1.00 mmol) in 1.0 mL of nitrobenzene, following general procedure **B**. Purification by flash column chromatography (SiO_2; PE/Et_2O = 10/1) afforded compound **3o** (124 mg, 40% yield) as a pale yellow oil.

(**3o**) ^{1}H-NMR (300 MHz, $CDCl_3$): δ = 3.04 (t, *J* = 7.6 Hz, 4H), 1.82 (q, *J* = 7.4 Hz, 4H), 1.25–1.47 (m, 12H), 0.83–0.92 (m, 6H) ppm. ^{13}C-NMR (75 MHz, $CDCl_3$): δ = 172.6, 148.4, 35.1, 31.6, 29.9, 28.8, 22.6, 14.2 ppm. IR (KBr): $\tilde{\nu}$ = 2927, 1467 cm^{-1}. ESI-MS: *m/z* = 311 $[M+H]^+$. ESI-HRMS (ion trap) *m/z* calcd for $C_{16}H_{27}N_2S_2$ $[M+1]^+$ 311.1610. Found 311.1615.

2,5-Dicyclohexyl-thiazolo[5,4-*d*]thiazole (3p).

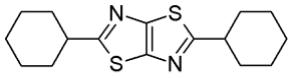

3p

Aldehyde **4p** (897 mg, 8.01 mmol) was reacted with dithiooxamide **2** (240 mg, 2.00 mmol) following general procedure **A**. After purification, compound **3p** (245 mg, 40% yield) was obtained as a light brown solid.

(**3p**): mp = 140–141 °C. ^{1}H-NMR (300 MHz, $CDCl_3$): δ = 3.03 (tt, *J* = 11.4 and 3.2 Hz, 2H), 2.14–2.19 (m, 4H), 1.84–1.89 (m, 4H), 1.72–1.77 (m, 2H), 1.52–1.66 (m, 4H), 1.26–1.47 (m, 6H) ppm. ^{13}C-NMR (75 MHz, $CDCl_3$): δ = 178.0, 148.0, 44.1, 33.6, 26.1, 25.9 ppm. IR (KBr): $\tilde{\nu}$ = 2923, 1465 cm^{-1}. ESI-MS: *m/z* = 307 $[M+H]^+$. Anal. calcd for $C_{16}H_{22}N_2S_2$: C, 62.70; H, 7.24; N, 9.14. Found: C, 62.94; H, 7.59; N, 9.13%.

2,5-Di-t-butyl-thiazolo[5,4-*d*]thiazole (3q).

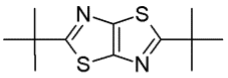

3q

Aldehyde **4q** (172 mg, 2.00 mmol) was reacted with dithiooxamide **2** (120 mg, 1.00 mmol) and 1.0 mL of nitrobenzene, following general procedure **B**. Purification by flash chromatography (SiO_2; PE/Et_2O = 10/1) afforded compound **3q** (84 mg, 33% yield) as a brown solid.

(**3q**): mp = 109–111 °C. ^{1}H-NMR (300 MHz, $CDCl_3$): δ = 1.48 (s, 18H) ppm. ^{13}C-NMR (75 MHz, $CDCl_3$): δ = 182.4, 148.4, 39.0, 30.7 ppm. IR (KBr) $\tilde{\nu}$ = 2961, 1484 cm^{-1}. ESI-MS: *m/z* = 255 $[M+H]^+$. Anal. calcd for $C_{12}H_{18}N_2S_2$: C, 56.65; H, 7.13; N, 11.01. Found: C, 56.33; H, 7.01; N, 10.64%.

2,5-Distyryl-thiazolo[5,4-*d*]thiazole (3r).[2]

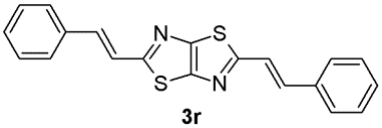

3r

Aldehyde **4r** (264 mg, 2.00 mmol) was reacted with dithiooxamide **2** (120 mg, 1.00 mmol) and 1.0 mL of nitrobenzene, following general procedure **B**. Compound **3r** (31 mg, 9% yield) was obtained as a black solid.

(**3r**): mp = >260 °C (lit.2 242–243 °C). ^{1}H-NMR (300 MHz, $CDCl_3$): δ = 7.55–7.58 (m, 4H), 7.49 (d, *J* = 16.2 Hz, 2H), 7.35–7.44 (m, 6H), 7.30 (d, *J* = 16.2 Hz, 2H); ^{13}C-NMR (75 MHz, $CDCl_3$): δ = 168.3, 150.5, 135.5, 135.1, 129.5, 129.1, 127.4, 122.2 ppm. IR (KBr): $\tilde{\nu}$ = 3057, 1653, 1570 cm^{-1}. ESI-MS: *m/z* = 347 $[M+H]^+$.

2,5-Bis[3,5-di(oct-1-yn-1-yl)phenyl]-thiazolo[5,4-d]thiazole (6).

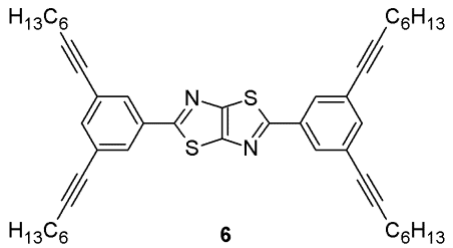

6

Compound **3g** (110 mg, 0.18 mmol), was suspended in triethylamine (6.0 mL), and reacted with oct-1-yne (199 mg, 1.80mmol), CuI (3.4mg, 0.018 mmol), and $Pd(PPh_3)_2Cl_2$ (13 mg, 0.018 mmol). The resulting slurry was heated to 105 °C and stirred for 20 h, then it was cooled to room temperature. The reaction mixture was filtered on a short pad of Celite® and the filter cake was washed several times with $CHCl_3$; the filtrate solution was washed with water (100 mL) and brine (100 mL) and dried with Na_2SO_4. Evaporation gave a dark oil which was purified by flash column chromatography (SiO_2, PE/Et_2O = 98/2) to give, after further recrystallization from AcOEt, pure compound **6** (15 mg, 11% yield) as a yellow sticky solid.

(**6**): ^{1}H-NMR (400 MHz, $CDCl_3$): δ = 7.90 (d, *J* = 1.4 Hz, 4H), 7.48 (s, 2H), 2.42 (t, *J* = 7.1 Hz, 8H), 1.55–1.65 (m, 8H), 1.46–1.49 (m, 8H), 1.31–1.36 (m, 16H), 0.92 (t, *J* = 6.9 Hz, 12H) ppm. ^{13}C-NMR (75 MHz, $CDCl_3$): δ = 168.2, 151.2, 136.5, 134.1, 128.4, 125.5, 92.4, 79.3, 31.5, 28.8, 28.7, 22.7, 19.6, 14.3 ppm. IR (KBr): $\tilde{\nu}$ = 2929, 2229, 1582, 1466 cm^{-1}. ESI-MS: *m/z* = 727 $[M+H]^+$. ESI-HRMS (ion trap) *m/z* calcd for $C_{48}H_{59}N_2S_2$ $[M+1]^+$ 727.4114. Found 727.4113.

3.4. References

[1] Ephraim J. *Ber. Dtsch. Chem. Ges.*, **1891**, *24*, 1026

[2] Johnson J. R., Ketcham R. *J. Am. Chem. Soc.*, **1960**, *82*, 2719

[3] Bevk D., Marin L., Lutsen L., Vanderzande D., Maes W. *RSC Adv.*, **2013**, *3*, 11418

[4] Johnson J. R., Rotenberg D. H., Ketcham R. *J. Am. Chem. Soc.*, **1970**, *92*, 4046

[5] Naraso, Wudl F. *Macromolecules*, **2008**, *41*, 3169

[6] Cheng C., Yu C., Guo Y., Chen H., Fang Y., Yu G., Liu Y. *Chem. Commun.*, **2013**, *49*, 1998

[7] Peng Q., Peng J.-B., Kang E. T., Neoh K. G., Cao Y. *Macromolecules*, **2005**, *38*, 7292

[8] Ando S., Nishida J.-I., Inoue Y., Tokito S., Yamashita Y. *J. Mater. Chem.*, **2004**, *14*, 1787

[9] Osaka I., Sauvé G., Zhang R., Kowalewski T., McCullough R. D. *Adv. Mater.*, **2007**, *19*, 4160

[10] Zani L., Calamante M., Mordini A., Reginato G. in *Targets in Heterocyclic Systems* (Eds.: Attanasi O. A., Spinelli D.), Società Chimica Italiana, Rome, **2014**, vol. 17, p. 87

[11] a) Thomas D. A. *J. Heterocycl. Chem.*, **1970**, *7*, 457. b) Jung I. H., Yu J., Jeong E., Kim J., Kwon S., Kong H., Lee K., Woo H. Y., Shim H.-K *Chem. Eur. J.*, **2010**, *16*, 3743. c) Hisamatsu S., Masu H., Azumaya I., Takahashi M., Kishikawa K., Kohmoto S. *Cryst. Growth Des.*, **2011**, *11*, 5387

[12] a) Ando S., Nishida J.-I., Fujiwara E., Tada H., Inoue Y., Tokito S., Yamashita Y. *Chem. Lett.*, **2004**, *33*, 1170. b) Ando S., Kumaki D., Nishida J.-I., Tada H., Inoue Y., Tokito S., Yamashita Y. *J. Mater. Chem.*, **2007**, *17*, 553

[13] Knighton R. C., Hallet A. J., Kariuki B. M., Pope S. J. A. *Tetrahedron Lett.*, **2010**, *51*, 5419

[14] a) Hansen P., Liebich W. DD154978 (**1982**). b) Roethling T., Schroeder A., Kibbel H., Kochmann K., Naumann K. DD208354 (**1984**) and DD210457 (**1984**). c) Roethling T., Polanek M., Hansen P., Kibbel H., Naumann K., Thust U. DD216241 (**1984**).

[15] Jung I. H., Jung Y. K., Lee J., Park J.-H., Woo H. Y., Lee J.-I., Chu H. Y., Shim H. K. *J. Polym. Sci., Part A: Polym. Chem.*, **2008**, *46*, 7148

[16] a) Polshettiwar V., Varma R. S. *Acc. Chem. Res.*, **2008**, *41*, 629. b) Kappe C. O., Stadler A. , Dallinger D. *Microwaves in Organic and Medicinal Chemistry*, Wiley-VCH, Weinheim, 2nd edn, **2012**

[17] Sharma A., Appukkuttan P., Van der Eycken E. *Chem. Commun.*, **2012**, *48*, 1623

[18] Li D., Zhang Z., Zhao S., Wang Y., Zhang H. *Dalton Trans.*, **2011**, *40*, 1279

[19] US Pat. 2009/156827 A1, **2009** (TOYO INK MFG. CO. LTD). In this patent the structures of eight aliphatic derivatives are shown, but their synthesis and characterization are not described in the preparative examples

[20] Campbell I. B., The Sonogashira Cu-Pd-catalysed alkyne coupling reaction, in *Organocopper Reagents, a Practical Approach*, ed. R. J. K. Taylor, Oxford University Press, New York, **1994**

[21] a) Fikrat H. T., Oneto J. F. *J. Pharm. Sci.*, **1962**, *51*, 527. b) Ketcham R., Mah S. *J. Med. Chem.*, **1971**, *14*, 743

[22] Papernaya L. K., Shatrova A. A., Sterkhova I. V., Levkovskaya G. G., Rozntsveig I. B. *Russ. J. Org. Chem.*, **2015**, *51*, 3

[23] Zampese J. A., Keene F. R., Steel P. J. *Dalton Trans.*, **2004**, 4124

Chapter 4

Thiazolo[5,4-*d*]thiazole-based sensitizers for thin-layer Dye-Sensitized Solar Cells (DSSCs)

Dessì A., Calamante M., Mordini A., Peruzzini M., Sinicropi A., Basosi R., Fabrizi de Biani F., Taddei M., Colonna D., di Carlo A., Reginato G., Zani L. *Chem. Commun.*, **2014**, *50*, 13952

Dessì A., Calamante M., Mordini A., Peruzzini M., Sinicropi A., Basosi R., Fabrizi de Biani F., Taddei M., Colonna D., di Carlo A., Reginato G., Zani L. *RSC Adv.*, **2015**, *5*, 32657

4.1. Introduction and aim of the work

Once the procedure for the synthesis of the thiazolo[5,4-*d*]thiazole core was optimized, we considered the design of some possible new structures of TzTz-dyes for DSSC applications. In a previous study conducted in the laboratory where this work was carried out, a new family of D-π-A dyes featuring different bis-thiazole cores as π-conjugated spacers was prepared and tested,[1] and dye **TTZ1** (Figure 4.1), bearing a thiazolo[5,4-*d*]thiazole scaffold, was the best performing one, recording a maximum efficiency (η) of 3.53% in the presence of chenodeoxycholic acid (CDCA) as coadsorbent.

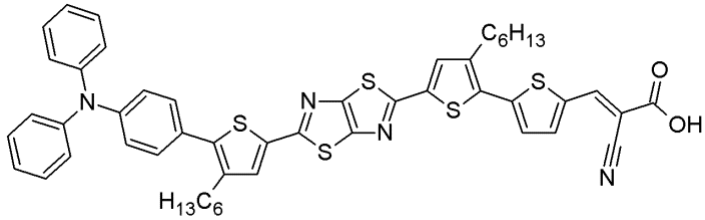

TTZ1

Figure 4.1. Structure of previously described TTZ1 dye.

TTZ1 exhibited a moderate absorption of solar light between 400 and 500 nm (λ_{max} = 472 nm; ε = 2.76 × 10^4 M^{-1} cm^{-1}) with an offset around 550 nm, a reversible electrochemical behavior and right redox potentials for electron injection in the TiO_2 layer and regeneration from the electrolyte. Despite fair values of open-circuit potential (V_{oc} = 0.58-0.62 mV) and *fill factor* (*ff* = 0.72-0.74), a low short-circuit photocurrent (J_{sc} = 5.48-6.42 mA cm^{-2}) did not allow to obtain higher efficiencies. The major drawbacks of **TTZ1**, which could be responsible for its moderate efficiency, were attributed to a limited light-harvesting ability, a poor solubility in the most common organic solvents and a tendency to form aggregates on the surface of TiO_2 layer, which was supported by the increased photocurrents observed when CDCA was added as a coadsorbent.

Starting from these results, we designed a new series of thiazolothiazole-based dyes (Figure 4.2) focusing, initially, on two main targets: increase their visible light absorption and try to minimize the undesired π-stacking effects. The first modification we decided to introduce was the substitution of the hexyl chains present in **TTZ1** with alkoxy substituents with the aim of reducing the aromatic stabilization of the thiophene rings. Such substitution, having the effect to increase

the HOMO energies of the new dyes, could cause a decrease of their HOMO-LUMO gaps, thus inducing a red-shift of their absorption spectra.

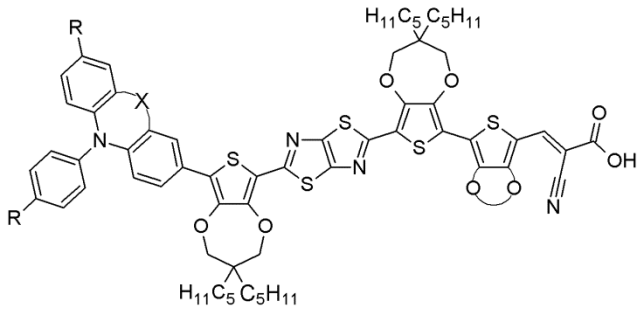

Figure 4.2. Generic structure of new TzTz-based dyes.

Our first choice was that of introducing the 3,4-ethylendioxythiophene (EDOT, Figure 4.3a) moiety on the dye scaffold, since sensitizers bearing EDOTs have already shown impressive performances in DSSCs.[2] However, the very low solubility of the corresponding TzTz derivative[3] **3n** (Figure 4.3b, see also Chapter 3, Table 3.2) in most of the common organic solvents prompted us to find a more suitable alternative.

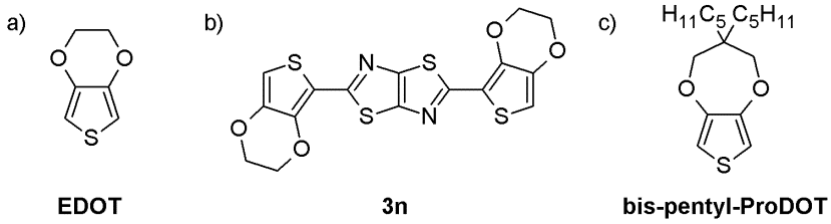

Figure 4.3. Structure of a) EDOT, b) TzTz compound 3n and c) bis-pentyl-ProDOT.

Therefore, we selected the structure of *bis*-pentylpropylenedioxythiophene (ProDOT, Figure 4.3c)[4] which conjugates the attractive properties of EDOT with a higher solubility, thanks to the presence of the two alkyl chains. Moreover, the presence of a tetrahedral central carbon in the cycloheptane ring, on which many different functional groups could be installed, enables the construction of three-dimensional branched structures which might be effective to minimize the undesired π-stacking effects. This would result not only in a reduction of dye aggregation on the surface of the semiconductor, but also in the shielding of the TiO_2 layer from the electrolyte, thus reducing charge recombination of injected electrons. Once the π-scaffold was selected, we planned to introduce different donor groups in order to further

modulate the electronic properties of the dyes and possibly enhance their photovoltaic performances.

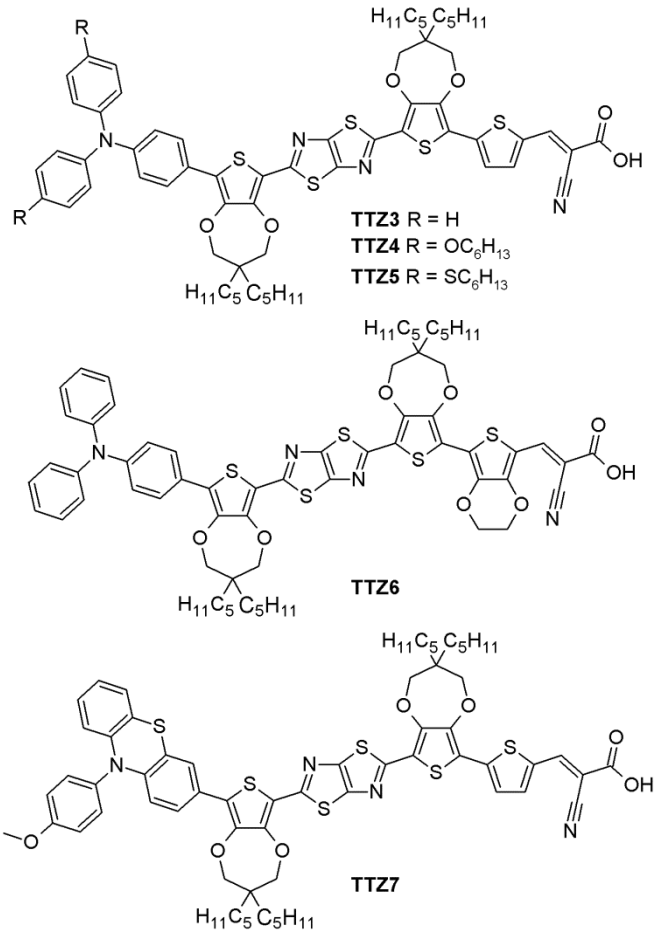

Figure 4.4. Structures of new TzTz-based dyes TTZ3-7

We designed five different molecules as reported in Figure 4.4. The terminal triphenylamine group was decorated with hexyloxy- chains (**TTZ4**), in order to increase its electron-donating character and get a further red-shift of the absorption spectrum, but also with hexylthio- chains (**TTZ5**), as these substituents had been reported to enhance dye-regeneration and increase the V_{oc} value compared to their oxygenated counterparts.[5] Moreover we planned to introduce an additional electronrich EDOT ring in place of the terminal thiophene (**TTZ6**) and also to test a different donor group, such as phenothiazine[6] (**TTZ7**).

The selected structures **TTZ3**-**7** were computationally analyzed in order to predict the energies and shapes of their frontier molecular orbitals (FMOs) and the light-absorption properties of the dyes. Then, the synthesis of the molecules was accomplished; the dyes were characterized through spectroscopic and electrochemical analysis and, finally, some test solar cells containing **TTZ3**-**7** were built to assess their photovoltaic properties.

4.2. Results and discussion

4.2.1. Computational analysis

Before approaching the synthesis of **TTZ3**-**7**, a computational analysis which could predict the absorption maxima of the dyes and the energy levels and shapes of their HOMO and LUMO was performed. This was possible thank to a collaboration with Dr. Adalgisa Sinicropi in Siena University who carried out all the theoretical calculations reported in this work.

In the calculations, the alkyl chains present on the molecules were replaced by simple methyl groups to reduce the computational burden, without affecting the length and nature of the conjugate system. Initially, the selected structures having both ProDOT rings in the most stable "chair" conformation were optimized *in vacuo* by means of TD-DFT calculations, which were performed with the Gaussian09 program package,[7] at the B3LYP/6-31G* level.[8] The energy and the shape of the frontier molecular orbitals (FMOs) were calculated.

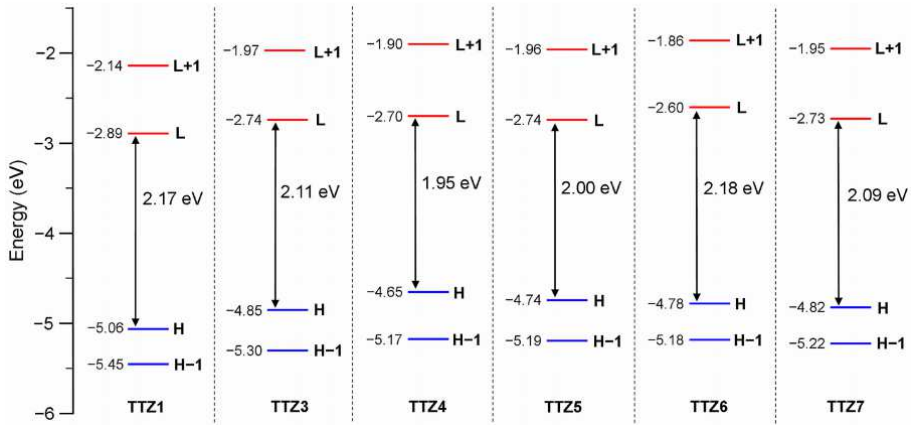

Figure 4.5. Computed (B3LYP/6-31G) HOMO–LUMO energy gaps of compounds TTZ1 and TTZ3-7.*

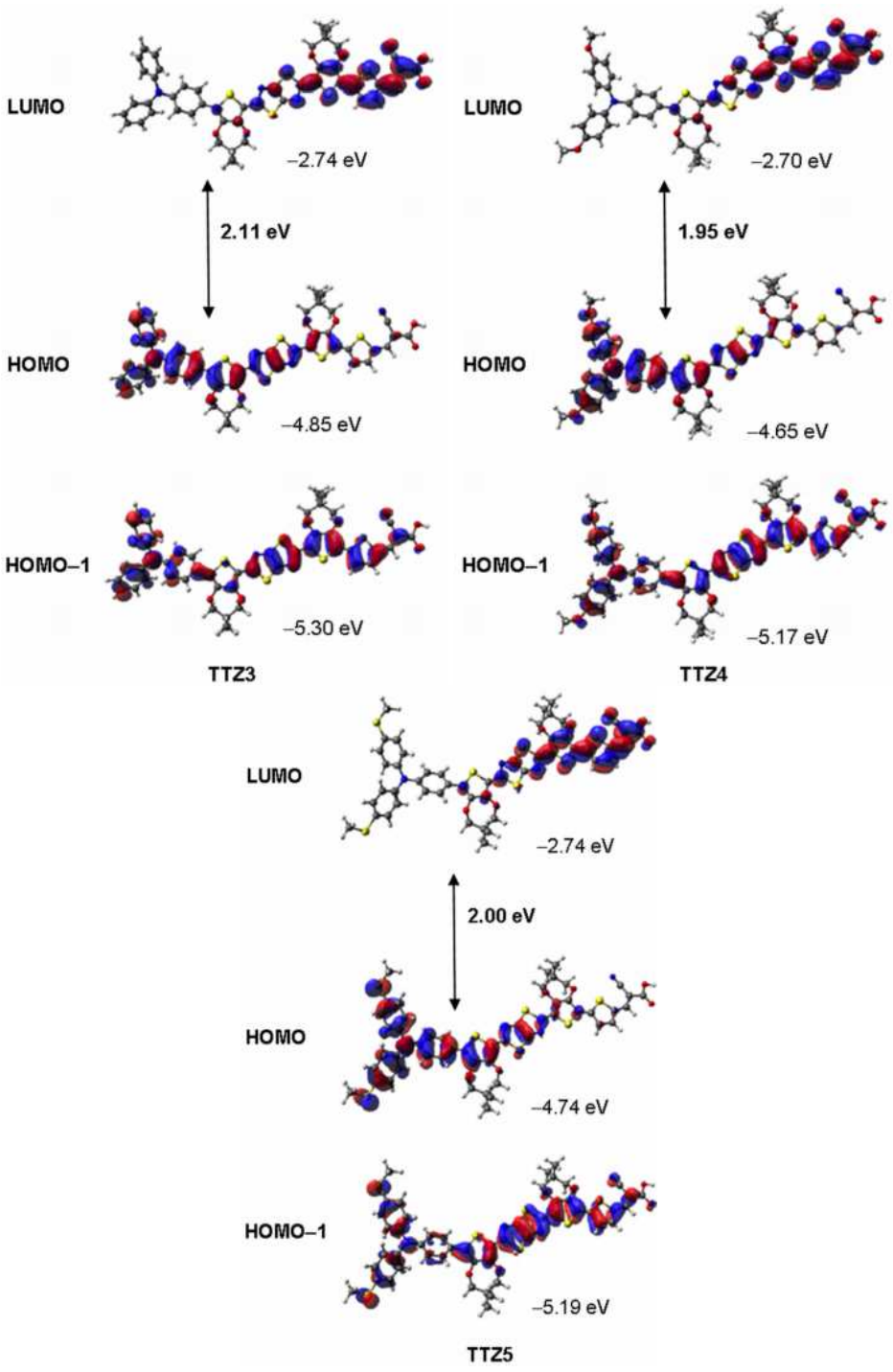

Figure 4.6. Isodensity plots and computed energies for the frontier molecular orbitals of compounds TTZ3-7 at the B3LYP/6-31G level.*

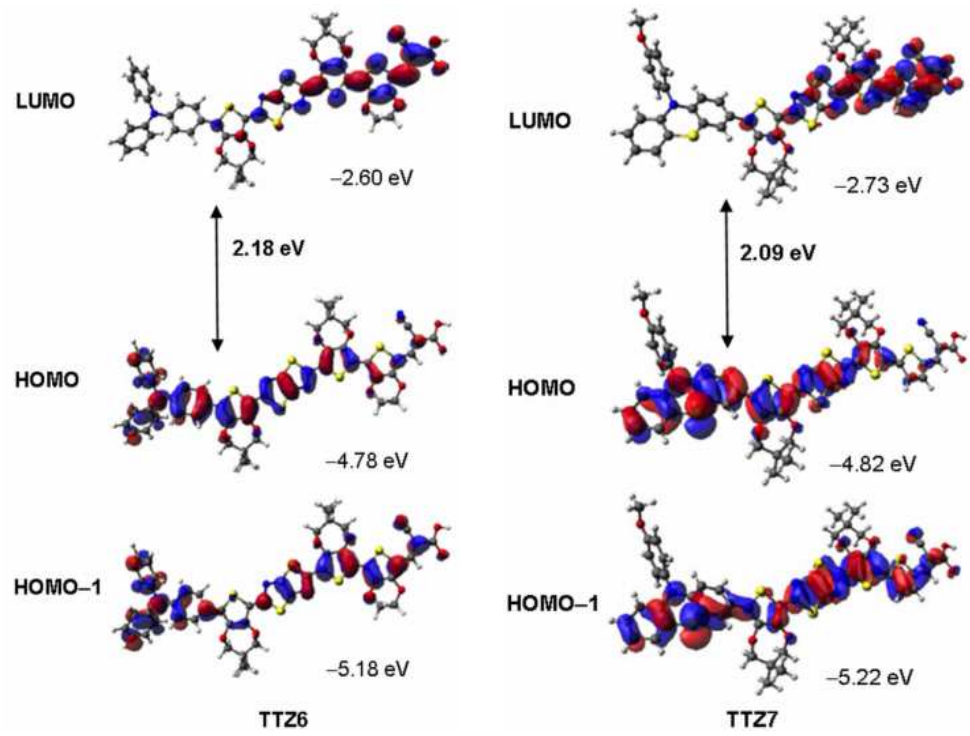

Figure 4.6. (continued) Isodensity plots and computed energies for the frontier molecular orbitals of compounds TTZ3-7 at the B3LYP/6-31G* level.

The HOMO/LUMO energy gaps, compared with those previously found for **TTZ1** as a reference,[1] are reported in Figure 4.5, while the wavefunction plots of **TTZ3**-**7** are drawn in Figure 4.6.

All the **TTZ3**-**7** dyes had smaller HOMO/LUMO energy gaps than **TTZ1**, which was mostly due to the HOMO destabilization, as expected by the introduction of ProDOT rings in place of simple thiophenes: this effect is particularly evident comparing the energy gaps of **TTZ1** and **TTZ3** (2.17 eV vs. 2.11 eV). The introduction of hexyloxy-chains in **TTZ4** increased the electron-donating properties of the triphenylamine group leading to a corresponding increase of the HOMO energy compared to **TTZ3** (+ 0.20 eV). Hexylthio- chains (**TTZ5**) had a similar, but smaller, effect on the HOMO energy, resulting in a FMO gap of 2.00 eV. On the other hand, the introduction of a more electronrich group in proximity of the electron-withdrawing moiety (**TTZ6**) caused a destabilization of the LUMO orbital without affecting the HOMO and, consequently, an increase of the HOMO/LUMO energy gap (2.18 eV), which is the largest one in this series of structures. Finally, the substitution of triphenylamine with

phenothiazine (**TTZ7**) did not alter significantly the FMO gap (2.09 eV). All the TzTz-compounds had similar frontier orbital shapes (Figure 4.6): while the HOMO–1 was distributed along the entire conjugated system, the HOMO and LUMO orbitals were mostly localized on the donor and the acceptor moieties, respectively.

Table 4.1. CAMB3LYP/6-31G absorption maxima (λ_{max}), oscillator strengths (f), vertical excitation energies (E_{exc}) and main electronic transitions for dyes TTZ1 (taken as a reference) and TTZ3-7 in THF.*

Compound	λ_{max} [nm]	*f*	E_{exc} [eV]	Main transitions (%)
TTZ1[a]	482	2.45	2.57	H−1 → L 51.2
				H → L 29.2
TTZ3	503	2.61	2.46	H → L 42.0
				H−1 → L 38.2
TTZ4	507	2.67	2.45	H−1 → L 47.4
				H → L 30.5
TTZ5	504	2.66	2.46	H−1 → L 48.7
				H → L 29.3
TTZ6	509	2.54	2.43	H → L 47.0
				H−1 → L 36.6
TTZ7	501	2.59	2.47	H → L 45.4
				H−1 → L 34.6

a) Values taken from ref. 1.

To learn more on the electronic transitions of the new organic sensitizers, the absorption maxima (λ_{max}), oscillator strengths (*f*) and vertical excitation energies (E_{exc}) in the most stable conformation were assessed by TD-DFT calculations in THF at the CAM-B3LYP/6-31G* level[9] (Table 4.1).

The computational results were in agreement with our expectations because the predicted absorption maxima of all the dyes were higher than 500 nm and red-shifted of 20-30 nm relative to **TTZ1**, while the higher oscillator strengths suggested the possibility of more intense light absorption. Mixed HOMO–1 → LUMO and HOMO → LUMO transitions characterized the excitation process in the visible region; interestingly, although **TTZ6** was the compound with the highest computed HOMO-LUMO gap, the larger H→L component in its excitation process caused a slightly red-shifted absorption maximum, if compared to the other dyes.

4.2.2. Synthesis of TTZ3–7 dyes

4.2.2.1. Retrosynthesis

All the **TTZ3**-**7** dyes could be synthesized following the same retrosynthetic approach depicted in Scheme 4.1 for **TTZ3**. Six steps are necessary to build the common π-scaffold **11**, while donor and acceptor moieties can be introduced in three subsequent steps. Introduction of the cyanoacrylic moiety can be performed by a Knoevenagel reaction between cyanoacetic acid (**8**) and aldehyde **7**, which is obtained through two consecutive cross-coupling reactions using the proper organometallic reagents **10** and **12.** Accordingly, the donor group and a formyl-thiophene are introduced, starting from the diiodide **11**. Thus, all the structural modifications which characterize every dye could be introduced starting from common π-scaffold **11**, which in turn could be obtained by electrophilic iodination of compound **13**. The TzTz-scaffold of **13** is obtained starting from aldehyde **14** and dithiooxamide (**2**) using our optimized condensation/oxidation sequence for the synthesis of thiazolo[5,4-*d*]thiazoles[3] (see Chapter 3). Aldehyde **14** is then prepared by formylation of ProDOT **15**, obtained by transetherification of commercially available 3,4-dimethoxythiophene **16** and diol **17**. Finally, diol **17** is synthesized by simple reduction of diester **18** and alkylation of diethylmalonate (**19**).

4.2.2.2. Synthesis of π–scaffold 11

According to the above analysis, aldehyde **14** was thus prepared following a four steps procedure which had already been described in the literature[10] (Scheme 4.2):

I. Alkylation of diethylmalonate (**19**) using 1-bromopentane as the electrophile and sodium hydride as the base in anhydrous THF gave desired product **18**, which was purified by distillation.
II. Reduction of diester **18** with lithium aluminum hydride in anhydrous diethyl ether gave the corresponding diol **17**, which was used in the following step without any further purification.
III. Transetherification between thiophene **16** and diol **17** was catalyzed by *p*-toluenesulfonic acid and performed in toluene, using a Soxhlet apparatus with activated molecular sieves (MS-4Å) to remove the formed methanol. This was necessary, in order to shift the equilibrium between the two ethers **15** and **16** towards the formation of ProDOT **15,** which was purified by flash column chromatography. The unreacted excess of diol **17** could be recovered as well for later reuse.

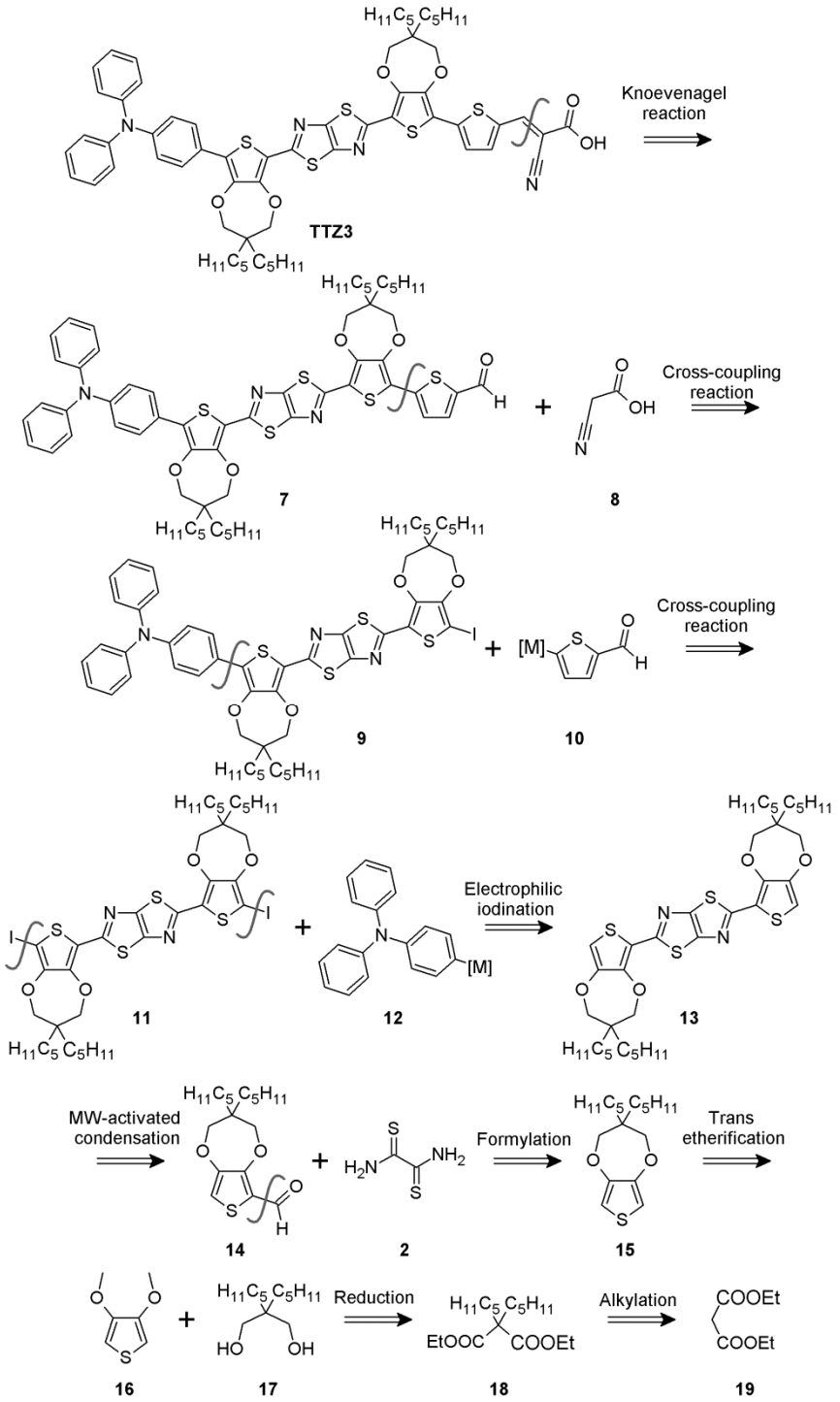

Scheme 4.1. Retrosynthesis of TTZ3 dye.

IV. Monolithiation of ProDOT **15** in 2-position was accomplished using *n*-butyllithium in anhydrous THF. Subsequent formylation of the organolithium derivative-with *N*,*N*-DMF as the electrophile gave aldehyde **14**, which was purified by flash column chromatography.

All these steps were high yielding and could be performed on multi-gram scale, leading to the desired aldehyde in an overall yield of approximately 50%.

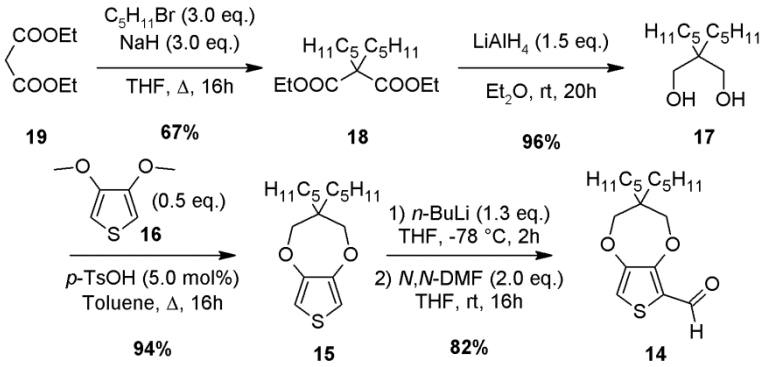

19 **67%** **18** **96%** **17**

94% **16** **15** **82%** **14**

Scheme 4.2. Synthesis of π-scaffold 11.

Once aldehyde **14** had been obtained, our protocol for the synthesis of thiazolo[5,4-*d*]thiazoles[3] was applied to the preparation of TzTz-derivative **13.** Unfortunately, the final product did not precipitate, as usual, from the reaction mixture (see Chapter 3) thus requiring purification by flash column chromatography followed by washing with methanol several times to completely remove nitrobenzene and obtain pure thiazolothiazole **13** in 27% yield (Table 4.2, entry 1).

Clearly, the presence of the long alkyl chains on the ProDOT ring affected the solubility of the final compounds making its purification more difficult. For this reason, we decided to modify the reaction conditions using *n*-BuOH as the solvent[11] since the latter could be more easily removed from the crude reaction mixture compared to nitrobenzene. Due to the lower boiling point of *n*-BuOH, it was necessary to reduce the reaction temperature to 120 °C and extend the reaction time to 2.5 hours (entry 2). Under these conditions, desired product **13** was easily isolated with an improved yield of 42%. A control experiment carried out under thermal heating (entry 3) proved also in this case the accelerating effect of microwaves, since almost 24 hours were necessary to obtain the desired product with approximately the same yield.

Table 4.2. Optimization of the synthesis of TzTz-derivative 13.

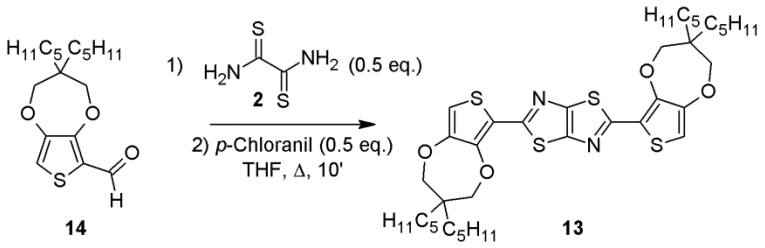

Entry	Solvent	Heating	Time (h)	Temperature (°C)	Yield (%)
1	Nitrobenzene	MW	0.5	150	27%
2	*n*-butanol	MW	2.5	120	42%
3	*n*-butanol	Thermal	24	120	41%

Electrophilic iodination of compound **13** was performed using *N*-iodosuccinimide in a 1/1 mixture of chloroform and acetic acid (Scheme 4.3). Diiodide **11**, being insoluble, precipitated from the reaction mixture, from which it was recovered in high yield after washing with methanol and ethyl acetate.

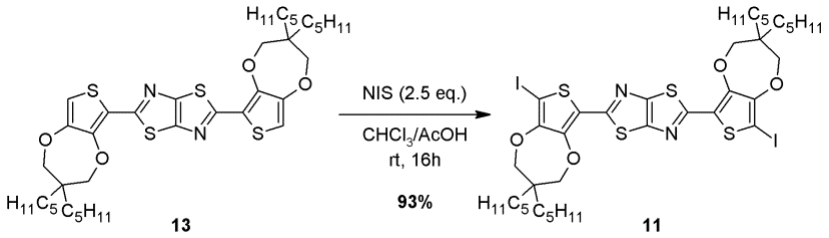

Scheme 4.3. Iodination of TzTz-containing scaffold 13.

4.2.2.3. Insertion of donor groups

Diiodide **11** is the key intermediate of our synthetic strategy and was used as starting material for the preparation of all **TTZ3**-**7** dyes. The Suzuki-Miyaura cross-coupling reaction was the procedure selected for the insertion of four different donor groups, using boronic esters **21**-**23** and boronic acid **20** (Figure 4.7) as the organometallic counterparts. Except for boronic acid **20**, which is commercially available, reagents **21**-**23** had to be synthesized.

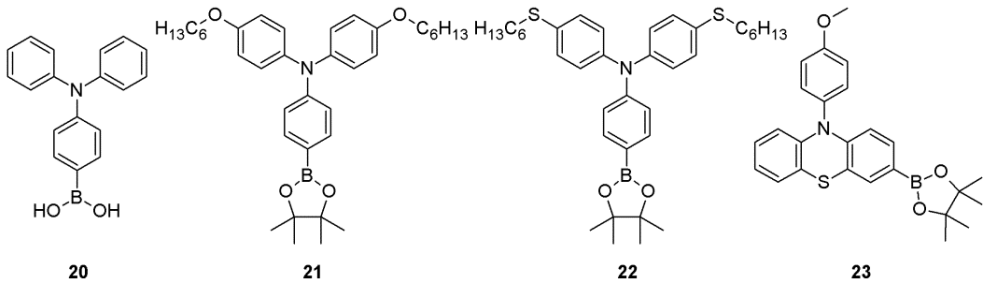

Figure 4.7. Structures of boronic acid/esters 20-23 used for the Suzuki reaction.

4.2.2.3.1. Synthesis of boronic esters 21–23

Organoboron compound **21** was prepared using a slight modification of a previously reported three-step sequence, which was necessary to assemble the triarylamine scaffold and introduce the boronic ester function (Scheme 4.4).[12] The first step was based on a Pd-catalyzed Buchwald-Hartwig reaction between 4-bromohexyloxybenzene **24** and 4-aminohexyloxybenzene **25**: the required catalytic complex was formed *in situ* by using $Pd_2(dba)_3$ as a precatalyst and 1,1'-bis(diphenylphosphino)ferrocene (dppf) as the ligand, while sodium *tert*-butoxide was chosen as the base and anhydrous and degassed toluene as the solvent.[13] Under these conditions compound **26** was obtained in high yield (84%).

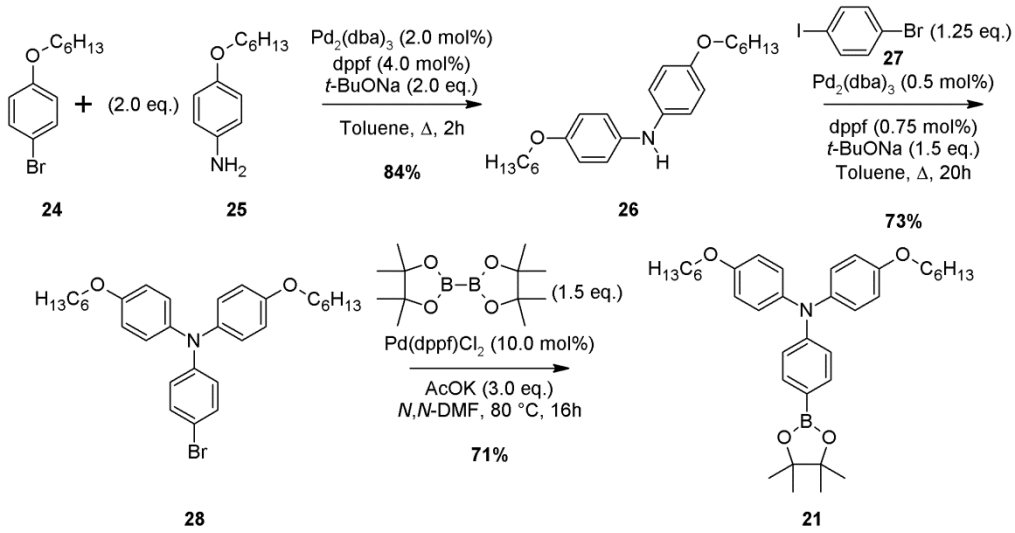

Scheme 4.4. Synthesis of boronic ester 21.

Very similar conditions were applied to react amine **26** and 1-bromo-4-iodobenzene (**27**):[14] taking advantage of the different reactivity of the carbon-iodine and carbon-bromine bonds, it was possible to isolate brominated triarylamine **28** in good yield (73%). Finally, the synthesis of the desired organoboron compound **21** was accomplished applying Miyaura borylation reaction conditions.[15] Using bis(pinacolato)diboron as a borylating agent, $Pd(dppf)Cl_2$ as the catalyst, potassium acetate as the base and anhydrous and degassed *N*,*N*-DMF as the solvent, boronic ester **21** was prepared with a yield of 71%. The synthesis of compound **21** was accomplished with an overall yield of 44%.

Boronic ester **22,** bearing two hexylthio- chains, had already been synthesized by Berlinguette *et al.*[16] starting from 4-bromo-*N*-(4-bromophenyl)-*N*-phenylaniline, using a three-steps synthesis with an overall yield of 10%. In order to increase the yield of the desired product, we elaborated a different synthetic sequence, starting from 1-bromo-4-iodobenzene (**27**) (Scheme 4.5).

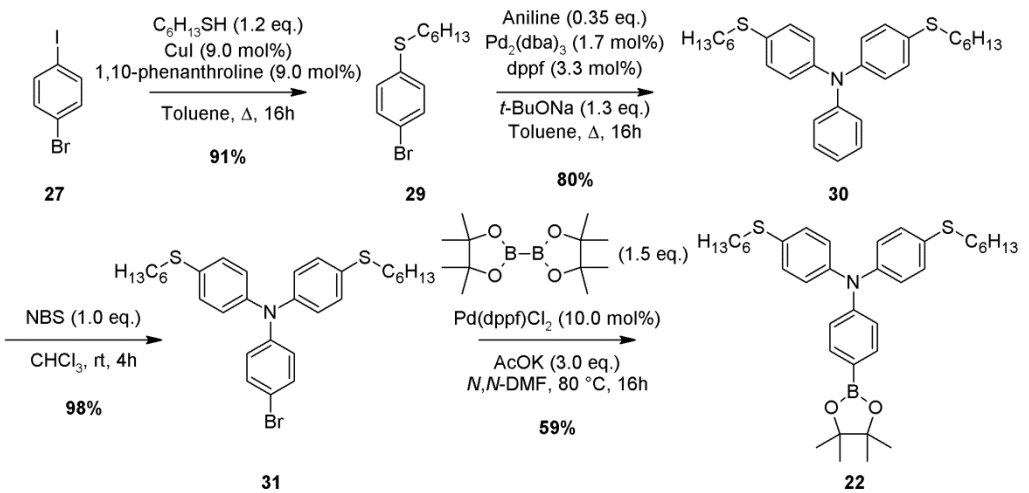

Scheme 4.5. Synthesis of boronic ester 22.

The reaction conditions described by Venkataraman *et al.*[17] for the synthesis of thioethers were applied to accomplish a Ullmann-type reaction between compound **27** and 1-hexanethiol under catalysis of copper iodide and 1,10-phenanthroline. The catalytic system was able to discriminate the two different carbon-halogen bonds of **27,** producing 1-bromo-4-hexylthiobenzene (**29**) in a very high yield (91%). Using the same Buchwald-Hartwig conditions described for the synthesis of compounds **26** and **28** (Scheme 4.4), triarylamine **30** was obtained in good yield and quantitatively

halogenated with *N*-bromosuccinimide (NBS) to bromo-derivative **31**. Finally, boronic ester **22** was prepared applying the same experimental conditions used for the synthesis of **21** (Scheme 4.4). The whole sequence allowed the preparation of ester **22** with an overall yield of 42%, which was a remarkable improvement if compared to the previously reported procedure.[16]

Finally, boronic ester **23** was previously unreported and was prepared employing the synthetic procedure depicted in Scheme 4.6. This time, the usual Buchwald-Hartwig conditions proved unsatisfactory when applied to the reaction between phenothiazine (**32**) and 4-iodoanisole (**33**): indeed, in this case, after one night at reflux in toluene, the reaction mixture still contained approximately half of the starting material **32**. However, a simple switch of the ligand from dppf to the more hindered tri-*tert*-butylphosphine enabled the complete conversion of phenothiazine (**32**) and the isolation of desired product **34** with a good yield (75%). The electrophilic monobromination of **34** was initially performed using a stoichiometric amount of *N*-bromosuccinimide or elemental bromine as brominating reagents: under these conditions, an inseparable mixture of starting material **34**, desired monobromide **35** and dibrominated product was always found.

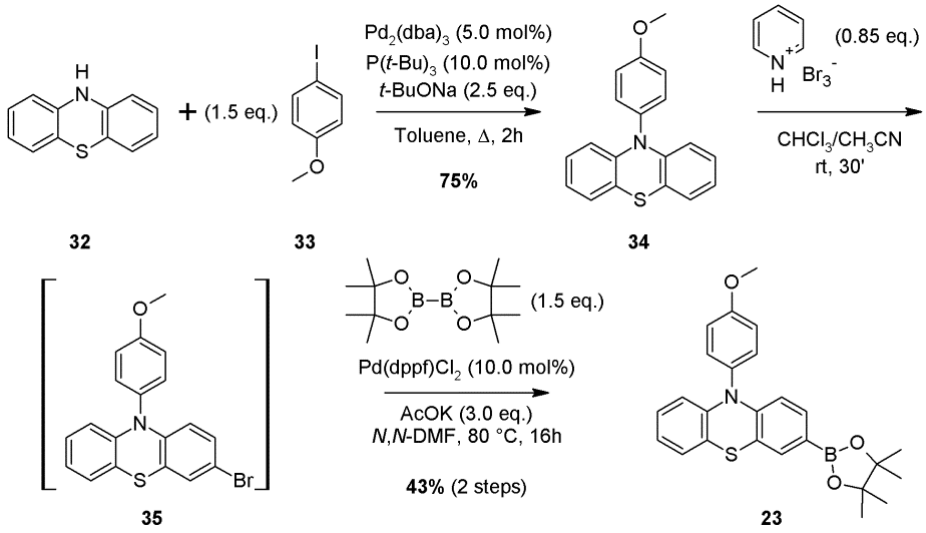

Scheme 4.6. Synthesis of boronic ester 23.

Therefore, a different brominating reagent such as pyridinium bromide perbromide[18] (PBPB, Scheme 4.6) was employed: several different reaction conditions were tested and, finally, we found that, using a sub-stoichiometric amount of PBPB, it was

possible to obtain a composition of the crude mixture (**35**:**34** = 3:1 molar ratio), suitable to be used in the following borylation reaction. Using the already described conditions (see Scheme 4.4 and Scheme 4.5) pure boronic ester **23** was isolated after separation from unreacted **34** by flash column chromatography, with an overall yield of 32%.

4.2.2.3.2. Introduction of the donor: first Suzuki–Miyaura cross-coupling

As shown in Scheme 4.1, organoboron reagents **20**-**23** were reacted with diiodide **11** in order to insert the different donor moieties on the TzTz-scaffold (Scheme 4.7; compounds **9**, **36**-**38**).

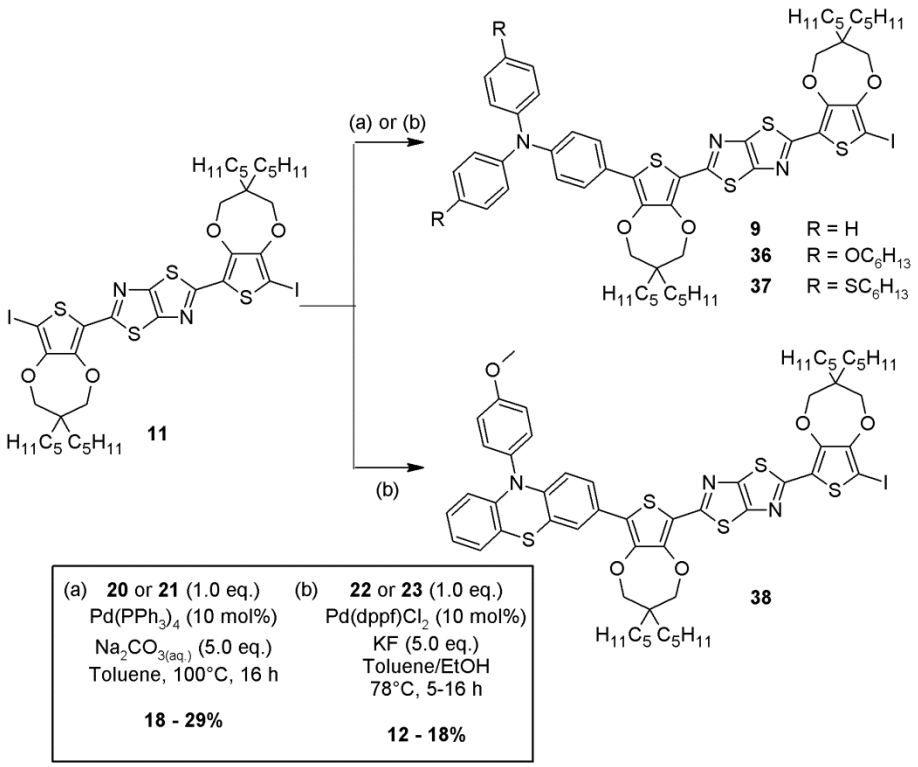

Scheme 4.7. Insertion of donor groups: Suzuki-Miyaura cross-coupling.

This Suzuki-Miyaura cross-coupling was indeed the most challenging step of the whole synthetic procedure, since it implied the desymmetrization of the π-scaffold, thus requiring a differentiation of two indistinguishable reactive sites. To achieve this goal we had already observed[1] that the best choice was to use a stoichiometric

amount of organoboron reagent and that the reaction progress had to be carefully followed in order to stop the process before complete conversion of **11**. In such a way, it was possible to minimize the production of the undesired symmetrical double-coupling product and to separate easily, by flash chromatography, the coupling compound from the unreacted diiodide, leading to isolation of products **9** and **36**-**38** in 18-29% yields. Although the yields of the desired products were not very high, a not negligible amount of unreacted diiodide **11** was always recovered after chromatographic purification and could be reused for further reactions.

Two different sets of reaction conditions were applied: in the case of reagents **20**-**21**, the most classical Suzuki-Miyaura conditions required $Pd(PPh_3)_4$ as the catalyst and an aqueous solution of sodium carbonate (Na_2CO_3) as the base (Scheme 4.7). In the case of boronic esters **22**-**23**, due to their lower reactivity, $Pd(dppf)Cl_2$ had to be used as the catalyst, potassium fluoride (KF) as the base and a mixture of toluene and ethanol as the solvent. In both cases degassed solvents were used.

4.2.2.4. Introduction of the acceptor: second Suzuki–Miyaura cross-coupling and Knoevenagel condensation

The introduction of the acceptor moiety was performed in two steps: first, a cross-coupling reaction with a formyl thiophene boronic acid and then a Knoevenagel condensation. These two steps were carried out for all the dyes except **TTZ6**. Due to the presence of an EDOT ring in place of a simple thiophene in the structure of **TTZ6** (Figure 4.4), it was necessary to optimize a different cross-coupling procedure to introduce the appropriate acceptor moiety.

4.2.2.4.1. Synthesis of TTZ3-5 and TTZ7

Introduction of an additional thiophene ring bearing a formyl moiety was accomplished through a Suzuki-Miyaura cross-coupling with commercially available boronic acid **42** (Scheme 4.8). The cross–coupling reaction was carried out using $Pd(dppf)Cl_2$ as the catalyst, KF as the base and a mixture of toluene and methanol as the solvent. Microwave activation[1] enabled to shorten reaction times and minimize undesired by-products which could derive, for example, from protodehalogenation reactions. Aldehydes **7** and **39**-**41** were isolated after flash column chromatography with good yields (57-74%).

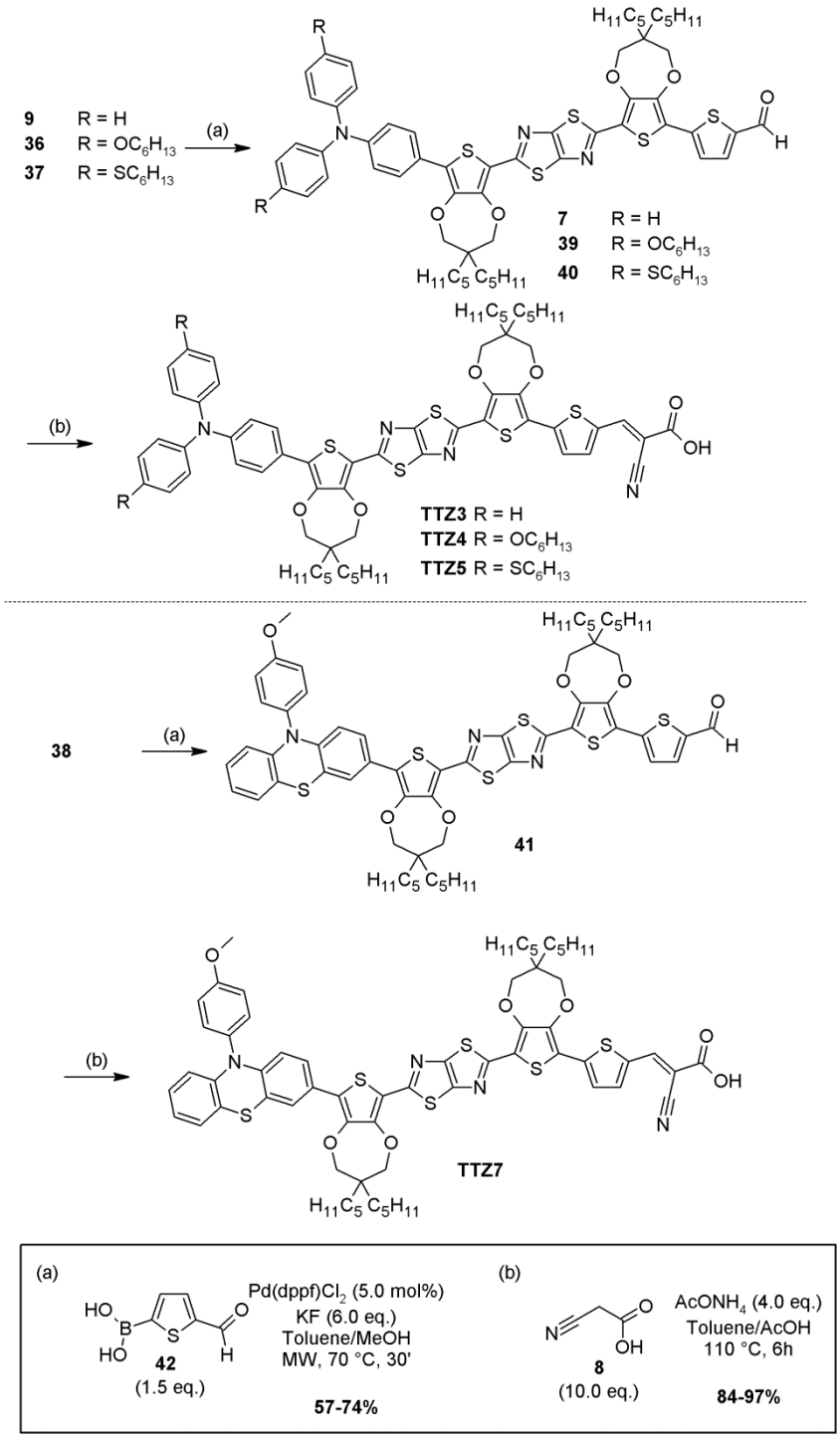

Scheme 4.8. Introduction of the acceptor group: cross-coupling/condensation sequence (TTZ3-5, TTZ7).

Finally, Knoevenagel condensation with cyanoacetic acid **8** and ammonium acetate in toluene/acetic acid mixture gave an almost complete conversion of starting aldehydes to **TTZ3**-**5** and **TTZ7** dyes.

4.2.2.4.2. Synthesis of TTZ6

EDOTs containing a formyl group and a proper moiety to achieve a cross-coupling with the iodide **9** are not commercially available and have never been reported in literature. Since the synthesis of different aromatic derivatives containing both formyl- and stannyl-moieities was already known,[19] we decided to prepare stannane **44** (Scheme 4.9) in order to employ it in a Stille cross-coupling reaction with intermediate **9**.

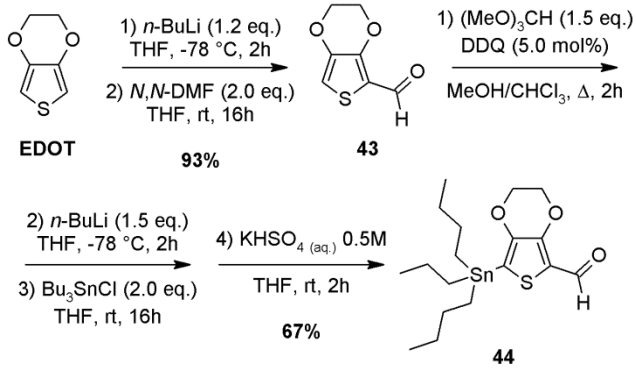

Scheme 4.9. Synthesis of stannane 44.

After a simple formylation of EDOT,[20] a *one-pot* procedure led to stannane **44**. Initially, the aldehyde moiety of **43** was protected by using trimethylorthoformate and DDQ as the catalyst;[21] the resulting dimethylacetal was then treated with *n*-butyllithium and, subsequently, with tributyltin chloride. At the end of the reaction, work-up with an aqueous solution of $KHSO_4$ deprotected selectively the formyl group without affecting the carbon-tin bond.

The synthesis of **TTZ6** (Scheme 4.10) was finally concluded with a classical Pd-catalyzed Stille cross-coupling among stannane **44** and iodide **9** in order to obtain aldehyde **45**, which was then almost quantitatively converted to **TTZ6** dye applying the same Knoevenagel reaction conditions used for the preparation of the other sensitizers.

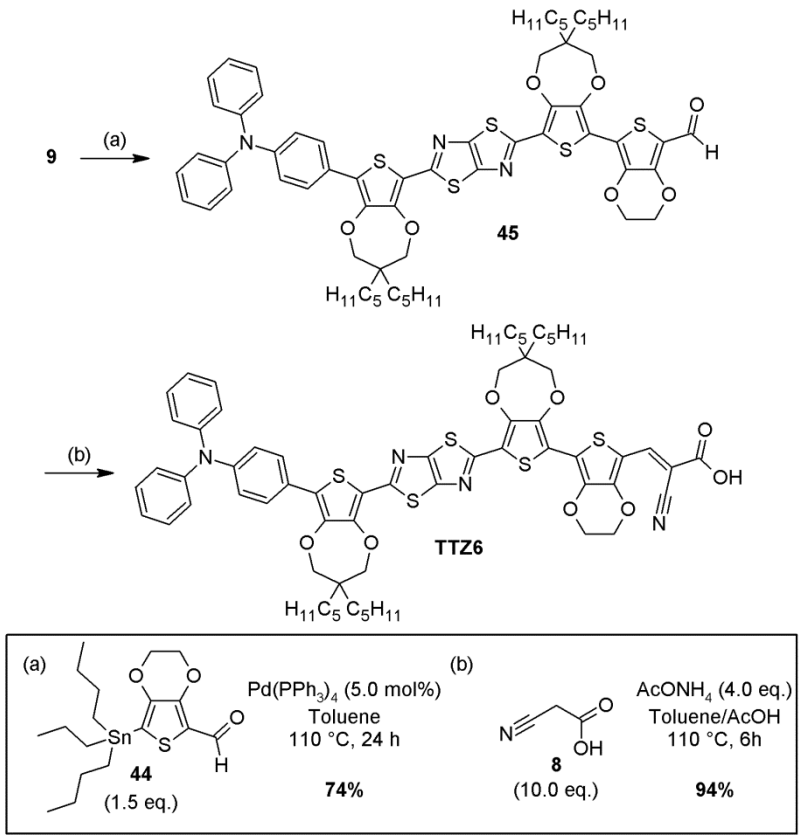

Scheme 4.10. Introduction of the acceptor group: cross-coupling/condensation sequence (TTZ6).

4.2.3. Characterization of dyes TTZ3–7

UV-Vis spectra of dyes **TTZ3**-**7** both in THF solution and adsorbed on TiO_2 were recorded (Figure 4.8). All the dyes showed a broad and intense absorption of solar light with very high extinction molar coefficients (ε up to 9.76×10^4 M^{-1} cm^{-1} in THF, see Table 4.3) and, as expected from the computational analysis (see Paragraph 4.2.1), they displayed a bathochromic shift of 40-50 nm compared to **TTZ1**,[1] with maxima in the 510-521 nm range in solution and in the 484-492 range when adsorbed on TiO_2 (Table 4.3). The blue-shifted light absorption of the dyes upon their attachment to TiO_2 could be due to the deprotonation of the carboxylic acid group on the semiconductor surface.[22] Generally, **TTZ4** and **TTZ6**, which had the strongest electron-donating group and the largest HOMO→LUMO component in the excitation process, respectively, showed the most red-shifted absorption spectra.

Table 4.3 Spectroscopic and electrochemical data for dyes TTZ3–7.

Dye	$\lambda_{max\ abs.}$ [a] [nm] (ε [$M^{-1}\,cm^{-1}$])	$\lambda_{max\ emi.}$ [a] [nm]	$\lambda_{max\ abs.}$ on TiO_2 [nm]	$E_{ox.}$ [b] [V]	$E^*_{ox.}$ [c] [V]	$E_{0\text{-}0}$ [d] [eV]	$E_{0\text{-}0}$ [e] [eV]	Γ [10^{-7} mol cm^{-2}]
TTZ3	510 (81400)	587	484	1.02	– 1.23	2.25	2.16	0.99
TTZ4	518 (86600)	601	491	0.77	– 1.42	2.19	2.12	1.08
TTZ5	510 (94100)	573	487	0.91	– 1.33	2.24	2.16	1.19
TTZ6	521 (94500) 548 (85100)	636	498	0.93	– 1.21	2.14	2.12	1.25
TTZ7	513 (96700)	596	492	0.85	– 1.37	2.22	2.16	1.75

a) THF solution. b) Potentials vs. NHE. c) Calculated from $E_{ox} - E_{0\text{-}0}$. d) Estimated from the intersection of normalized absorption and emission spectra. e) Determined from Tauc Plot.[23]

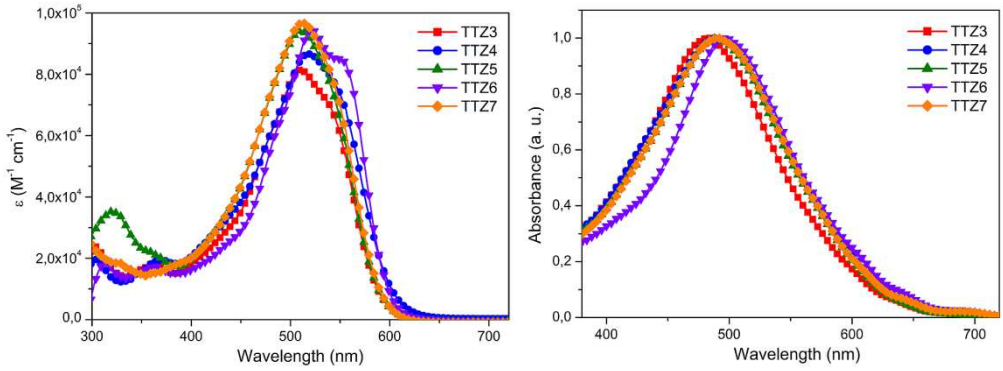

Figure 4.8. (left) UV-Vis spectra of dyes TTZ3-7 in THF solution; concentrations: TTZ3, 8.47 × 10^{-6} M; TTZ4, 8.89 × 10^{-6} M; TTZ5, 8.96 ×10^{-6} M; TTZ6, 7.61 × 10^{-6} M; TTZ7, 9.57 × 10^{-6} M. (right) Normalized UV-Vis spectra of dyes TTZ3-7 adsorbed on TiO_2.

All the dyes exhibited fluorescence emission in THF solution: the intersection of the normalized absorption and emission spectra (Figure 4.9.a-e) allowed to estimate the optical band-gaps ($E_{0\text{-}0}$, Table 4.3), which were comprised in the 2.14-2.25 eV range, with **TTZ6** having the smallest and **TTZ3** the largest $E_{0\text{-}0}$ values. These values were in good agreement with those derived from the corresponding Tauc plots,[23] which were in the 2.12-2.16 eV range and in the same relative order (Figure 4.9.f).

The amount of dyes adsorbed on the TiO_2 layer was calculated through the desorption method: electrodes were sensitized with **TTZ3**-**7**, and then dipped in a 0.1 M KOH solution in THF/MeOH until their complete discoloration. The absorbance of the resulting solution was measured and the amount of dye desorbed from the electrode could therefore be calculated. All the dyes exhibited similar values of

density (Γ = 0.99-1.75 × 10^{-7} mol cm^{-2}), which were consistent with those usually found for other organic DSSC sensitizers (10^{-7}-10^{-8} mol cm^{-2}).

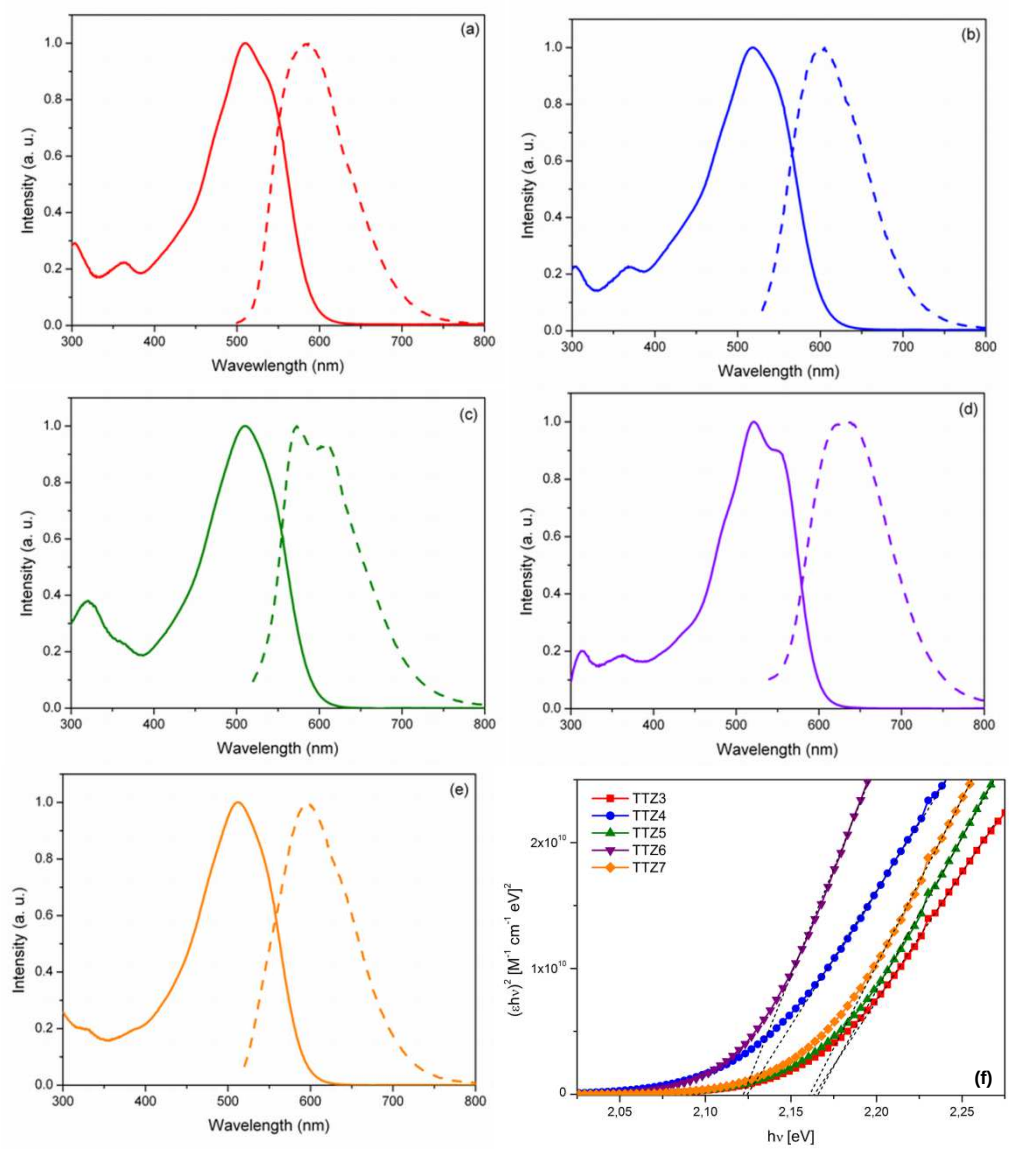

Figure 4.9. (a-e) Intersection between the normalized UV-Vis absorption (solid line) and fluorescence emission (dashed line) spectra for compounds TTZ3-7 in THF solution. (a) TTZ3; (b) TTZ4; (c) TTZ5; (d) TTZ6; (e) TTZ7 – (f) Tauc plot for the determination of the optical band-gap of sensitizers TTZ3-7 in THF solution.

Cyclic voltammetry* measurements of all dyes in CH_2Cl_2 were carried out to determine the ground-state oxidation potentials (Table 4.3). All the potentials were comprised in the 0.77-1.02 V range, therefore being positive enough to ensure regeneration by the iodide/triiodide redox couple (*ca.* 0.5 V *vs*. NHE).[24] As expected, the strong electron-donating character resulting from the introduction of hexyloxy chains on the triarylamine moiety of **TTZ4** was reflected by its relatively low E_{ox} value (0.77 V vs. NHE, compared to 1.02 V for **TTZ3**), with the introduction of phenothiazine in **TTZ7** also showing a similar effect (E_{ox} = 0.85 V).

Subtracting the optical band-gaps ($E_{0\text{-}0}$) to the ground-state oxidation potentials ($E_{ox.}$), it was possible to calculate the excited state oxidation potentials (Table 4.3; $E^*_{ox.} = E_{ox.} - E_{0\text{-}0}$). These values were always more negative than the conduction band edge of TiO_2 (*ca.* –0.4 eV vs. NHE), which means that electron injection from the excited state of the dye to the conduction band of the semiconductor could occur properly during cell operation.

4.2.4. Photovoltaic measurements†

4.2.4.1. Small-scale DSSCs

After characterization, small-scale test DSSCs (0.25 cm^2) containing compounds **TTZ3**-**7** as sensitizers were built in order to evaluate and compare their photovoltaic performances. Since molar extinction coefficients of **TTZ3**-**7** were very high (Table 4.3) suggesting the possibility of an extremely efficient light-harvesting, we reasoned that these dyes could be appropriate for the construction of DSSCs with a thinner TiO_2 layer compared to typical devices. For this reason, two series of cells were assembled: a first series with a transparent photoanode of 5.5 µm thickness (obtained with commercial Dyesol 18NR-T paste), and a second series with an opaque electrode of 6.5 µm thickness (Dyesol 18NR-AO). The performances of our dyes were compared with those of standard organic dye **D5**[25] and organometallic sensitizer **Z907**[26] (Figure 4.10). A commercial electrolyte solution based on the most classical I^-/I_3^- redox couple (Dyesol HPE) was used in the cells. This solution is still the most used one for practical applications, such as BIPV, since it is usually the best

* Cyclic voltammetry measurements were performed by Dr. Fabrizia Fabrizi de Biani from the University of Siena.

† All the photovoltaic measurements were carried out by Dr. Daniele Colonna and Prof. Aldo di Carlo from C.H.O.S.E., University of Rome "Tor Vergata".

performing one with ruthenium sensitizers. Typical J/V curves measured on the transparent solar cells are shown in Figure 4.11a, while the corresponding IPCE spectra are displayed in Figure 4.11b.

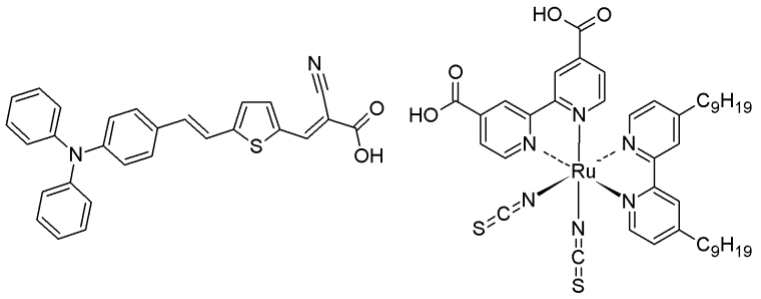

Figure 4.10. Structures of reference dyes D5 and Z907.

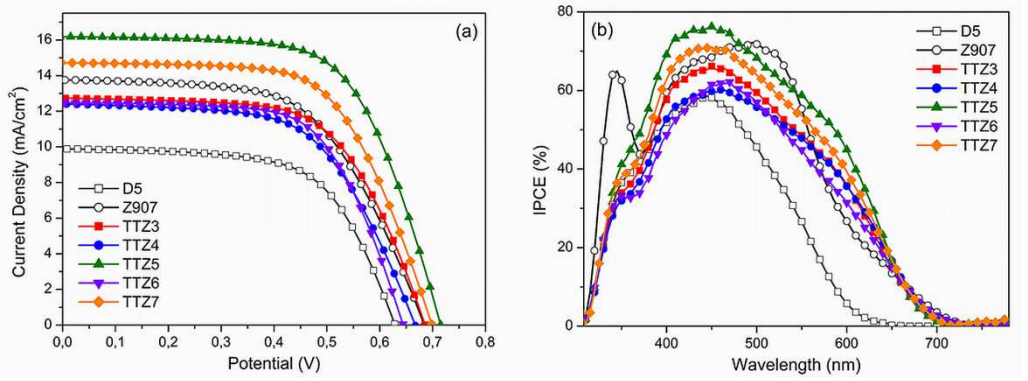

Figure 4.11. Typical J/V curves (a) and IPCE spectra (b) for transparent cells built with dyes D5, Z907 and TTZ3-7.

In the case of transparent cells (Table 4.4), dyes **TTZ3**-**7** showed efficiency values between 4.85 and 7.39%, with **TTZ5** and **TTZ7** being the best two sensitizers. Remarkably, all new thiazolo[5,4-*d*]thiazole dyes gave better efficiencies than standard organic dye **D5**, while **TTZ5** and **TTZ7** surpassed even the performance provided by ruthenium sensitizer **Z907** (η 6.35-7.39% vs. 5.51%). This result was particularly significant, since **Z907** is one of the sensitizers of choice for applications in BIPV.[27] All new compounds gave broad IPCE spectra with onsets around 700 nm (Figure 4.11b), in agreement with their UV-Vis spectra recorded on TiO_2: in particular, the IPCE of dye **TTZ5** was superior to **Z907** in the 370-480 and 550-660 nm regions, consistent with its higher photocurrent.

Table 4.4. Photovoltaic parameters for transparent DSSCs built with dyes D5, Z907 and TTZ3-7.[a]

Dye	J_{sc} [mA cm^{-2}]	V_{oc} [V]	*ff* [%]	η [%]
D5	9.60	0.624	63	3.78
Z907	13.50	0.686	60	5.51
TTZ3	12.79	0.687	61	5.41
TTZ4	12.18	0.669	60	4.85
TTZ5	**16.20**	**0.716**	**63**	**7.39**
TTZ6	12.29	0.646	63	5.01
TTZ7	14.99	0.686	62	6.35

a) Average values of three devices; active surface area 0.25 cm^2; TiO_2 layer thickness 5.5 µm.

Apparently the presence of alkylthio-chains on the donor portion of the molecule improved the photovoltaic performance of dye **TTZ5** compared to the other sensitizers. This is in agreement with previous studies by Berlinguette *et al*.,[5] who found that this substituent was able to induce superior photocurrent and photovoltage in DSSCs compared to its oxygenated analogue. These beneficial effects were attributed to a much faster dye regeneration which, according to the authors, could either be due to formation of an adduct between iodide from the electrolyte and the "soft" sulphur atoms, or simply arise from the greater HOMO coefficients found on the S atoms compared to the O atoms. The latter observation could be made also in our case when comparing the HOMO isodensity plots of **TTZ4** and **TTZ5** derived from our computational analysis (see Paragraph 4.2.1, Figure 4.6).

Regarding the other dyes, their lower efficiencies could be justified by a combination of several factors: for example, **TTZ3** had the lowest extinction molar coefficient and dye density on TiO_2, which could result in a lower light-harvesting efficiency. **TTZ4**, having the highest E_{ox} value among all dyes, could be affected by a less efficient dye-regeneration, while **TTZ6** could suffer from faster electron recombination since its HOMO coefficients were partially located on the terminal portion of the molecule.

Data obtained for opaque cells were generally consistent with those recorded for transparent devices (Table 4.5), with **TTZ5** and **TTZ7** being once again the two best sensitizers, albeit with slightly reduced efficiency values (η 6.08-6.91%). Generally, the relatively low *fill factors* observed for all the cells (55-63%) were likely due to the small thickness of the TiO_2 layer employed, combined with the absence of a blocking layer, which probably favored electron recombination through direct contact between the conductive substrate and the electrolyte solution.

Table 4.5. Photovoltaic parameters for opaque DSSCs built with dyes D5, Z907 and TTZ3-7.[a]

Dye	J_{sc} [mA cm^{-2}]	V_{oc} [V]	*ff* [%]	η [%]
D5	11.04	0.619	58	3.99
Z907	13.85	0.687	58	5.61
TTZ3	13.65	0.671	60	5.45
TTZ4	12.99	0.665	57	4.93
TTZ5	**16.05**	**0.721**	**60**	**6.91**
TTZ6	13.00	0.644	56	4.70
TTZ7	15.26	0.680	59	6.08

a) Average values of three devices; active surface area 0.25 cm^2; TiO_2 layer thickness 6.5 µm.

Although the tridimensional structure of alkyl chains in ProDOT rings should have minimized the aggregation effects of dyes **TTZ3**-**7** on TiO_2 layer, two new series of transparent and opaque solar cells were built by staining the photoanode in a solution containing chenodeoxycholic acid (CDCA) in addition to the appropriate dye. The photovoltaic values obtained in this case are reported in Table 4.6.

Table 4.6. Photovoltaic parameters for DSSCs built with dyes TTZ3-7 and CDCA as coadsorbent.[a]

Transparent DSSCs[b]				
Dye	J_{sc} [mA cm^{-2}]	V_{oc} [V]	*ff* [%]	η [%][d]
TTZ3	15.62	0.697	60	6.55 (+21%)
TTZ4	14.27	0.692	59	5.85 (+21%)
TTZ5	**16.59**	**0.717**	**59**	**7.08 (–4%)**
TTZ6	10.68	0.640	57	3.90 (–22%)
TTZ7	15.97	0.694	60	6.61 (+4%)
Opaque DSSCs[c]				
TTZ3	16.52	0.683	58	6.54 (+20%)
TTZ4	15.18	0.675	55	5.71 (+16%)
TTZ5	**18.33**	**0.709**	**59**	**7.71 (+12%)**
TTZ6	13.86	0.646	56	5.03 (+7%)
TTZ7	17.22	0.689	58	6.94 (+14%)

a) Average values of three devices; active surface area 0.25 cm^2; 1mM CDCA added in the sensitizing bath (0.1 mM dye in THF). b) TiO_2 layer thickness 5.5 µm. c) TiO_2 layer thickness 6.5 µm. d) Comparison with DSSCs without CDCA.

In both device classes, higher photocurrent densities were observed for all the sensitizers, with the sole exception of **TTZ6**, maybe because the steric bulk of its terminal EDOT ring minimized the aggregation even in the absence of CDCA, while the largest enhancement was displayed by dye **TTZ3** (+20-21%). In the presence of

CDCA, the best result was provided by **TTZ5**-containing opaque cells, which recorded an average efficiency of 7.71% with a remarkable photocurrent of 18.33 mA cm^{-2}.

Except for the devices built with dyes **TTZ3** and, partially, **TTZ4**, the adding of CDCA did not provide huge increases of the efficiency values of our devices, which were able to furnish good photovoltaic performances without it. This result was particularly appreciated because it fulfilled our initial goal, that is the construction of efficient solar devices using simplified procedures and materials. In particular, no blocking layer of TiO_2 was deposed either on the conductive glass substrate or on the nanocrystalline semiconductor layer by treatment with aq. $TiCl_4$, and no light-scattering layer was employed in photoanode fabrication. All these features represented the first essential condition for a possible future large-scale production of DSSC modules based on the new TzTz-dyes.

4.2.4.2. Strip DSSCs

Having obtained promising results with small-scale DSSCs (0.25 cm^2), built under very simple conditions, the next step was to investigate how an increase in the cell active surface area could affect device efficiency and stability. For this reason, we decided to build larger area (3.6 cm^2) strip cells, in view of a possible scale-up of the system. Accordingly, we also introduced some changes in device fabrication:

i. Transparent TiO_2 electrodes with a thickness of 3 to 5 µm were prepared in order to minimize semiconductor employment and enhance transparency.
ii. A different commercial electrolytic solution (Dyesol HSE) was used, which is still based on the I^-/I_3^- redox couple, but is designed to improve device stability at the cost of maximum performance.
iii. Only dyes **TTZ3**-**5** were used in these experiments, due to their easier preparation procedure.

Two series of cells were prepared for each electrode thickness, either by addition of CDCA to the sensitizing bath or not. The well-known organic dye **D35** (Figure 4.12) was selected as reference standard,[28] since this compound has recently been established worldwide as a reference organic sensitizer for DSSCs, due to its good performances coupled with high transparency and excellent stability.[29]

The relevant photovoltaic parameters of strip cells are listed in Table 4.7, while their J/V curves and their IPCE spectra are shown in Figure 4.13 and Figure 4.14 respectively.

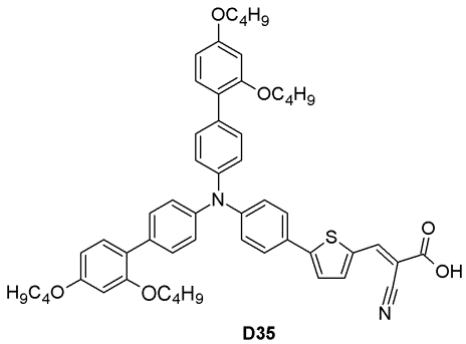

D35

Figure 4.12. Structure of reference dye D35.

Table 4.7. Photovoltaic parameters for strip DSSCs built with dyes D35 and TTZ3-5.[a]

Dye	Thickness [µm]	CDCA[b]	J_{sc} [mA cm^{-2}]	V_{oc} [V]	*ff* [%]	η [%]
D35	3	–	9.93	0.758	54	4.06
		+	9.52	0.754	55	3.93
TTZ3	3	–	14.65	0.693	53	5.40
		+	13.80	0.696	47	4.52
	5	–	15.70	0.678	52	5.58
		+	16.31	0.667	50	5.48
TTZ4	3	–	13.14	0.682	52	4.70
		+	12.62	0.690	52	4.55
	5	–	13.51	0.667	52	4.71
		+	14.31	0.677	52	5.04
TTZ5	3	**–**	**15.78**	**0.732**	**53**	**6.20**
		+	15.29	0.722	54	6.03
	5	**–**	**17.00**	**0.705**	**53**	**6.35**
		+	16.38	0.711	50	5.88

a) Average values of two devices; active surface area 3.6 cm^2. b) "–": without CDCA; "+": with 1mM CDCA added in the sensitizing bath (0.1 mM dye in THF).

Remarkably, strip DSSCs built with dyes **TTZ3**-**5** recorded higher efficiencies than those containing standard sensitizer **D35**, with the best result provided once again by **TTZ5** (6.35% average efficiency for the 5 µm cell without CDCA). The superior efficiencies were mostly due to the higher photocurrents induced by the TzTz-containing dyes compared to **D35**; such difference could be explained considering their wider and, in the case of **TTZ5**, also higher IPCE spectra (Figure 4.14).

Comparing cells with different thicknesses, DSSCs with a 5µm-layer of TiO_2 gave slightly improved performances, but differences in efficiency were rather small.

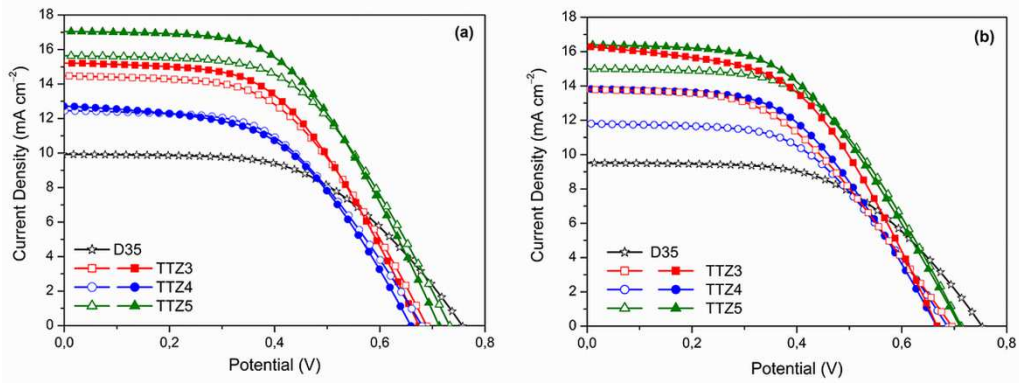

Figure 4.13. Typical J/V curves for transparent strip cells built with dyes D35 and TTZ3-5 in the absence (a) and in the presence (b) of CDCA. Hollow symbols: 3 µm devices; full symbols: 5 µm devices.

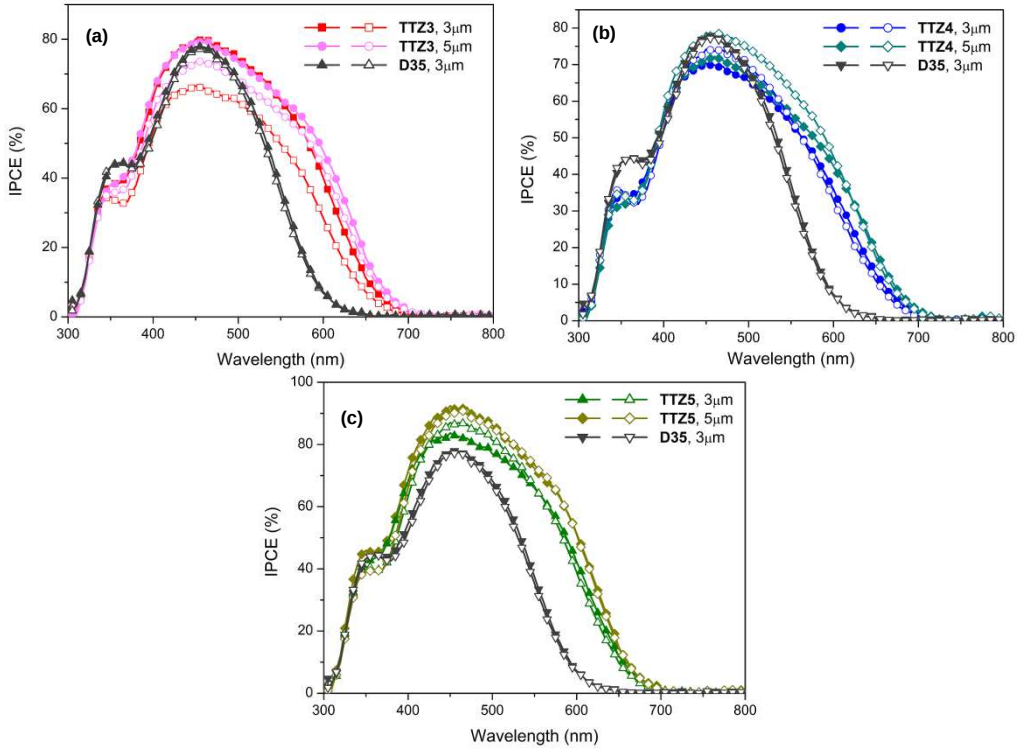

Figure 4.14. IPCE curves measured for strip DSSCs built with dye TTZ3 (a), TTZ4 (b), TTZ5 (c); solid symbols: no CDCA; hollow symbols: CDCA added to the sensitizing bath. The corresponding curves obtained with reference dye D35 have been added for comparison.

As expected, photocurrents increased by using a thicker semiconductor layer, since a larger amount of dye was adsorbed on the electrode, but the open-circuit voltages

were smaller, probably due to higher electron recombination. Generally, *fill factors* of strip cells were lower than those of small-scale cells due to the higher series resistance usually observed for larger DSSCs.[30]

Unlike what was observed in the case of small-scale cells, the introduction of CDCA decreased the performances of the larger-area devices (Table 4.7), with the sole exception of the 5 µm device built with dye **TTZ4**. In general, photocurrent was not improved by the presence of CDCA, highlighting a lower tendency of the dyes to aggregate under these conditions. Accordingly, we suppose that, during staining of the larger electrodes, a more homogeneous distribution of the sensitizer was achieved, which caused a reduction of stacking and other aggregation phenomena and the elimination of all potential benefits brought by the co-adsorbent.

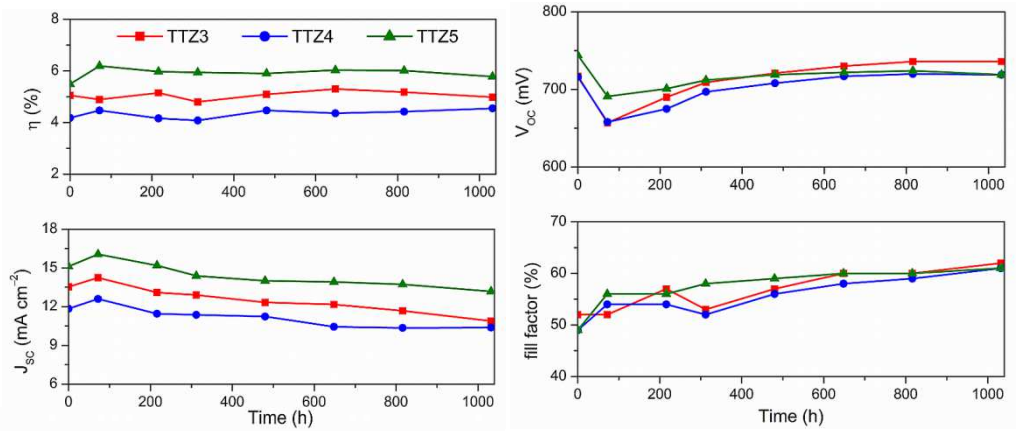

Figure 4.15. Stability test conducted with 3 µm-thick DSSCs sensitized with dyes TTZ3-5 over the course of 1000 h. Ageing in the dark at 85°C.

At this stage, the stability of the strip cells fabricated with dyes **TTZ3**-**5** (Figure 4.15) was also tested. A new series of 3 µm-thick devices was built and all the photovoltaic parameters measured under standard illumination over a period of approx. 1000 h, during which they were stored in the dark at 85°C. All the devices showed excellent stability during this period of time, with final efficiencies comparable to the initial ones (for **TTZ4**-**5** a slight increase was even observed within the first 72 h). In particular, the efficiency of compound **TTZ5** was constant around 6% for the entire duration of the experiment, consistent with the results described above.

Generally, during the course of the experiment, photocurrents increased during the first 100 hours and then slowly decreased, while an opposite pattern was observed

for photovoltages, with an initial drop followed by a subsequent recovery; similarly, *fill factors* increased slightly during the experiment. All these results regarding efficiency and stability indicated that TzTz-sensitizers are promising candidates for the potential fabrication of large-scale thin-film DSSC modules due to their good performances coupled with high photochemical stability and easy building techniques.

4.2.4.3. Electrochemical impedance spectroscopy

In the final part of our studies, we analyzed more in detail the charge transfer processes taking place in the cells by means of electrochemical impedance spectroscopy (EIS),[31] which is a powerful tool for the study of charge accumulation, transport and recombination under the different operating conditions of DSSC, as well as to make a general assessment of device electrical properties. Measurements for 5µm-strip cells containing dyes **TTZ3**-**5** were performed in the dark at –0.60 V forward bias over the 0.1 Hz-100 KHz frequency range: the corresponding Nyquist plots (i.e. the plots showing the minus imaginary part of the impedance –Z'' *vs.* the real part Z' when sweeping the frequency) are shown in Figure 4.16a, while Bode phase plots (i.e. the plots showing the current/voltage phase shift *vs.* the frequency) are shown in Figure 4.16b.

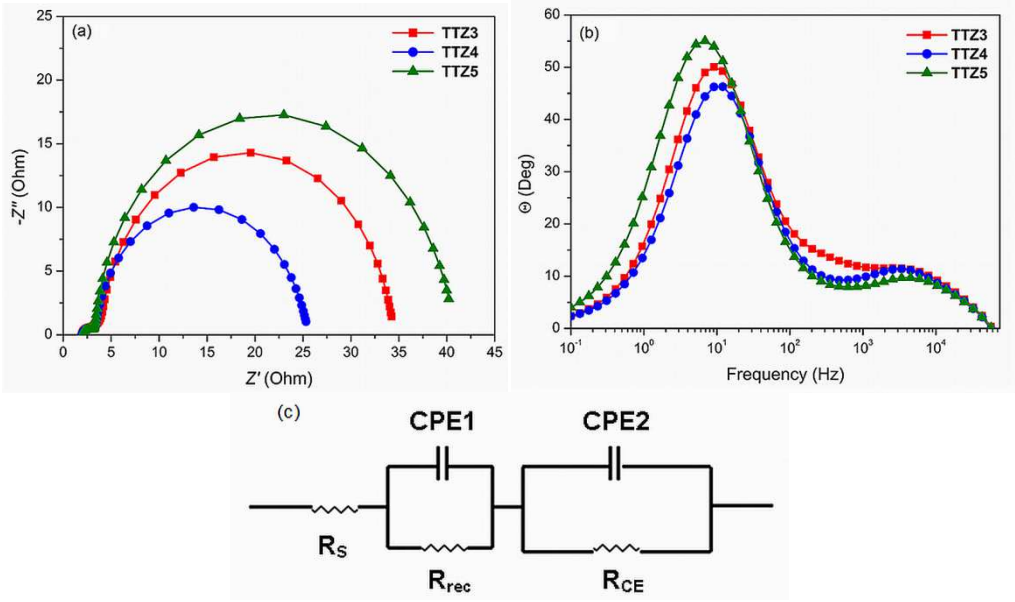

Figure 4.16. Electrochemical impedance spectra for compounds TTZ3-5 measured in the dark at –0.60 V forward bias: (a) Nyquist plot; (b) Bode phase plot; (c) equivalent circuit.

In the Nyquist plots, due to the use of a liquid electrolyte, two semicircles were observed: the small semicircle at higher frequencies corresponds to charge transfer processes at the Pt-electrolyte interface, while the larger semicircle at lower frequencies derives from the charge transfer processes at the TiO_2-dye-electrolyte interface. Several parameters can be obtained by fitting the spectra with a known electrochemical model (see the equivalent circuit in Figure 4.16c), namely the series resistance of the cell (R_s), the charge transfer resistance at the TiO_2-dye-electrolyte interface (R_{rec}) and the charge transfer resistance at the counter electrode (R_{CE}). Here, while R_s and R_{CE} were comparable for all dyes (reflecting the similar fabrication conditions and the same materials used in the counter electrode), R_{rec} values increased in the order **TTZ4** (22.0 Ω) < **TTZ3** (30.2 Ω) < **TTZ5** (37.2 Ω), suggesting that for the latter dye a slower charge recombination was taking place at the photoanode.

Considering the Bode phase plots, the frequency of the peaks observed in the middle-frequency domain can be used to evaluate the electron lifetime within the semiconductor (τ_e),[32] providing another indication of the charge recombination rate. In agreement with the previous measurements, we found that electron lifetimes increased in the order **TTZ4** (15.1 ms) < **TTZ3** (17.5 ms) < **TTZ5** (23.2 ms), confirming that electron recombination was more efficiently prevented by the dye with the alkylthio-terminal chains. As recently pointed out in other studies,[33] electron lifetime, influenced by factors such as molecular size and dye adsorption behavior, exerts a strong influence on cell photovoltage. Indeed, also here, the trend in τ_e values was in good agreement with V_{oc} values measured for the cells and reported in Table 4.7.

4.3. Experimental section

4.3.1. Synthetic procedures

Diethyl 2,2-dipentylmalonate (18)[34]

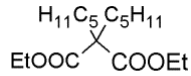

18

1-bromopentane (34.9 g, 0.23 mol, 3.0 eq.) was dissolved in THF, then sodium hydride (5.54 g, 0.23 mol, 3.0 eq.) was added. After cooling to 0 °C, diethyl malonate (**19**, 12.3 g, 0.077 mol, 1.0 eq.) was added into the flask during one hour, after which the resulting mixture was heated to reflux for 16 h. After cooling to 0 °C, water was added until neutralization of the excess of sodium hydride. The resulting mixture was extracted with Et_2O (2 × 150 mL), then the combined organic phases were washed with brine and dried with Na_2SO_4. After filtration, removal of the solvent under vacuum afforded a pale yellow oil, which was purified by distillation under reduced pressure to give pure **18** (15.6 g, 0.052 mol, 67% yield) as a colorless liquid.

(**18**): ^{1}H-NMR (300 MHz, $CDCl_3$): δ = 4.15 (q, *J* = 7.1 Hz, 4H), 1.80–1.88 (m, 4H), 1.24–1.28 (m, 8H), 1.22 (t, *J* = 7.1 Hz, 6H), 1.09–1.16 (m, 4H), 0.83–0.89 (m, 6H) ppm. ^{13}C-NMR (75 MHz, $CDCl_3$): δ = 172.2, 61.0, 57.7, 32.2, 32.1, 23.7, 22.5, 14.2, 14.1 ppm. IR (KBr): $\tilde{\nu}$ = 2956, 2929, 2862, 1736, 1459, 1036 cm^{-1}.

2,2-dipentylpropan-1,3-diol (17)[35]

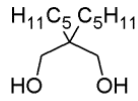

17

Lithium aluminum hydride (2.95 g, 0.078 mol, 1.5 eq.) and Et_2O (100 mL) were introduced in a Schlenk flask then, after cooling to 0 °C, diester **18** (15.6 g, 0.052 mol, 1.0 eq.) was added within an hour. The reaction mixture was left under stirring at room temperature for 16 hours, then was cooled to 0 °C. A first portion of water (3 mL), a 15% NaOH aqueous solution (3 mL) and a second portion of water (9 mL) were added to the reaction mixture, then, after stirring at room temperature for 20 minutes, Na_2SO_4 (*ca.* 10 g) was added to the reaction mixture, which was stirred for further 20 minutes, and then filtered over a short pad of Celite®. The organic phase was washed with brine and dried with Na_2SO_4. After filtration, removal of the solvent

under vacuum afforded diol **17** (10.8 g, 0.050 mol, 96% yield) as a colorless oil, which was used for the next step without further purification.

(**17**): ^{1}H–NMR (300 MHz, $CDCl_3$): δ = 3.56 (d, *J* = 4.3 Hz, 4H), 2.27 (bs, 2H), 1.21–1.32 (m, 16H), 0.89 (t, *J* = 6.7 Hz, 6H) ppm. ^{13}C–NMR (75 MHz, $CDCl_3$): δ = 68.7, 41.2, 32.9, 30.9, 22.8, 22.7, 14.2 ppm. IR (KBr): $\tilde{\nu}$ = 3360, 2955, 2930, 2860, 1466, 1053 cm^{-1}.

3,3-dipentyl-3,4-dihydro-2H-thieno[3,4-*b*][1,4]dioxepine (ProDOT, 15)[10]

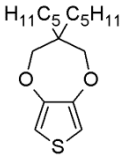

15

3,4-dimethoxythiophene (**16**, 1.67 g, 11.6 mmol, 1.0 eq.), toluene (100 mL), diol **17** (5.00 g, 23.2 mmol, 2.0 eq.) and *p*-toluenesulfonic acid (0.220 g, 1.16 mmol, 10 mol%) were introduced in a Schlenk flask equipped with a Soxhlet extractor containing activated molecular sieves (4Å). The reaction mixture was heated at reflux for 16 hours, then allowed to cool to room temperature, washed with water (100 mL) and brine, and dried with Na_2SO_4. After filtration and evaporation of the solvent under reduced pressure, the crude product was purified by flash column chromatography (SiO_2, petroleum ether / dichloromethane 3:2, then ethyl acetate) to give pure product **15** (3.22 g, 10.9 mmol, 94% yield) as a pale yellow oil, as well as starting material **17** (1.99 g, 9.2 mmol, 40% recovery).

(**15**): ^{1}H–NMR (300 MHz, $CDCl_3$): δ = 6,42 (s, 2H), 3.85 (s, 4H), 1.26–1.38 (m, 16H), 0.89 (t, *J* = 6.9 Hz, 6H) ppm. ^{13}C–NMR (75 MHz, $CDCl_3$): δ = 149.9, 104.8, 77.7, 43.9, 32.8, 32.0, 22.7, 22.6, 14.2 ppm. IR (KBr): $\tilde{\nu}$ = 3112, 2955, 2930, 2860, 1459, 1376, 1188, 1022 cm^{-1}. ESI–MS: *m/z* = 297.06 $[M+1]^+$.

3,3-dipentyl-3,4-dihydro-2H-thieno[3,4-*b*][1,4]dioxepine-6-carboxaldehyde (14)

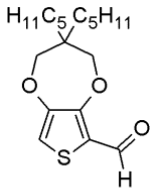

14

ProDOT **15** (1.09 g, 3.68 mmol, 1.0 eq.) was dissolved in THF (30 mL), then, after cooling to –78 °C, a 1.6 M solution of *n*-BuLi in hexane (4.78 mmol, 3.0 mL, 1.3 eq.) was added dropwise. The resulting mixture was left under stirring at –78 °C for 2 hours, then *N*,*N*-DMF (0.538 g, 7.35 mmol, 0.57 mL, 2.0 eq.) was added. The reaction mixture was allowed to return to room temperature and left under stirring for 16 h. A saturated aqueous solution of NH_4Cl (50 mL) and Et_2O (100 mL) were added, the two phases were separated, and the organic phase was washed with brine and dried with Na_2SO_4. After filtration, removal of the solvent under vacuum afforded a bright yellow oil which was purified by flash column chromatography (SiO_2, petroleum ether / CH_2Cl_2 2:1) to give pure aldehyde **14** (0.972 g, 3.00 mmol, 82% yield) as a pale yellow oil.

(**14**): ^{1}H–NMR (300 MHz, $CDCl_3$): δ = 9.91 (d, *J* = 1.2 Hz, 1H), 6.86 (d, *J* = 1.2 Hz, 1H), 4.06 (s, 2H), 3.90 (s, 2H), 1.22–1.43 (m, 16H), 0.90 (t, *J* = 6.9 Hz, 6H) ppm. ^{13}C–NMR (75 MHz, $CDCl_3$): δ = 181.4, 156.5, 149.6, 122.2, 115.3, 78.1, 77.9, 43.9, 32.7, 32.2, 22.7, 22.6, 14.2 ppm. IR (KBr): $\tilde{\nu}$ = 3101, 2955, 2930, 2860, 1661, 1487, 1379, 1030 cm^{-1}. ESI–MS: *m/z* = 325.14 $[M+1]^+$.

2,5-bis(3,3-dipentyl-3,4-dihydro-2H-thieno[3,4-*b*][1,4]dioxepin-6-yl)thiazolo[5,4-*d*]thiazole (13)

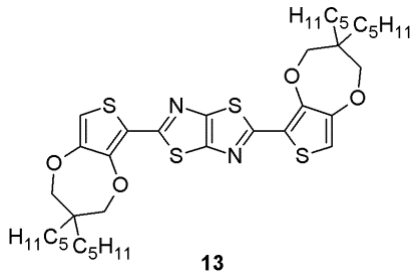

13

Dithiooxamide (106 mg, 0.88 mmol), aldehyde **14** (570 mg, 1.76 mmol, 2.0 eq.) and *n*-butanol (1.5 mL) were introduced in a microwave vial equipped with a magnetic stirrer. The resulting mixture was heated under microwave irradiation at 120°C for 2.5 h. After cooling to room temperature, THF (*ca.* 5 mL) and chloranil (108 mg, 0.44 mmol, 0.5 eq.) were added to the reaction mixture, which was transferred to a flask, heated to reflux and stirred for 10 min. Removal of the solvent *in vacuo* afforded a dark thick oil, which was purified by flash column chromatography (SiO_2; petroleum ether / toluene 3:2) to give compound **2** as a light brown solid (269 mg, 0.37 mmol, 42% yield).

(**2**): mp = 207–208 °C. ^{1}H–NMR (400 MHz, $CDCl_3$): δ = 6.56 (s, 2H), 4.10 (s, 4H), 3.92 (s, 4H), 1.42–1.46 (m, 8H), 1.28–1.36 (m, 24H), 0.91 (t, *J* = 6.8 Hz, 12H) ppm. ^{13}C–NMR (75 MHz, $CDCl_3$): δ = 159.7, 150.2, 149.7, 148.6, 117.5, 107.0, 78.1, 77.9, 44.1, 32.8, 32.2, 22.7, 14.2 ppm. IR (KBr): $\tilde{\nu}$ = 3100, 2930, 2860, 1500, 1039 cm^{-1}. ESI–MS: *m/z* = 731.32 $[M]^+$.

2,5-bis(8-iodo-3,3-dipentyl-3,4-dihydro-2H-thieno[3,4-*b*][1,4]dioxepin-6-yl)thiazolo [5,4-*d*]thiazole (11)

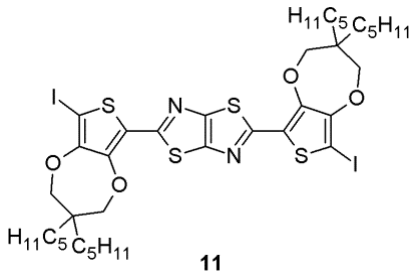

11

Thiazolo[5,4-*d*]thiazole **13** (847 mg, 1.16 mmol) and *N*-iodosuccinimmide (652 mg, 2.89 mmol, 2.5 eq.) were dissolved into a mixture of $CHCl_3$ (20 mL) and glacial acetic acid (20 mL). The reaction mixture was stirred overnight in the dark, at room temperature. The solid obtained was filtered and washed with several portions (50 mL) of methanol and ethyl acetate to afford diiodide **11** as a yellow solid (1.06 g, 1.08 mmol, 93% yield). Compound **11** was used in the following steps without any further purification.

(**11**): mp = 228–230 °C. ^{1}H–NMR (400 MHz, $CDCl_3$): δ = 4.09 (s, 4H), 3.98 (s, 4H), 1.42–1.46 (m, 8H), 1.28–1.36 (m, 24H), 0.91 (t, *J* = 6.7 Hz, 12H) ppm. ^{13}C–NMR (75 MHz, $CDCl_3$): δ = 159.0, 152.0, 150.4, 146.8, 122.0, 78.3, 78.2, 61.0, 44.1, 32.7, 32.1, 22.7, 22.6, 14.2 ppm. IR (KBr): $\tilde{\nu}$ = 2929, 2858, 1492, 1370, 1057 cm^{-1}. ESI–MS: *m/z* = 983.09 $[M]^+$.

4,4'-dimethoxydiphenyl amine (26)[13]

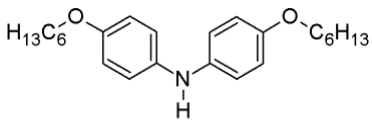

26

1-bromo-4-hexyloxybenzene (**24**, 3.70 g, 14.4 mmol, 3.0 mL, 1.0 eq.) was mixed with toluene (30 mL), dppf (0.319 g, 0.575 mmol, 4.0 mol%) and $Pd_2(dba)_3$ (0.263 g, 0.288

mmol, 2.0 mol%). The resulting mixture was stirred for 20 minutes at room temperature while the color turned from black to red, then 4-hexyloxyaniline (**25**, 5.56 g, 28.8 mmol, 2.0 eq.) and sodium *tert*-butoxide (2.77 g, 28.8 mmol, 2.0 eq.) were added. The reaction mixture was heated to reflux for 2 hours, then allowed to cool down to room temperature. After filtration over Celite®, CH_2Cl_2 (150 mL) and water (150 mL) were added, the two phases were separated, the organic phase was washed with brine and dried with Na_2SO_4. After filtration and evaporation of the solvent under vacuum, the crude product was purified by flash column chromatography (SiO_2, petroleum ether / Et_2O 12:1) to give pure amine **26** (4.49 g, 12.1 mmol, 84% yield) as an off-white solid.

(**26**): ^{1}H–NMR (400 MHz, Acetone-d_6): δ = 6.95 (d, *J* = 9.0 Hz, 4H), 6.81 (d, *J* = 8.9 Hz, 4H), 3.92 (t, *J* = 6.5 Hz, 4H), 3.73–3.76 (m, 1H), 1.73 (q, *J* = 6.7 Hz, 4H), 1.41–1.53 (m, 4H), 1.29–1.38 (m, 8H), 0.90 (t, *J* = 7.0 Hz, 6H) ppm. The analytical data were in agreement with those reported in the literature.[36]

***N*,*N*-bis(4'-methoxyphenyl)-4-bromoaniline (28)**[14]

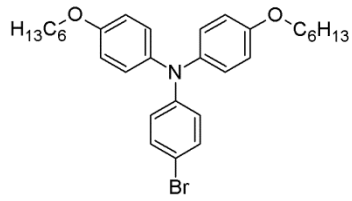

28

1-bromo-4-iodobenzene (**27**, 2.39 g, 8.46 mmol, 1.25 eq.) was mixed with toluene (25 mL), dppf (0.028 g, 0.051 mmol, 0.75 mol%) and $Pd_2(dba)_3$ (0.031 g, 0.034 mmol, 0.5 mol%). The resulting mixture was stirred for 20 minutes at room temperature, then 4,4'-dimethoxydiphenyl amine (**26**, 2.50 g, 6.76 mmol, 1.0 eq.) and sodium *tert*-butoxide (0.975 g, 10.2 mmol, 1.5 eq.) were added. The reaction mixture was heated to reflux for 20 hours, then allowed to cool down to room temperature. After filtration over Celite®, ethyl acetate (200 mL) and water (150 mL) were added, the two phases were separated, the organic phase was washed with brine and dried with Na_2SO_4. After filtration and evaporation of the solvent under vacuum, the crude product was purified by flash column chromatography (SiO_2, petroleum ether / toluene 5:1) to give pure triarylamine **28** (2.59 g, 4.94 mmol, 73% yield) as a colorless oil.

(**28**): ^{1}H-NMR (300 MHz, Acetone-d_6): δ = 7.28 (d, *J* = 9.1 Hz, 2H), 7.04 (d, *J* = 9.1 Hz, 4H), 6.90 (d, *J* = 9.1 Hz, 4H), 6.74 (d, *J* = 9.1 Hz, 2H), 3.98 (t, *J* = 6.5 Hz, 4H), 1.76 (qu, *J* = 6.5 Hz, 4H), 1.45–1.51 (m, 4H), 1.29–1.41 (m, 8H), 0.86–0.94 (m, 6H) ppm. ^{13}C-NMR (75 MHz, Acetone-d_6): δ = 157.1, 149.4, 141.0, 132.6, 127.9, 122.0, 116.4, 112.1, 68.8, 32.4, 26.5, 23.3, 14.3 ppm. The analytical data were in agreement with those reported in the literature.[5]

*Note: In the ^{13}C-NMR of compound **28** recorded in acetone-d_6, one aliphatic signal was covered by the signal belonging to acetone.*

1-bromo-4-hexylthiobenzene (29)[17]

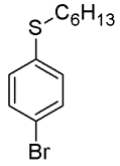

29

1-bromo-4-iodobenzene (**27**, 5.66 g, 20.0 mmol, 1.0 eq.) was mixed with toluene (55 mL), copper iodide (0.340 g, 1.80 mmol, 9.0 mol%), 1,10-phenanthroline (0.324 g, 1.8 mmol, 9.0 mol%) and sodium *tert*-butoxide (2.88 g, 30.0 mmol, 1.5 eq.). 1-hexanethiol (2.84 g, 24.0 mmol, 0.832 mL, 1.2 eq.) was added to the resulting mixture, which was heated to reflux for 16 h. After cooling to room temperature, the reaction mixture was diluted with ethyl acetate (150 mL) and filtrated over Celite®, then the solvent was removed under reduced pressure. Purification of the crude reaction mixture by flash column chromatography (SiO_2, petroleum ether) afforded pure **29** (4.94 g, 18.1 mmol, 91% yield) as a colorless oil.

(**29**): ^{1}H–NMR (400 MHz, $CDCl_3$): δ = 7.38 (d, *J* = 8.4 Hz, 2H), 7.16 (d, *J* = 8.4 Hz, 2H), 2.89 (t, *J* = 7.4 Hz, 2H), 1.57–1.68 (m, 2H), 1.36–1.48 (m, 2H), 1.22–1.39 (m, 4H), 0.85–0.94 (m, 3H) ppm. ^{13}C–NMR (100 MHz, $CDCl_3$): δ = 136.4, 131.9, 130.4, 119.4, 33.7, 31.4, 29.1, 28.9, 22.6, 14.1 ppm. The analytical data were in agreement with those reported in the literature.[17]

4-(Hexylthio)-*N*-(4-(hexylthio)phenyl)-*N*-phenylaniline (30)

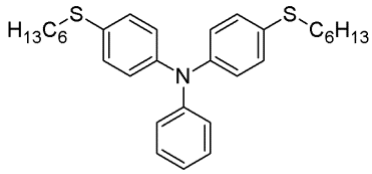

30

1-Bromo-4-hexylthiobenzene (**29**, 4.74 g, 17.3 mmol, 3.0 eq.) was dissolved in toluene (55 mL). The solution was degassed, then $Pd_2(dba)_3$ (300 mg, 0.29 mmol, 5.0 mol%) and dppf (321 mg, 0.57 mmol, 10 mol%) were added. The mixture was stirred for 15 min at room temperature while the color turned from black to red, then aniline (539 mg, 5.79 mmol, 0.480 mL, 1.0 eq.) and sodium *tert*-butoxide (2.22 g, 23.1 mmol, 4.0 eq.) were added. The reaction mixture was heated to reflux and stirred for 20 h. After cooling and filtration over Celite®, the resulting solution was diluted with Et_2O (200 mL), washed with water (150 mL) and brine (200 mL), and dried with Na_2SO_4. Filtration, removal of the solvent and purification by flash column chromatography (SiO_2, petroleum ether / toluene, gradient from 10:1 to 5:1) gave compound **30** (2.22 g, 4.65 mmol, 80% yield) as a pale yellow oil.

(**30**): ^{1}H–NMR (400 MHz, C_6D_6): δ = 7.21 (d, *J* = 8.5 Hz, 4H), 7.04 (m, 4H), 6.95 (d, *J* = 8.5 Hz, 4H), 6.84 (m, 1H), 2.67 (t, *J* = 7.2 Hz, 4H), 1.53 (qu, *J* = 7.5 Hz, 4H), 1.05–1.32 (m, 12H), 0.83 (t, *J* = 7.1 Hz, 6H) ppm. The analytical data were in agreement with those reported in the literature.[16]

4-Bromo-*N,N-bis*(4-(hexylthio)phenyl)aniline (31)

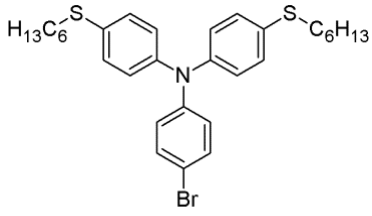

31

Compound **30** (1.53 g, 3.20 mmol, 1.0 eq.), was dissolved in dry $CHCl_3$ (30 mL) together with *N*-bromosuccinimide (569 mg, 3.20 mmol, 1.0 eq.). The brown solution was stirred at room temperature in the dark for 4 hours, while the color turned to pale yellow, then diluted with $CHCl_3$ (100 mL), washed with water (150 mL) and brine (200 mL), and dried with Na_2SO_4. Filtration and removal of the solvent gave

compound **31** (1.75 g, 3.15 mmol, 98% yield) as a pale orange oil, which was used for the following reaction without further purification.

(**31**): ^{1}H–NMR (400 MHz, C_6D_6): δ = 7.20 (d, *J* = 8.6 Hz, 4H), 7.13 (d, *J* = 8.8 Hz, 2H), 6.84 (d, *J* = 8.6 Hz, 4H), 6.68 (d, *J* = 8.8 Hz, 2H), 2.68 (t, *J* = 7.3 Hz, 4H), 1.54 (q, *J* = 7.4 Hz, 4H), 1.06–1.32 (m, 12H), 0.83 (t, *J* = 7.1 Hz, 6H) ppm. The analytical data were in agreement with those reported in the literature.[16]

10-(4-Methoxyphenyl)-10H-phenothiazine (34)

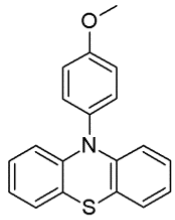

34

4-iodoanisole (**33**, 11.6 g, 49.5 mmol, 1.5 eq.) was dissolved in toluene (150 mL). The solution was degassed, then $Pd_2(dba)_3$ (1.71 g, 1.65 mmol, 5.0 mol%) and tri-*tert*-butylphosphine (0.667 g, 3.30 mmol, 0.834 mL, 10 mol%) were added. The mixture was stirred for 30 min at room temperature, then phenothiazine (**32**, 6.57 g, 33.0 mmol, 1.0 eq.) and sodium *tert*-butoxide (7.92 g, 82.4 mmol, 2.5 eq.) were added. The reaction mixture was heated to reflux and stirred for 20 h. After cooling and filtration over Celite®, the resulting solution was diluted with ethyl acetate (300 mL), washed with water (300 mL) and brine (300 mL), and dried with Na_2SO_4. Filtration, removal of the solvent and purification by flash column chromatography (SiO_2, petroleum ether / Et_2O 10:1, then $CHCl_3$) gave compound **34** (7.51 g, 24.6 mmol, 75% yield) as a dark yellow solid.

(**34**): ^{1}H–NMR (300 MHz, $CDCl_3$): δ = 7.31 (d, *J* = 9.0 Hz, 2H), 7.12 (d, *J* = 8.9 Hz, 2H), 6.99 (dd, *J* = 8.6, *J* = 2.0 Hz, 2H), 6.76–6.85 (m, 4H), 6.19 (dd, *J* = 8.1, *J* = 1.6 Hz, 2H), 3.90 (s, 3H) ppm. The analytical data were in agreement with those reported in the literature.[37]

10-(4-Methoxyphenyl)-3-bromo-10H-phenothiazine (35)

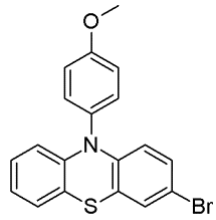

35

10-(4-methoxyphenyl)-10H-phenothiazine (**34**, 3.05 g, 10.0 mmol, 1.0 eq.) was dissolved in a mixture of dry CH_2Cl_2 (100 mL) and dry CH_3CN (60 mL), and treated with pyridinium bromide perbromide (2.72 g, 8.50 mmol, 0.85 eq.), which was added in four portions during 20 minutes. The reaction mixture was stirred at room temperature for 10 minutes, the solvents were removed and ethyl acetate (150 mL) was added. The organic phase was washed with a saturated aqueous solution of $NaHCO_3$ (100 mL), water (100 mL) and brine (100 mL). After drying with Na_2SO_4, filtration and removal of the solvent, the crude product was purified by flash column chromatography (SiO_2, petroleum ether/toluene 3:1). Purification yielded a 3:1 mixture of compound **35** and starting material **34**, which was used as such in the following step.

(**35**): ^{1}H–NMR (400 MHz, C_6D_6): δ = 7.06 (d, *J* = 2.3 Hz, 1H), 6.85 (dd, *J* = 7.4 Hz, *J* = 1.6 Hz, 1H), 6.82 (d, *J* = 8.9 Hz, 2H), 6.77 (dd, *J* = 8.8 Hz, *J* = 2.3 Hz, 1H), 6.54–6.70 (m, 4H), 6.17 (dd, *J* = 8.1 Hz, *J* = 1.2 Hz, 1H), 5.91 (d, *J* = 8.8 Hz, 1H), 3.24 (s, 3H) ppm.

General procedure for the synthesis of compounds 21–23[15]

The appropriate bromide (**28**, **31** or **35**, 1.0 eq.) was dissolved in *N*,*N*-DMF together with bis(pinacolato)diboron (1.5 eq.), Pd(dppf)Cl_2 (10 mol%) and potassium acetate (3.0 eq.). The resulting mixture was heated to 80°C for 16 h, then allowed to cool to room temperature. After dilution with water (100 mL) and CH_2Cl_2 (100 mL), the two phases were separated and the organic phase was washed with water (5 × 100 mL) and brine and then dried with Na_2SO_4. After filtration and evaporation of the solvent, the crude product was purified by flash column chromatography.

4-(hexyloxy)-*N*-(4-(hexyloxy)phenyl)-*N*-(4-(4,4,5,5-tetramethyl-1,3,2-dioxaborolan-2-yl)phenyl)aniline (21)

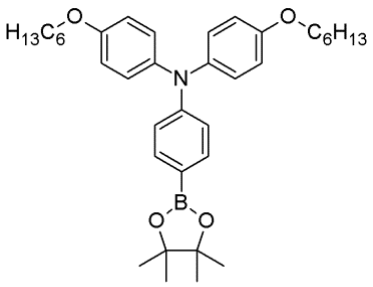

21

Bromide **28** (2.60 g, 4.96 mmol) was dissolved in *N*,*N*-DMF (25 mL) with $Pd(dppf)Cl_2$ (404 mg, 0.496 mmol), bis(pinacolato)diboron (1.89 g, 7.44 mmol) and potassium acetate (1.46 g, 14.9 mmol). The reaction mixture was heated at 80°C for 16h. After work-up, evaporation of the solvent gave a brown oil which was purified by flash column chromatography (SiO_2; petroleum ether / toluene 1:3) to give pure ester **21** (2.02 g, 3.54 mmol, 71% yield) as a light brown oil.

(**21**): ^{1}H–NMR (300 MHz, $CDCl_3$): δ = 7.59 (d, *J* = 8.6 Hz, 2H), 7.05 (d, *J* = 8.9 Hz, 4H), 6.85 (d, *J* = 8.6 Hz, 2H), 6.81 (d, *J* = 9.0 Hz, 4H), 3.93 (t, *J* = 6.5 Hz, 4H), 1.76 (q, *J* = 6.7 Hz, 4H), 1.42–1.53 (m, 4H), 1.24–1.39 (m, 20H), 0.86–0.94 (m, 6H) ppm. The analytical data were in agreement with those reported in the literature.[12]

4-(Hexylthio)-*N*-(4-(hexylthio)phenyl)-*N*-(4-(4,4,5,5-tetramethyl-1,3,2-dioxaborolan-2-yl)phenyl)aniline (22)

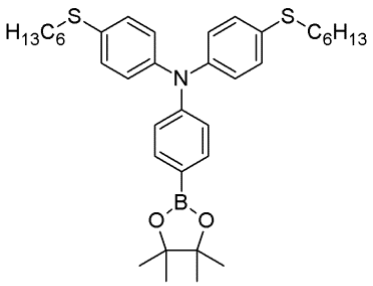

22

Bromide **31** (1.23 g, 2.20 mmol) was dissolved in *N*,*N*-DMF (20 mL) with $Pd(dppf)Cl_2$ (161 mg, 0.22 mmol), bis(pinacolato)diboron (838 mg, 3.30 mmol) and potassium acetate (648 mg, 6.60 mmol). The reaction mixture was heated at 80°C for 16h. After

work-up, evaporation of the solvent gave a brown oil which was purified by flash column chromatography (SiO_2; petroleum ether / toluene, gradient from 1:1 to 1:2) to give pure ester **22** (788 mg, 1.31 mmol, 59% yield) as a light green oil.

(**22**): ^{1}H–NMR (400 MHz, $CDCl_3$): δ = 7.66 (d, *J* = 7.9 Hz, 2H), 7.21 (d, *J* = 8.6 Hz, 4H), 6.98–7.03 (m, 6H), 2.88 (t, *J* = 7.4 Hz, 4H), 1.64 (q, *J* = 7.5 Hz, 4H), 1.37–1.46 (m, 4H), 1.33 (s, 12H), 1.24–1.32 (m, 8H), 0.89 (t, J = 6.7 Hz, 6H) ppm. Analytical data were in agreement with those found in the literature.[16]

10-(4-Methoxyphenyl)-3-(4,4,5,5-tetramethyl-1,3,2-dioxaborolan-2-yl)-10H-phenothiazine (23)

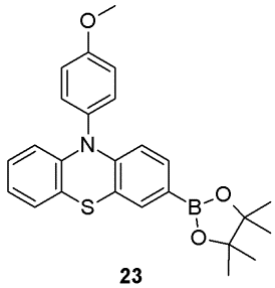

23

The 3:1 mixture of compounds **35**/**34** (corresponding to 2.00 g, 3.86 mmol of 10-(4-methoxyphenyl)-3-bromo-10H-phenothiazine **35**) was dissolved in *N*,*N*-DMF (20 mL) with $Pd(dppf)Cl_2$ (283 mg, 0.39 mmol), bis(pinacolato)diboron (1.47 g, 5.79 mmol) and potassium acetate (1.14 g, 11.6 mmol). The reaction mixture was heated at 80°C for 16h. After work-up, evaporation of the solvent gave a brown oil which was purified by flash column chromatography (SiO_2; toluene) to give pure ester **23** (1.38 g, 3.20 mmol, 83% yield) as a colorless solid.

(**23**): mp = 197–199 °C. ^{1}H–NMR (300 MHz, C_6D_6): δ = 8.03 (d, *J* = 1.4 Hz, 1H), 7.73 (dd, *J* = 8.2 Hz, *J* = 1.3 Hz, 1H), 6.87 (dd, *J* = 7.3 Hz, *J* = 1.9 Hz, 1H), 6.83 (d, *J* = 8.7 Hz, 2H), 6.63 (d, *J* = 8.8 Hz, 2H), 6.54–6.59 (m, 2H), 6.35 (d, *J* = 8.2 Hz, 1H), 6.16 (dd, *J* = 7.8 Hz, *J* = 1.6 Hz, 1H), 3.20 (s, 3H), 1.09 (s, 12H) ppm. ^{13}C–NMR (75 MHz, C_6D_6): δ = 159.5, 147.7, 144.8, 134.4, 134.1, 133.3, 132.3, 127.1, 126.9, 123.0, 120.6, 119.6, 116.3, 116.1, 115.5, 83.6, 54.9, 24.9 ppm. IR (KBr): $\tilde{\nu}$ = 3058, 2976, 2924, 1598, 1510, 1351, 1295, 1143, 1032 cm^{-1}. ESI–MS: *m/z* = 431.33 $[M]^+$.

General procedure for the synthesis of compounds 9 and 36

2,5-Bis(8-iodo-3,3-dipentyl-3,4-dihydro-2*H*-thieno[3,4-*b*][1,4]dioxepin-6-yl)thiazolo[5,4-*d*]thiazole (**11**, 1.0 eq.) was dissolved in toluene together with $[Pd(PPh_3)_4]$ (0.1 eq.). The appropriate boronic acid or ester (**20** or **21**) (1.0 eq.) was then added, followed by Na_2CO_3 (2.0 M aqueous solution, 5.0 eq.). The resulting mixture was heated at 100°C and stirred for 16 h, then allowed to cool to room temperature and diluted with H_2O (150 mL) and CH_2Cl_2 (150 mL). The phases were separated and the aqueous layer washed with CH_2Cl_2 (2 × 50 mL). The combined organic layers were washed with brine and dried with Na_2SO_4. After filtration and evaporation of the solvent, the crude product was purified by flash column chromatography.

4-(8-(5-(8-Iodo-3,3-dipentyl-3,4-dihydro-2H-thieno[3,4-*b*][1,4]dioxepin-6-yl)thiazolo[5,4-*d*]thiazol-2-yl)-3,3-dipentyl-3,4-dihydro-2H-thieno[3,4-*b*][1,4]dioxepin-6-yl)-*N*,*N*-diphenylaniline (9)

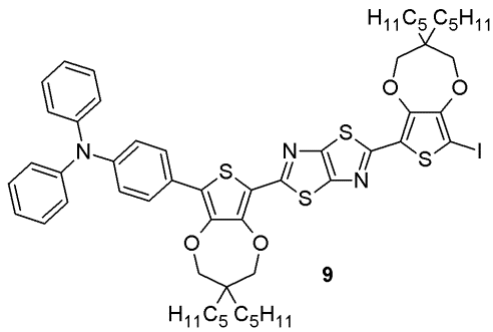

9

Diiodide **11** (800 mg, 0.81 mmol) was dissolved in toluene (30 mL) with $[Pd(PPh_3)_4]$ (94 mg, 0.08 mmol) and reacted with 4-(diphenylamino)benzeneboronic acid (**20**, 235 mg, 0.81 mmol) and Na_2CO_3 (2.0 M aqueous solution, 2.0 mL, 4.07 mmol) at 100°C for 16h. After work-up, evaporation of the solvent gave a dark-red oil which was purified by flash column chromatography (SiO_2; petroleum ether / toluene 3:1 to 1:1) to give pure **9** (285 mg, 0.26 mmol, 29% yield) as an orange solid as well as starting material **11** (239 mg, 30% recovery).

(**9**): mp = 91–93 °C. ^{1}H–NMR (400 MHz, $CDCl_3$): δ = 7.63 (d, *J* = 8.7 Hz, 2H), 7.27 (t, *J* = 8.2 Hz, 4H), 7.13 (d, *J* = 7.8 Hz, 4H), 7.03–7.07 (m, 4H), 4.15 (s, 2H), 4.09 (s, 2H), 4.01 (s, 2H), 3.98 (s, 2H), 1.44–1.48 (m, 8H), 1.28–1.36 (m, 24H), 0.91 (t, *J* = 6.7 Hz, 12H) ppm. ^{13}C–NMR (100 MHz, $CDCl_3$): δ = 159.8, 158.4, 152.0, 150.5, 150.2, 149.4, 147.5, 146.6, 145.1, 129.5, 127.7, 126.4, 125.0, 124.4, 123.5, 123.0, 122.1, 118.0, 113.7,

78.3, 78.2, 77.93, 77.89, 60.7, 44.11, 44.08, 32.8, 32.7, 32.3, 32.1, 29.8, 22.71, 22.69, 22.67, 22.6, 14.2 ppm. IR (KBr): $\tilde{\nu}$ = 3058, 2927, 2857, 1590, 1491, 1057 cm^{-1}. ESI–MS: *m/z* = 1100.26 $[M+1]^+$.

4-(Hexyloxy)-*N*-(4-(hexyloxy)phenyl)-*N*-(4-(8-(5-(8-iodo-3,3-dipentyl-3,4-dihydro-2H-thieno[3,4-*b*][1,4]dioxepin-6-yl)thiazolo[5,4-*d*]thiazol-2-yl)-3,3-dipentyl-3,4-dihydro-2H-thieno[3,4-*b*][1,4]dioxepin-6-yl)phenyl)aniline (36)

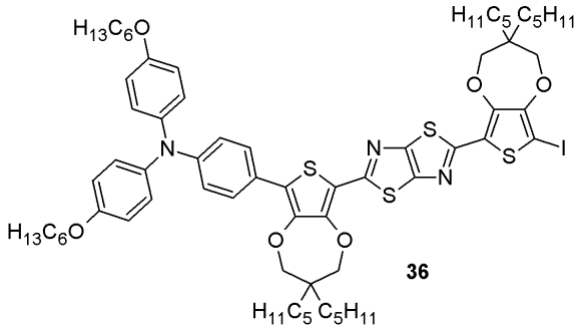

36

Diiodide **11** (750 mg, 0.76 mmol) was dissolved in toluene (30 mL) with $[Pd(PPh_3)_4]$ (176 mg, 0.15 mmol) and reacted with 4-(hexyloxy)-*N*-(4-(hexyloxy)phenyl)-*N*-(4-(4,4,5,5,-tetramethyl-1,3,2-dioxaborolan-2-yl)phenyl)aniline (**21**, 436 mg, 0.76 mmol) and Na_2CO_3 (2.0 M aqueous solution, 1.9 mL, 3.82 mmol) at 100°C for 16h. After work-up, evaporation of the solvent gave a dark-red oil which was purified by flash column chromatography (SiO_2, petroleum ether/toluene 2:1 to 1:1) to give pure **36** (174 mg, 0.13 mmol, 18% yield) as a sticky orange solid, as well as starting material **11** (223 mg, 30% recovery).

(**36**): ^{1}H-NMR (400 MHz, C_6D_6): δ = 7.84 (d, *J* = 8.8 Hz, 2H), 7.11 (d, *J* = 8.9 Hz, 6H), 6.80 (d, *J* = 8.9 Hz, 4H), 3.69 (s, 2H), 3.65 (t, *J* = 6.4 Hz, 4H), 3.61 (s, 2H), 3.54 (s, 2H), 3.49 (s, 2H), 1.62 (q, *J* = 6.5 Hz, 4H), 1.05–1.47 (m, 44H), 0.84–0.97 (m, 18H) ppm. ^{13}C-NMR (100 MHz, C_6D_6): δ = 160.3, 158.6, 156.4, 152.4, 151.3, 151.0, 150.0, 149.0, 146.9, 145.3, 141.0, 128.8, 127.3, 125.5, 125.3, 123.0, 120.7, 115.8, 114.5, 78.0, 77.7, 77.6, 68.2, 61.2, 43.8, 43.7, 33.0, 32.9, 32.4, 32.1, 31.9, 30.2, 29.7, 26.1, 23.0, 22.94, 22.90, 22.8, 22.7, 14.34, 14.32, 14.27 ppm. IR (KBr): $\tilde{\nu}$ = 2952, 2925, 2852, 1602, 1508, 1060 cm^{-1}. ESI-MS: *m/z* = 1300.52 $[M+1]^+$.

General procedure for the synthesis of compounds 37 and 38

2,5-Bis(8-iodo-3,3-dipentyl-3,4-dihydro-2*H*-thieno[3,4-*b*][1,4]dioxepin-6-yl)thiazolo[5,4-*d*]thiazole (**11**), (1.0 eq.) was dissolved in toluene together with [Pd(dppf)Cl_2] (0.1 eq.). The appropriate boronic ester (**22** or **23**) (1.0 eq.) was then added, followed by KF (5.0 eq.) and ethanol. The resulting mixture was heated at 78°C and stirred for 5-16h, then allowed to cool to room temperature and filtered over a short pad of Celite®. After evaporation of the solvent, the crude product was purified by flash column chromatography.

4-(Hexylthio)-*N*-(4-(hexylthio)phenyl)-*N*-(4-(8-(5-(8-iodo-3,3-dipentyl-3,4-dihydro-2H-thieno[3,4-*b*][1,4]dioxepin-6-yl)thiazolo[5,4-*d*]thiazol-2-yl)-3,3-dipentyl-3,4-dihydro-2Hthieno[3,4-*b*][1,4]dioxepin-6-yl)phenyl)aniline (37)

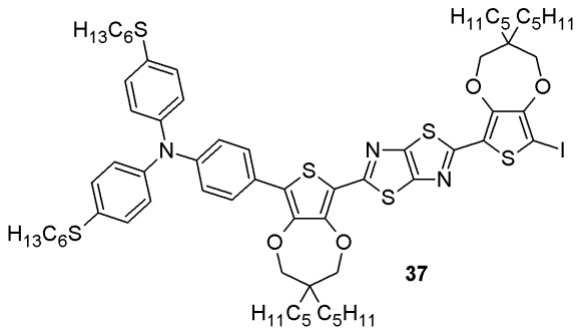

37

Diiodide **11** (750 mg, 0.76 mmol) was dissolved in toluene (15 mL) with [Pd(dppf)Cl_2] (56 mg, 0.08 mmol) and reacted with 4-(hexylthio)-*N*-(4-(hexylthio)phenyl)-*N*-(4-(4,4,5,5,-tetramethyl-1,3,2-dioxaborolan-2-yl)phenyl)aniline (**22**, 461 mg, 0.76 mmol), KF (222 mg, 3.82 mmol) and ethanol (15 mL) at 78°C for 5h, then a second portion of [Pd(dppf)Cl_2] (28 mg, 0.04 mmol) was added and stirring was continued for 2 hours. After work-up, evaporation of the solvent gave a dark-red oil which was purified by flash column chromatography (SiO_2, petroleum ether / toluene 2:1 to 1:1) to give pure **37** (178 mg, 0.13 mmol, 18% yield) as a sticky orange solid, as well as starting material **11** (495 mg, 66% recovery).

(**37**): ^{1}H-NMR (400 MHz, C_6D_6): δ = 7.81 (d, *J* = 8.8 Hz, 2H), 7.23 (d, *J* = 8.4 Hz, 4H), 7.04 (d, *J* = 8.8 Hz, 2H), 6.96 (d, *J* = 8.0 Hz, 4H), 3.68 (s, 2H), 3.62 (s, 2H), 3.53 (s, 2H), 3.48 (s, 2H), 2.70 (t, *J* = 7.2 Hz, 4H), 1.55 (q, *J* = 7.6 Hz, 4H), 1.04–1.38 (m, 44H), 0.91 (m, 12H), 0.84 (t, *J* = 6.8 Hz, 6H) ppm. ^{13}C-NMR (100 MHz, C_6D_6): δ = 160.0, 159.3, 158.8, 152.4, 151.3, 151.1, 149.8, 147.3, 147.2, 147.0, 145.8, 145.7, 131.9, 131.2,

125.4, 124.6, 123.7, 122.9, 115.1, 77.9, 77.7, 77.6, 61.4, 43.7, 43.6, 34.6, 33.0, 32.9, 32.3, 32.1, 31.7, 29.6, 28.8, 22.93, 22.91, 22.89, 22.8, 22.7, 14.3, 14.2 ppm. IR (KBr): $\tilde{\nu}$ = 3025, 2928, 2857, 1587, 1490, 1060 cm^{-1}. ESI-MS: *m/z* = 1332.11 $[M+1]^+$.

3-(8-(5-(8-Iodo-3,3-dipentyl-3,4-dihydro-2H-thieno[3,4-*b*][1,4]dioxepin-6-yl)thiazolo[5,4-*d*]thiazol-2-yl)-3,3-dipentyl-3,4-dihydro-2H-thieno[3,4-*b*][1,4]dioxepin-6-yl)-10-(4-methoxyphenyl)-10H-phenothiazine (38)

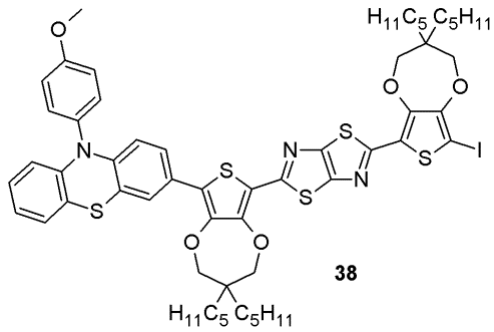

38

Diiodide **11** (750 mg, 0.76 mmol) was dissolved in toluene (15 mL) with $[Pd(dppf)Cl_2]$ (56 mg, 0.08 mmol) and reacted with 10-(4-methoxyphenyl)-3-(4,4,5,5-tetramethyl-1,3,2-dioxaborolan-2-yl)-10H-phenothiazine (**23**) (329 mg, 0.76 mmol), KF (222 mg, 3.82 mmol) and ethanol (15 mL) at 78°C for 5h, then a second portion of $[Pd(dppf)Cl_2]$ (28 mg, 0.04 mmol) was added and stirring was continued for further 16h. After work-up, evaporation of the solvent gave a dark-red oil which was purified by flash column chromatography (SiO_2, petroleum ether / toluene 2:1 to 1:1) to give pure **38** (102 mg, 0.09 mmol, 12% yield) as a sticky orange solid, as well as starting material **11** (117 mg, 16% recovery).

(**38**): ^{1}H-NMR (400 MHz, C_6D_6): δ = 7.85 (d, *J* = 2.1 Hz, 1H), 7.33 (dd, *J* = 8.7 Hz, *J* = 2.1 Hz, 1H), 6.94 (d, *J* = 8.9 Hz, 2H), 6.91 (dd, *J* = 7.5 Hz, *J* = 1.6 Hz, 1H), 6.74 (d, *J* = 8.9 Hz, 2H), 6.63–6.69 (m, 1H), 6.57–6.61 (m, 1H), 6.23 (dd, *J* = 8.2 Hz, *J* = 1.2 Hz, 1H), 6.19 (d, *J* = 8.7 Hz, 1H), 3.72 (s, 2H), 3.58 (s, 4H), 3.51 (s, 2H), 3.29 (s, 3H), 0.98–1.36 (m, 32H), 0.93 (t, *J* = 7.1 Hz, 6H), 0.91 (t, *J* = 7.3 Hz, 6H) ppm. ^{13}C-NMR (100 MHz, C_6D_6): δ = 160.0, 159.7, 158.7, 152.4, 151.3, 151.0, 149.7, 147.0, 145.6, 144.8, 144.5, 133.4, 132.5, 127.1, 125.9, 125.4, 123.8, 122.9, 120.7, 120.1, 116.2, 114.8, 78.0, 77.8, 77.7, 77.6, 61.3, 55.1, 43.74, 43.71, 33.0, 32.9, 32.4, 32.1, 23.0, 22.9, 22.8, 22.7, 14.4, 14.3 ppm. IR (KBr): $\tilde{\nu}$ = 3064, 2928, 2857, 1510, 1461, 1057 cm^{-1}. ESI-MS: *m/z* = 1160.06 $[M]^+$.

General procedure for cross-coupling with 5-formylthiophen-2-ylboronic acid (42).

Compound **9** or **36**–**38** (1.0 eq.) was dissolved in anhydrous toluene together with [Pd(dppf)Cl_2] (0.05 eq.) and introduced in a microwave vial equipped with a magnetic stirrer. Boronic acid **42** (1.5 eq.) and KF (6.0 eq.) were dissolved in MeOH and the resulting pink solution was transferred into the microwave vial. The reaction mixture was heated under microwave irradiation at 70°C for 30 min. After cooling to room temperature, the reaction mixture was diluted with water (30 mL) and CH_2Cl_2 (30 mL), the layers were separated and the aqueous layer was extracted with CH_2Cl_2 (20 mL). The combined organic layers were washed with brine (50 mL) and dried with Na_2SO_4. Removal of the solvent *in vacuo* yielded a black solid, which was purified by flash column chromatography.

5-(8-(5-(8-(4-(Diphenylamino)phenyl)-3,3-dipentyl-3,4-dihydro-2H-thieno[3,4-*b*][1,4]dioxepin-6-yl)thiazolo[5,4-*d*]thiazol-2-yl)-3,3-dipentyl-3,4-dihydro-2H-thieno[3,4-*b*][1,4]dioxepin-6-yl)thiophene-2-carbaldehyde (7)

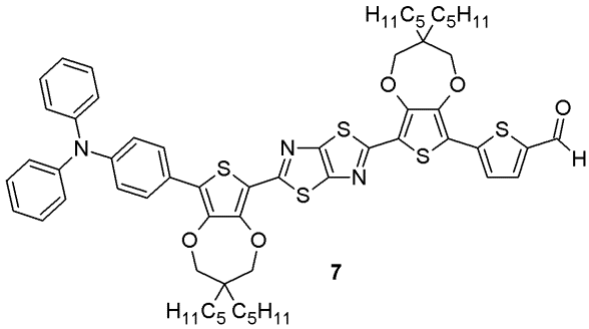

7

Compound **9** (123 mg, 0.11 mmol) and [Pd(dppf)Cl_2] (5 mg, 0.006 mmol) were dissolved in toluene (6.0 mL) and reacted with 5-formyl-2-thiopheneboronic acid (**42**) (26 mg, 0.17 mmol) and KF (39 mg, 0.67 mmol) in MeOH (3.0 mL) under microwave irradiation at 70°C for 30 min. Work-up and evaporation of the solvent yielded a black solid, which was purified by flash column chromatography (SiO_2, toluene / petroleum ether 3:1) to give compound **7** (89 mg, 0.08 mmol, 74% yield) as a dark-red solid.

(**7**): mp = 229–231 °C. ^{1}H-NMR (400 MHz, $CDCl_3$): δ = 9.89 (s, 1H), 7.67 (d, *J* = 4.1 Hz, 1H), 7.63 (d, *J* = 8.8 Hz, 2H), 7.26–7.32 (m, 5H), 7.13 (d, *J* = 8.5 Hz, 4H), 7.03–7.07 (m, 4H), 4.16 (s, 4H), 4.13 (s, 2H), 4.02 (s, 2H), 1.46–1.52 (m, 8H), 1.29–1.36 (m, 24H), 0.89–0.94 (m, 12H) ppm. ^{13}C-NMR (100 MHz, $CDCl_3$): δ = 183.0, 160.1, 157.9, 151.1,

150.5, 149.6, 148.1, 147.5, 147.4, 147.3, 145.1, 144.1, 142.0, 136.7, 129.5, 127.7, 126.2, 125.0, 124.6, 123.8, 123.5, 122.9, 117.0, 116.9, 113.5, 78.4, 78.1, 77.9, 44.2, 44.0, 32.8, 32.7, 32.2, 32.1, 29.8, 22.7, 14.2 ppm. IR (KBr): $\tilde{\nu}$ = 3025, 2928, 2857, 1654, 1054 cm^{-1}. ESI-MS: *m/z* = 1083.62 $[M]^+$.

5-(8-(5-(8-(4-(*Bis*(4-(hexyloxy)phenyl)amino)phenyl)-3,3-dipentyl-3,4-dihydro-2H-thieno[3,4-*b*][1,4]dioxepin-6-yl)thiazolo[5,4-*d*]thiazol-2-yl)-3,3-dipentyl-3,4-dihydro-2H-thieno[3,4-*b*][1,4]dioxepin-6-yl)thiophene-2-carbaldehyde (39)

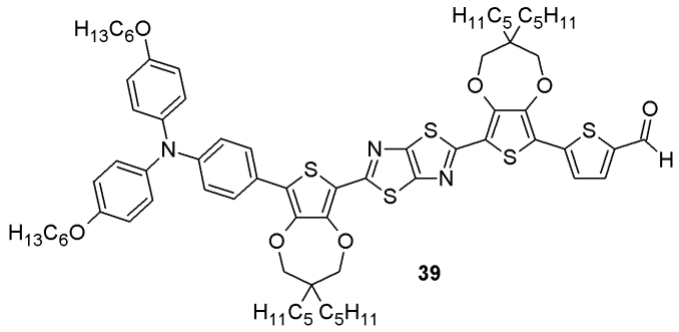

39

Compound **36** (187 mg, 0.14 mmol) and [Pd(dppf)Cl_2] (6 mg, 0.007 mmol) were dissolved in toluene (4.0 mL) and reacted with 5-formyl-2-thiopheneboronic acid (**42**) (42 mg, 0.22 mmol) and KF (50 mg, 0.86 mmol) in MeOH (2.0 mL) under microwave irradiation at 70°C for 30 min. Work-up and evaporation of the solvent yielded a black solid, which was purified by flash column chromatography (SiO_2, toluene / petroleum ether 3:1) to give compound **39** (116 mg, 0.09 mmol, 63% yield) as a dark-red sticky solid.

(**39**)**:** ^{1}H-NMR (400 MHz, C_6D_6): δ = 9.57 (s, 1H), 7.84 (d, *J* = 8.8 Hz, 2H), 7.10–7.17 (m, 6H), 6.97 (d, *J* = 4.0 Hz, 1H), 6.90 (d, *J* = 4.0 Hz, 1H), 6.82 (d, *J* = 8.8 Hz, 4H), 3.78 (s, 2H), 3.64–3.68 (m, 8H), 3.60 (s, 2H), 1.63 (q, *J* = 8.8 Hz, 4H), 1.02–1.41 (m, 44H), 0.93 (t, *J* = 7.1 Hz, 12H), 0.88 (t, *J* = 6.8 Hz, 6H) ppm. ^{13}C-NMR (100 MHz, C_6D_6): δ = 182.2, 160.6, 158.2, 156.4, 152.0, 151.2, 150.2, 149.1, 148.6, 147.5, 145.3, 143.4, 143.0, 140.9, 136.1, 127.3, 126.6, 125.8, 125.2, 123.8, 120.6, 117.7, 117.6, 115.8, 114.3, 78.1, 78.0, 77.7, 77.6, 68.2, 43.7, 33.0, 32.9, 32.3, 32.2, 32.0, 30.2, 29.7, 26.1, 23.0, 22.9, 22.8, 22.7, 14.3, 14.2 ppm. IR (KBr): $\tilde{\nu}$ = 3036, 2929, 2857, 1655, 1438, 1054 cm^{-1}. ESI-MS: *m/z* = 1285.40 $[M+1]^+$.

5-(8-(5-(8-(4-(Bis(4-(hexylthio)phenyl)amino)phenyl)-3,3-dipentyl-3,4-dihydro-2H-thieno[3,4-*b*][1,4]dioxepin-6-yl)thiazolo[5,4-*d*]thiazol-2-yl)-3,3-dipentyl-3,4-dihydro-2H-thieno[3,4-*b*][1,4]dioxepin-6-yl)thiophene-2-carbaldehyde (40)

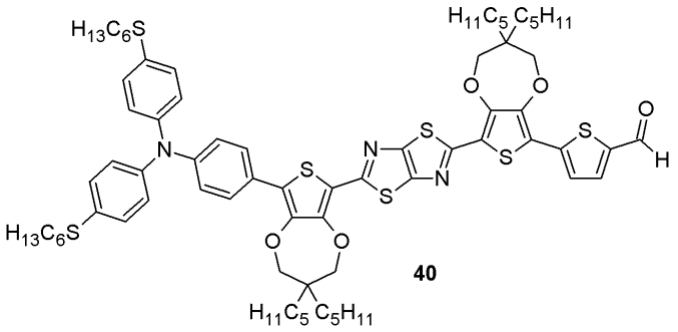

Compound **37** (160 mg, 0.12 mmol) and [Pd(dppf)Cl_2] (5 mg, 0.006 mmol) were dissolved in toluene (6.0 mL) and reacted with 5-formyl-2-thiopheneboronic acid (**42**) (35 mg, 0.18 mmol) and KF (42 mg, 0.72 mmol) in MeOH (3.0 mL) under microwave irradiation at 70°C for 30 min. Work-up and evaporation of the solvent yielded a black solid, which was purified by flash column chromatography (SiO_2; Toluene) to give compound **40** (90 mg, 0.07 mmol, 57% yield) as a dark-red sticky solid.

(**40**): ^{1}H-NMR (400 MHz, C_6D_6): δ = 9.57 (s, 1H), 7.82 (d, *J* = 8.7 Hz, 2H), 7.24 (d, *J* = 8.6 Hz, 4H), 7.05 (d, *J* = 8.7Hz, 2H), 6.97 (d, *J* = 8.6 Hz, 4H), 6.94 (d, *J* = 4.0 Hz, 1H), 6.87 (d, *J* = 4.0 Hz, 1H), 3.73 (s, 2H), 3.64 (s, 2H), 3.61 (s, 2H), 3.55 (s, 2H), 2.70 (t, *J* = 7.3 Hz, 4H), 1.56 (q, *J* = 7.5 Hz, 4H), 0.96–1.41 (m, 44H), 0.93 (t, *J* = 7.0 Hz, 12H), 0.85 (t, *J* = 7.0 Hz, 6H) ppm. ^{13}C-NMR (100 MHz, C_6D_6): δ = 182.2, 160.3, 158.4, 151.9, 151.4, 150.0, 148.7, 147.5, 147.4, 145.7, 143.4, 143.0, 136.1, 132.0, 131.2, 131.0, 127.4, 125.7, 125.5, 124.9, 123.8, 123.6, 117.7, 117.6, 115.0, 78.2, 78.0, 77.7, 43.8, 34.6, 33.0, 32.96, 32.4, 32.3, 31.7, 29.6, 28.8, 22.95, 22.93, 22.85, 22.78, 14.4, 14.3 ppm. IR (KBr): $\tilde{\nu}$ = 3025, 2924, 2852, 1653, 1438, 1057 cm^{-1}. ESI-MS: *m/z* = 1315.27 $[M]^+$.

5-(8-(5-(8-(10-(4-Methoxyphenyl)-10H-phenothiazin-2-yl)-3,3-dipentyl-3,4-dihydro-2H-thieno[3,4-*b*][1,4]dioxepin-6-yl)thiazolo[5,4-*d*]thiazol-2-yl)-3,3-dipentyl-3,4-dihydro-2H-thieno[3,4-*b*][1,4]dioxepin-6-yl)thiophene-2-carbaldehyde (41).

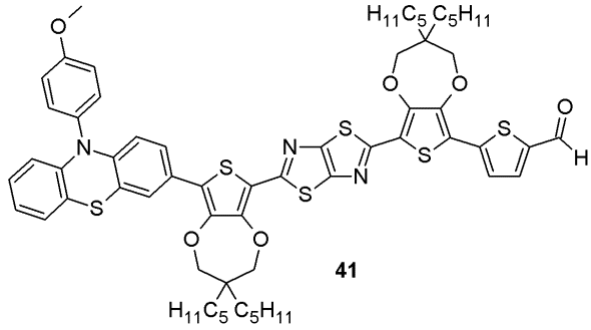

41

Compound **38** (97 mg, 0.08 mmol) and [Pd(dppf)Cl_2] (3.0 mg, 0.004 mmol) were dissolved in toluene (4.0 mL) and reacted with 5-formyl-2-thiopheneboronic acid (**42**) (19 mg, 0.12 mmol) and KF (29 mg, 0.50 mmol) in MeOH (2.0 mL) under microwave irradiation at 70°C for 30 min. Work-up and evaporation of the solvent yielded a black solid, which was purified by flash column chromatography (SiO_2; Toluene) to give compound **41** (70 mg, 0.06 mmol, 73% yield) as a dark-red sticky solid.

(**41**): mp = 232–235 °C. ^{1}H-NMR (400 MHz, C_6D_6): δ = 9.57 (s, 1H), 7.87 (d, *J* = 2.1 Hz, 1H), 7.33 (dd, *J* = 8.7 Hz, J = 2.1 Hz, 1H), 6.90–6.97 (m, 4H), 6.88 (d, *J* = 4.0 Hz, 1H), 6.75 (d, *J* = 8.9 Hz, 2H), 6.64–6.69 (m, 1H), 6.56–6.62 (m, 1H), 6.25 (dd, *J* = 8.2 Hz, *J* = 1.2 Hz, 1H), 6.20 (d, *J* = 8.6 Hz, 1H), 3.72 (s, 2H), 3.61 (s, 2H), 3.57 (s, 2H), 3.54 (s, 2H), 3.29 (s, 3H), 1.15–1.36 (m, 24H), 1.00–1.13 (m, 8H), 0.94 (t, *J* = 7.2 Hz, 6H), 0.93 (t, *J* = 7.2 Hz, 6H) ppm. ^{13}C-NMR (100 MHz, C_6D_6): δ = 182.2, 160.3, 159.7, 158.3, 152.0, 151.3, 150.0, 148.6, 147.5, 145.7, 144.8, 144.6, 143.4, 143.0, 136.1, 133.3, 132.4, 127.2, 125.9, 125.4, 124.2, 123.8, 123.0, 120.8, 120.0, 117.7, 116.22, 116.19, 114.7, 78.2, 78.0, 77.8 (×2), 55.0, 43.72, 43.70, 33.01, 32.96, 32.4, 32.2, 23.0, 22.9, 22.83, 22.77, 14.4 ppm. IR (KBr): $\tilde{\nu}$ = 3064, 2929, 2857, 1661, 1439, 1055 cm^{-1}. ESI-MS: *m/z* = 1158.20 $[M+CH_3]^+$.

2,3-Dihydrothieno[3,4-*b*][1,4]dioxine-5-carbaldehyde (43)

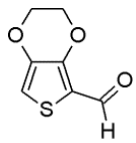

43

3,4-Ethylenedioxythiophene (EDOT, 2.00 g, 14.1 mmol, 1.0 eq.) was dissolved in THF (30 mL), then, after cooling to –78 °C, a 1.6 M solution of *n*-BuLi in hexane (16.9 mmol, 10.6 mL, 1.2 eq.) was added dropwise. The resulting mixture was left under stirring at –78 °C for 2 hours, then *N*,*N*-DMF (2.06 g, 28.2 mmol, 2.17 mL, 2.0 eq.) was added. The reaction mixture was allowed to return to room temperature and left under stirring for 16 h. Water (120 mL) was added to induce precipitation of the crude product, which was isolated by vacuum filtration. Recrystallization by ethanol afforded product **43** (2.23 g, 13.1 mmol, 93% yield) as a light yellow solid.

(**43**) ^{1}H-NMR (300 MHz, $CDCl_3$): δ = 9.89 (s, 1H), 6.79 (s, 1H), 4.35 (m, 2H), 4.26 (m, 2H) ppm. Analytical data were in agreement with those found in the literature.[20]

7-(Tributylstannyl)-2,3-dihydrothieno[3,4-*b*][1,4]dioxine-5-carbaldehyde (44)

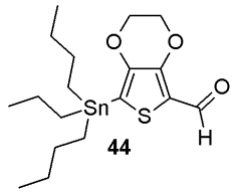

44

2,3-Dihydrothieno[3,4-*b*][1,4]dioxine-5-carbaldehyde (**43**, 900 mg, 5.29 mmol, 1.0 eq.) was dissolved in a mixture of anhydrous chloroform (10 mL) and anhydrous methanol (25 mL). Trimethyl orthoformate (842 mg, 7.93 mmol, 1.5 eq.) and 2,3-dichloro-5,6-dicyano-1,4-benzoquinone (DDQ, 60 mg, 0.26 mmol, 0.05 eq.) were added and the reaction mixture was stirred at 50°C for 2 h. The solvent was removed and anhydrous THF (30 mL) was added. The resulting solution was cooled to –78°C and reacted with *n*-BuLi (1.6 M solution in hexanes, 4.96 mL, 7.93 mmol, 1.5 eq.). After stirring at –78°C for 2 h, tributylstannyl chloride (3.44 g, 10.6 mmol, 2.0 eq.) was added. The reaction mixture was warmed to room temperature and stirred for 16 h, then $KHSO_4$ was added (40 mL, 2.5 M solution in water) and stirring was continued for further 2 h. After dilution with CH_2Cl_2 (150 mL) and Na_2CO_3 (150 mL, 0.1 M solution in water), the layers were separated and the organic phase washed with brine (100 mL) and dried with Na_2SO_4. Evaporation of the solvent yielded a dark oil, which was purified by column chromatography (SiO_2; petroleum ether / AcOEt 8:1) to afford compound **44** (1.62 g, 3.53 mmol, 67% yield) as a light yellow oil.

(**44**): ^{1}H-NMR (300 MHz, $CDCl_3$): δ = 9.80 (s, 1H), 4.29–4.34 (m, 2H), 4.20–4.24 (m, 2H), 1.52–1.59 (m, 6H), 1.28–1.36 (m, 6H), 1.12–1.19 (m, 6H), 0.85–0.93 (m, 9H) ppm. ^{13}C-NMR (100 MHz, $CDCl_3$): δ = 179.4, 148.5, 147.6, 125.5, 124.0, 65.3, 64.4, 29.0,

27.3, 13.8, 10.9 ppm. IR (KBr): $\tilde{\nu}$ = 2957, 2924, 2846, 1649, 1469, 1083 cm^{-1}. ES-MS: *m/z* = 461.08 $[M+1]^+$.

7-(8-(5-(8-(4-(Diphenylamino)phenyl)-3,3-dipentyl-3,4-dihydro-2H-thieno[3,4-*b*][1,4]dioxepin-6-yl)thiazolo[5,4-*d*]thiazol-2-yl)-3,3-dipentyl-3,4-dihydro-2H-thieno[3,4-*b*][1,4]dioxepin-6-yl)-2,3-dihydrothieno[3,4-*b*][1,4]dioxine-5-carbaldehyde (45).

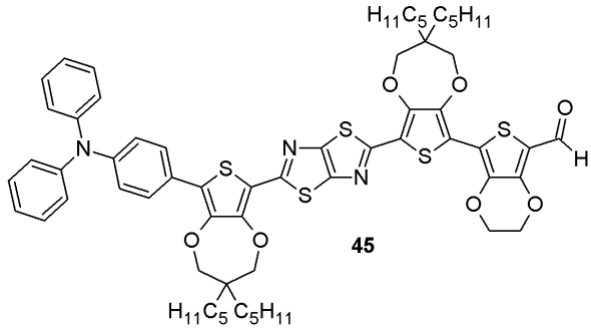

45

Compound **9** (200 mg, 0.18 mmol) was dissolved in toluene (8.0 mL) together with 7-tributylstannyl-2,3-dihydrothieno[3,4-*b*][1,4]dioxine-5-carbaldehyde (**44**) (125 mg, 0.27 mmol, 1.5 eq.), and $[Pd(PPh_3)_4]$ (11 mg, 0.009 mmol, 0.05 eq.). The resulting mixture was stirred at 110°C for 24h, then it was allowed to cool to room temperature and diluted with H_2O (150 mL) and CH_2Cl_2 (150 mL). The phases were separated and the organic layer was washed with brine (200 mL) and dried with Na_2SO_4. After filtration and evaporation of the solvent, a dark-red oil was obtained, which was purified by flash column chromatography (SiO_2; Toluene) to give compound **45** (154 mg, 0.13 mmol, 74% yield) as a dark red solid.

(**45**): mp = 305–306 °C. ^{1}H-NMR (300 MHz, $CDCl_3$): δ = 9.87 (s, 1H), 7.62 (d, *J* = 9.0 Hz, 2H), 7.25–7.32 (m, 4H), 7.10–7.17 (m, 4H), 7.10–7.17 (m, 4H), 4.43 (s, 4H), 4.16 (s, 2H), 4.14 (s, 2H), 4.09 (s, 2H), 4.02 (s, 2H), 1.43–1.59 (m, 8H), 1.26–1.40 (m, 24H), 0.86–0.994 (m, 12H) ppm. ^{13}C-NMR (75 MHz, $CDCl_3$): δ = 180.0, 159.7, 158.5, 150.9, 150.5, 149.5, 147.9, 147.8, 147.5, 147.1, 145.1, 137.7, 129.5, 127.7, 126.3, 125.0, 124.5, 123.5, 123.0, 121.0, 117.9, 116.3, 115.4, 113.7, 78.4, 78.3, 78.0, 77.9, 65.4, 65.0, 44.1, 44.0, 32.8, 32.7, 32.3, 32.1, 29.8, 22.7, 14.2 ppm. IR (KBr): $\tilde{\nu}$ = 3034, 2928, 2857, 1638, 1459, 1061 cm^{-1}. ESI-MS: *m/z* = 1142.37 $[M]^+$.

General procedure for Knoevenagel condensation with cyanoacetic acid

In a Schlenk flask equipped with a magnetic stirrer aldehyde **7**, **39**–**41** or **45** (1.0 eq.) was dissolved in toluene together with cyanoacetic acid (10.0 eq.), ammonium acetate (4.0 eq.), and glacial acetic acid. The reaction mixture was stirred at 110°C for 6 h, then cooled to room temperature and diluted with $CHCl_3$ (150 mL). The organic phase was washed with a saturated solution of $NaHCO_3$ (100 mL) and brine (100 mL), and then it was dried with Na_2SO_4. Evaporation of the solvent gave a black solid, which was purified by consecutive washing with ethyl acetate, methanol and pentane and dried under vacuum.

2-Cyano-3-(5-(8-(5-(8-(4-(diphenylamino)phenyl)-3,3-dipentyl-3,4-dihydro-2H-thieno[3,4-*b*][1,4]dioxepin-6-yl)thiazolo[5,4-*d*]thiazol-2-yl)-3,3-dipentyl-3,4-dihydro-2H-thieno[3,4-*b*][1,4]dioxepin-6-yl)thiophen-2-yl)acrylic acid (TTZ3)

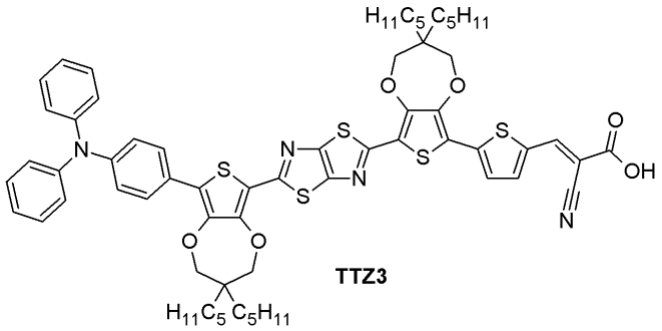

TTZ3

Aldehyde **7** (89 mg, 0.08 mmol), cyanoacetic acid (70 mg, 0.82 mmol) and ammonium acetate (25 mg, 0.33 mmol) were dissolved in toluene (4.0 mL) and glacial acetic acid (6.0 mL). The reaction mixture was stirred at 110°C for 6 h. Work-up and purification afforded compound **TTZ3** (80 mg, 0.07 mmol, 84% yield) as a dark solid.

(**TTZ3**): mp = 288–291 °C. ^{1}H-NMR (400 MHz, THF-d_8): δ = 8.31 (s, 1H), 7.83 (d, *J* = 4.2 Hz, 1H), 7.64 (d, *J* = 8.8 Hz, 2H), 7.44 (d, *J* = 4.1 Hz, 1H), 7.23–7.30 (m, 4H), 7.09–7.12 (m, 4H), 7.00–7.08 (m, 4H), 4.28 (s, 2H), 4.24 (s, 2H), 4.22 (s, 2H), 4.06 (s, 2H), 1.52–1.59 (m, 8H), 1.28–1.42 (m, 24H), 0.89–0.96 (m, 12H) ppm. ^{13}C-NMR (100 MHz, THF-d_8): δ = 160.2, 158.2, 151.7, 151.1, 150.4, 149.1, 148.3, 148.0, 145.9, 143.9, 138.0, 136.3, 130.0, 128.2, 127.2, 125.5, 125.2, 125.0, 124.0, 123.4, 117.9, 117.8, 116.7, 116.6, 114.5, 78.9, 78.8, 78.5, 78.4, 44.7, 44.5, 33.50, 33.48, 32.8, 23.2, 14.2 ppm. IR (KBr): $\tilde{\nu}$ = 3025, 2928, 2578, 2217, 1689, 1058 cm^{-1}. ESI-MS: *m/z* = 1151.47 [M]$^+$. Anal. calcd. for $C_{64}H_{70}N_4O_6S_5$: C, 66.75; H, 6.13; N, 4.87. Found: C, 66.46; H, 6.35; N, 4.52.

3-(5-(8-(5-(8-(4-(*Bis*(4-(hexyloxy)phenyl)amino)phenyl)-3,3-dipentyl-3,4-dihydro-2H-thieno[3,4-*b*][1,4]dioxepin-6-yl)thiazolo[5,4-*d*]thiazol-2-yl)-3,3-dipentyl-3,4-dihydro-2H-thieno[3,4-*b*][1,4]dioxepin-6-yl)thiophen-2-yl)-2-cyanoacrylic acid (TTZ4)

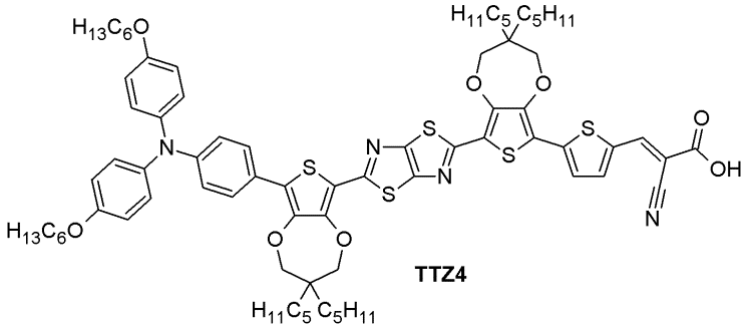

TTZ4

Aldehyde **39** (108 mg, 0.08 mmol), cyanoacetic acid (72 mg, 0.84 mmol) and ammonium acetate (26 mg, 0.34 mmol) were dissolved in toluene (5.0 mL) and glacial acetic acid (7.0 mL). The reaction mixture was stirred at 110°C for 4 h. Work-up and purification afforded compound **TTZ4** (103 mg, 0.08 mmol, 90% yield) as a dark sticky solid.

(**TTZ4**): ^{1}H-NMR (400 MHz, THF-d_8): δ = 8.33 (s, 1H), 7.85 (d, *J* = 4.2 Hz, 1H), 7.56 (d, *J* = 8.8 Hz, 2H), 7.46 (d, *J* = 4.1 Hz, 1H), 7.04 (d, *J* = 8.9 Hz, 4H), 6.85 (d, *J* = 8.9 Hz, 6H), 4.27 (s, 2H), 4.23 (s, 2H), 4.22 (s, 2H), 4.04 (s, 2H), 3.94 (t, *J* = 6.4 Hz, 4H), 1.73–1.79 (m, 4H), 1.32–1.60 (m, 44H), 0.90–0.95 (m, 18H) ppm. ^{13}C-NMR (100 MHz, THF-d_8): δ = 164.0, 160.3, 158.0, 156.9, 151.7, 151.0, 150.5, 149.4, 149.0, 148.0, 146.0, 145.4, 144.1, 140.9, 138.2, 136.1, 128.0, 127.6, 125.9, 124.91, 124.89, 120.0, 117.84, 117.77, 116.6, 115.9, 113.8, 99.1, 78.9, 78.8, 78.4, 78.3, 68.6, 44.7, 44.5, 33.51, 33.49, 32.80, 32.75, 32.4, 30.1, 26.6, 23.4, 23.3, 14.3, 14.2 ppm. IR (KBr): $\tilde{\nu}$ = 3030, 2928, 2852, 2213, 1684, 1505, 1057 cm^{-1}. ESI-MS: *m/z* = 1351.38 $[M+1]^+$. Anal. calcd. for $C_{76}H_{94}N_4O_8S_5$: C, 67.52; H, 7.01; N, 4.14. Found C, 66.98; H, 7.11; N, 4.08.

3-(5-(8-(5-(8-(4-(*Bis*(4-(hexylthio)phenyl)amino)phenyl)-3,3-dipentyl-3,4-dihydro-2H-thieno[3,4-*b*][1,4]dioxepin-6-yl)thiazolo[5,4-*d*]thiazol-2-yl)-3,3-dipentyl-3,4-dihydro-2H-thieno[3,4-*b*][1,4]dioxepin-6-yl)thiophen-2-yl)-2-cyanoacrylic acid (TTZ5)

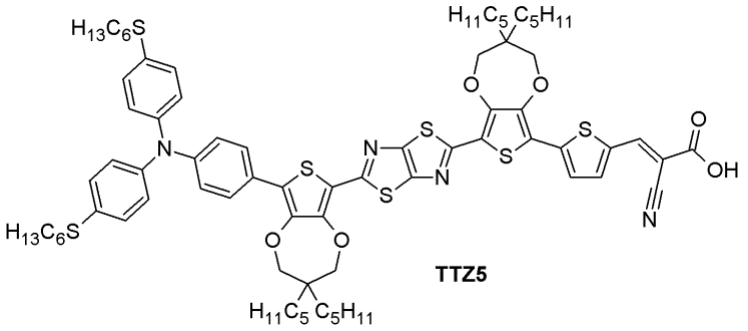

TTZ5

Aldehyde **40** (84 mg, 0.06 mmol), cyanoacetic acid (54 mg, 0.64 mmol) and ammonium acetate (20 mg, 0.25 mmol) were dissolved in toluene (3.0 mL) and glacial acetic acid (3.0 mL). The reaction mixture was stirred at 110°C for 3 h. Work-up and purification afforded compound **TTZ5** (85 mg, 0.06 mmol, 97% yield) as a dark sticky solid.

(**TTZ5**): ^{1}H-NMR (400 MHz, THF-d_8): δ = 8.30 (s, 1H), 7.83 (d, *J* = 4.0 Hz, 1H), 7.64 (d, *J* = 8.6 Hz, 2H), 7.43 (d, *J* = 4.0 Hz, 1H), 7.26 (d, *J* = 8.5 Hz, 4H), 7.00–7.05 (m, 6H), 4.28 (s, 2H), 4.24 (s, 2H), 4.22 (s, 2H), 4.06 (s, 2H), 2.90 (t, *J* = 7.3 Hz, 4H), 1.62–1.68 (m, 4H), 1.53–1.59 (m, 8H), 1.27–1.51 (m, 36H), 0.88–0.95 (m, 18H) ppm. ^{13}C-NMR (100 MHz, THF-d_8): δ = 164.0, 160.1, 158.2, 151.7, 151.1, 150.3, 149.1, 148.0, 147.7, 146.0, 145.9, 144.0, 138.2, 136.2, 132.3, 131.3, 128.2, 127.4, 125.7, 125.0, 124.9, 123.5, 117.9, 117.7, 116.7, 114.5, 99.2, 78.9, 78.8, 78.5, 78.3, 67.8, 44.7, 44.5, 34.6, 33.50, 33.49, 32.8, 32.7, 32.2, 30.0, 29.2, 23.27, 23.26, 14.3, 14.2 ppm. IR (KBr): $\tilde{\nu}$ = 3020, 2924, 2857, 2213, 1678, 1563, 1407, 1057 cm^{-1}. ESI-MS: *m/z* = 1383.89 $[M+1]^+$. Anal. calcd. for $C_{76}H_{94}N_4O_6S_7$: C, 65.95; H, 6.85; N, 4.05. Found: C, 65.69; H, 6.94; N, 4.00.

2-Cyano-3-(7-(8-(5-(8-(4-(diphenylamino)phenyl)-3,3-dipentyl-3,4-dihydro-2H-thieno[3,4-*b*][1,4]dioxepin-6-yl)thiazolo[5,4-*d*]thiazol-2-yl)-3,3-dipentyl-3,4-dihydro-2H-thieno[3,4-*b*][1,4]dioxepin-6-yl)-2,3-dihydrothieno[3,4-*b*][1,4]dioxin-5-yl)acrylic acid (TTZ6)

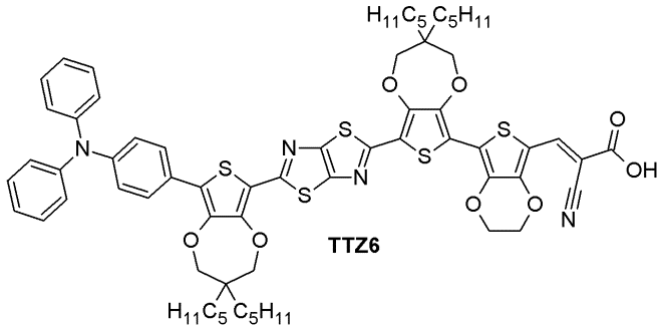

TTZ6

Aldehyde **45** (102 mg, 0.09 mmol), cyanoacetic acid (76 mg, 0.89 mmol, 10.0 eq.) and ammonium acetate (28 mg, 0.36 mmol, 4.0 eq.) were dissolved in toluene (3.0 mL) and glacial acetic acid (4.0 mL). The reaction mixture was stirred at 110°C for 3 h. Work-up and purification afforded compound **TTZ6** (102 mg, 0.08 mmol, 94% yield) as a dark amorphous solid.

(**TTZ6**): mp = 292–294 °C. ^{1}H-NMR (300 MHz, THF-d_8): δ = 8.30 (s, 1H), 7.65 (d, J = 8.8 Hz, 2H), 7.27 (m, 4H), 7.10 (d, J = 7.7 Hz, 4H), 7.04 (m, 4H), 4.49 (s, 4H), 4.25 (s, 4H), 4.18 (s, 2H), 4.07 (s, 2H), 1.48–1.64 (m, 8H), 1.32–1.46 (m, 24H), 0.87–0.99 (m, 12H). IR (KBr): $\tilde{\nu}$ = 3025, 2928, 2578, 2217, 1689, 1058 cm^{-1}. ESI-MS: *m/z* = 1209.42 [M]$^{+}$. Anal. calcd. for $C_{66}H_{72}N_4O_8S_5$: C, 65.53; H, 6.00; N, 4.63. Found: C, 66.17; H, 6.35; N, 4.32.

*Note: due to its limited solubility in a vast range of organic solvents, a ^{13}C-NMR spectrum of compound **TTZ6** could not be recorded.*

2-Cyano-3-(5-(8-(5-(8-(10-(4-methoxyphenyl)-10H-phenothiazin-3-yl)-3,3-dipentyl-3,4-dihydro-2H-thieno[3,4-*b*][1,4]dioxepin-6-yl)thiazolo[5,4-*d*]thiazol-2-yl)-3,3-dipentyl-3,4-dihydro-2H-thieno[3,4-*b*][1,4]dioxepin-6-yl)thiophen-2-yl)acrylic acid (TTZ7).

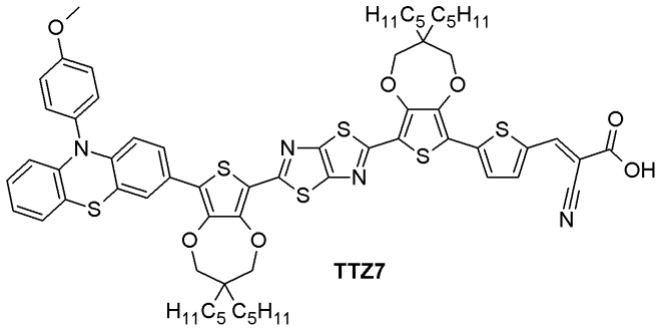

TTZ7

Aldehyde **41** (70 mg, 0.06 mmol), cyanoacetic acid (52 mg, 0.61 mmol, 10.0 eq.) and ammonium acetate (19 mg, 0.24 mmol, 4.0 eq.) were dissolved in toluene (3.0 mL) and glacial acetic acid (3.0 mL). The reaction mixture was stirred at 110°C for 5 h. Work-up and purification afforded compound **TTZ7** (67 mg, 0.05 mmol, 91% yield) as a dark solid.

(**TTZ7**): mp = 277–279 °C. ^{1}H-NMR (400 MHz, THF-d_8): δ = 8.30 (s, 1H), 7.83 (d, *J* = 4.1 Hz, 1H), 7.43 (d, *J* = 4.1 Hz, 1H), 7.38 (d, *J* = 2.0 Hz, 1H), 7.32 (d, *J* = 8.8 Hz, 2H), 7.17–7.24 (m, 3H), 6.95 (dd, *J* = 7.3 Hz, J = 1.6 Hz, 1H), 6.75 – 6.82 (m, 2H), 6.18 (d, *J* = 8.9 Hz, 1H), 6.15 (d, *J* = 8.7 Hz, 1H), 4.27 (s, 2H), 4.23 (s, 2H), 4.21 (s, 2H), 4.05 (s, 2H), 3.82 (s, 3H), 1.50–1.63 (m, 8H), 1.25–1.46 (m, 24H), 0.89–0.96 (m, 12H) ppm. ^{13}C-NMR (100 MHz, THF-d_8): δ = 164.0, 160.6, 160.1, 158.1, 151.7, 151.1, 150.3, 149.1, 148.0, 146.0, 145.9, 144.9, 144.8, 144.0, 138.2, 136.2, 133.7, 132.8, 127.6, 127.5, 127.1, 125.9, 124.9, 124.8, 124.2, 123.1, 120.6, 119.9, 117.9, 117.8, 116.7, 116.4, 116.2, 114.4, 99.2, 78.9, 78.8, 78.5, 78.4, 55.6, 44.7, 44.5, 33.8, 33.52, 33.49, 32.8, 31.6, 30.5, 23.3, 14.3 ppm. IR (KBr): $\tilde{\nu}$ = 2957, 2862, 2213, 1560, 1415, 1096 cm^{-1}. ESI-MS: *m/z* = 1211.34 [M]$^{+}$. Anal. calcd. for $C_{65}H_{70}N_4O_7S_6$: C, 64.43; H, 5.82; N, 4.62. Found: C, 63.97; H, 5.90; N, 4.58.

4.3.2. Electrochemical characterization

Cyclic voltammetry measurements were carried out in commercially available anhydrous 99.9%, HPLC grade dichloromethane for electrochemistry. The supporting electrolyte used was electrochemical grade $[N(Bu)_4]PF_6$. Cyclic voltammetry was performed in a three-electrode C-3 *BAS* Cell having a glassy carbon working electrode, a platinum counter electrode and the aqueous Ag/AgCl NaCl (3M) reference electrode. A *BAS* 100A electrochemical analyzer was used as a polarizing unit. Under these experimental conditions, the one-electron oxidation of ferrocene occurs at E°' = + 0.42 V.

4.3.3. Measurement of the density of adsorbed dyes on TiO_2

A nanocrystalline TiO_2 electrode (surface area 0.88 cm^2) similar to those used for the photovoltaic measurements was immersed in 1.0×10^{-4} M solutions of dyes **TTZ3**-**7** in THF at room temperature for 16 h. The stained electrode was removed from the solution, washed with EtOH, dried under a stream of nitrogen and immersed in 5 mL of a 0.1 M KOH solution in THF/MeOH 9:1 at room temperature until full discoloration was observed. The absorbance of the resulting orange-yellow solution was measured by UV-Vis spectroscopy and compared to that of a standard solution of sensitizer in the same solvent/base mixture. The amount of dye present in the unknown solution was calculated and divided by the electrode surface area, yielding the density values.

4.3.4. DSSC fabrication and photoelectrochemical measurements

Transparent photoanodes for small-scale DSSCs were prepared by screen-printing a commercial TiO_2 paste (Dyesol 18NR-T) on a 8 Ω sq^{-1} conductive glass substrate (Pilkington), and by sintering the resulting electrodes at 520 °C for 30 minutes. After sintering, the thickness of the semiconductor layer was measured by means of a profiler (Dektak 150, Veeco) and determined to be 5.5 µm. Opaque photoanodes were obtained following an analogous procedure, but using a different commercial titania paste (Dyesol 18NR-AO); their final thickness was 6.5 µm. In both cases, the electrode active area was 0.25 cm^2. Counter electrodes were obtained by screen printing a commercial platinum-containing paste (Chimet) on pre-drilled conductive

glass plates and by heating at 420 °C for 15 minutes. TiO_2 photo-electrodes were sensitized by overnight immersion at room temperature into the appropriate dye solution (0.1 mM in THF for dyes **TTZ3**–**7**, 0.2 mM in EtOH for dye **D5**, 0.3 mM in EtOH for dye **Z907**), either in the absence or in the presence of 1 mM chenodeoxycholic acid (CDCA). After sensitization, the anodes were rinsed with EtOH and deionized water, and then dried. A TiO_2-sensitized photoanode and a Pt counter electrode were assembled into a sealed sandwich-type cell using a 25 µm hot-melt Surlyn® gasket (Solaronix). A drop of the I^-/I_3^- containing commercial HPE electrolyte solution (Dyesol) was placed on the drilled hole on the back of the counter electrode and was driven into the cell by vacuum backfilling. The hole was finally sealed by using additional sealing film and a small glass cover. Fabrication of strip cells (3.6 cm^2 active area) was carried out following the same procedure, except that only transparent photoanodes were prepared, in a thickness of 3 and 5 µm, and a different electrolyte (Dyesol HSE) was used to fill the cells. Sensitization of the photoanodes with standard sensitizer **D35** was performed using a 0.3 mM solution of the dye in 1-methoxy-2-propanol. The devices underwent photovoltaic characterization by using a AM 1.5G solar simulator equipped with a Xenon lamp (KHS Solar Constant 1200). The measurements were performed with a power of incoming radiation of 100 mW cm^{-2}. J/V curves were obtained by applying an external bias to the cell and measuring the generated photocurrent with a Keithleymodel 2400 digital source-meter, under the control of dedicated LabTracer 2.0 software. A black shading mask was used to avoid overestimation of the measured parameters. IPCE spectra were measured with a dedicated apparatus built with the following components: Newport model 70612 Xenon lamp (150 W), Cornerstone 130 1/8 m monochromator and Keithley model 2400 digital source-meter. Electrochemical impedance spectroscopy (EIS) measurements were performed in the dark using a AUTOLAB 302N potentiostat (Metrohm) equipped with a Nova electrochemical interface system, working at –0.80 V, –0.60 V and –0.45 V forward bias. The spectra were recorded over a frequency range of 10^{-1} Hz to 10^5 Hz with an amplitude of 10 mV. Data fitting was carried out using the EC-Lab software (V9.46).

4.4. References

[1] Dessì A., Barozzino Consiglio G., Calamante M., Reginato G., Mordini A., Peruzzini M., Taddei M., Sinicropi A., Parisi M. L., Fabrizi de Biani F., Basosi R., Mori R., Spatola M., Bruzzi M., Zani L. *Eur. J. Org. Chem.*, **2013**, 1916

[2] a) Liu W.-H., Wu I-C., Lai C.-H., Lai C.-H., Chou P.-T., Li Y.-T., Chen C.-L., Hsu Y.-Y., Chi Y. *Chem. Commun.*, **2008**, 5152. b) Zhang G., Bala H., Cheng Y., Shi D., Lv X., Yu Q., Wang P. *Chem. Commun.*, **2009**, 2198

[3] Dessì A., Calamante M., Mordini A., Zani L., Taddei M., Reginato G. *RSC Adv.*, **2014**, *4*, 1322

[4] a) Welsh D. M., Kumar A., Meijer E. W., Reynolds, J. R. *Adv. Mater.*, **1999**, *11*, 1379. b) Nielsen C. B., Bjørnholm T. *Macromolecules*, **2005**, *38*, 10379. c) Hammond S. R., Clot O., Firestone K. A., Bale D. H., Lao D., Haller M., Phelan G. D., Carlson B., Jen A. K. Y., Reid P. J., Dalton L. R. *Chem. Mater.*, **2008**, *20*, 3425. d) Liang Y., Peng B., Liang J., Tao Z., Chen J. *Org. Lett.*, **2010**, *12*, 1204

[5] Robson K. C. D., Hu K., Meyer G. J., Berlinguette C. P. *J. Am. Chem. Soc.*, **2013**, *135*, 1961

[6] Tian H., Yang X., Chen R., Pan Y., Li L., Hagfeldt A., Sun L. *Chem. Commun.*, **2007**, 3741

[7] Gaussian 09, Revision C.01, Frisch M. J., Trucks G. W., Schlegel H. B., Scuseria G. E., Robb M. A., Cheeseman J. R., Scalmani G., Barone V., Mennucci B., Petersson G. A., Nakatsuji H., Caricato M., Li X., Hratchian H. P., Izmaylov A. F., Bloino J., Zheng G., Sonnenberg J. L., Hada M., Ehara M., Toyota K., Fukuda R., Hasegawa J., Ishida M., Nakajima T., Honda Y., Kitao O., Nakai H., Vreven T., Montgomery Jr. J. A., Peralta J. E., Ogliaro F., Bearpark M., Heyd J. J., Brothers E., Kudin K. N., Staroverov V. N., Kobayashi R., Normand J., Raghavachari K., Rendell A., Burant J. C., Iyengar S. S., Tomasi J., Cossi M., Rega N., Millam J. M., Klene M., Knox J. E., Cross J. B., Bakken V., Adamo C., Jaramillo J., Gomperts R., Stratmann R. E., Yazyev O., Austin A. J., Cammi R., Pomelli C., Ochterski J. W., Martin R. L., Morokuma K., Zakrzewski V. G., Voth G. A., Salvador P., Dannenberg J. J., Dapprich S., Daniels A. D., Farkas Ö., Foresman J. B., Ortiz J. V., Cioslowski J., Fox D. J., Gaussian, Inc., Wallingford CT, 2009.

[8] a) Becke A. D. J. *J. Chem. Phys.*, **1993**, *98*, 5648. b) Lee C., Yang W., Parr R. G. *Phys. Rev. B: Condens. Matter Mater. Phys.*, **1988**, *37*, 785. c) Stephens P. J., Devlin F. J., Chabalowski C. F., Frisch M. J., *J. Phys. Chem.*, **1994**, *98*, 11623

[9] Yanai T., Tew D., Handy N. *Chem. Phys. Lett.*, **2004**, *393*, 51

[10] Thompson B. C., Kim Y.-G., McCarley T. D., Reynolds J. R. *J. Am. Chem. Soc.*, **2006**, *128*, 12714

[11] Ziessel R., Nano A., Heyer E., Bura T., Retailleau P. *Chem.–Eur. J.*, **2013**, *19*, 2582

[12] Li R., Liu J., Kai N., Zhang M., Wang P. J. *J. Phys. Chem. B*, **2010**, *114*, 4461

[13] Odom S. A., Lancaster C., Beverina L., Lefler K. M., Thompson N. J., Coropceanu V., Bredas J.-L., Marder S. R., Barlow S. *Chem.–Eur. J.*, **2007**, *13*, 9637

[14] Lambert C., Schelter J., Fiebig T., Mank D., Trifonov A. *J. Am. Chem. Soc.*, **2005**, *127*, 10600

[15] Chen L., Zhang B., Cheng Y., Xie Z., Wang L., Jing X., Wang F. *Adv. Funct. Mater.* **2010**, *20*, 3143

[16] Robson K. C. D., Koivisto B. D., Berlinguette C. P. *Inorg. Chem.*, **2012**, *51*, 1501

[17] Bates C. G., Gujadhur R. K., Venkataraman D. *Org. Lett.*, **2002**, *4*, 2803

[18] Djerassi C., Scholz C. R. *J. Am. Chem. Soc.*, **1948**, *70*, 417

[19] Creary X., Mehrsheikh-Mohammadi M. E., McDonald S. *J. Org. Chem.*, **1987**, *52*, 3254

[20] Mohanakrishnan A. K., Hucke A., Lyon M. A., Lakshmikantham M. V., Cava M. P. *Tetrahedron*, **1999**, *55*, 11745

[21] Karimi B., Ashtiani A. M. *Chem. Lett.*, **1999**, 1199

[22] Chang Y. J., Chow T. J. *J. Mater. Chem.*, **2011**, *21*, 9523

[23] a) Tauc J. *Mater. Res. Bull.*, **1968**, *3*, 37. An application on molecular dyes: b) Coluccini C., Manfredi N., Salamone M. M., Ruffo R., Lobello M. G., De Angelis F., Abbotto A. *J. Org. Chem.*, **2012**, *77*, 7945

[24] Boschloo G., Hagfeldt A. *Acc. Chem. Res.*, **2009**, *42*, 1819

[25] a) Hagberg D. P., Edvinsson T., Marinado T., Boschloo G., Hagfeldt A., Sun L. *Chem. Commun.*, **2006**, 2245. b) Hagberg D. P., Marinado T., Karlsson K. M., Nonomura K., Qin P., Boschloo G., Brinck T., Hagfeldt A., Sun L. *J. Org. Chem.*, **2007**, *72*, 9550

[26] a) Wang P., Zakeeruddin S. M., Moser J. E., Nazeeruddin M. K., Sekiguchi T., Grätzel M. *Nat. Mater.*, **2003**, *2*, 402. b) Heiniger L.-P., O'Brien P. G., Soheilnia N., Yang Y., Kherani N. P., Grätzel M., Ozin G. A., Tétrault N., *Adv. Mater.*, **2013**, *25*, 5734

[27] Schmidt-Mende L., Kroeze J. E., Durrant J. R., Nazeeruddin M. K., Grätzel M. *Nano Lett.*, **2005**, *5*, 1315

[28] Hagberg D. P., Jiang X., Gabrielsson E., Linder M., Marinado T., Brinck T., Hagfeldt A., Sun L. *J. Mater. Chem.*, **2009**, *19*, 7232

[29] Dye **D35** is commercially available from Dyenamo AB (Sweden). For a list of references regarding applications of such dye, see: http://www.dyenamo.se/dyenamo_dyes.php.

[30] Huang Y., Dai S., Chen S., Zhang C., Sui Y., Xiao S., Hu L. *Appl. Phys. Lett.*, **2009**, *95*, 243503.

[31] Fabregat-Santiago F., Garcia-Belmonte G., Mora-Serò I., Bisquert J., *Phys. Chem. Chem. Phys.*, **2011**, *13*, 9083

[32] Li Q., Lu L., Zhong C., Huang J., Huang Q., Shi J., Jin X., Peng T., Qin J., Li Z. *Chem.–Eur. J.*, **2009**, *15*, 9664

[33] Yang L., Zheng Z., Li Y., Wu W., Tian H., Wang Z. *Chem. Commun.*, **2015**, *51*, 4842

[34] a) Snyder S. A., Treitler D. S., Schall A. *Tetrahedron*, **2010**, *66*, 4796. b) Reeves B. D., Grenier C. R. G., Argun A. A., Cirpan A., McCarley T. D., Reynolds J. R. *Macromolecules*, **2004**, 37, 7559

[35] Leznoff C. C., Drew D. M. *Can. J. Chem.*, **1996**, *74*, 307

[36] Nguyen W. H. , Bailie C. D. , Burschka J. , Moehl T. , Grätzel M. , D.McGehee M., Sellinger A. *Chem. Mater.*, **2013**, *25*, 1519

[37] Seo Y.-H., Lee W.-H., Park J.-H., Bae C., Hong Y., Park J.-W., Kang, I.-N. *J. Polym. Sci. A Polym. Chem.*, **2012**, *50*, 649

Chapter 5

Synthesis of near-IR D-A-π-A sensitizers for Dye-Sensitized Solar Cells (DSSCs)

5.1. Introduction and aim of the work

The solar cells built with dyes **TTZ3**-**7** described in the previous chapter, besides being highly transparent, recorded also remarkable results in terms of efficiency and stability. Nevertheless, the major drawback of those sensitizers was their inability to absorb light (Figure 4.8) in the red/near infrared (NIR) region of the solar spectrum; consequently, their IPCE spectrum (Figure 4.11b) showed quite a steep decrease of the incident photon-to-current conversion efficiency above 600 nm, with the onset around 700 nm. Accordingly, if we were able to synthesize dyes with an extended absorption in the red/NIR light regions ($\lambda_{abs.}$ = 600-800 nm), which corresponds to approximately 45% of total solar irradiance, higher photocurrents and improved efficiencies could be obtained.[1] Besides, dyes featuring such properties would be very attractive from an aesthetic point of view due to their blue/green color, which is relatively unusual among commercial sensitizers[2] and quite sought after by professionals working in the BIPV sector.

Few dyes are currently reported to show a strong absorption of solar light in the red/NIR region thanks to presence of particular chromophores, such as squaraine,[3] perylene,[4] BODIPY[5] and cyanine[6] (Figure 5.1).

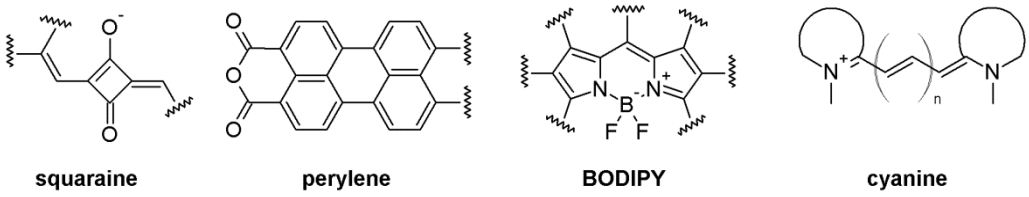

Figure 5.1. Structures of some NIR chromophores.

Squaraine-based sensitizers have recently received great attention owing to their excellent absorption features (600 < λ_{max} < 750 nm; ε up to 3.0 × 10^6 M^{-1} cm^{-1}). The first examples of symmetrical squaraine dyes recorded quite low efficiency values (up to 3.0-3.5%), while better results were obtained with asymmetrical squaraine dyes featuring a D-π-A structure, such as dye **DTS-CA**[7] (Figure 5.2), whose cells showed a remarkable η of 8.9% with an impressive photocurrent of 19.1 mA cm^{-2}. Generally, squaraine-based dyes showed tricky synthetic processes as well as a fast decomposition once adsorbed on the TiO_2 layer. Dyes containing the other functional groups depicted in Figure 5.1 showed intense, but too narrow absorption bands in the red/NIR region; in addition to this drawback, when employed in DSSCs, high

recombination rates and the aggregation of the dyes on the TiO_2 surface usually led to devices with low efficiency values.

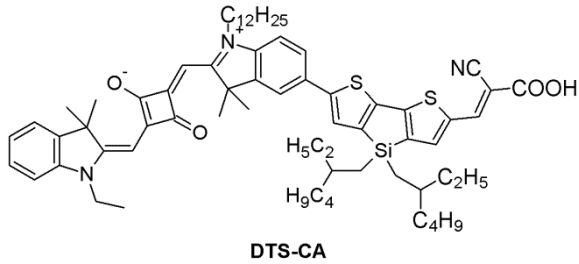

DTS-CA

Figure 5.2. Structure of best-performing squaraine dye DTS-CA.

In 2011, Zhu *et al*. proposed a new generation of sensitizers based on an alternative D-A-π-A[8] design capable of inducing a broad absorption of visible and NIR light.[9] Indeed, the introduction of an auxiliary acceptor group in the π-bridge of the sensitizer can modulate the frontier molecular orbitals energy levels by lowering the energy of the LUMO and, consequently, reducing the HOMO-LUMO gap. Moreover, both the HOMO and LUMO orbitals of a D-A-π-A dye are often distributed on the acceptor central unit, resulting in a partial superposition which should enhance the charge transfer from the donor to the acceptor / anchoring group.

Many different auxiliary acceptor groups have been tested (e.g., benzooxadiazole **46**, benzothiadiazole **47**, benzotriazole **48** and quinoxaline **49**; Figure 5.3), inducing a red-shift in the absorption spectra of the resulting D-A-π-A dyes up to 100 nm. In a recent review, Grätzel *et al*.[10] compared absorption properties of dyes having the same donor, π-bridge and anchor, but different auxiliary acceptor groups (**46**-**49**) and showed that, the larger the electronwithdrawing nature of the additional acceptor unit, the larger the red shift in the photoresponse.

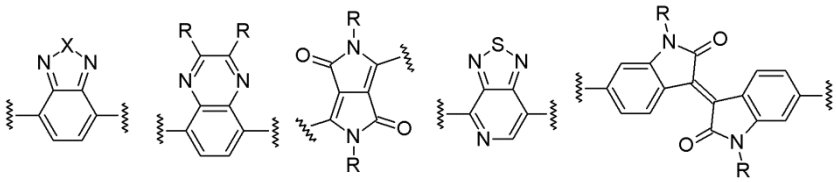

46 (X = O)
47 (X = S)
48 (X = NR)

49 **50** **51** **52**

Figure 5.3. Some examples of auxiliary acceptor units.

Following these guidelines, more electronwithdrawing units, such as diketopyrrolopyrrole (**50**), thiadiazolo[5,4-*c*]pyridine (**51**) and isoindigo (**52**), were introduced with the aim to shift the maximum light absorption over 600 nm. Some examples of NIR-absorbing dyes containing **50**-**52** as acceptor units are depicted in Figure 5.4. Dye **PT2**[11] exhibited a broad absorption spectrum in the visible/NIR region up to 750 nm and a cell efficiency of 6.7% when used together with an iodine based redox system and CDCA as a coadsorbent, while isoindigo-based dye **ICD3**[12] showed the maximum light absorption at 610 nm and its cells yielded a good efficiency of 7.55%. Even better results were obtained with diketopyrrolopyrrole-based dyes **DPP17**[13] and **DPP21**[14]; both sensitizers contained an elaborated donor group and exhibited a broad absorption of red/NIR light and an intense blue color. **DPP21** recorded a conversion efficiency value of 7.65%, while an impressive η of 10.1% was obtained by **DPP17**-containing cells employing a cobalt-based redox shuttle.

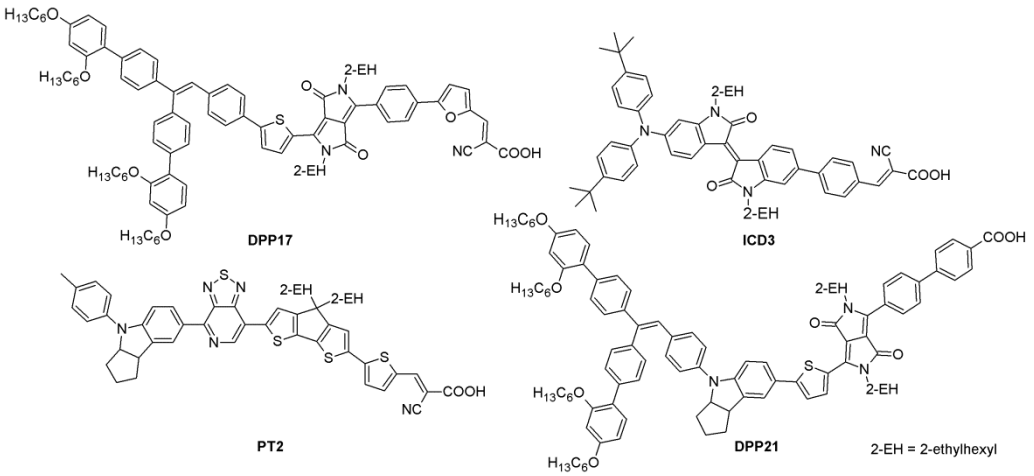

Figure 5.4. Structures of best-performing NIR-absorbing D-A-π-A dyes.

With the aim of introducing a different auxiliary acceptor unit and build a new family of NIR-absorbing D-A-π-A dyes, which could show that blue-green color which is still a challenge in the field of organic dyes, we focused our attention on the structure of (*E*)-3,3'-bifuranylidene-2,2'-dione (**53a**, Figure 5.5), also known as Pechmann-dye,[15] a strong electron-withdrawing system with a brilliant red-purple color, which took its name from the chemist who synthesized the first derivative in 1882 (R = phenyl).[16] For almost 60 years very few papers were published about the chemistry of Pechmann dyes, but more recently their particular optical properties have attracted

great interest,[17] and the possibility to insert the Pechmann-unit in a much longer conjugated system has been investigated.

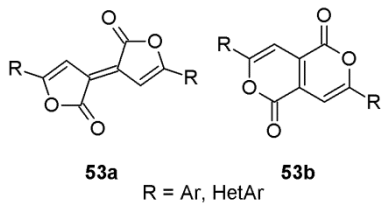

Figure 5.5. Structure of Pechmann-dye 53a and its isomer 53b.

The molecules depicted in Figure 5.6 have been used as organic semiconductors in organic field-effect transistors (OFET): **P_{55}-1**,[18] which contained the typical bis-lactone system of Pechmann-dye, showed intense light absorption between 500 and 750 nm, with the maximum peak at 674 nm and $\varepsilon = 6.5 \times 10^4\ M^{-1}\ cm^{-1}$, while **BPD**,[19] which is a nitrogenous analogue of classical Pechmann-dye **53a**, absorbed solar light until 800 nm (λ_{max} = 666 nm; $\varepsilon = 5.3 \times 10^4\ M^{-1}\ cm^{-1}$). Furthermore, the aza-Pechmann unit has been incorporated in the structure of polymers, which have been used as semiconductors for OFETs as well.[20]

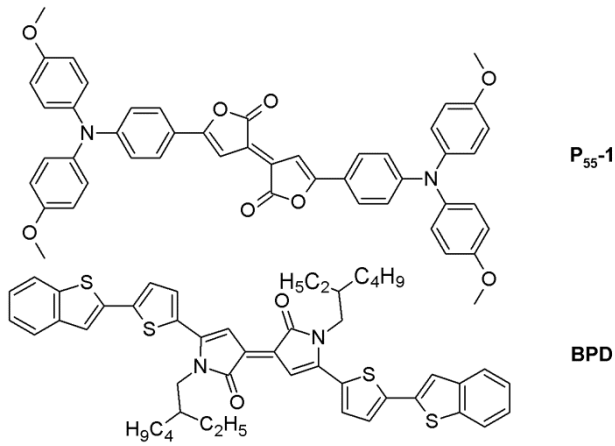

Figure 5.6. Some conjugated structures containing Pechmann-dye and its aza-derivative.

Since the optical properties of **P_{55}-1** and **BPD** were very promising, we decided to design and synthesize a new D-A-π-A molecule containing a Pechmann-dye as auxiliary acceptor unit (Figure 5.7) aiming to check its optical and electrochemical properties in view of a possible subsequent use as DSSC sensitizer.

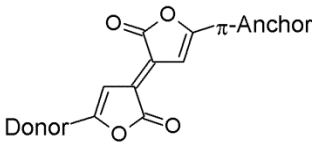

Figure 5.7. Introduction of the Pechmann-unit in D-π-A structure.

5.2. Results and discussion

5.2.1. Possible synthetic routes for Pechmann-dyes

The first report related to this kind of compounds is due to Von Pechmann,[16] who intended to prepare 1,4-naphtoquinone (**55**) by dehydration of β-benzoyl-acrylic acid (**54**), but, instead of the product, he isolated a brilliant red pigment with the same empirical formula as **55** (Figure 5.8 left). Von Pechmann gave a careful description of the product properties, but did not propose a structure for it. Twenty-four years later, Kozniewski and Marchlewski[21] repeated Von Pechmann's experiments and suggested that the product was 2,5-dibenzoylbenzoquinone (**56**, Figure 5.8 right), but a subsequent synthesis of this compound demonstrated that it was a different species than the original Pechmann-dye.[22]

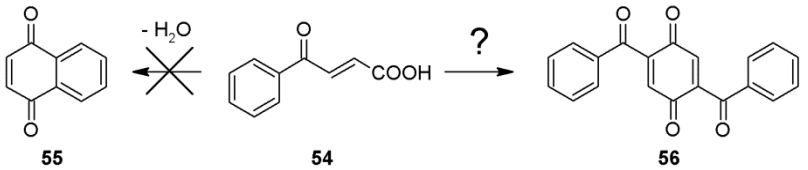

Figure 5.8. Attempt to prepare naphtoquinone 55 by Von Pechmann (left) and wrong suggestion of the product structure by Kozniewski and Marchlewski (right).

Even earlier, in 1924, Bogert and Ritter[23] showed that Pechmann product behaved like a bifunctional lactone and proposed structure **53a**, which was officially accepted in 1944.[24] They also assigned structure **53b** (Figure 5.5) to the yellow isomers of the Pechmann-dyes. Then, in 1951, Fang and Bergmann[25] reported the first general procedures for the synthesis of aromatic derivatives of Pechmann-dyes: following their protocols, we could draw two different retrosynthetic schemes for the preparation of a D-A-π-A Pechmann-dye (Scheme 5.1).

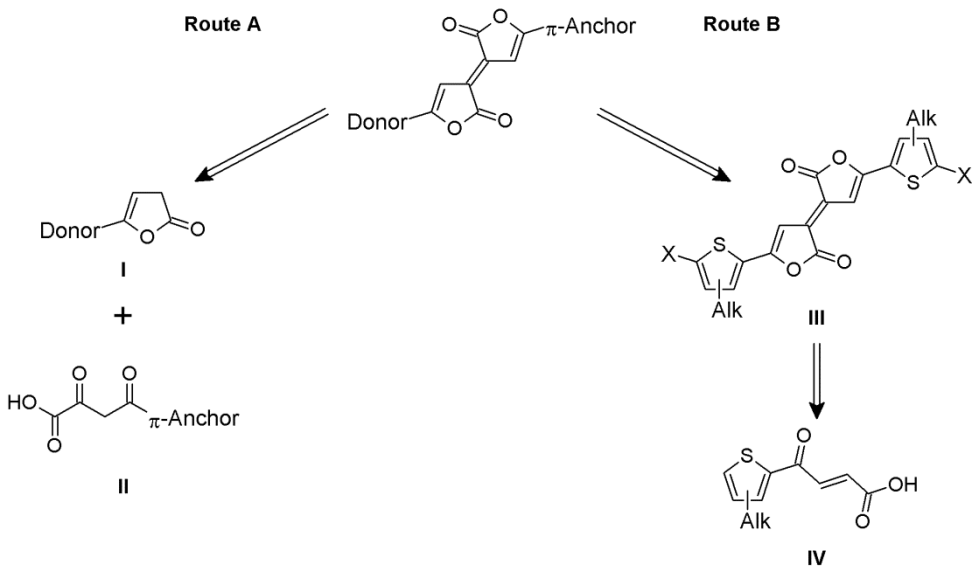

Scheme 5.1. Retrosynthetic analysis of a generic D-A-π-A Pechmann-dye.

Route **A** was expected to provide the desired structure by condensation of the two building blocks **I** and **II** bearing the appropriate donor and anchor groups respectively. On the other side (route **B**), different donor and anchor could be installed on the common π-spacer **III** through cross-coupling reactions analogously to the TzTz-synthesis (see Chapter 4), while the Pechmann-unit could be formed by a condensation/dimerization reaction sequence starting from the compound **IV**. Since route **A** theoretically enabled the synthesis of the desired dye through a convergent process, we selected this protocol and elaborated the structure of a possible D-A-π-A dye (**57**), which is reported in Figure 5.9.

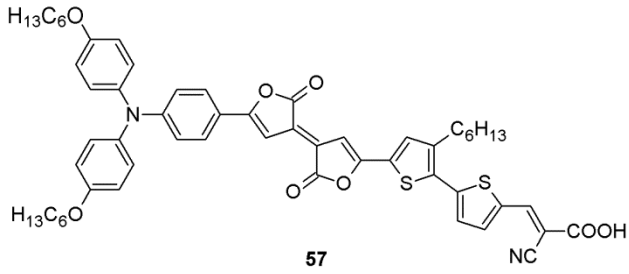

Figure 5.9. Selected structure for the synthesis of a Pechmann-containing dye for DSSCs.

In addition to the Pechmann unit, the molecule **57** contained a *p*-hexyloxy substituted triarylamine as the donor group, two thiophene rings as π-spacers and

cyanoacrylic acid as the anchor. An additional alkyl chain was placed on the central thiophene ring to improve the solubility of the final molecule.

5.2.2. Computational analysis

As already done for dyes **TTZ3**-**7**, before to approach the synthesis of such compound **57**, a computational analysis was performed, thanks to the collaboration with Dr. Adalgisa Sinicropi from the University of Siena, in order to predict the absorption maxima of the dyes and the HOMO-LUMO energy levels. In the calculations, the alkyl chains present on the molecule were replaced by simple methyl groups to reduce the computational burden, without affecting the length and nature of the conjugate system.

The structure of **57** was optimized *in vacuo* by means of DFT calculations performed with the Gaussian09 program package[26] at the B3LYP/6-31G* level.[27] The energy and shape of the frontier molecular orbitals (FMOs) of dye **57** were calculated and compared with those previously found for **TTZ4**, since both molecules contained the same donor (*p*-hexyloxy-substituted triarylamine) and anchoring (cyanoacrylic acid) group (Figure 5.10, Figure 5.11).

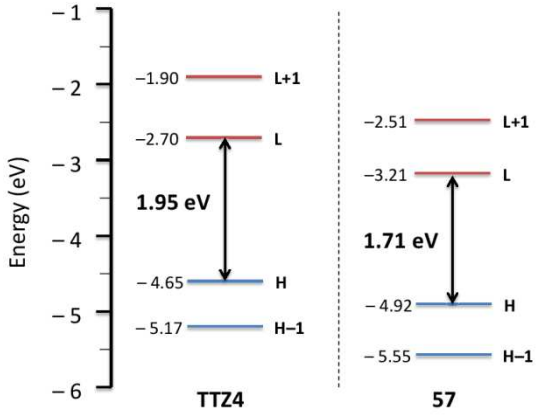

Figure 5.10. Computed (B3LYP/6-31G) HOMO–LUMO energy gaps of compounds TTZ4 and 57.*

As expected, the introduction of a strong auxiliary acceptor unit changed the energy levels significantly: compared to **TTZ4**, both HOMO and LUMO levels of **57** were shifted to more negative energy values (Δ HOMO = –0.27 eV; Δ LUMO = –0.51 eV) and the orbital energy gap was smaller as well (1.71 eV *vs*. 1.95 eV). Indeed, the more negative HOMO energy of dye **57** relative to that of **TTZ4** could be considered an

advantage since the worse photovoltaic performances of **TTZ4** compared to those of the other TzTz-dyes could be ascribed to a slower dye-regeneration caused by its high-lying HOMO (see paragraph 4.2.4.1). As well as for other D-A-π-A dyes,[8,10] the HOMO and LUMO orbitals of dye **57** were mostly localized on the donor and the anchor, respectively, but both of them were partially distributed on the auxiliary acceptor unit too, while **TTZ4** showed a more definite spatial separation of the orbitals.

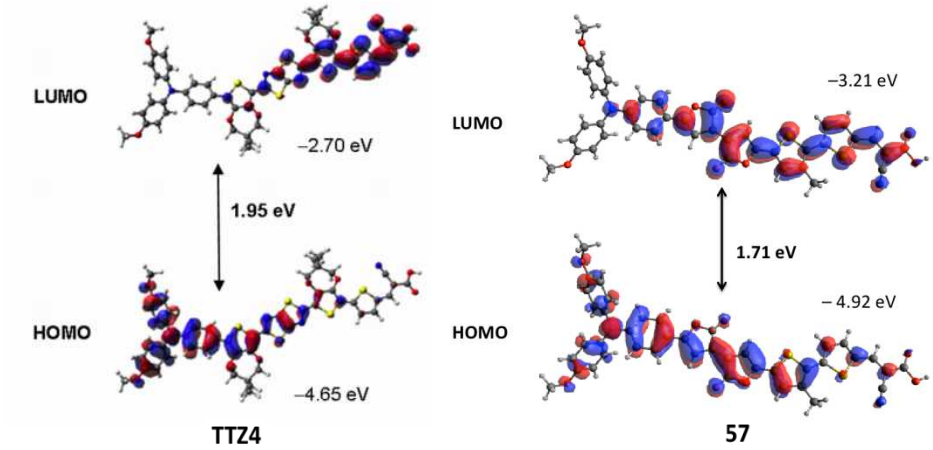

Figure 5.11. Isodensity plots and computed energies for the frontier molecular orbitals of compounds TTZ4 (left) and 57 (right) at the B3LYP/6-31G level.*

Finally, the absorption maxima (λ_{max}), oscillator strengths (*f*) and vertical excitation energies (E_{exc}) of dye **57** were assessed by TD-DFT calculations in THF at the CAM-B3LYP/6-31G* level[28] and were compared with the values found for **TTZ4** (Table 5.1). As expected, the decrease of the HOMO-LUMO energy gap of dye **57** compared to that of **TTZ4** was directly connected with a deep red-shift of the absorption maximum (507 nm *vs*. 669 nm), which was located in the red region of the solar spectrum. Moreover, differently from **TTZ4**, the excitation process was almost a pure HOMO → LUMO transition (85%), while the lower value of the oscillator strength (*f*) suggested the possibility of a less intense light absorption.

Table 5.1. CAMB3LYP/6-31G absorption maxima (λ_{max}), oscillator strengths (f), vertical excitation energies (E_{exc}) and main electronic transitions for dyes TTZ4 and 57 in THF.*

Compound	λ_{max} [nm]	*f*	E_{exc} [eV]	Main transitions (%)	
TTZ4	507	2.67	2.45	H−1 → L: 47.4	H → L: 30.5
57	669	1.85	2.43	H → L: 85	

5.2.3. Route A: synthesis of Pechmann-dye 57

5.2.3.1. Retrosynthesis

Once the properties of the selected dye **57** were checked by the computational analysis, a complete retrosynthetic analysis was worked out. Taking advantage of the previous work on TzTz-dyes, the last two steps of the synthesis of dye **57** were the Knoevenagel condensation of aldehyde **58** with cyanoacetic acid (**8**) and the cross-coupling reaction of bromide **59** with the appropriate organometallic reagent **10** (Scheme 5.2).

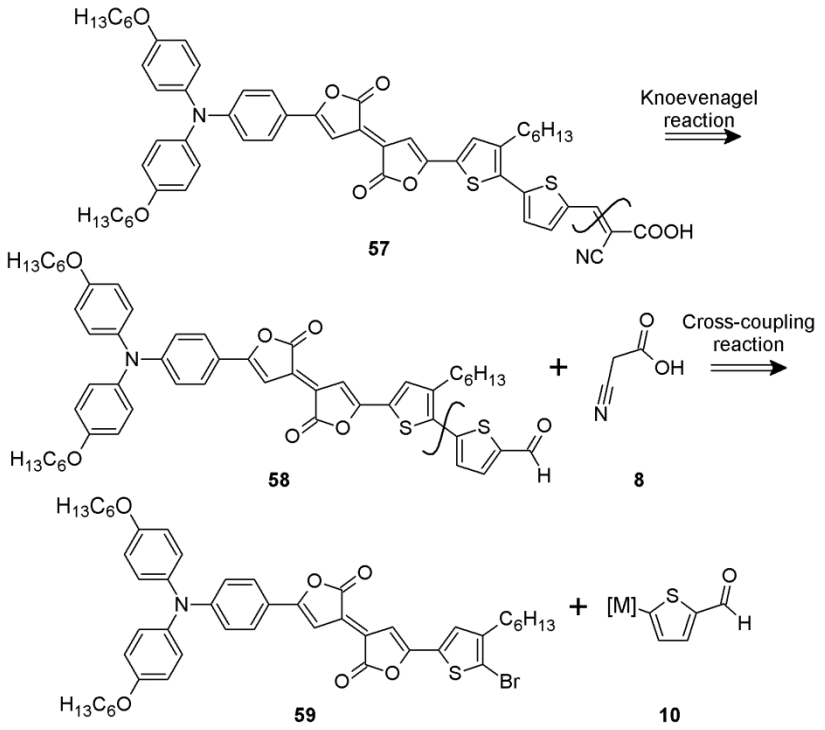

Scheme 5.2. Retrosynthetic analysis of dye 57: last steps.

The key-intermediates for the formation of the Pechmann-unit were the lactone **60,** bearing the donor moiety, and α,γ-diketoacid **61**. Both the building blocks **60** and **61** could be prepared following the retrosynthetic analysis in Scheme 5.3.

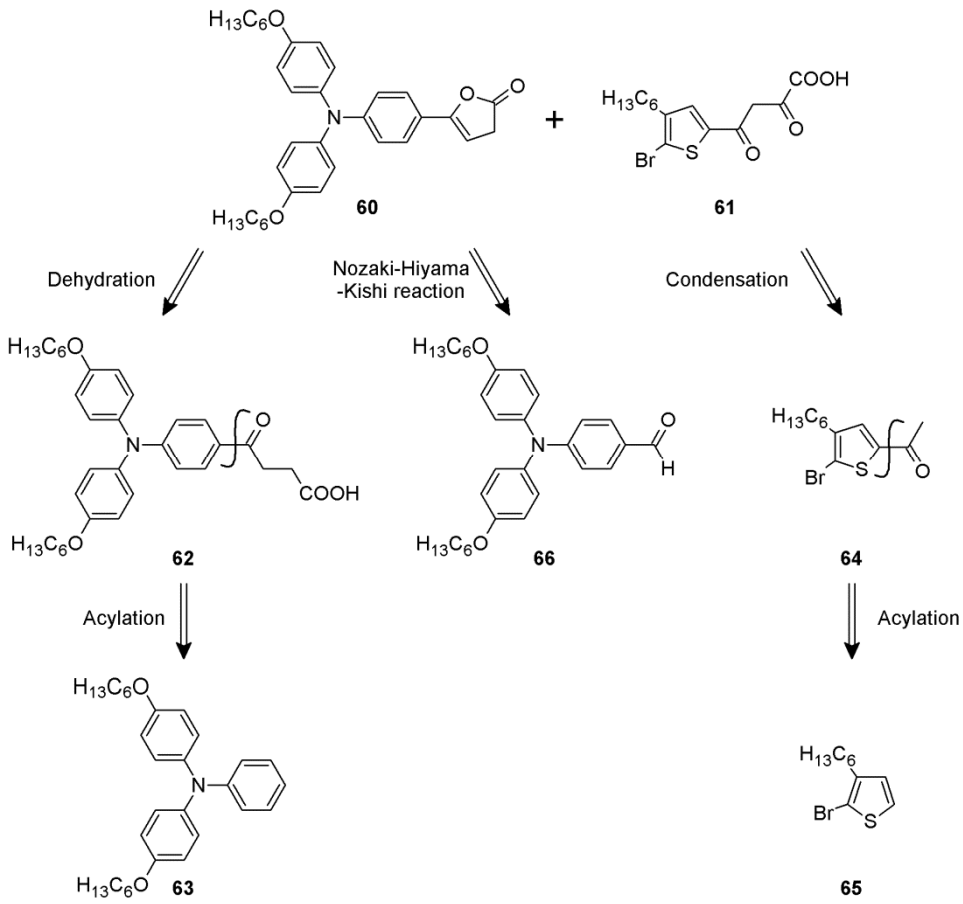

Scheme 5.3. Retrosynthetic analysis of dye 57: construction of building blocks 60 and 61.

5.2.3.2. Synthesis of intermediate 61

A two-step synthesis of intermediate **61** was accomplished following the procedure depicted in Scheme 5.4. Friedel-Crafts acetylation of commercially available 2-bromo-3-hexylthiophene (**65**) was carried out by using a two-fold excess of acetyl chloride and aluminum chloride as a Lewis acid promoter: although the thiophene ring partially decomposed in the presence of a strong Lewis acid such as $AlCl_3$, optimal experimental conditions afforded the desired product **64** with a moderate yield (40%) after chromatographic purification. The second step was a Claisen condensation of compound **64** with diethyl oxalate as the electrophile:[29] the reaction was performed in anhydrous THF by using a solution of sodium methoxide in anhydrous methanol as the base, and product **61** was isolated in high yield (80%) after recrystallization.

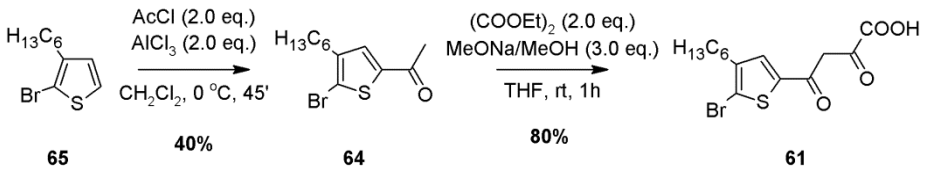

Scheme 5.4. Synthesis of intermediate 61.

5.2.3.3. Synthesis of intermediate 60

The preparation of intermediate **60** could be carried out following two different procedures, which used triarylamines **63** and **66** as starting materials, respectively.[30]

In the first approach (Scheme 5.5) we started with a Friedel-Crafts acylation of triarylamine **63** with succinic anhydride. Initially, we applied the same reaction conditions already used for the synthesis of compound **64** (Scheme 5.4), but only a very low conversion of the starting material (about 16%) was achieved in this case even increasing the temperature to 40 °C for 24 hours. Changing the solvent from dichloromethane to 1,2-dichloroethane enabled to raise the temperature to 85 °C, allowing to obtain γ-ketoacid **62** with a high yield (81%).

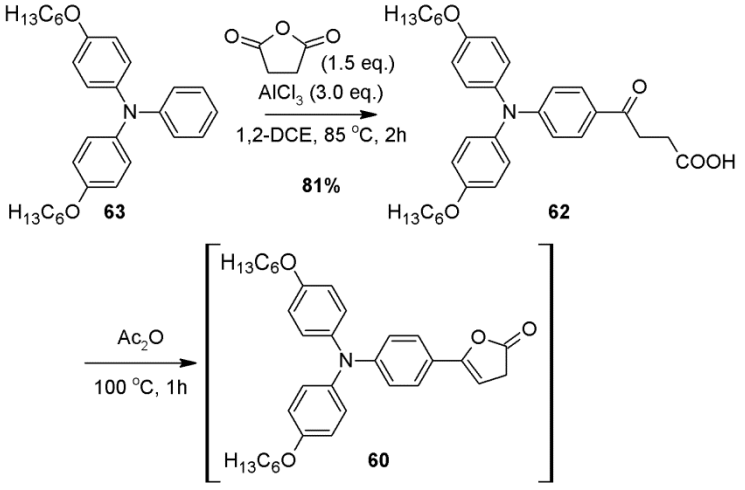

Scheme 5.5. Synthesis of intermediate 60 (route A).

The second step was a dehydration/cyclization sequence promoted by acetic anhydride[31] which was used as reaction solvent too. The conversion of the starting material to product was complete after one hour at 100 °C, but the instability of

compound **60** towards air humidity allowed to isolate just a mixture of compounds **60**:**62** in a 70/30 ratio.

The second procedure we used is based on a Nozaki-Hiyama-Kishi reaction, which is a nickel/chromium-mediated reaction forming an alcohol starting from an aldehyde and an allyl or vinyl halide.[32] The reaction is very selective towards aldehydes and tolerates many functional groups such as ketones, esters, amides and nitriles. Knochel *et al.*[33] studied the reactivity of chromium-based organometallics and reported the synthesis of a simple aromatic five-membered lactone (**69**, Scheme 5.6) by employing vinyl iodide **67**, benzaldehyde, chromium- and nickel dichloride.

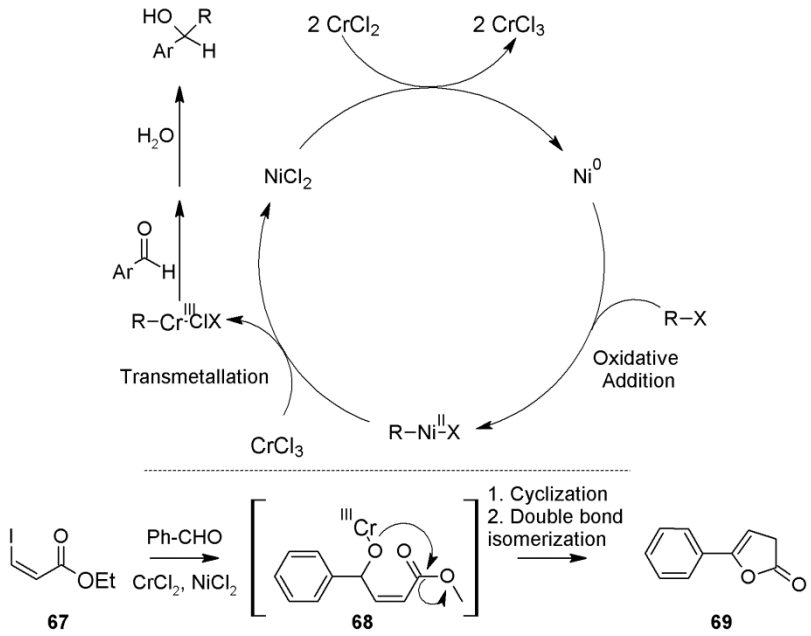

Scheme 5.6. Mechanism of Nozaki-Hiyama-Kishi reaction (up) and Knochel reaction (down).

The reaction mechanism (Scheme 5.6) starts with the reduction of Ni^{2+} to Ni^{0} by Cr^{2+}, then proceeds with the oxidative addition of Ni^{0} in the carbon-halogen bond of the halide and the transmetallation of the intermediate organo-nickel species with Cr^{3+}. The so-formed organo-chromium reagent can react with an aldehyde to afford, after hydrolysis, the alcohol. In the Knochel reaction,[33] the expected intermediate **68** could give an intramolecular reaction with the formation of the lactone ring and elimination of chromium methoxide bishalide. A final double bond isomerization afforded product **69**.

These reaction conditions were applied to aldehyde **66** in view of obtaining compound **60** in a single step (Scheme 5.7): heating to a temperature of 50 °C was necessary to start the reaction and complete conversion of **66** was achieved within 16 hours. The reaction looked very sensitive to the quality of chromium chloride and the presence of water was detrimental. Unfortunately, many by-products were formed and compound **60** was isolated, after chromatographic purification, with a yield of 38%. Likewise the first procedure, a variable amount of open-chain product **62** (5-10%) was always obtained.

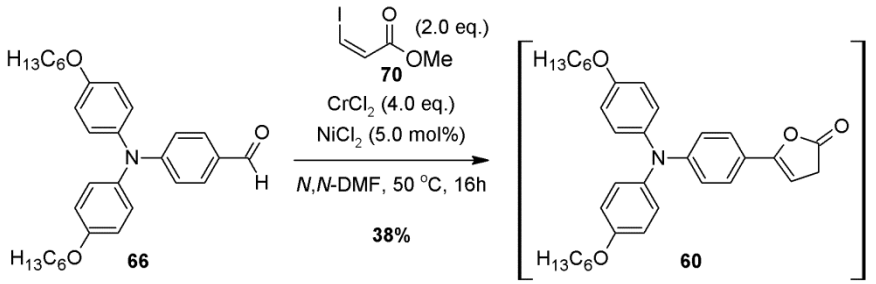

Scheme 5.7. Synthesis of intermediate 60 (route B).

We can thus conclude that although both the methods used allowed to obtain the desired intermediate **60**, the first one (Scheme 5.5) gave better results affording a higher yield and a more straightforward experimental procedure. Since it was impossible to isolate compound **60** in a pure form, its mixture with **62** was used as such for the subsequent reaction.

5.2.3.4. Preparation of the bis-lactonic unit

The first systematic study concerning the synthesis of Pechmann-dyes was accomplished by Fang and Bergmann in 1951.[25] In that paper, they showed that the condensation of lactone **71** with benzoylpyruvic acid **72** in acetic anhydride afforded non-symmetrical Pechmann product **74** in high yield (Scheme 5.8). The authors suggested that lactone **71** performed a nucleophilic attack on the carbonyl group in α-position to the carboxylic acid of **72** with loss of water and formation of intermediate **73**, which could evolve to product **74** after cyclization and elimination of a second molecule of water. The presence of acetic anhydride was required to assist the dehydration processes.

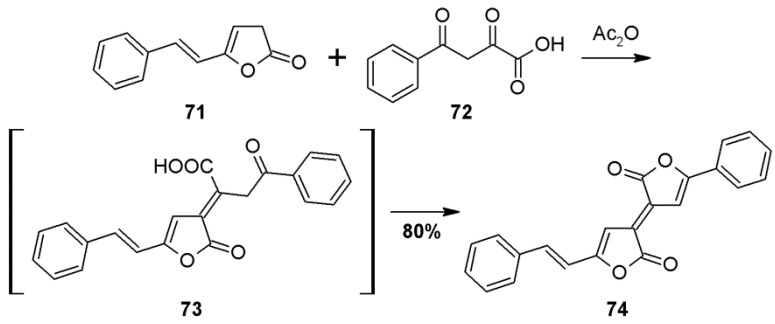

Scheme 5.8. Synthesis of non-symmetrical Pechmann-dyes by Fang and Bergmann.[25]

To the best of our knowledge, compound **74** is the only non-symmetrical Pechmann-derivative ever reported in the literature. This precedent prompted us to test this reaction on our substrates in order to obtain non-symmetrical derivative **59** (Scheme 5.9): several attempts were carried out.

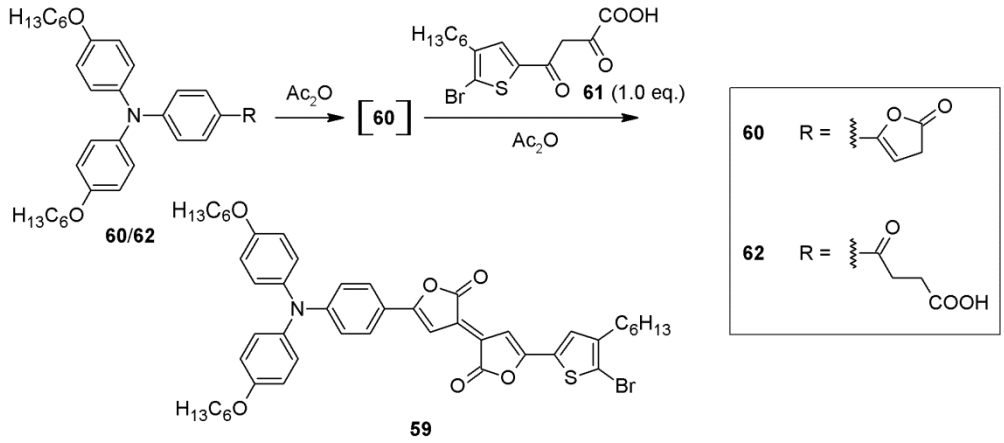

Scheme 5.9. Generic reaction scheme for the synthesis of Pechmann-intermediate 59.

Thus we decided to heat at 100 °C the mixture of compounds **60** and **62** obtained by dehydration/cyclization promoted by acetic anhydride[31] (see Scheme 5.5) in order to convert all γ-ketoacid **62** to lactone **60**. After 30 minutes conversion of compound **62** was complete and α,γ-diketoacid **61** was added *in situ*, then the reaction mixture was heated to 100 °C for 6 hours. Although the starting materials were consumed, the desired compound **59** was isolated with a very low yield (approx. 4%) due to the formation of many by-products. Using an higher reaction temperature (120 °C) caused a faster disappearance of the starting materials, but the yield of the product did not increase.

Some of the by-products (Scheme 5.10) were identified: among them, compound **75**, a dimer of lactone **60**, and ketone **64**, which was an intermediate for the synthesis of α,γ-diketoacid **61** (Scheme 5.4), were found. Indeed, in the presence of acetic anhydride, α,γ-diketoacid **61** could dehydrate and afford dioxofuran **76** (Scheme 5.10 down) by means of a thermal decomposition already known in the literature.[34] The loss of carbon monoxide generated a very reactive ketene (**77**) which could produce intermediate **64** and other unidentified by-products.

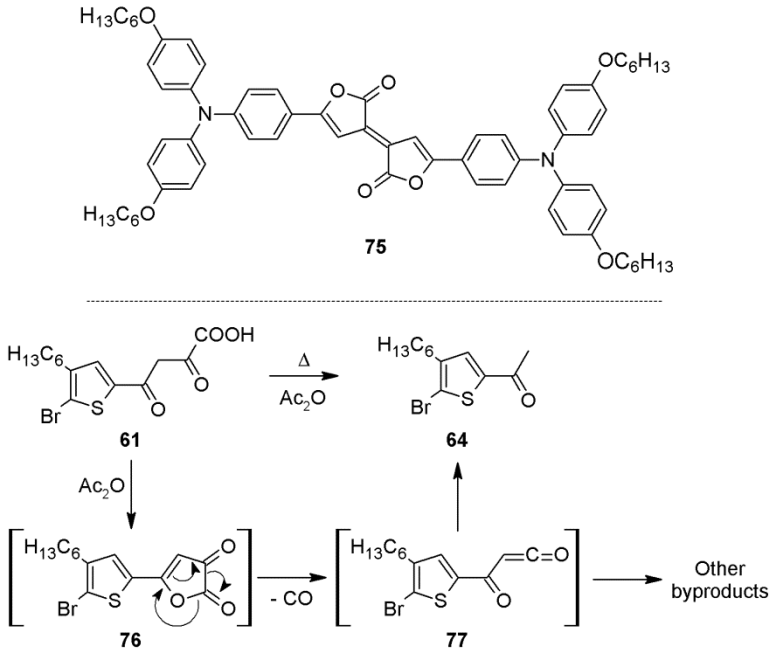

Scheme 5.10. Byproduct 75 (up) and an hypothesis of decomposition of 61 (down).

Several attempts were carried out at different reaction conditions, including temperatures and reaction times, use of acid and basic additives, however all our efforts were frustrated by very low yields of the desired product **59** and the formation of many by-products, mostly stemming from decomposition reactions of α,γ-diketoacid **61**.

Since dioxofuran **76** seemed to be a key-intermediate in the condensation reaction, we attempted a different synthesis of **76** (Scheme 5.11), not requiring the use of Ac_2O, and using compound **64** as starting material.[34] The first step was the formation of silylenolether **78**, which was obtained quantitatively using LDA as a base and trapping the enolate with trimethylchlorosilane. Then, silylenolether **78** was reacted

with oxalyl chloride. The reaction was carried out twice at different temperatures (25 and –78 °C), but in each case dioxofuran **76** was not formed and only starting material **64** was recovered from the reaction mixture. A strong acid Lewis such as trimethylsilyl triflate was also employed to increase the electrophilicity of oxalyl chloride, but the only product we were able to isolate was once again ketone **64**.

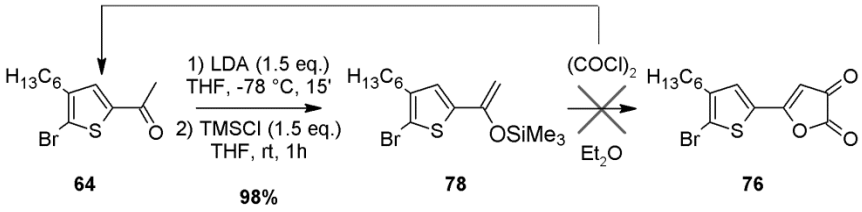

Scheme 5.11. Attempt to synthesize the dioxofuran 76.

Since our efforts to reproduce the direct synthesis of an asymmetric Pechmann-unit by Fang and Bergmann[25] were unsuccessful, we abandoned the synthesis of dye **57** and turned our attention to a different approach.

5.2.4. Route B: preparation of a symmetric Pechmann-unit

Once abandoned the first retrosynthetic approach (route **A**, Scheme 5.1), we investigated the feasibility of the route **B** which provided the preparation of a symmetric Pechmann-scaffold **III** and its subsequent derivatization in cross-coupling reactions in order to introduce different donor and anchor moieties.

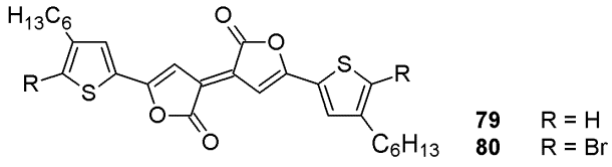

Figure 5.12. Structures of the desired symmetric Pechmann-dyes.

Compound **79** and its dibrominated derivative **80** (Figure 5.12) were chosen as new key intermediates: for this purpose, two synthetic procedures which were already known in literature for the synthesis of symmetric Pechmann-dyes were investigated.

5.2.4.1. First procedure – pyridinium ylide route

The most recent procedure was reported in 2014 by Belei *et al.*,[35] who discovered serendipitously that Pechmann-dye **83** could be obtained with a good yield (Scheme 5.12) adding dimethyl maleate (**82**) to an *in situ*-generated pyridinium ylide, in turn obtained by deprotonation of *N*-phenacyl-4-dimethylamino-pyridinium bromide (**81**) with 1,8-diazabicycloundec-7-ene (DBU). Few *p*-substituted aromatic Pechmann-derivatives were prepared following this protocol with moderate yields (32-45%).

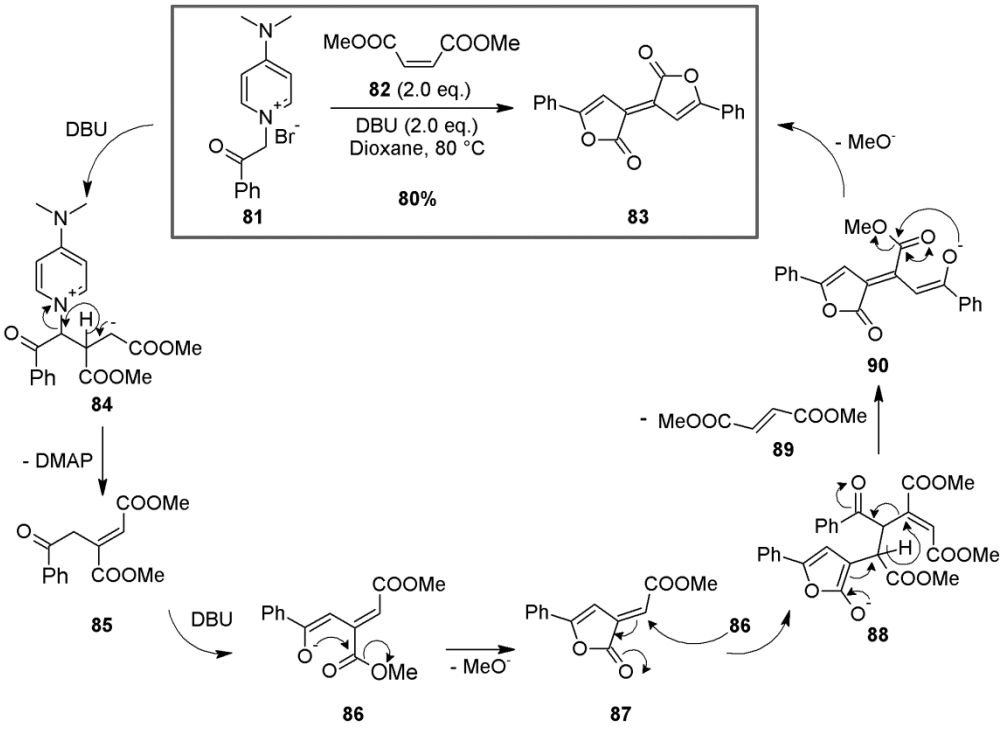

Scheme 5.12. Belei's procedure and its mechanism for the synthesis of Pechmann-dyes.

Based on some experimental evidences, authors suggested a plausible mechanism which is drawn in Scheme 5.12: ylide generated by deprotonation of pyridinium salt **81** with DBU undergoes a Michael addition to dimethyl maleate (**82**) generating adduct **84**, which affords intermediate **85** after a formal hydride shift and elimination of DMAP. A second equivalent of DBU can deprotonate **85** to form enolate **86**, which provides lactone **87** by intramolecular cyclization. Then, a second Michael addition of enolate **86** to the same lactone **87** affords intermediate **88**, which, after a second hydride shift followed by elimination of dimethyl fumarate (**89**), forms compound **90**.

Finally, cyclization of enolate **90** affords Pechmann-dye **83** upon elimination of methanol.

In order to test the feasibility of this procedure for our purposes, we had to prepare the appropriate pyridinium salt (**92**, Scheme 5.13) to provide symmetric Pechmann-derivative **80**. Starting from compound **64**, α-mono-bromination of the ketone with pyridinium bromide perbromide (PBPB)[36] produced intermediate **91**, which was easily converted to pyridinium salt **92** by reaction with DMAP[37] in refluxing acetone, with 59% overall yield.

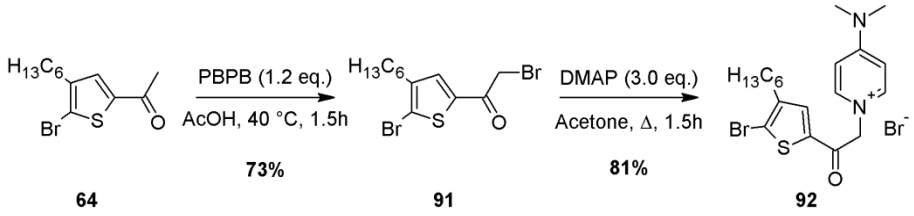

Scheme 5.13. Synthesis of pyridinium salt 92.

Subsequently, pyridinium salt **92** was reacted with two equivalents of maleate **82** and DBU in refluxing ethanol (Scheme 5.14). Disappointingly no traces of desired compound **80** were formed after 16 hours, despite complete disappearance of the starting material. ^{1}H-NMR analysis of the crude reaction mixture just showed the hydrobromide salt of DBU, DMAP, dimethyl maleate (**82**) and dimethyl fumarate (**89**).

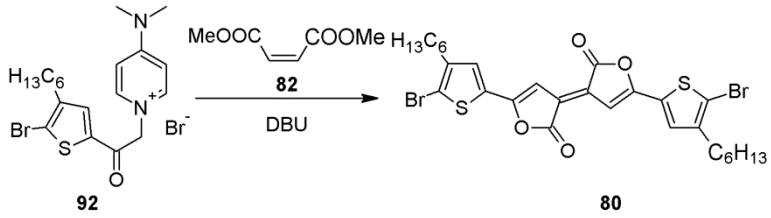

Scheme 5.14. Generic scheme for the synthesis of compound 80.

The reaction was repeated at room temperature to assess if a lower temperature could avoid decomposition of the starting material, but the analysis of crude material did not show a better result. Use of a different solvent (dioxane or CH_2Cl_2), of a substoichiometric amount of maleate **82,** or isolation of the pre-formed pyridinium ylide of **92** using NaOH before reacting with maleate **82** and DBU, did not allow the isolation of any reaction intermediate.

5.2.4.2. Second procedure – β-aroylacrylic acid route

Consequently we decide to abandon the first procedure and try a different approach based on the method described by Fang and Bergmann[25] in their first systematic study about the preparation of such compounds. In such context, the authors elaborated a synthetic procedure based on the reaction of β-aroylacrylic acids (**93a-c**) with copper (I) chloride and ammonium acetate under air in refluxing acetic anhydride (Scheme 5.15).

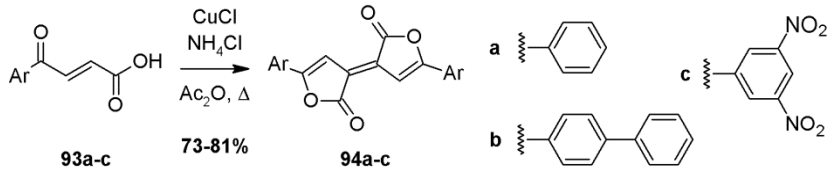

Scheme 5.15. Symmetric Pechmann-dyes prepared by Fang and Bergmann[25].

Products **94a**-**c** were isolated with high yields, but each substrate required a very different amounts of CuCl (0.35–1.30 eq.) and NH_4Cl (0.70–4.70 eq.) to be efficiently converted. Authors did not justify these significant differences and did not propose a plausible mechanism, which was postulated only thirty years later by Begley *et al.* (Scheme 5.16).[38]

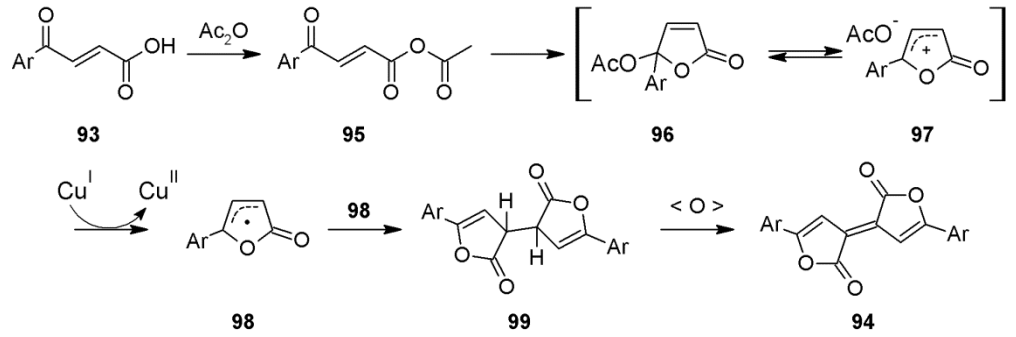

Scheme 5.16. Reaction mechanism proposed by Begley et al.[38]

These authors observed that, when the reaction was carried out in the absence of air, no product was formed and only mixed anhydride **95** could be isolated. Accordingly, they supposed that compound **95** is an intermediate for the formation of **94**, which could evolve to acetyl-lactol **96** and/or cation **97**. Then, they suggested that product **94** could be formed by single-electron transfer from Cu^{I} (**98**), followed by radical coupling (**99**) and final dehydrogenation under air. However, except for the

formation of mixed anhydride **95**, no experimental evidence was provided of the other intermediates featured in this mechanistic hypothesis. This reaction was recently applied by Sullivan *et al*.[17] for the synthesis of two thiophene-containing Pechmann-dyes with good results (Scheme 5.17) by using sub-stoichiometric amounts of CuCl (0.30–0.37 eq.) and NH_4Cl (0.60–0.73 eq.).

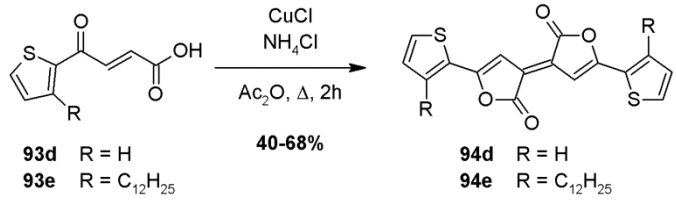

Scheme 5.17. Symmetric Pechmann-dyes prepared by Sullivan et al.[17]

Thus, the promising results obtained in the synthesis of some aromatic and heteroaromatic Pechmann-derivatives (**94**) prompted us to test these conditions for the preparation of compounds **79** and **80**. Initially, synthesis of β-heteroaroylacrylic acids **102**-**104** was carried out through Friedel-Crafts acylation of 3-hexylthiophene (**100**) and 2-bromo-3-hexylthiophene (**65**) with maleic anhydride (**101**) and aluminum trichloride as Lewis acid (Scheme 5.18). The desired compounds were obtained with moderate yields.

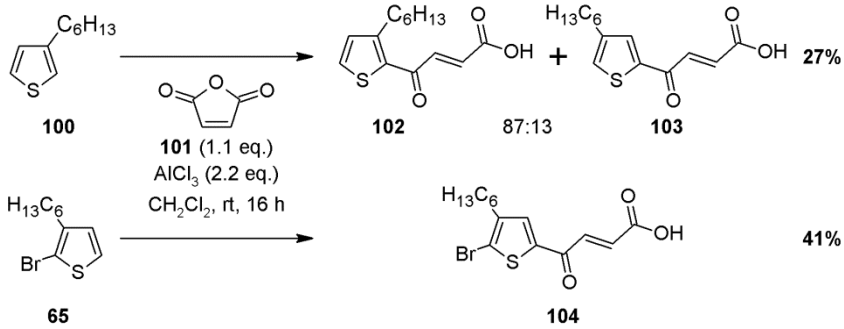

Scheme 5.18. Synthesis of β-heteroaroylacrylic acids 102-104.

Unfortunately, the acylation of thiophene **100** with anhydride **101** was not completely regioselective: the ratio of acids **102**/**103** in the reaction crude was approximately 80:20, which could only be increased to 87:13 after some recrystallizations from toluene. The same experimental conditions, however, afforded acid **104** as a unique product.

Based on Sullivan's procedure, we decided to use the mixture of isomers **102**-**103** as a substrate to optimize the reaction conditions (Table 5.2). Initially the reaction was performed by heating to reflux a mixture of the starting material and substoichiometric amounts of CuCl and NH_4Cl in acetic anhydride for two hours (entry 1). A 95:5 mixture of the two isomers **105**-**106** was always obtained, but, unlike the preparation of compounds **94d-e** (Scheme 5.17), in rather low yield. The ^{1}H-NMR analysis of the crude reaction mixture showed the absence of the starting material, and the presence of a mixed anhydride akin to **95** (Scheme 5.16) and other unidentified products in high amount. We supposed that the backlog of reaction intermediates and by-products at the end of the reaction could be due to an inefficient dehydrogenation step (see Scheme 5.16), thus chloranil was used to accelerate this step together with a stoichiometric amount of CuCl. No product was formed when chloranil was added at the beginning of the reaction with the other reagents (entry 2), and its addition to the crude reaction mixture was ineffective as well (entry 3).

Table 5.2. Optimization of the synthesis of symmetric Pechmann-derivatives 105-106.

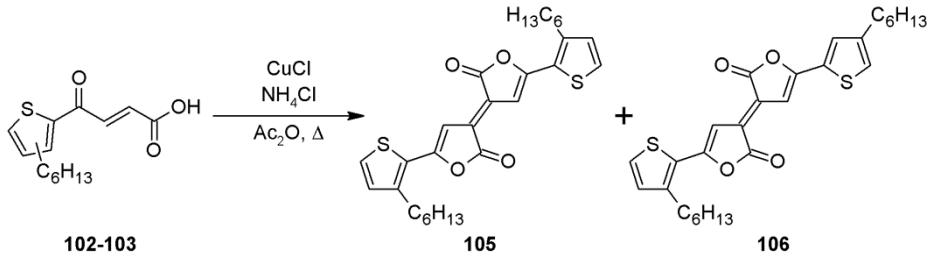

Entry	CuCl (eq.)	NH_4Cl (eq.)	chloranil (eq.)	Time (h)	Yield **105**-**106** (%)[a]
1	0.30	0.60	-	2	12
2	1.0	0.60	0.5[b]	2	-
3	1.0	0.60	0.5[c]	2	11
4	1.2	2.4	-	6	34
5	1.2	2.4	-	16	41
6[d]	1.2	2.4	-	0.5	27

a) **105**/**106** ratio ≈ 95:5. b) Added to the reaction mixture with the other reagents. c) Added to the crude reaction mixture after dissolving in THF. d) The reaction was performed under MW heating.

Better results were obtained by using excess amounts of CuCl and NH_4Cl and longer reaction times (entries 4-5): in these conditions the reaction yield was finally improved up to 41%. However, despite a complete disappearance of both the starting material and the reaction intermediates, the final yield was always limited by

the formation of a black decomposition product, probably obtained by reaction of some intermediates with acetic anhydride itself. Performing the reaction under MW heating (entry 6) shortened reaction times, but the yield of the isolated product was limited by the formation of undesired by-products (**107**-**108**; Figure 5.13) stemming from Friedel-Crafts acetylation of the desired compounds.

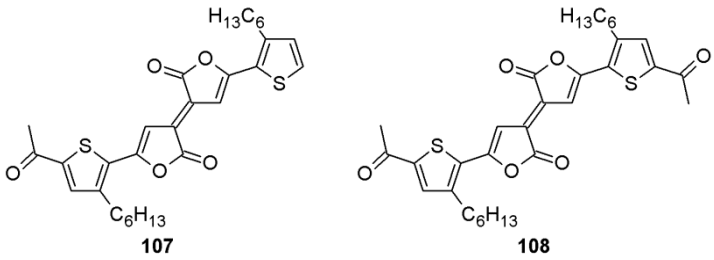

Figure 5.13. By-products of the MW-activated reaction (entry 6, Table 5.2).

In general, the optimization effort described above allowed us to prepare the desired Pechmann-unit with a moderate yield, but, even after chromatographic purification, a mixture of the two different isomers **105**-**106** was always obtained. For this reason, we tested our best reaction conditions on acid **104** (Scheme 5.19) hoping to prepare compound **80** as a unique isomer.

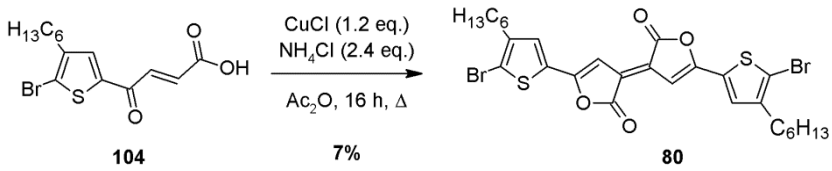

Scheme 5.19. Synthesis of Pechmann-derivative 80.

In this case, a large amount of a blue insoluble material was formed at the end of the reaction, in addition to other undesired dark-colored by-products. Therefore, unlike the former reaction (entry 5, Table 5.2), product **80** was isolated with a very low yield (7%). Probably the carbon-bromine bond in the outer thiophene rings of **80** was sensitive to the presence of copper and to single-electron transfer (SET) conditions, and thus the blue solid which was isolated at the end of the reaction could be due to an undesired polymerization reaction.

Since bromo-derivative **104** did not tolerate our reaction conditions and the employment of a non-symmetrical thiophene such as **100** afforded a mixture of

isomers, we selected a slightly different Pechmann-derivative (**109** - Figure 5.14) as the new target molecule.

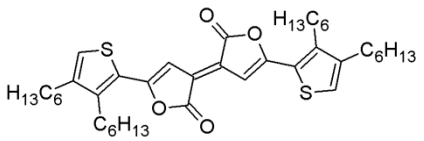

109

Figure 5.14. Structure of target molecule 109.

5.2.4.3. Synthesis of intermediate 109

The structure of compound **109** was chosen as new synthetic target because we supposed that its precursor, β-heteroaroylacrylic acid **110,** would have reacted with CuCl and NH_4Cl similarly to compound **102**, while 3,4-dihexylthiophene (**111**), unlike 3-hexylthiophene (**100),** would not pose any regioselectivity issue in the Friedel-Crafts acylation (Figure 5.15). As the starting material of this synthesis we used 3,4-dibromothiophene (**112**), which was easily prepared in a multi-gram scale following a well-known procedure.[39]

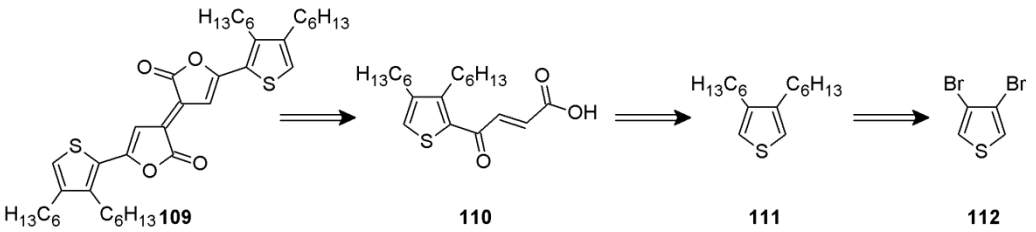

Figure 5.15. Retrosynthetic sequence of compound 109.

Compound **111** was prepared as already reported,[40] using a Kumada cross-coupling reaction (Scheme 5.20): $Ni(dppp)Cl_2$ was employed as the catalyst, while 1-hexylmagnesiumbromide was formed *in situ* starting from 1-bromohexane and magnesium. Then, the usual Friedel-Craft acylation with maleic anhydride (**101**) gave a crude reaction mixture containing the desired product (*E*)-**110** and a fraction together with its (*Z*)-isomer, which was isomerized by washing repeatedly the reaction crude with $HCl_{(aq)}$.[41] Finally pure acid (*E*)-**110** was obtained in good yield.

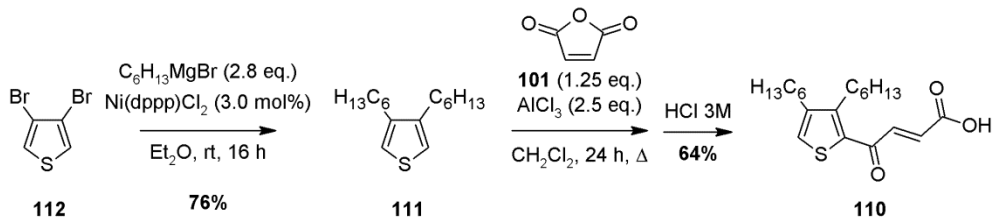

Scheme 5.20. Synthesis of the β-heteroaroylacrylic acid 110.

Then, the optimized conditions (entry 5, Table 5.2) were applied to acid **110** which indeed reacted in the presence of CuCl and NH_4Cl similarly to its analogue **102**, even if a longer reaction time (40 hours *vs*. 16 hours) was necessary to obtain a comparable yield (38% *vs*. 41%) of the Pechmann-product **109** (Scheme 5.21).

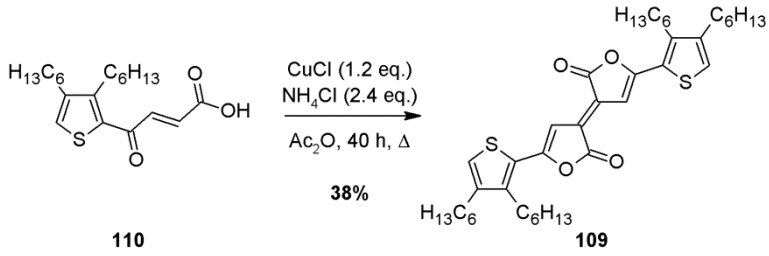

Scheme 5.21. Synthesis of Pechmann-derivative 109.

Although the obtained yields were not very high, we decided to go further and use key intermediate **109** for our purposes. However, by our experience, it appears that there is a lack of synthetic procedures in the literature, as the described ones resulted in our hands either not general nor high yielding. This fact could be ascribed to the absence of an established reaction mechanism.

5.2.5. Synthesis of D-A-π-A dyes AD351 and AD364

The two structures we selected **AD351**-**AD364** are reported in Figure 5.16. This two dyes differ for two different donor groups, a simple triphenylamine (**AD351**), and a hexylthio *p*-substituted triphenylamine (**AD364**). Such substitution was introduced on the donor group referring on our precedent results about TzTz-dyes (see Chapter 4), where, apparently, the presence of alkylthio chains on the donor portion of the molecule improved the photovoltaic performance which was probably due to a much faster dye regeneration.[42]

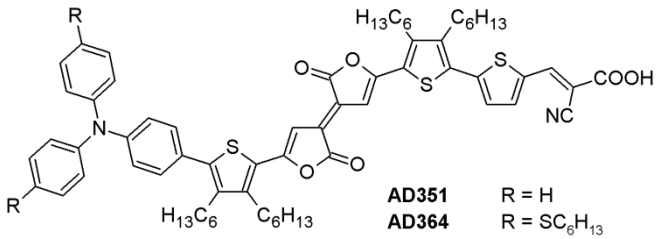

Figure 5.16. Structures of dyes AD351 and AD364.

5.2.5.1. Computational analysis of AD351 and AD364

DFT computational analysis was then repeated for structures **AD351** and **AD364**. The HOMO/LUMO energy levels (Figure 5.17) and the wavefunction plots (Figure 5.18) of the two dyes were compared with those previously found for sensitizers **TTZ3** and **TTZ5** which contained the same donor (triphenylamine for **AD351** and **TTZ3**; *p*-hexlythio-substituted triarylamine for **AD364** and **TTZ5**) and anchoring (cyanoacrylic acid) groups. As already outlined for compound **57**, when compared to **TTZ3**-**TTZ5**, the presence of the Pechmann-unit in **AD351** and **AD364** shifted both HOMO and LUMO energy levels to more negative values (Δ HOMO = 0.14-0.16 eV; Δ LUMO = 0.55-0.56 eV) with a remarkable decrease of the HOMO-LUMO energy gap of 0.39-0.41 eV.

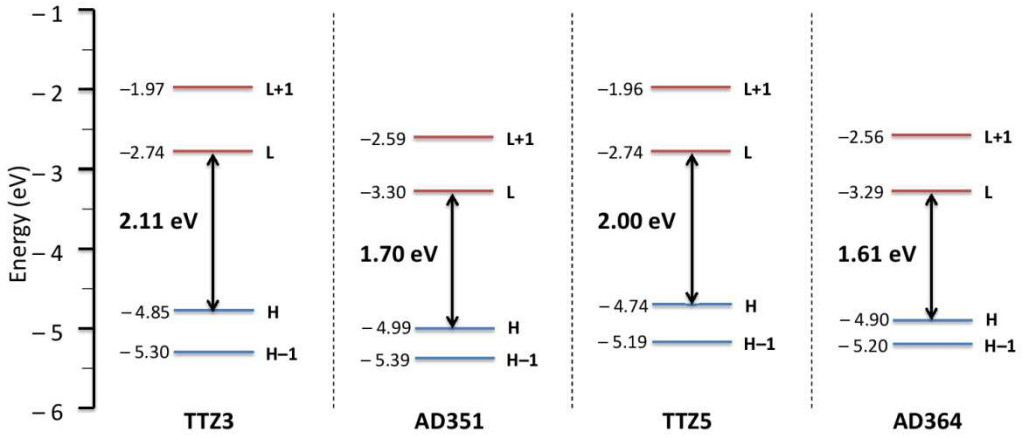

Figure 5.17. Computed (B3LYP/6-31G) HOMO–LUMO energy gaps of compounds AD351-AD364 and, for comparison, TTZ3-TTZ5.*

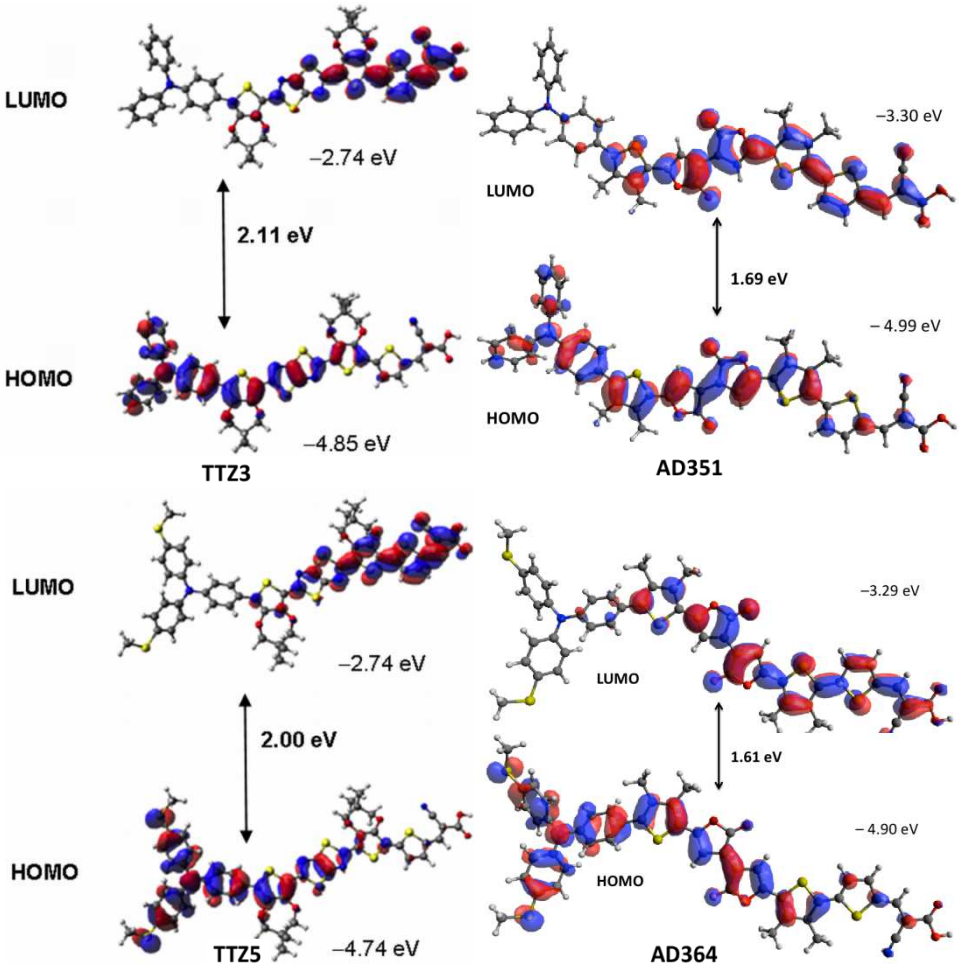

Figure 5.18. Isodensity plots and computed energies for the frontier molecular orbitals of compounds AD351-AD364 and, for comparison, TTZ3-TTZ5 at the B3LYP/6-31G* level.

In particular, the introduction of *p*-hexylthio chains in **AD364** slightly raised the HOMO level without affecting the LUMO leading to a smaller energy gap (**AD351**/**AD364**: 1.70 eV *vs.* 1.61 eV). Similarly to **57** and other D-A-π-A dyes,[8,10] the HOMO/LUMO orbitals of **AD351** and **AD364** were mostly localized on donor and anchor respectively, but both were present on the Pechmann-unit as well, thus giving rise to an extended superimposition and therefore ensuring strong intramolecular charge transfer upon photoexcitation.

Finally, Table 5.3 lists the absorption maxima (λ_{max}), oscillator strengths (*f*) and vertical excitation energies (E_{exc}) obtained from TD-DFT analysis of dyes **AD351**, **AD364** compared with those of **TTZ3** and **TTZ5**. The results were once again in line

with those provided by dye **57**: Pechmann-dyes **AD351** and **AD364** were predicted to have a strongly red-shifted absorption spectrum (503-504 nm vs. 674-691 nm in THF), with a large HOMO → LUMO component of the excitation process, unlike TzTz-dyes.

Table 5.3. CAMB3LYP/6-31G absorption maxima (λ_{max}), oscillator strengths (f), vertical excitation energies (E_{exc}) and main electronic transitions for dyes TTZ3, AD351, TTZ5 and AD364 in THF.*

Compound	λ_{max} [nm]	*f*	E_{exc} [eV]	Main transition (%)	
TTZ3	503	2.61	2.46	H–1 → L: 38.2	H→ L: 42
AD351	674	1.84	2.23	H → L: 83	
TTZ5	504	2.66	2.46	H–1 → L: 48.7	H→ L: 29.3
AD364	691	1.80	2.25	H → L: 72	

5.2.5.2. Retrosynthesis

A new retrosynthetic sequence traced on that already validated for dyes **AD351** and **AD364** was conceived as reported in Scheme 5.22. Again the cyanoacrylic anchor could be introduced through a Knoevenagel reaction starting from aldehydes **113**-**114**, which, in turn, could be synthesized through a cross-coupling reaction between a suitable organometallic reagent **10** and intermediates **115**-**116**. The two different donor groups could be installed at this point through cross-coupling of organometallics **12a**,**b** with dibromide **117**, which could in turn be obtained through bromination of compound **109**, whose preparation has been already described in the previous paragraphs.

5.2.5.3. Bromination of intermediate 109

Two different procedures (**A** and **B**, Table 5.4) were tested. Electrophilic bromination with *N*-bromosuccinimide (NBS) was carried out at room temperature for one hour (entries 1-2) using a slight excess of NBS and a mixture of acetic acid and CH_2Cl_2 as solvent. Despite the mild reaction conditions, dibromide **117** was isolated only with a low yield (15%) due to the formation of many decomposition products.

Elimination of the acid component and substitution of the reaction solvent from CH_2Cl_2 to *N*,*N*-DMF in order to increase the reaction temperature did not allow the formation of the desired product (entry 3). Since the presence of AcOH seemed essential, a lower amount of acid was employed (entry 4) which led the yield to increase up to 54%. Finally, the use of a catalytic amount of acid (entry 5) allowed to obtain desired product **117** in just 20 minutes with a 64% yield.

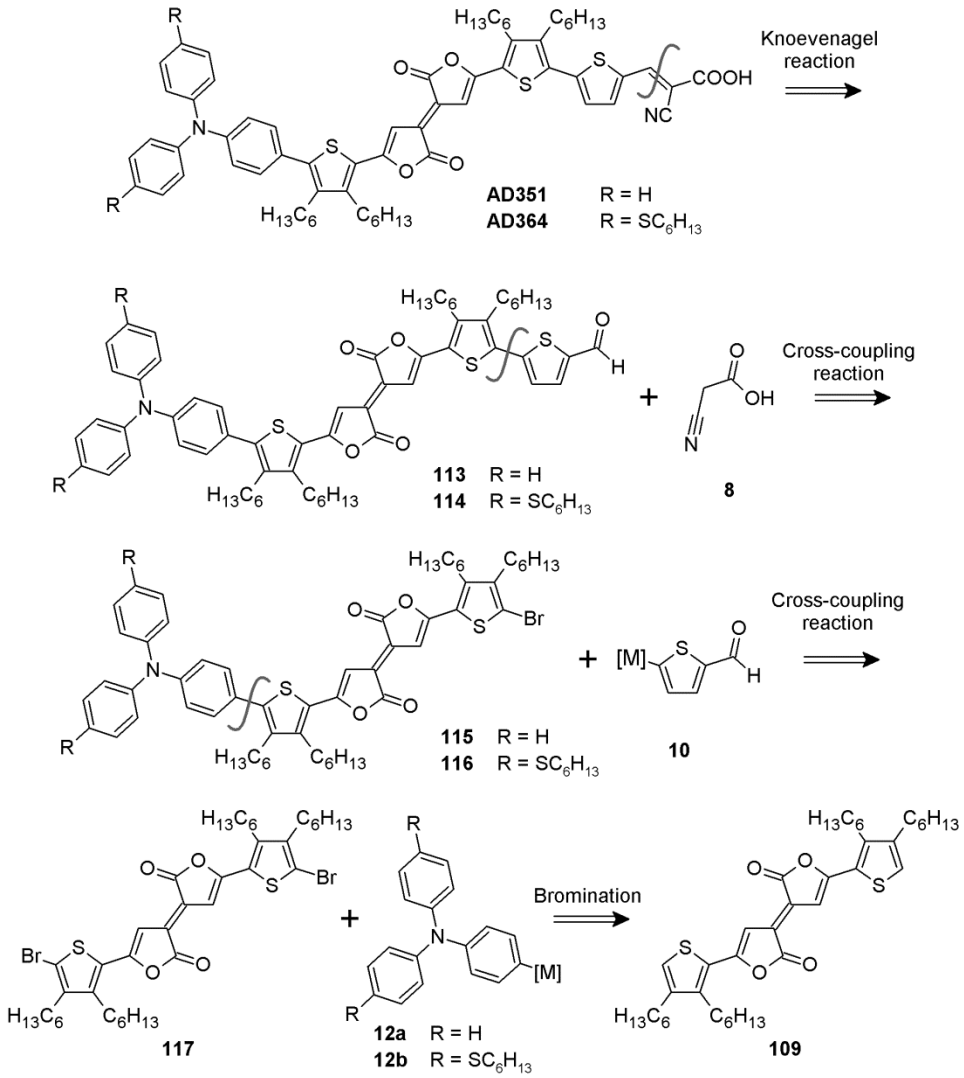

Scheme 5.22. Retrosynthetic sequence of dyes AD351 and AD364.

A different procedure for the bromination of some thiophene-containing aza-Pechmann derivatives based on use of lithium diisopropylamide (LDA) to deprotonate the outer thiophene rings in α-position and 1,2-dibromotetrachloroethane to quench the incipient lithium salt was also reported.[19,20] In order to verify a possible increase of the final yield of **117**, we decided to try also these conditions. However, both performing the reaction at –78 °C for one hour (entry 6) or raising the temperature from –78 to 25 °C overnight (entry 7), no trace of the desired compound was recovered.

Table 5.4. Optimization of the bromination reaction of compound 109.

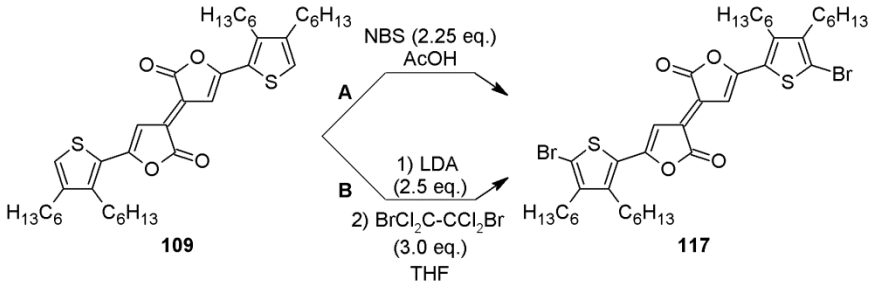

	Procedure A				
Entry	Solvent	AcOH (eq.)	Temperature (°C)	Time (h)	**117** yield (%)
1	CH_2Cl_2	≈ 350	25	1	15
2	CH_2Cl_2	≈ 35	25	1	15
3	*N*,*N*-DMF	-	25 → 100	16	-
4	CH_2Cl_2	2.25	25	1	54
5	CH_2Cl_2	0.10	25	0.33	64

	Procedure B		
Entry	Temperature (°C)	Time (h)	**117** yield (%)
6	–78	1	-
7	–78 → 25	16	-

5.2.5.4. Introduction of the donors: first Stille cross-coupling

The first reaction we decided to use to introduce the donor groups was a Suzuki-Miyaura cross-coupling of dibromide **117** with boronic acid **20** (Scheme 5.23); the reaction was performed using two different sets of reaction conditions, in particular changing the catalyst, the base and the reaction temperature. In both cases, starting material **117** decomposed completely within one hour.

This result led us to suppose that the Pechmann moiety is too sensitive to tolerate the basic conditions employed in the Suzuki reactions, and therefore we decided to switch to a milder process. Among cross-couplings the Stille reaction, which is characterized by the use of organostannane as organometallic counterpart, requiring quite mild conditions,[43] usually allows to perform difficult synthetic transformations using a neutral environment.

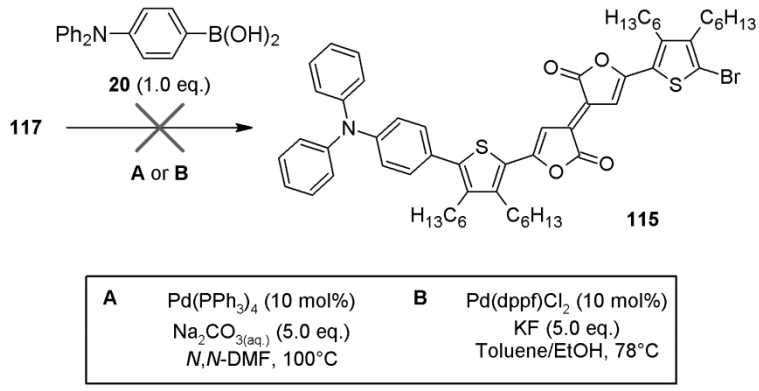

Scheme 5.23. Attempts of Suzuki-Miyaura cross-coupling.

To perform this process the proper organostannanes **119-120** needed to be prepared. This was done, starting from the corresponding bromoanilines **31** and **118** through metal-halogen exchange with *n*-BuLi at –78 °C followed by reaction with Bu_3SnCl as the electrophile (Scheme 5.24). In both cases, the conversion of starting materials was almost complete: although approx. 5-10% of dehalogenated triarylamine by-products were present, the crude reaction mixtures were used without purification for the next cross-coupling step, since attempts to purify the organostannanes by flash column chromatography caused a partial decomposition of the reagents.

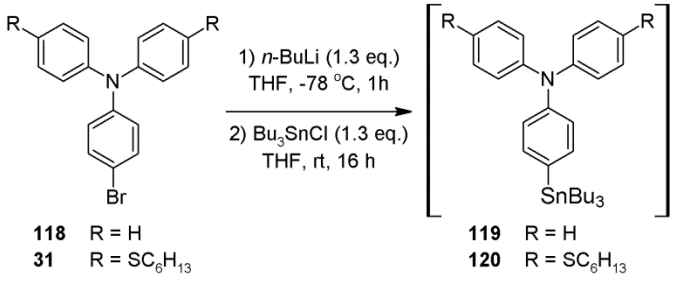

Scheme 5.24. Synthesis of organostannane 119-120.

The optimization of the Stille reaction was performed by using stannane **119**: the reaction was performed in toluene, using a stoichiometric amount of the stannane, and stopped before complete conversion of the starting material in order to avoid the formation of the symmetric double-coupling product. Unlike the Suzuki reaction, the milder experimental conditions required in this case, allowed the formation of desired product **115.** After a small screening of the catalysts (Table 5.5), we found

that employment of $Pd_2(dba)_3$ as pre-catalyst and tris-2-furylphosphine as ligand (entry 3) allowed to shorten the reaction time, decrease the reaction temperature to 70 °C and, consequently, improve the yield of the isolated product and reduce the decomposition of the starting material. The same catalyst was used successfully to react dibromide **117** with organostannane **120.** The reaction was carried out at a lower temperature (60 °C) and afforded monobromide **116** with 27% yield after purification.

Table 5.5. Optimization of Stille cross-coupling reaction.

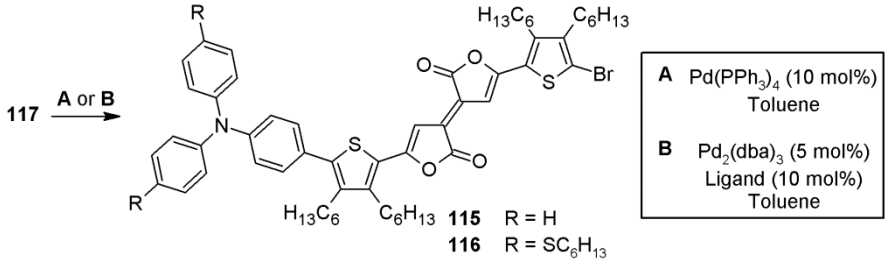

Entry	Stannane	Procedure	Ligand	T (°C)	Time (h)	Conversion (%)	Yield (%)
1	**119**	**A**	PPh_3[a]	110	5,5	70	18
2	**119**	**B**	P(*o*-tolyl)$_3$	105	5	75	20
3	**119**	**B**	P(2-furyl)$_3$	70	2	72	25
4	**120**	**B**	P(2-furyl)$_3$	60	2	72	27

a) Preformed $Pd(PPh_3)_4$ was used as catalyst.

Despite the final yields of this step were not very high, as already observed in the case of the TZ-TZ series, a variable amount of the starting dibromide **117** could always be recovered after chromatographic purification. Furthermore it should be remarked that this result represents the first example of a cross-coupling reaction performed on this kind of bis-lactonic unit and thus can open the way to the preparation of a wide array of such derivatives which are structurally connected with Pechmann-dyes[*].

[*] To the best of our knowledge, only few examples of cross-coupling reactions of aza-Pechmann dyes were described in literature.[19,20]

5.2.5.5. Introduction of the acceptor: second Stille cross-coupling and Knoevenagel reaction

Since the former Stille cross-coupling was successfully carried out, we decided to perform the same reaction also to introduce the formyl-thiophene moiety (Scheme 5.22), and obtain compounds **113**-**114**. To do that, the proper organotin reagent **123** was prepared (Scheme 5.25)[44] by reaction with lithium *N*,*O*-dimethylhydroxylamide, formed *in situ* by reaction of *n*-butyllithium and *N*,*O*-dimethylhydroxylammonium chloride, at –40 °C. Addition on the formyl moiety of compound **121**, afforded intermediate **122**, which, after deprotonation with *n*-BuLi, reacted with Bu_3SnCl to form the desired carbon-tin bond. Finally, addition of a weakly acid aqueous solution restored the formyl moiety by elimination of *N*,*O*-dimethylhydroxylammonium salt.

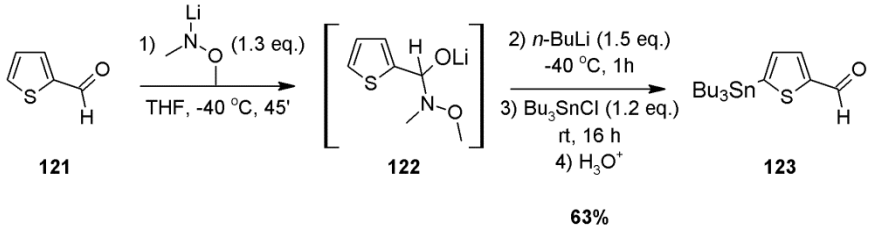

Scheme 5.25. Synthesis of organotin reagent 123.

Organostannane **123** (Scheme 5.26) was reacted with bromides **115**-**116** using our optimized reaction conditions for the Stille cross-coupling (Table 5.5, entries 3-4) and in both cases desired products **113**-**114** were obtained with good yields, confirming that the Stille reaction is a powerful tool for the chemical modification of Pechmann-derivatives.

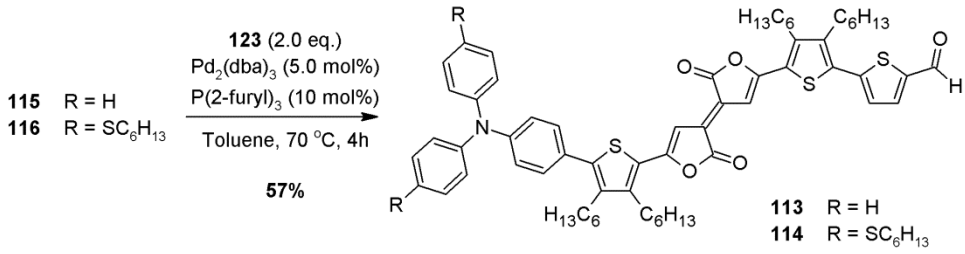

Scheme 5.26. Synthesis of the intermediates 113-114.

Finally, the anchoring group had to be installed on our dyes in order to complete the synthetic path, which is usually done through Knoevenagel condensation. Usual conditions for the transformation (see Chapter 4, Paragraph 4.2.2.4) required a

mixture of toluene and acetic acid and use of a large excess of cyanoacetic acid and ammonium acetate. In consideration that, during the bromination step (see paragraph 5.2.5.3), the Pechmann-dyes proved to be quite sensitive to the presence of acetic acid, we decided to slightly modify these conditions and carry out the Knoevenagel reaction by using a stoichiometric amount of piperidine[45] as the base and a mixture of toluene and acetonitrile as the solvents (Scheme 5.27).

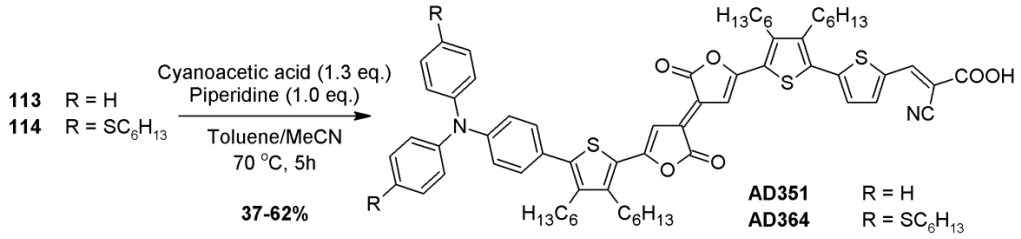

Scheme 5.27. Synthesis of the Pechmann-dyes AD351 and AD364.

After 5 hours at 70 °C, the reaction was stopped before complete conversion of the starting material in order to minimize its degradation: despite that, the final dyes **AD351** and **AD364** were isolated with a yield of 37% and 62% respectively. The moderate yield of the dye **AD351** could be ascribed to its lower solubility which hampered its final purification.

5.2.6. Characterization of dyes AD351 and AD364

First of all, we recorded the UV-Vis spectra of the $CHCl_3$ solutions of all synthetic intermediates to dye **AD351** containing the Pechmann-moiety (namely **109**, **113**, **115** and **117**; see Scheme 5.22 and Figure 5.19): the comparison in Figure 5.20 clearly shows the red-shift and widening of the absorption bands due to the elongation of the conjugated skeleton. Experimental values were compared with TD-DFT CAM-B3LYP/6-31G* and MPW1K/6-31G* computed absorption maxima in chloroform (Table 5.6) and a very good agreement between theoretical and experimental data was generally found. In particular, the computed maxima of **AD351** were almost perfectly aligned with the experimental values.

Then, UV-Vis spectra of dyes **AD351** and **AD364** were recorded both in $CHCl_3$ solution (Figure 5.21) and with the dyes adsorbed on TiO_2 (Figure 5.22). As expected, the two dyes showed an intense cyan color in solution due to their broad absorption of

red/NIR light between 550 and 800 nm, with high extinction molar coefficients and maxima at 676 and 681 nm for **AD351** and **AD364**, respectively (Table 5.7).

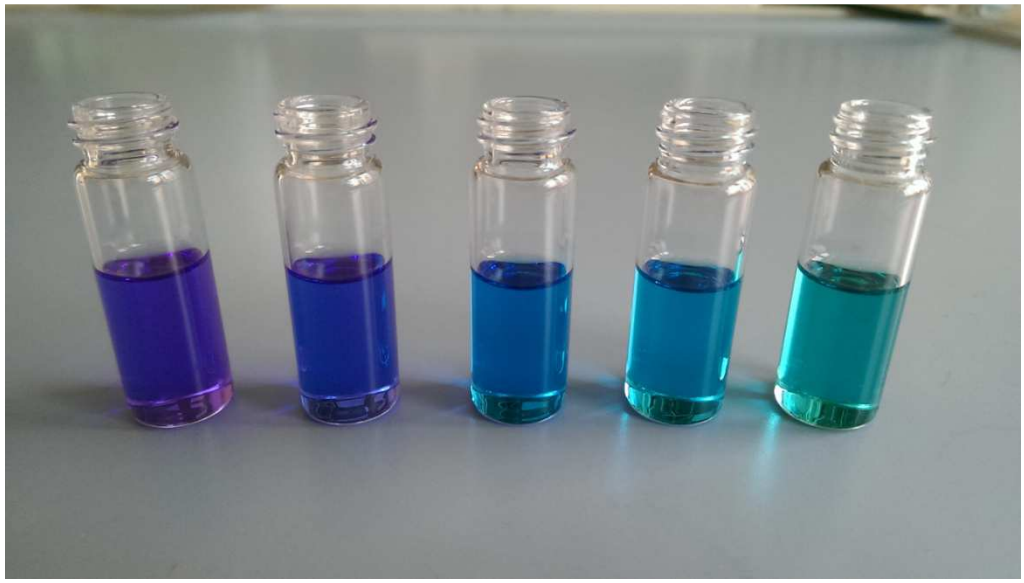

Figure 5.19. Picture of reaction intermediates (from left to right) 109, 117, 115 and 113 and AD351.

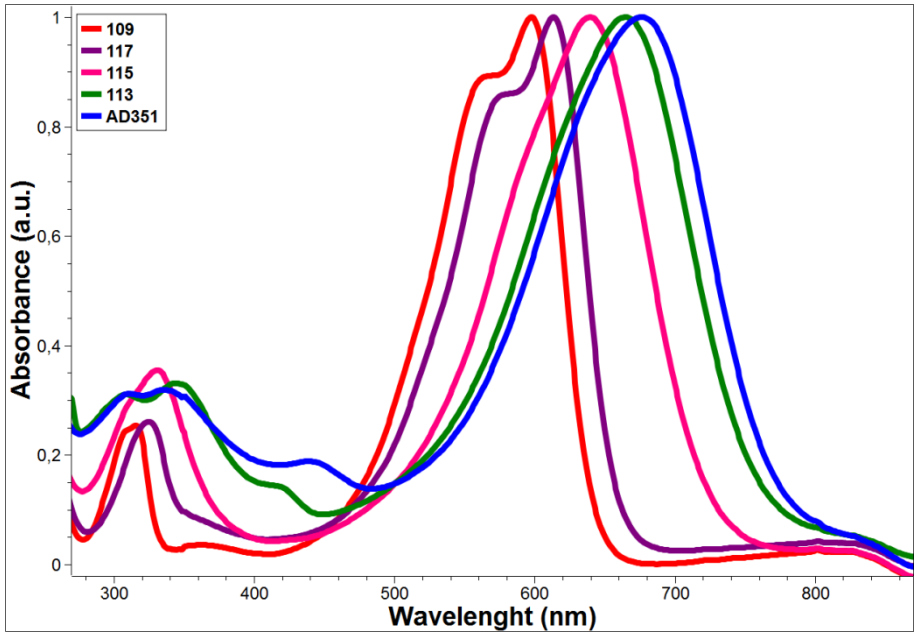

Figure 5.20. UV-Vis spectra of dye AD351 and its reaction intermediates 109, 113, 115 and 117.

Table 5.6. TD-DFT computed and experimental absorption maxima and related main transition of dye AD351 and its reaction intermediates 109, 113, 115 and 117 in $CHCl_3$.

Dyes	$\lambda_{max\ comp.}$ [nm]		$\lambda_{max\ exp.}$ [nm]	Main transition
	CAM-B3LYP/6-31G*	MPW1K/6-31G*		
AD351	675	703	676	H → L
	417	450	438	H → L+1
	335	359	336	H–3 → L
	318	328	311	H → L+2
113	651	671	665	H → L
	374	388	345	H–2 → L
	319	330	308	H → L+2
115	616	629	639	H → L
	317	329	331	H → L+1
117	587	589	613	H → L
	289	288	325	H → L+2
109	576	577	598	H → L
	278	277	316	H → L+2

Moreover, less intense absorption peaks were observed in the 300-500 nm range as well (Figure 5.21), and a very wide absorption band (500-800 nm) was observed when the dyes were adsorbed on the TiO_2 layer (Figure 5.22). Optical band-gaps ($E_{0\text{-}0}$, Table 5.7) were estimated both from the intersection of the normalized absorption and emission spectra of the dyes, and from the corresponding Tauc plots[46] (Figure 5.23), obtaining very similar values (1.66-1.69 eV), which were in agreement with the results of computational analysis (1.61-1.69 eV; see paragraph 5.2.5.1).

Table 5.7. Spectroscopic and electrochemical data for dyes AD351 and AD364.

Dye	$\lambda_{max\ abs.}$[a] [nm] (ε [$M^{-1}\,cm^{-1}$])	$\lambda_{max\ emi.}$[a] [nm]	$\lambda_{max\ abs.}$ on TiO_2 [nm]	$E_{ox.}$[b] [V]	$E^*_{ox.}$[c] [V]	$E_{0\text{-}0}$[d] [eV]	$E_{0\text{-}0}$[e] [eV]
AD351	676 (58500)	799	617	1.10	–0.58	1.68	1.67
AD364	681 (72300)	788	604	1.05	–0.64	1.69	1.66

a) $CHCl_3$ solution. b) Potentials vs. NHE. c) Calculated from $E_{ox} – E_{0\text{-}0}$. d) Estimated from the intersection of normalized absorption and emission spectra. e) Determined from Tauc Plot.

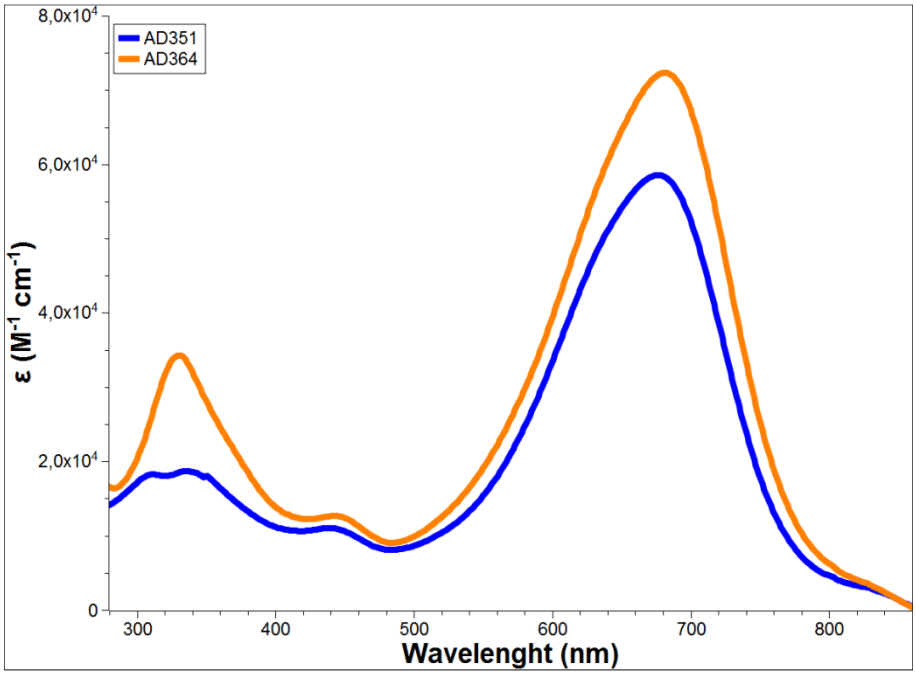

Figure 5.21. UV-Vis spectra of dyes AD351 and AD364 in $CHCl_3$ solution; concentrations: AD351, 7.95 × 10^{-6} M; AD364, 8.80 × 10^{-6} M.

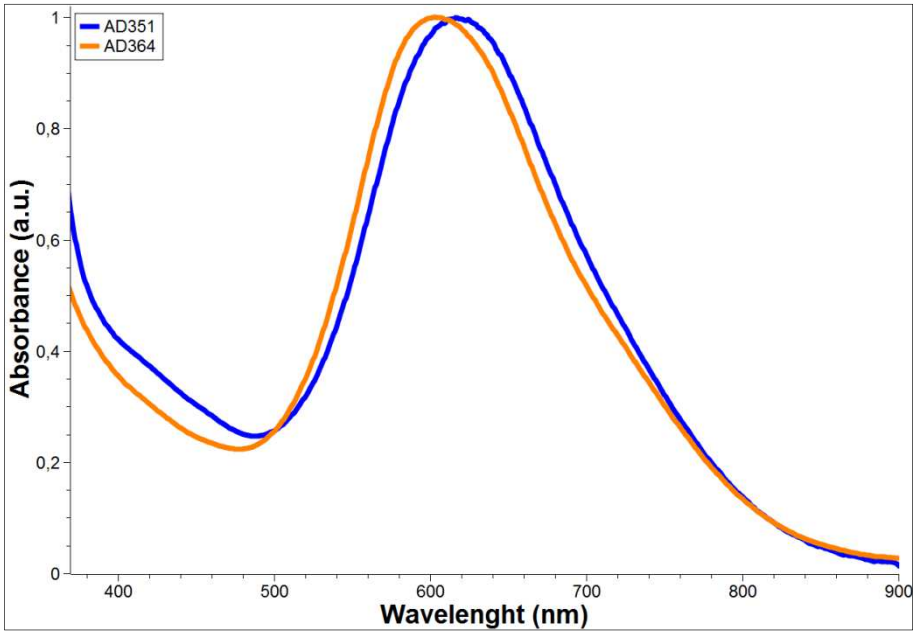

Figure 5.22. Normalized UV-Vis spectra of dyes AD351 and AD364 adsorbed on TiO_2.

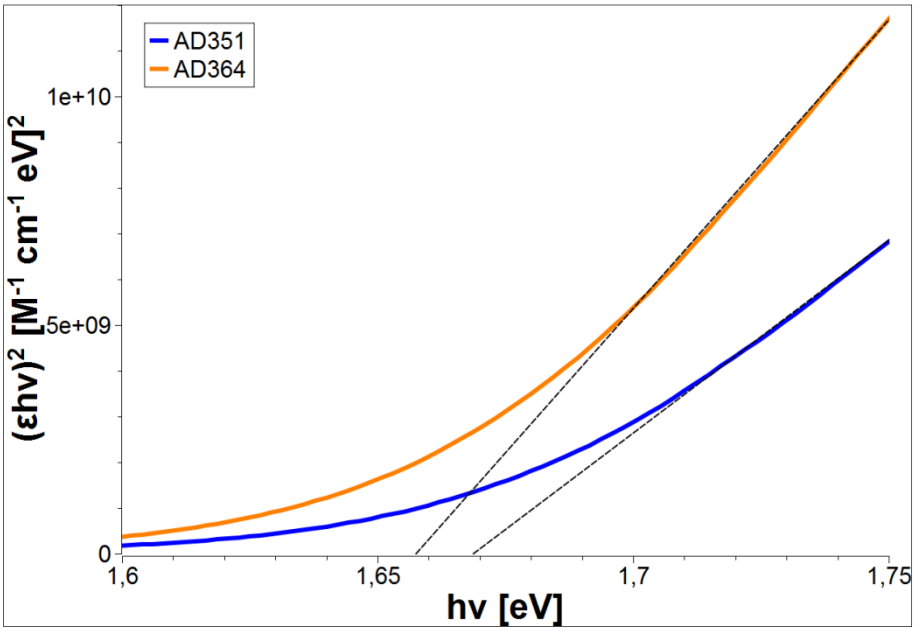

Figure 5.23. Tauc plots[46] for the determination of the optical band-gap of sensitizers AD351 and AD364 in $CHCl_3$ solution.

Finally, cyclic voltammetry[†] measurements of both dyes were carried out in CH_2Cl_2 solution: ground-state oxidation potentials ($E_{ox.}$, Table 5.7) were similar for both compounds (1.05-1.10 V *vs*. NHE), and were more positive than the reduction potentials of the most common redox couples[47,48] (*ca.* 0.5 V *vs*. NHE for I^-/I_3^-; *ca.* 0.56 V *vs*. NHE for $[Co(bpy)_3]^{2+/3+}$), ensuring a good regeneration of the dyes after electron injection. The excited-state oxidation potentials ($E^*_{ox.}$; Table 5.7) were also calculated by subtracting the optical band-gaps ($E_{0\text{-}0}$) from the ground-state oxidation potentials ($E_{ox.}$). These values (–0.58/–0.64 V) were more negative than the conduction band edge of TiO_2 (*ca.* –0.4 eV vs. NHE), suggesting a proper electron injection from the excited state of the dye to the conduction band of the TiO_2 during cell operation.

[†] Cyclic voltammetry measurements were performed by Dr. Fabrizia Fabrizi de Biani from the University of Siena.

5.3. Experimental section

5.3.1. Synthetic procedures

3,4-dihexylthiophene (111)[40]

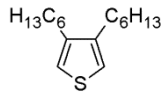

111

Activated magnesium turnings (3.24 g, 134 mmol, 4.0 eq.) were suspended in Et_2O (50 mL), then a crystal of iodine was added. After cooling at 0 °C, 1-bromohexane (15.7 g, 94.8 mmol, 2.8 eq.) was added into the flask. The resulting mixture was stirred at room temperature for 10 minutes and then at 50 °C for one hour. In a second flask 3,4-dibromothiophene (**112**, 8.23 g, 34.0 mmol, 3.76 mL, 1.0 eq.) and Ni(dppp)Cl_2 (0.577 g, 1.06 mmol, 3.0 mol%) were dissolved in Et_2O (50 mL) and the resulting solution was cooled to 0 °C. The ethereal solution of 1-hexylmagnesiumbromide was added dropwise in the second flask, then the resulting mixture was stirred at 50 °C for two hours and at room temperature for 16 hours. After cooling at 0 °C, an aqueous solution of HCl 1M (100 mL) was added and the resulting mixture was stirred for 30 minutes. Two phases were separated and the organic phase was washed with brine and dried with Na_2SO_4. After filtration and removal of the solvent under reduced pressure, the crude product was purified by flash column chromatography (SiO_2, petroleum ether) to give pure product **111** (6.51 g, 25.8 mmol, 76%) as a colorless liquid.

(**111**): ^{1}H–NMR (300 MHz, $CDCl_3$): δ = 6.94 (s, 2H), 2.56 (t, *J* = 7.6 Hz, 4H), 1.62–1.72 (m, 4H), 1.27–1.40 (m, 12H), 0.92–0.98 (m, 6H) ppm. EI–MS: *m/z* = 252 $[M]^+$. Analytical data were in agreement with those reported in the literature.[49]

(*E*)-4-(3,4-dihexylthiophen-2-yl)-4-oxobut-2-enoic acid (110)[17]

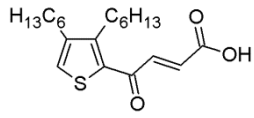

110

3,4-dihexylthiophene (**111**, 2.25 g, 8.91 mmol, 1.0 eq.) and maleic anhydride (**101**, 1.09 g, 11.1 mmol, 1.25 eq.) were dissolved in CH_2Cl_2 (40 mL), then, after cooling to 0

°C, aluminum chloride (2.97 g, 22.3 mmol, 2.5 eq.) was added into the flask. The resulting red mixture was stirred at 0 °C for 30 minutes, then at room temperature for other 30 minutes and at reflux temperature for 23 hours. After cooling at room temperature, a mixture of ice and HCl 3M (50 mL) was added into the flask and the mixture was stirred for 30 minutes, then two phases were separated. The organic phase was diluted again with HCl 3M (50 mL) and the resulting mixture was stirred at room temperature for 24 hours. After separation of the phases, the organic phase was washed with brine and dried with Na_2SO_4. After filtration, removal of the solvent afforded a light brown solid which was recrystallized (hexane) to give pure product **110** (2.01 g, 5.73 mmol, 64%) as a light yellow solid.

(**110**): ^{1}H–NMR (300 MHz, $CDCl_3$): δ = 7.77 (d, *J* = 15.2 Hz, 1H), 7.29 (s, 1H), 6.87 (d, *J* = 15.2 Hz, 1H), 2.97 (t, *J* = 6.7 Hz, 2H), 2.57 (t, *J* = 7.5 Hz, 2H), 1.56–1.65 (m, 2H), 1.27–1.63 (m, 14H), 0.87–0.92 (m, 6H) ppm. ^{13}C–NMR (75 MHz, $CDCl_3$): δ = 181.0, 171.0, 152.4, 146.0, 141.1, 135.3, 130.3, 128.4, 31.8, 31.7, 30.1, 29.9 (x2), 29.3, 28.8, 28.7, 22.8, 22.7, 14.3 (x2) ppm. IR (KBr): $\tilde{\nu}$ = 3423, 3094, 2926, 2857, 1701, 1655, 1612, 1424, 1306 cm^{-1}. ESI–MS: *m/z* = 349.74 [M-H]$^-$.

(3*E*)-5,5'-(3,4-dihexylthiophen-2-yl)-3,3'-bifuranylidene-2,2'-dione (109)

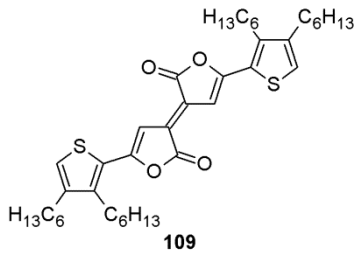

109

Acid **110** (1.20 g, 3.42 mmol, 1.0 eq.), copper (I) chloride (0.407 g, 4.11 mmol, 1.2 eq.), ammonium chloride (0.440 g, 8.22 mmol, 2.4 eq.) and acetic anhydride (16 mL) were divided into eight test tubes and stirred under air at 145 °C for 40 hours. After cooling to room temperature, the purple mixture was diluted with chloroform (100 mL) and filtered over Celite®, then the solvent was removed under vacuum. Chromatographic purification (SiO_2, petroleum ether / toluene 5:2) afforded pure bislactone **109** (430 mg, 0.65 mmol, 38%) as a dark purple solid.

(**109**): ^{1}H–NMR (300 MHz, $CDCl_3$): δ = 7.26 (s, 2H), 7.17 (s, 2H), 2.82 (t, *J* = 6.7 Hz, 4H), 2.54 (t, *J* = 7.3 Hz, 4H), 1.46–1.70 (m, 12H), 1.28–1.44 (m, 20H), 0.88–0.93 (m, 12H) ppm. ^{13}C–NMR (75 MHz, $CDCl_3$): δ = 167.1, 154.9, 146.6, 145.3, 126.1, 126.0, 124.7,

103.7, 31.8, 31.7, 29.9, 29.8, 29.7, 29.3, 28.9, 28.7, 22.8 (x2), 14.2 (x2) ppm. IR (KBr): $\tilde{\nu}$ = 3105, 2924, 2855, 1757, 1559, 1439, 1198 cm^{-1}. ESI–MS: *m/z* = 663.79 $[M-1]^+$. UV-Vis ($CHCl_3$): λ_{max} (ε [M^{-1} cm^{-1}]) = 598 (53900), 316 (13600) nm.

(3*E*)-5,5'-(5-bromo-3,4-dihexylthiophen-2-yl)-3,3'-bifuranylidene-2,2'-dione (117)

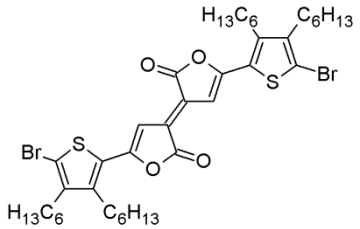

117

Compound **109** (0.133 g, 0.20 mmol, 1.0 eq.) was dissolved in CH_2Cl_2 (10 mL), then NBS (0.080 g, 0.45 mmol, 2.25 eq.) and acetic acid (0.02 mmol, 1.1 µL, 10 mol%) were added into the flask, which was shielded from light. After stirring at room temperature for 20 minutes, water (20 mL) was added, two phases were separated and the organic phase was washed with brine and dried with Na_2SO_4. After filtration and evaporation of the solvent under vacuum, flash column chromatography (SiO_2, petroleum ether / toluene 4:1) afforded pure product **117** (0.106 g, 0.13 mmol, 64%) as a dark blue solid.

(**117**): ^{1}H–NMR (400 MHz, $CDCl_3$): δ = 7.22 (s, 2H), 2.84–2.79 (m, 4H), 2.56 (t, *J* = 7.3 Hz, 4H), 1.45–1.62 (m, 12H), 1.30–1.44 (m, 20H), 0.88–0.93 (m, 12H) ppm. ^{13}C–NMR (75 MHz, $CDCl_3$): δ = 166.7, 153.6, 146.4, 144.7, 126.1, 124.8, 117.3, 104.0, 31.7, 31.6, 30.0, 29.9, 29.7 (x2), 29.4, 28.5, 22.7 (x2), 14.2 (x2) ppm. IR (KBr): $\tilde{\nu}$ = 2926, 2855, 1757, 1559, 1383, 1197 cm^{-1}. ESI–MS: *m/z* = 823.54 $[M+1]^+$. UV-Vis ($CHCl_3$): λ_{max} (ε [M^{-1} cm^{-1}]) = 613 (64000), 325 (16700) nm.

General procedure for the synthesis of stannanes 119 and 120

The appropriate bromide (**118** or **31**, 1.0 eq.) was dissolved in THF, then, after cooling to –78 °C, a 1.6 M solution of *n*-BuLi (1.3 eq.) in hexane was added. The reaction mixture was stirred at –78 °C for one hour, then Bu_3SnCl (1.3 eq.) was added. The resulting mixture was stirred for 16 hours during which the temperature was allowed to return to 25°C. After addition of water (50 mL) and ethyl acetate (50 mL), two phases were separated and the organic layer was washed with water (30 mL) and

brine, and dried with Na_2SO_4. After filtration, removal of the solvent under vacuum afforded the crude product which was used as such for the following reaction.

4-Tributylstannyl-*N*,*N*-diphenylaniline (119)[50]

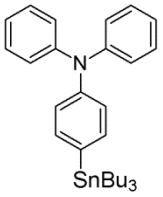

119

4-bromo-*N*,*N*-diphenylaniline (**118**, 0.324 g, 1.0 mmol) was dissolved in THF (5 mL) and reacted with a 1.6 M solution of *n*-BuLi (0.813 mL, 1.3 mmol) in hexane for one hour and, then, with Bu_3SnCl (0.423 g, 1.3 mmol, 0.353 mL) for 16 hours. After work-up and evaporation of the solvent, crude product **119** was isolated as a pale yellow oil.

(**119**): ^{1}H–NMR (400 MHz, $CDCl_3$): δ = 7.31 (d, *J* = 8.3 Hz, 2H), 7.21–7.27 (m, 4H), 7.07–7.12 (m, 4H), 6.98–7.06 (m, 4H), 1.53–1.59 (m, 6H), 1.28–1.38 (m, 6H), 1.02–1.07 (m, 6H), 0.90 (t, *J* = 7.3 Hz, 9H) ppm. Analytical data were in agreement with those reported in the literature.[50]

4-Tributylstannyl-*N*,*N*-(4-hexylthiophenyl)aniline (120)

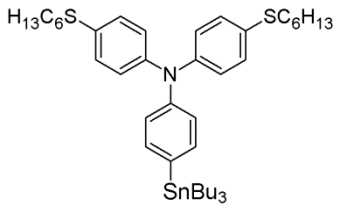

120

4-bromo-*N*,*N*-(4-hexylthiophenyl)aniline (**31**, 0.200 g, 0.36 mmol) was dissolved in THF (2 mL) and reacted with a 1.6 M solution of *n*-BuLi (0.292 mL, 0.47 mmol) in hexane for one hour and, then, with Bu_3SnCl (0.152 g, 0.47 mmol, 0.127 mL) for 16 hours. After work-up and evaporation of the solvent, crude product **120** was isolated as a pale yellow oil.

(**120**): ^{1}H–NMR (300 MHz, $CDCl_3$): δ = 7.31 (d, *J* = 8.3 Hz, 2H), 7.19–7.24 (m, 4H), 6.96–7.06 (m, 6H), 2.87 (t, *J* = 7.3 Hz, 4H), 1.48–1.62 (m, 10H), 1.18–1.45 (m, 18H), 1.02–1.07 (m, 6H), 0.85–0.92 (m, 15H) ppm.

General procedure for the synthesis of compounds 115 and 116

Dibromide **117** (1.0 eq.) was dissolved in toluene, then a solution of $Pd_2(dba)_3$ (5.0 mol%) and P(2-furyl)$_3$ (10 mol%) in toluene and the appropriate stannane (**119** or **120**, 1.0 eq.) were added. The resulting mixture was heated and stirred for 2 h, then it was allowed to cool to room temperature and diluted with H_2O (50 mL) and ethyl acetate (100 mL). The phases were separated and the organic layers were washed with brine and dried with Na_2SO_4. After filtration and evaporation of the solvent, the crude product was purified by flash column chromatography.

(3*E*)-5-(5-(4-(diphenylamino)phenyl)-3,4-dihexylthiophen-2-yl)-5'-(5-bromo-3,4-dihexylthiophen-2-yl)-3,3'-bifuranylidene-2,2'-dione (115)

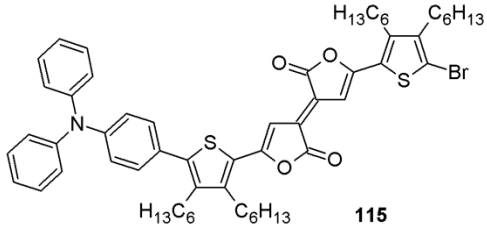

115

Dibromide **117** (185 mg, 0.225 mmol) was dissolved in toluene (15.0 mL) and reacted with a solution of $Pd_2(dba)_3$ (12 mg, 0.011 mmol) and P(2-furyl)$_3$ (5.2 mg, 0.022 mmol) in toluene (3.0 mL) and 4-tributylstannyl-*N*,*N*-diphenylaniline (**119**, 120 mg, 0.225 mmol) at 70 °C for 2h. After work-up, evaporation of the solvent gave a dark-black solid which was purified by flash column chromatography (SiO_2; petroleum ether / toluene 6:1 to 2:1) to give pure **115** (56 mg, 0.056 mmol, 25% yield) as a dark-blue solid together with starting material **117** (52 mg, 28% recovery).

(**115**): ^{1}H–NMR (400 MHz, $CDCl_3$): δ = 7.27–7.33 (m, *7*H), 7.23 (s, 1H), 7.15 (d, *J* = 7.5 Hz, 4H), 7.06–7.10 (m, 4H), 2.81–2.85 (m, 4H), 2.51–2.62 (m, 4H), 1.47–1.66 (m, 12H), 1.24–1.43 (m, 20H), 0.79–0.91 (m, 12H) ppm. ^{13}C–NMR (75 MHz, $CDCl_3$): δ = 167.2, 166.9, 155.0, 152.8, 148.7, 148.3, 147.4, 145.8, 145.5, 144.5, 141.0, 129.9, 129.6, 127.3, 126.3, 125.3, 125.2, 124.0, 123.8, 123.5, 122.5, 116.6, 104.1, 104.0, 31.7, 31.6, 31.5, 31.0, 30.2, 30.0, 29.9, 29.7, 29.6, 29.5, 29.4, 28.5, 27.4, 22.7, 14.2 ppm. IR (KBr):

$\tilde{\nu}$ = 3029, 2924, 2853, 1762, 1559, 1199 cm^{-1}. ESI–MS: *m/z* = 987.28 $[M+1]^+$. UV-Vis ($CHCl_3$): λ_{max} (ε [M^{-1} cm^{-1}]) = 639 (58400), 331 (20711) nm.

(3*E*)-5-(5-(4-(*bis*(4-(hexylthio)phenyl)amino)phenyl)-3,4-dihexylthiophen-2-yl)-5'-(5-bromo-3,4-dihexylthiophen-2-yl)-3,3'-bifuranylidene-2,2'-dione (116)

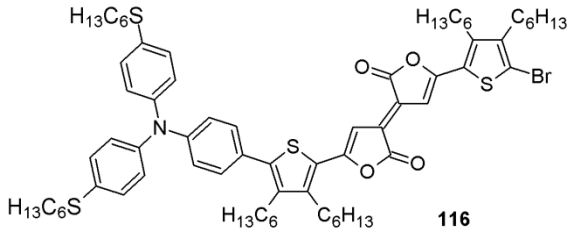

116

Dibromide **117** (180 mg, 0.218 mmol) was dissolved in toluene (12.0 mL) and reacted with a solution of $Pd_2(dba)_3$ (11 mg, 0.011 mmol) and P(2-furyl)$_3$ (5.1 mg, 0.021 mmol) in toluene (3.0 mL) and 4-tributylstannyl-*N*,*N*-(4-hexylthiophenyl)aniline (**120**, 168 mg, 0.218 mmol) at 60°C for 2h. After work-up, evaporation of the solvent gave a dark-black solid which was purified by flash column chromatography (SiO_2; petroleum ether / toluene 6:1 to 2:1) to give pure **116** (72 mg, 0.059 mmol, 27% yield) as a blue gummy solid together with starting material **117** (51 mg, 28% recovery).

(**116**): ^{1}H–NMR (300 MHz, C_6D_6): δ = 7.47 (s, 1H), 7.31–7.38 (m, 3H), 7.25 (d, *J* = 8.7 Hz, 4H), 7.06 (d, *J* = 8.6 Hz, 2H), 6.98 (d, *J* = 8.6 Hz, 4H), 2.81–2.92 (m, 2H), 2.58–2.76 (m, 8H), 2.40–2.49 (m, 2H), 1.70–1.82 (m, 2H), 1.05–1.68 (m, 46H), 0.95–1.02 (m, 6H), 0.79–0.94 (m, 12H) ppm. ^{13}C–NMR (75 MHz, C_6D_6): δ = 166.8, 166.5, 155.0, 153.0, 148.4, 148.3, 145.6, 145.4, 145.3, 144.5, 141.0, 132.6, 131.4, 131.0, 130.4, 125.8, 125.5, 125.0, 124.8, 124.0, 122.8, 116.7, 104.43, 104.39, 34.4, 31.94, 31.87, 31.76, 31.66, 31.3, 30.4, 30.2, 30.1, 30.0, 29.9, 29.8, 29.7, 29.6, 28.8, 28.6, 27.7, 23.13, 23.07, 22.98, 22.91, 14.39, 14.36, 14.31, 14.25 ppm. IR (KBr): $\tilde{\nu}$ = 3014, 2927, 2855, 1762, 1560, 1199 cm^{-1}. ESI–MS: *m/z* = 1220.32 $[M+1]^+$.

2-Tributylstannyl-5-formylthiophene (123)

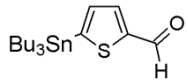

123

N,O-dimethylhydroxylammonium chloride (0.317 g, 3.25 mmol, 1.3 eq.) was suspended in THF (10 mL), then, after cooling to –40 °C, a 1.6 M solution of *n*-BuLi (6.50 mmol, 4.06 mL, 2.6 eq.) in hexane was added and the resulting solution was stirred for 30 minutes at –40 °C. 2-thiophenecarboxaldehyde (**121**, 0.280 g, 2.50 mmol, 0.234 mL, 1.0 eq.) was added and the solution was stirred for 45 minutes at –40 °C. A second portion of the 1.6 M solution of *n*-BuLi (3.75 mmol, 2.34 mL, 1.5 eq.) in hexane was added, then, after one hour stirring at –40 °C, Bu_3SnCl (0.977 g, 3.00 mmol, 0.814 mL, 1.2 eq.) was added and the resulting mixture was allowed to return to room temperature and was stirred for 16 hours. A saturated aqueous solution of NH_4Cl (30 mL) and ethyl acetate (30 mL) were added, the two phases were separated and the organic layer was washed with brine and dried with Na_2SO_4. After filtration, removal of the solvent under vacuum afforded the crude product which was purified by flash column chromatography (SiO_2; petroleum ether / ethyl acetate 20:1) to give desired product **123** (0.627 g, 1.56 mmol, 63%) as a yellow liquid.

(**123**): ^{1}H–NMR (400 MHz, $CDCl_3$): δ = 9.94 (s, 1H), 7.84 (d, *J* = 3.5 Hz, 1H), 7.26 (d, *J* = 3.5 Hz, 1H), 1.52–1.60 (m, 6H), 1.29–1.38 (m, 6H), 1.13–1.17 (m, 6H), 0.89 (t, *J* = 7.3 Hz, 9H) ppm. ^{13}C–NMR (75 MHz, $CDCl_3$): δ = 182.0, 151.6, 149.3, 136.8, 136.3, 29.0, 27.3, 13.7, 11.1 ppm.

General procedure for the synthesis of compounds 113 and 114

The appropriate bromide (**115** or **116**, 1.0 eq.) was dissolved in toluene, then a solution of $Pd_2(dba)_3$ (5.0 mol%) and P(2-furyl)$_3$ (10 mol%) in toluene and 2-tributylstannyl-5-formylthiophene (**123**, 2.0 eq.) were added. The resulting mixture was heated to 70 °C and stirred for 4 hours, then it was allowed to cool to room temperature and diluted with H_2O (50 mL) and ethyl acetate (100 mL). The phases were separated and the organic layers were washed with brine, and dried with Na_2SO_4. After filtration and evaporation of the solvent, the crude product was purified by flash column chromatography.

(3*E*)-5-(5-(4-(diphenylamino)phenyl)-3,4-dihexylthiophen-2-yl)-5'-(5-(5-formylthiophen-2-yl)-3,4-dihexylthiophen-2-yl)-3,3'-bifuranylidene-2,2'-dione (113)

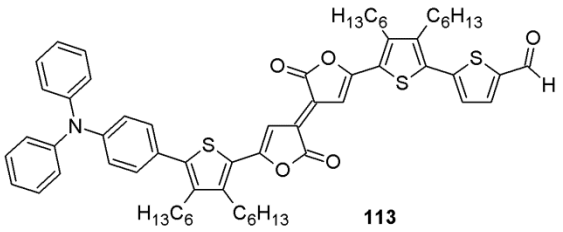

113

Bromide **115** (73 mg, 0.074 mmol) was dissolved in toluene (9.0 mL) and reacted with a solution of $Pd_2(dba)_3$ (3.8 mg, 3.7 µmol) and P(2-furyl)$_3$ (1.7 mg, 7.4 µmol) in toluene (3.0 mL) and 2-tributylstannyl-5-formylthiophene (**123**, 59 mg, 0.148 mmol). Work-up and purification by flash column chromatography (SiO_2; petroleum ether / toluene 2:1 to 1:3) afforded pure aldehyde **113** (43 mg, 0.042 mmol, 57% yield) as a black solid.

(**113**): ^{1}H–NMR (400 MHz, $CDCl_3$): δ = 9.91 (s, 1H), 7.73 (d, *J* = 4.0 Hz, 1H), 7.34 (s, 1H), 7.27–7.33 (m, 8H), 7.15 (d, *J* = 7.7 Hz, 4H), 7.06–7.10 (m, 4H), 2.66–2.88 (m, 6H), 2.57–2.64 (m, 2H), 1.48–1.66 (m, 16H), 1.25–1.42 (m, 16H), 0.85–0.94 (m, 12H) ppm. ^{13}C–NMR (100 MHz, $CDCl_3$): δ = 182.7, 167.1, 166.9, 155.3, 152.7, 149.0, 148.4, 147.6, 147.4, 145.9, 145.2, 143.6, 143.5, 141.1, 136.7, 134.6, 129.9, 129.6, 127.4, 127.2, 126.5, 125.6, 125.3, 124.0, 123.8, 123.2, 122.4, 105.3, 104.2, 31.7, 31.64, 31.61, 31.5, 31.0, 30.5, 30.2, 30.0, 29.9, 29.8, 29.7, 29.5, 29.4, 29.1, 28.2, 27.5, 22.79, 22.77, 22.74, 22.72, 14.2 ppm. IR (KBr): $\tilde{\nu}$ = 3062, 2924, 2854, 1757, 1661, 1551, 1201 cm^{-1}. ESI–MS: *m/z* = 1063.70 $[M+C_2H_6O]^+$. UV-Vis ($CHCl_3$): λ_{max} (ε [M^{-1} cm^{-1}]) = 665 (64600), 345 (21400), 308 (20100) nm.

(3*E*)-5-(5-(4-(*bis*(4-(hexylthio)phenyl)amino)phenyl)-3,4-dihexylthiophen-2-yl)-5'-(5-(5-formylthiophen-2-yl)-3,4-dihexylthiophen-2-yl)-3,3'-bifuranylidene-2,2'-dione (114)

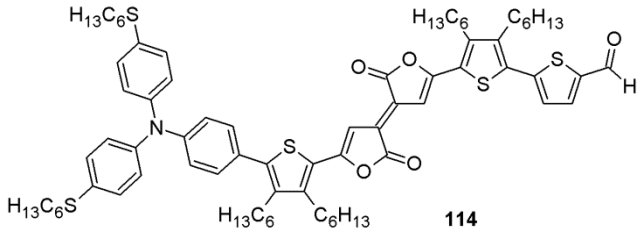

114

$Pd_2(dba)_3$ (3.8 mg, 3.7 µmol) and P(2-furyl)$_3$ (1.7 mg, 7.4 µmol) were dissolved in toluene (10 mL) and reacted with bromide **116** (90 mg, 0.074 mmol) and 2-tributylstannyl-5-formylthiophene (**123**, 59 mg, 0.148 mmol). Work-up and purification by flash column chromatography (SiO_2; petroleum ether / toluene 2:1 to 1:3) afforded pure aldehyde **114** (52 mg, 0.042 mmol, 57% yield) as a blue gummy solid.

(**114**): ^{1}H–NMR (300 MHz, C_6D_6): δ = 9.46 (s, 1H), 7.49 (s, 1H), 7.48 (s, 1H), 7.35 (d, *J* = 8.3 Hz, 2H), 7.25 (d, *J* = 8.3 Hz, 4H), 7.07 (d, *J* = 8.6 Hz, 2H), 6.98 (d, *J* = 8.4 Hz, 4H), 6.93 (d, *J* = 3.8 Hz, 1H), 6.84 (d, *J* = 3.8 Hz, 1H), 2.82–2.94 (m, 2H), 2.56–2.79 (m, 10H), 1.68–1.82 (m, 2H), 1.05–1.68 (m, 46H), 0.95–1.02 (m, 6H), 0.79–0.94 (m, 12H) ppm. ^{13}C–NMR (75 MHz, C_6D_6): δ = 181.8, 166.8, 166.6, 155.2, 153.1, 148.7, 148.3, 147.7, 145.6, 145.4, 144.3, 144.1, 143.4, 141.1, 136.1, 135.2, 132.7, 131.0, 130.4, 127.4, 126.8, 125.9, 125.7, 124.9, 123.8, 122.8, 105.6, 104.5, 34.4, 32.0, 31.9, 31.74, 31.66, 31.3, 30.5, 30.4, 30.2, 30.1, 29.8, 29.6, 29.3, 28.8, 28.3, 27.7, 23.1, 23.0, 22.9, 14.4, 14.3, 14.2 ppm. IR (KBr): $\tilde{\nu}$ = 3027, 2925, 2853, 1752, 1655, 1552, 1203 cm^{-1}. ESI–MS: *m/z* = 1251.42 $[M+1]^+$.

*<u>Note:</u> In the ^{13}C-NMR of compound **114** recorded in C_6D_6, one aromatic signal was covered by the signal belonging to benzene.*

General procedure for the synthesis of dyes AD351 and AD364

The appropriate aldehyde (**113** or **114**, 1.0 eq.) was dissolved in toluene, then a solution of cyanoacetic acid (1.3 eq.) and piperidine (1.0 eq.) in MeCN was added. The resulting mixture was heated to 70 °C and stirred for 5 hours, then chloroform (100 mL) and an aqueous solution of HCl 3M (100 mL) were added. After separation of the phases, the solvent was evaporated. The resulting black solid was purified by consecutive washing with pentane, diethyl ether, methanol and ethyl acetate and dried under vacuum.

2-Cyano-3-(5-(5-((3*E*)-3-(2-oxo-5-(5-(4-(diphenylamino)phenyl)-3,4-dihexylthiophen-2-yl)-furan-3(2*H*)-ylidene)-furan-2(3*H*)-on-5-yl)-3,4-dihexylthiophen-2-yl)thiophen-2-yl)acrylic acid (AD351)

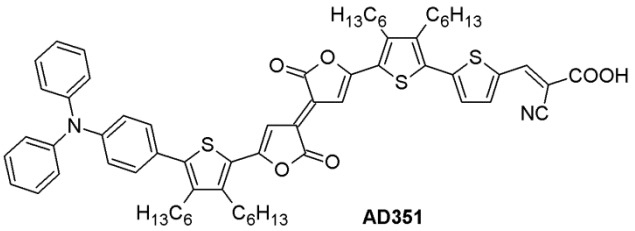

Aldehyde **113** (30 mg, 0.029 mmol) was dissolved in toluene (4.0 mL) and reacted with a solution of cyanoacetic acid (3.2 mg, 0.038 mmol) and piperidine (2.5 mg, 0.029 mmol, 2.9 µL) in MeCN (2.0 mL). Work-up and purification afforded compound **AD351** (12 mg, 0.011 mmol, 37% yield) as a dark solid.

(**AD351**): ^{1}H–NMR (300 MHz, THF-d_8): δ = 8.37 (s, 1H), 7.80–7.91 (m, 1H), 7.43–7.52 (m, 1H), 7.22–7.41 (m, 8H), 6.99–7.19 (m, 8H), 2.81–2.97 (m, 6H), 2.61–2.74 (m, 2H), 1.51–1.68 (m, 12H), 1.21–1.49 (m, 20H), 0.79–0.98 (m, 12H) ppm. ^{13}C–NMR (75 MHz, THF-d_8): δ = 166.8, 166.6, 163.7, 155.5, 153.3, 149.2, 149.0, 148.2, 148.1, 146.1, 145.9, 144.6, 144.2, 141.5, 139.9, 139.1, 137.5, 135.6, 130.4, 130.1, 128.0, 127.8, 126.9, 125.8, 124.6, 124.4, 123.9, 122.8, 116.4, 105.6, 104.3, 100.5, 32.4, 32.3, 32.2, 31.5, 31.2, 30.6, 30.48, 30.46, 30.41, 30.3, 30.1, 29.8, 29.5, 28.9, 27.9, 23.40, 23.34, 23.30, 14.3 ppm. IR (KBr): $\tilde{\nu}$ = 3421, 3067, 2923, 2853, 2211, 1759, 1552, 1201 cm^{-1}. ESI–MS: *m/z* = 1084.93 [M]$^{+}$. UV-Vis ($CHCl_3$): λ_{max} (ε [M^{-1} cm^{-1}]) = 676 (58500), 438 (11000), 336 (18700), 311 (18200) nm.

2-Cyano-3-(5-(5-((3*E*)-3-(2-oxo-5-(5-(4-(*bis*(4-(hexylthio)phenyl)amino)phenyl)-3,4-dihexylthiophen-2-yl)-furan-3(2*H*)-ylidene)-furan-2(3*H*)-on-5-yl)-3,4-dihexylthiophen-2-yl)thiophen-2-yl)acrylic acid (AD364)

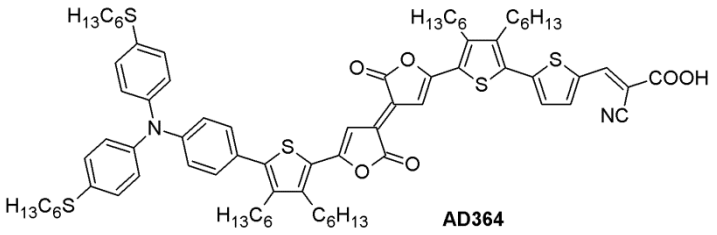

Aldehyde **114** (50 mg, 0.040 mmol) was dissolved in toluene (6.0 mL) and reacted with a solution of cyanoacetic acid (4.4 mg, 0.052 mmol) and piperidine (3.4 mg, 0.040 mmol, 4.0 µL) in MeCN (3.0 mL). Work-up and purification afforded compound **AD364** (33 mg, 0.025 mmol, 62% yield) as a dark solid.

(**AD364**): ^{1}H–NMR (300 MHz, THF-d_8): δ = 8.34 (s, 1H), 7.83 (d, *J* = 3.9 Hz, 1H), 7.45 (d, *J* = 3.9 Hz, 1H), 7.19–7.41 (m, 8H), 6.98–7.13 (m, 6H), 2.79–2.98 (m, 10H), 2.60–2.74 (m, 2H), 1.54–1.68 (m, 12H), 1.22–1.48 (m, 36H), 0.83–0.98 (m, 18H) ppm. ^{13}C–NMR (75 MHz, THF-d_8): δ = 166.7, 166.5, 163.6, 155.4, 153.3, 149.0, 148.7, 148.3, 145.90, 145.87, 145.7, 144.6, 144.2, 141.5, 139.1, 137.5, 135.6, 132.9, 131.1, 130.5, 128.00, 127.96, 126.9, 126.1, 125.8, 124.7, 123.9, 122.8, 116.4, 105.6, 104.3, 100.4, 34.5, 32.4, 32.3, 32.2, 30.51, 30.47, 30.43, 30.3, 30.1, 30.0, 29.2, 23.43, 23.41, 23.36, 23.32, 23.29, 14.3, 14.2 ppm. IR (KBr): $\tilde{\nu}$ = 3435, 2924, 2853, 2212, 1760, 1522, 1201 cm^{-1}. ESI–MS: *m/z* = 1316.41 $[M]^+$. UV-Vis ($CHCl_3$): λ_{max} (ε [M^{-1} cm^{-1}]) = 681 (72300), 443 (12600), 331 (34300) nm.

5.3.2. Electrochemical characterization

Cyclic voltammetry measurements were carried out in commercially available anhydrous 99.9%, HPLC grade dichloromethane for electrochemistry. The supporting electrolyte used was electrochemical grade $[N(Bu)_4]PF_6$. Cyclic voltammetry was performed in a three-electrode C-3 *BAS* Cell having a glassy carbon working electrode, a platinum counter electrode and the aqueous Ag/AgCl NaCl (3M) reference electrode. A *BAS* 100A electrochemical analyzer was used as a polarizing unit. Under these experimental conditions, the one-electron oxidation of ferrocene occurs at E°' = + 0.42 V.

5.4. References

[1] Snaith H. J. *Adv. Funct. Mater.*, **2010**, *20*, 13

[2] http://www.dyenamo.se/dyenamo_dyes.php

[3] Qin C., Wong W.-Y., Han L. *Chem. Asian J.*, **2013**, *8*, 1706

[4] Jin Y., Hua J., Wu W., Ma X., Meng F. *Synth. Metals*, **2008**, *158*, 64

[5] Singh S. P., Gayathri T. *Eur. J. Org. Chem.*, **2014**, 4689

[6] a) Wu W. J., Guo F. L., Li J., He J. X., Hua J. L. *Synth. Met.*, **2010**, *160*, 1008. b) Tang J., Wu W. J., Hua J. L., Li J., Li X., Tian H. *Energy Environ. Sci.*, **2009**, *2*, 982

[7] Jradi F. M., Kang X., O'Neil D., Pajares G., Getmanenko Y. A., Szymanski P., Parker T. C., El-Sayed M. A., Marder S. R. *Chem. Mater.*, **2015**, *27*, 2480

[8] Wu Y., Zhu W. H. *Chem. Soc. Rev.*, **2013**, *42*, 2039

[9] Zhu W. H., Wu Y. Z., Wang S. T., Li W. Q., Li X., Chen J., Wang Z. S., Tian H. *Adv. Funct. Mater.*, **2011**, *21*, 756

[10] Wu Y., Zhu W. H., Zakeeruddin S. M., Grätzel M. *ACS Appl. Mater. Interfaces*, **2015**, *7*, 9307

[11] Mao J., Yang J., Teuscher J., Moehl T., Yi C., Humphry-Baker R., Comte P., Grätzel C., Hua J., Zakeeruddin S. M., Tian H., Grätzel M. *J. Phys. Chem. C*, **2014**, *118*, 17090

[12] Li S.-G., Jiang K.-J., Huang J.-H., Yang L.-M., Song Y.-L. *Chem. Commun.*, **2014**, *50*, 4309.

[13] Yum J.-H., Holcombe T. W., Kim Y., Rakstys K., Moehl T., Teuscher J., Delcamp J. H., Nazeeruddin M. K., Grätzel M. *Scientific Reports*, **2013**, *3*, 2446

[14] Ganesan P., Yella A., Holcombe T. W., Gao P., Rajalingam R., Al-Muhtaseb S. A., Grätzel M., Nazeeruddin M. K. *ACS Sustainable Chem. Eng.*, **2015**, *3*, 2389

[15] Kingsberg E. *Chem. Rev.*, **1954**, *54*, 59

[16] Von Pechmann H. *Ber.*, **1882**, *15*, 885

[17] a) Norsten T. B., Kantchev E. A. B., Sullivan M. B. *Org. Lett.*, **2010**, *12*, 4816. b) Kantchev E. A. B., Norsten T. B., Tan M. L. Y., Ng J. J. Y., Sullivan M. B. *Chem. Eur. J.*, **2012**, *18*, 695. c) Kantchev E. A. B., Norsten T. B., Sullivan M. B. *Org. Biomol. Chem.*, **2012**, *10*, 6682

[18] Hayashi M., Toshimitsu F., Sakamoto R., Nishihara H. *J. Am. Chem. Soc.*, **2011**, *133*, 14518

[19] Cai Z., Guo Y., Yang S., Peng Q., Luo H., Liu Z., Zhang G., Liu Y., Zhang D. *Chem. Mater.*, **2013**, *25*, 471

[20] a) Cai Z., Luo H., Qi P., Wang J., Zhang G., Liu Z., Zhang D. *Macromolecules*, **2014**, *47*, 2899. b) Cai Z., Liu Z., Luo H., Qi P., Zhang G., Zhang D. *Chin. J. Chem.*, **2014**, *32*, 788

[21] Kozniewski T., Marchlewski L. *Chem. Zentr.*, **1906**, II, 1189

[22] Pummerer R., Buchta E. *Ber.*, **1936**, *69*, 1018

[23] Bogert M. T., Ritter J. J. *J. Am. Chem. Soc.*, **1924**, *46*, 2871

[24] Chovin P. *Bull. Chem. Soc. France*, **1944**, *11*, 91

[25] Fang C. S., Bergmann W. J. *Org. Chem.*, **1951**, *16*, 1231

[26] Gaussian 09, Revision C.01, Frisch M. J., Trucks G. W., Schlegel H. B., Scuseria G. E., Robb M. A., Cheeseman J. R., Scalmani G., Barone V., Mennucci B., Petersson G. A., Nakatsuji H., Caricato M., Li X., Hratchian H. P., Izmaylov A. F., Bloino J., Zheng G., Sonnenberg J. L., Hada M., Ehara M., Toyota K., Fukuda R., Hasegawa J., Ishida M., Nakajima T., Honda Y., Kitao O., Nakai H., Vreven T., Montgomery Jr. J. A., Peralta J. E., Ogliaro F., Bearpark M., Heyd J. J., Brothers E., Kudin K. N., Staroverov V. N., Kobayashi R., Normand J., Raghavachari K., Rendell A., Burant J. C., Iyengar S. S., Tomasi J., Cossi M., Rega N., Millam J. M., Klene M., Knox J. E., Cross J. B., Bakken V., Adamo C., Jaramillo J., Gomperts R., Stratmann R. E., Yazyev O., Austin A. J., Cammi R., Pomelli C., Ochterski J. W., Martin R. L., Morokuma K., Zakrzewski V. G., Voth G. A., Salvador P., Dannenberg J. J., Dapprich S., Daniels A. D., Farkas Ö., Foresman J. B., Ortiz J. V., Cioslowski J., Fox D. J., Gaussian, Inc., Wallingford CT, 2009.

[27] a) Becke A. D. J. *J. Chem. Phys.*, **1993**, *98*, 5648. b) Lee C., Yang W., Parr R. G. *Phys. Rev. B: Condens. Matter Mater. Phys.*, **1988**, *37*, 785. c) Stephens P. J., Devlin F. J., Chabalowski C. F., Frisch M. J., *J. Phys. Chem.*, **1994**, *98*, 11623

[28] Yanai T., Tew D., Handy N. *Chem. Phys. Lett.*, **2004**, *393*, 51

[29] Summa V., Petrocchi A., Pace P., Matassa V. G., De Francesco R., Altamura S., Tomei L., Koch U., Neuner P. *J. Med. Chem.*, **2004**, *47*, 14

[30] Franchi D., Calamante M., Reginato G., Zani L., Peruzzini M., Taddei M., Fabrizi de Biani F., Basosi R., Sinicropi A., Colonna D., Di Carlo A., Mordini A. *Tetrahedron*, **2014**, *70*, 6285

[31] Tamura Y., Shirouchi Y., Minamikawa J.-I., Haruta J.-I. *Chem. Pharm. Bull.*, **1985**, *33*, 551

[32] a) Okude Y., Hirano S., Hiyama T., Nozaki H. *J. Am. Chem. Soc.*, **1977**, *99*, 3179. b) Takai K., Tagashira M., Kuroda T., Oshima K., Utimoto K., Nozaki H. *J. Am. Chem. Soc.*, **1986**, *108*, 6048

[33] Knochel P., Rao C. J. *Tetrahedron*, **1993**, *49*, 29

[34] Saitoh T., Oyama T., Sakurai K., Niimura Y., Hinata M., Horiguchi Y., Toda J., Sano T. *Chem. Pharm. Bull.*, **1996**, *44*, 956

[35] Hopf H., Jones P. G., Nicolescu A., Bicu E., Birsa L. M., Belei D. *Chem. Eur. J.*, **2014**, *20*, 5565

[36] Djerassi C., Scholz C. R. *J. Am. Chem. Soc.*, **1948**, *70*, 417

[37] Sarkunam K., Nallu M. *J. Heterocycl. Chem.*, **2005**, *42*, 5

[38] Begley M. J., Crombie L., Griffiths G. L., Jones R. C. F., Rahmani M. *J. C. S. Chem. Commun.*, **1981**, 823

[39] Zhang Q. T., Tour J. M. *J. Am. Chem. Soc.*, **1998**, *120*, 5355

[40] Zhang W., Moore J. S. *Macromolecules*, **2004**, *37*, 3973

[41] Sugiyama N., Gasha T., Kataoka H., Kashima C. *Bull. Chem. Soc. Japan*, **1968**, *41*, 971

[42] Robson K. C. D., Hu K., Meyer G. J., Berlinguette C. P. *J. Am. Chem. Soc.*, **2013**, *135*, 1961

[43] Mitchell T. N. in: "Metal-catalyzed Cross-coupling Reactions, 2nd Edn.", ed. by A. de Meijere and F. Diederich, Wiley-VCH, Weinheim, **2004**, p. 125

[44] Roethle P. A., Trauner D. *Org. Lett.*, **2006**, *8*, 345

[45] Franchi D., Calamante M., Reginato G., Zani L., Peruzzini M., Taddei M., Fabrizi De Biani F., Basosi R., Sinicropi A., Colonna D., Di Carlo A., Mordini A. *Tetrahedron*, **2014**, *70*, 6285

[46] a) Tauc J. *Mater. Res. Bull.*, **1968**, *3*, 37. An application on molecular dyes: b) Coluccini C., Manfredi N., Salamone M. M., Ruffo R., Lobello M. G., De Angelis F., Abbotto A. *J. Org. Chem.*, **2012**, *77*, 7945

[47] Boschloo G., Hagfeldt A. *Acc. Chem. Res.*, **2009**, *42*, 1819

[48] Feldt S. M., Gibson E. A., Gabrielsson E., Sun L., Boschloo G., Hagfeldt A. *J. Am. Chem. Soc.*, **2010**, *132*, 16714

[49] Franco S., Garin J., Martinez de Baroja N., Perez-Tejada R., Orduna J., Yu Y., Lira-Cantù M. *Org. Lett*. **2012**, *14*, 752

[50] Quinton C., Chi S.-H., Dumas-Verdes C., Audebert P., Clavier G., Perry J. W., Alain-Rizzo V. *J. Mater. Chem. C*, **2015**, *3*, 8351

Chapter 6
Conclusions

This Ph.D. work has been focused on the design and synthesis of new organic photosensitizers suitable to be employed in DSSC devices. The target of this work has been the design and the synthesis of new structures of dyes having good photovoltaic performances, superior light-harvesting ability and long-term stability. To obtain this goal we selected two new classes of dyes, characterized by a thiazolo[5,4-*d*]thiazole and a 3,3'-bifuranylidene-2,2'-dione as π-scaffolds.

In the first part of this work (Chapter 3), a rapid and simple procedure for the microwave-activated synthesis of thiazolo[5,4-*d*]thiazoles by condensation of dithioxoamide with aromatic aldehydes, followed by oxidation (aromatization), was described. Thiazolo[5,4-*d*]thiazoles **3b-r** were obtained in good yields, using mild conditions and often reducing the excess of aldehydes employed in the process. Application of the reaction both on aromatic and aliphatic aldehydes, as well as further elaboration of the reaction products by cross-coupling chemistry, were demonstrated.

The synthesis and the characterization of five new thiazolo[5,4-*d*]thiazole-based dyes (**TTZ3**-**7**) has been achieved (Chapter 4 described). The optimized synthetic procedure proved to be general, robust and not sensitive to the modifications required to introduce different functional groups on the compounds common scaffold. The new sensitizers showed impressive visible light-harvesting properties, with absorption maxima over 500 nm and molar extinction coefficients up to 9.67 × 10^{-4} M^{-1} cm^{-2}. Such properties prompted us to use our dyes as sensitizers for thin-layer DSSCs: transparent and opaque small-scale (0.25 cm^2) solar cells containing dyes **TTZ3**-**7** afforded good power conversion efficiencies (η up to 7.71%) and both **TTZ5** and **TTZ7** recorded better photovoltaic performances than standard Ru-based dye **Z907**. Sensitizers **TTZ3**-**5** showed a similar behavior when they were employed for the construction of larger-scale (3.6 cm^2) strip solar cells containing a very thin layer (3-5 μm) of TiO_2. Moreover, all the TzTz-based dyes examined at this stage showed remarkable long-term stability, confirming their potential for a future use in the BIPV sector.

The first two Pechmann-dyes (**AD351** and **AD364**) with a potential application as photosensitizers for DSSC were synthesized and completely characterized (Chapter 5). The Pechmann-unit proved to be quite sensitive to the presence of bases and organic acids, but the employment of mild reaction conditions allowed the functionalization of the scaffold through cross-coupling reactions. To the best of our

knowledge, this is the first example of derivatization of a Pechmann-dye through cross-coupling reactions. As predicted by the computational analysis, the sensitizers **AD351** and **AD364** showed an intense cyan color in $CHCl_3$ solution due to a broad absorption of solar light in the red/NIR region between 500 and 800 nm. Ground- and excited-state oxidation potentials of the dyes were appropriate for their use in DSSCs. Test solar cells measurements are currently in progress to evaluate the photovoltaic performances of solar devices built with dyes **AD351** and **AD364**.

Annexes

List of abbreviations

^{13}C-NMR	^{13}carbon-Nuclear magnetic resonance
^{1}H-NMR	^{1}proton-Nuclear magnetic resonance
Ac_2O	Acetic anhydride
AcOEt	Ethyl acetate
BIPV	Building-integrated photovoltaics
Bu_3SnCl	Tributyltin chloride
CDCA	Chenodeoxycholic acid
dba	Dibenzylideneacetone
DBU	1,8-diazabicycloundec-7-ene
DDQ	2,3-Dichloro-5,6-dicyano-1,4-quinone
DFT	Density functional theory
DMAP	4-Dimethylaminopyridine
DMSO	Dimethylsulfoxide
dppf	1,1'-*bis*(diphenylphosphino)ferrocene
dppp	1,3-*bis*(diphenylphosphino)propane
DSSC	Dye-Sensitized Solar Cells
EDOT	Ethylenedioxythiophene
EIS	Electrochemical impedance spectroscopy
ESI-MS	Electrospray ionization-mass spectrometry
Et_2O	Diethyl ether
EtOH	Ethanol
FMOs	Frontier molecular orbitals
FTO	Fluorine-Tin oxide
HOMO	Highest occupied molecular orbital

HRMS	High-resolution mass spectrometry
ICT	Intramolecular charge transfer
IPCE	Incident photon-to-current conversion efficiency
IR	Infrared
ITO	Indium-Tin oxide
LDA	Lithium diisopropylamide
LHE	Light-harvesting efficiency
LUMO	Lowest unoccupied molecular orbital
MeCN	Acetonitrile
MeOH	Methanol
MLCT	Metal-to-ligand charge transfer
mp	Melting point
MS-4Å	Molecular sieves – 4 angstrom
MW	Microwave
***N*,*N*-DMF**	*N*,*N*-dimethylformamide
NBS	*N*-bromosuccinimide
***n*-BuLi**	*n*-butyllithium
***n*-BuOH**	*n*-butanol
NHE	Normal hydrogen electrode
NIR	Near infrared
NIS	*N*-iodosuccinimide
OFET	Organic field-effect transistor
PBPB	Pyridinium bromide perbromide
PE	Petroleum ether
ProDOT	Propylenedioxythiophene
PV	Photovoltaics
SET	Single-electron transfer
TBP	4-*tert*-butylpyridine

TCO	Transparent conductive oxide
TD-DFT	Time dependent – density functional theory
THF	Tetrahydrofuran
TzTz	Thiazolo[5,4-*d*]thiazole
UV-Vis	Ultraviolet-visible

General experimental remarks

All air-sensitive reactions were performed under inert atmosphere in a flame- or oven-dried apparatus using Schlenk techniques.[1] Solvents used in cross-coupling reactions were previously degassed by means of the "*freeze-pump-thaw*" method. Microwave-assisted transformations were carried out using a *CEM Discover Bench-Mate* reactor at fixed temperature (surface sensor monitoring) and variable power (max. power 300 W). Tetrahydrofuran (THF) was distilled over metallic sodium in the presence of benzophenone, dioxane was distilled over metallic sodium, methanol (MeOH) was distilled over metallic magnesium in the presence of a catalytic amount of iodine, CH_2Cl_2 was distilled over CaH_2, toluene, diethyl ether and acetonitrile were dried on a resin exchange Solvent Purification System (*MBraun*). Anhydrous *N*,*N*–dimethylformamide (DMF) and $CHCl_3$ were stored under nitrogen over 4 Å molecular sieves. Liquid aldehydes were distilled under vacuum before use. 3,4-Ethylenedioxythiophene-2-carboxaldehyde (**4n**)[2] and 3,4-dibromothiophene (**112**)[3] were prepared according to a published procedure. Dithiooxamide (**2**), 3,4-dimethoxythiophene (**16**), diethyl malonate (**19**), 4-(diphenylamino)benzeneboronic acid (**20**), 1-bromo-4-hexyloxybenzene (**24**), 4-hexyloxyaniline (**25**) 1-bromo-4-iodobenzene (**27**), phenothiazine (**32**), 4-iodoanisole (**33**), 5-formylthiophen-2-ylboronic acid (**42**), maleic anhydride (**101**), 4-bromo-*N*,*N*-diphenylaniline (**118**), 2-thiophenecarboxaldehyde (**121**) and all other chemicals employed were commercially available and used as received. Petroleum ether was the 40-60 °C boiling fraction. Thin-layer chromatography was carried out on aluminum-supported Merck 60 F254 plates; detection was carried out using UV light (λ = 254 and 365 nm) and permanganate or molybdophosphoric acid solutions followed by heating. Flash column chromatography was performed using Merck Kieselgel 60 (300-400 mesh) as the stationary phase. ^{1}H-NMR spectra were recorded at 300 or 400 MHz, and ^{13}C-NMR spectra were recorded at 75.5 or 100.6 MHz, respectively, on *Bruker* Avance or *Varian* Mercury series instruments. Chemical shifts were referenced to the residual solvent peak ($CDCl_3$, δ 7.26 ppm for ^{1}H-NMR and δ 77.16 ppm for ^{13}C-NMR; THF-d_8 δ 1.72 and 3.58 ppm for ^{1}H-NMR, δ 67.21 and 25.31 ppm for ^{13}C-NMR; C_6D_6, δ 7.16 ppm for ^{1}H-NMR, δ 128.06 ppm for ^{13}C-NMR; pyridine-d_5, δ 7.22, 7.58 and 8.74 ppm for ^{1}H-NMR, δ 123.9, 135.9 and 150.4 ppm for ^{13}C-NMR; DMSO-d_6, δ 2.50 ppm for ^{1}H-NMR; acetone-d_6, δ 2.05 ppm for ^{1}H-NMR, δ 206.7 and 29.92 ppm for ^{13}C-NMR). FT-IR spectra were recorded with a *Perkin-Elmer Spectrum BX* instrument in the range 4000-400 cm^{-1} with a 2 cm^{-1} resolution. GC-MS spectra were measured with a

Shimadzu gas-chromatograph (*GC-17A* or *GC-2010*) connected to a *Shimadzu* mass spectrometer (*MS-QP2010S* or *MS-QP5050a*) and are reported in the form *m/z* (intensity relative to base = 100). ESI-MS spectra were obtained by direct injection of the sample solution using a *Thermo Scientific* LCQ-FLEET instrument. UV-Vis spectra were recorded with a *Varian Cary* 400 spectrometer and a *Shimadzu* 2600 series spectrometer, and fluorescence spectra were recorded with a *Varian Eclipse* instrument, irradiating the sample at the wavelength corresponding to maximum absorption in the UV spectrum. Elemental analyses were determined using a CHN-S Flash E1112 *Thermo Finnigan* Elemental Analyser; the results were found to be in good agreement with the calculated values. Melting points are uncorrected.

[1] Shriver D. F., Drezdzon M. A. "*The Manipulation of Air-Sensitive Compounds*", John Wiley & Sons, Hoboken, **1986**

[2] Mohanakrishnan A. K., Hucke A., Lyon M. A., Lakshmikantham M. V., Cava M. P. *Tetrahedron*, **1999**, *55*, 11745

[3] Zhang Q. T., Tour J. M. *J. Am. Chem. Soc.*, **1998**, *120*, 5355

Ringraziamenti

… e dopo quasi 200 pagine di SCIIEENZA in inglese, almeno i ringraziamenti voglio che siano in italiano! Che dire…ormai ci siamo, mentre scrivo mancano pochi giorni alla consegna ufficiale e, fra le ultime correzioni e la formattazione delle pagine del maledetto word, prima di andare in stampa voglio aggiungere qualche ultima riga finale (poche perché la voglia di scrivere è definitivamente finita!). Condensare quello che è stato il lavoro di tre anni della propria vita in "poche" pagine non è certo facile, soprattutto perché dietro al risultato che si riporta, piccolo o grande che sia, c'è sempre un percorso molto più tortuoso, fatto di tantissime ore passate in lab, pranzi saltati, peregrinazioni continue a organica a cercare reagenti, colonne infinite, viaggi in treno, incazzature, corsi, spostamenti in bici, stalker, seminari, spettri NMR, imprecazioni e crisi di nervi. Ma anche, fortunatamente, risate, pause caffè, battute, congressi, pranzi, chiacchiere, bevute, viaggi, cene (trash e non) e merende pomeridiane. E tutto questo grazie ad una serie di persone senza le quali sarebbe stato tutto tremendamente più noioso.

Prima di chiunque altro devo ringraziare Gianna, che non contenta di avermi avuto tra i piedi per un anno come laureando, mi ha seguito in tutto questo percorso di dottorato e per tre anni mi ha aiutato, supportato e sopportato: grazie davvero, per tutto. E a ruota un ringraziamento altrettanto importante va a Lorenzo, per l'infinita pazienza, la sua presenza continua e per essere sempre stato un punto di riferimento, come scienziato e come persona: grazie di tutto. Altri ringraziamenti, più che doverosi, per il loro aiuto vanno poi ai boss di organica, Alessandro Mordini e "babbo" Massimo.

E poi ci sono loro, quelli del "Diamine Group", il gruppo di ricerca migliore, e sicuramente con più appetito, che avrei mai potuto trovare: innanzitutto Matteo (Bex) e MarcOlio, con i quali ho lavorato fianco a fianco per più tempo e condiviso la maggior parte dei bei momenti passati in lab, e poi Damiano, Ottavia, ancora Lorenzo e Massimo, Giovanna, Bianca, Daniele, Rocco e Matteo. Grazie di esserci stati in questi tre anni.

Voglio ringraziare le persone che ho trovato all'ICCOM e in particolare la mia "compagna di banco" Vanessa, con cui ho condiviso ufficio, lab, tre anni di dottorato, incazzature, risate, e i dolori della scrittura finale, e Giulia, l'altra pievarina, per tutti i

viaggi condivisi insieme e le disgrazie annesse. E grazie anche ai francesini in visita (quel *pisserò* di Alexandre, Cecile, Elodie e pure l'inquietante Tiphaine) che, pur avendomi spesso fatto dannare, hanno sicuramente arricchito l'esperienza in laboratorio. E un doveroso grazie a chi ha collaborato ai risultati di questa tesi, ad Adalgisa per le analisi computazionali, a Fabrizia per l'elettrochimica e al CHOSE di Roma per le misure sulle celle.

E infine grazie ai miei genitori che hanno sempre appoggiato le mie scelte e condiviso qualunque traguardo, piccolo o grande che fosse.

A tutte queste persone, grazie.